AFFDL-TR-65-88
Part I

INVESTIGATION OF STRUCTURAL SEALING PARAMETERS AND CONCEPTS FOR SPACECRAFT

PART I. DESIGN CRITERIA

Anton Hehn and Frank Iwatsuki
IIT Research Institute

TECHNICAL REPORT AFFDL-TR-65-88, Part I

1965

Air Force Flight Dynamics Laboratory
Research and Technology Division
Air Force Systems Command
Wright-Patterson Air Force Base, Ohio

NOTICES

When Government drawings, specifications, or other data are used for any purpose other than in connection with a definitely related Government procurement operation, the United States Government thereby incurs no responsibility nor any obligation whatsoever; and the fact that the Government may have formulated, furnished, or in any way supplied the said drawings, specifications, or other data, is not to be regarded by implication or otherwise as in any manner licensing the holder or any other person or corporation, or conveying any rights or permission to manufacture, use, or sell any patented invention that may in any way be related thereto.

Copies of this report should not be returned to the Research and Technology Division unless return is required by security considerations, contractual obligations, or notice on a specific document.

INVESTIGATION OF STRUCTURAL SEALING PARAMETERS AND CONCEPTS FOR SPACECRAFT

PART I. DESIGN CRITERIA

Anton Hehn and Frank Iwatsuki
IIT Research Institute

TECHNICAL REPORT AFFDL-TR-65-88, Part I

1965

Air Force Flight Dynamics Laboratory
Research and Technology Division
Air Force Systems Command
Wright-Patterson Air Force Base, Ohio

FOREWORD

The research summarized in this two-part report (Part I "Design Criteria," Part II "Leak Detection and Repair, General Environment, and Materials") was performed by IIT Research Institute, Chicago, Illinois, for the Applied Mechanics Branch, Structures Division, Air Force Flight Dynamics Laboratory, Wright-Patterson Air Force Base, under AF Contract AF 33(615)-2202. The research was concerned with the investigation of parameters for efficient sealing of pressurized spacecraft compartments and factors affecting the maintenance of efficient sealing. The Project Number is 1368, "Structural Design Concepts;" the Task Number is 136808, "Structures for Spacecraft." Frank E. Barnett of the Air Force Flight Dynamics Laboratory was the Project Engineer. The research was conducted from 4 November 1964 to 15 April 1965 by A. Hehn and F. Iwatsuki (Principal Investigators), W. Courtney, W. DeMuth, M. Glickman, C. Gustafson, and W. Jamison.

Publication of this report does not constitute Air Force approval of the report's findings or conclusions. It is published only for the exchange and stimulation of ideas.

RICHARD F. HOENER
Acting Chief
Structures Division

ABSTRACT

Part I: Design Criteria

Part II: Leak Detection - Repair, General Environment, and Material Properties

The many factors that influence the leakage of gases past a seal are discussed and analyzed, in Part I, to apprise the designer of pressurized spacecraft compartments of the problems of achieving and maintaining a seal when extremely low leakage rates are desired. The nature of the leakage path is described and the ways in which leakage occurs are categorized as interstitial, interfacial, and permeation flow. Methods of predicting leakage for these flow regimes are given with greatest emphasis placed on the interfacial flow phenomenon which is characteristic of lightly loaded, demountable seals. In the experimental phase of this program, the sealing characteristics of elastomers were studied to determine relationships between contact stress and leakage with hardness as a parameter. It is concluded that the analytical techniques presented are applicable to the evaluation or design of spacecraft seals.

The information contained in Part II is related to the overall problem of producing and maintaining a satisfactory seal but not directly applicable to spacecraft seal design or evaluation. It is included to apprise the designer of the potential detrimental effects of environment on a seal. The problems of leak detection and repair are discussed and techniques that have been investigated by various organizations are directly referenced. The general and induced environment to which spacecraft may be subjected are discussed to indicate the severity and almost endless combinations of environments. A brief discussion of the properties of rubber and plastic materials is included.

CONTENTS

CONTENTS (Cont.)

CONTENTS (Cont.)

LIST OF FIGURES

LIST OF FIGURES (Cont.)

LIST OF FIGURES (Cont.)

LIST OF FIGURES (Cont.)

LIST OF TABLES

NOMENCLATURE

A	=	area of leakage path
Ap	=	cross-section of flow channel
C	=	damped conductance factor
D	=	diffusion coefficient
E	=	modulus of elasticity
F	=	load/unit contact length
G	=	rate of evaporation
H	=	rubber hardness
K	=	solubility constant, proportionality constant
L	=	thickness of wall
M	=	molecular weight of gas
N_{Re}	=	Reynolds number
P_o	=	pressure at standard conditions
P_1	=	exit fluid pressure
P_2	=	inlet fluid pressure
Q	=	volume flow rate
Q_e	=	volume flow rate at pressure P_e
Q_o	=	volume flow rate at standard conditions
R	=	gas constant
T	=	temperature
W	=	weight rate of flow
	=	Poisson's ratio
	=	permeation rate

a = area of contact/unit length

d = diameter

f = friction factor

h = uniform separation height, conductance parameter

h_o = peak-to-valley roughness

m = 1/Poisson's ratio

n = Meyers strain hardening index

p_u = vapor pressure

r_1, r_2 = outside and inside radii

t = seal cross-section

y = deflection

ΔD = diametral difference

ΔP = pressure difference

λ = mean free molecular path

μ = absolute viscosity

υ_a = mean molecular speed

ρ = fluid density

ρ_o = fluid density at standard conditions

σ = stress at any point

σ_m = Meyers hardness

σ_x = local stress

τ = shear stress

ω = channel width

SECTION I

INTRODUCTION

This two-part report is the result of a 5-1/2-month program which was sponsored by the Air Force Flight Dynamics Laboratory, Research and Technology Division, in recognition of an important gap existing in the state-of-the-art of seal technology, particularly that of leakage prediction techniques. The inability to predict seal performance for new concepts of space vehicles has caused considerable guesswork for environmental control designers, as well as structural designers, with little assurance that the gas supply allowed for leakage make-up will be sufficient to accomplish a mission until a prototype has been built and tested. All too often, an overly optimistic estimate results in major structural modifications or reduced vehicle performance.

Part I purposely dwells at length on those subjects which will give the reader an insight into leakage phenomena and the factors which influence leakage. Also, it is intended that these discussions which indicate the complicated nature of leakage, and the difficulties of attempting to control leakage will create an appreciation of the importance of the need to analyze sealed areas and design for minimum leakage in the early stages of conceptual studies. This report demonstrates the methods by which analytical techniques can be used to reduce heavy dependence upon postfabrication leakage tests to guide final seal designs. It is not implied that an analytical approach alone is sufficient to solve all sealing problems, but rather that it can be an extremely useful initial step toward achieving a satisfactory seal with the least expenditure of time and funds.

An attempt has been made to show the validity of an orderly "seal engineering" approach by conducting the research program in the following sequence:

1. Analysis of leakage phenomena in seals.

2. Practical design techniques for controlling or predicting leakage.

3. Designation of future research areas deemed most likely to result in the advancement of seal technology.

SECTION II

MECHANISMS OF SEALING
(LEAKAGE FLOW PHENOMENA)

1. INTRODUCTION

The principal function of a seal is to exclude or prevent the flow of fluid from or to a particular area. In striving for this goal, an enormous amount of effort has been expended in seal research, primarily in the following areas:

- Structural analysis of seal and housing
- Seal materials
- Seal configuration design

A review of the literature indicates that most of the important parameters influencing seal performance have been recognized; however, the major difficulty has been the generation of theoretical or empirical relationships between the important sealing parameters which can lead to useful design criteria or prediction of seal performance.

In view of the vast amount of seal research to date, it is ironic that the area of seal leakage that is most important in sealing considerations is the one in which the least amount of quantitative information is available. In the past, the leakage requirements for many sealing applications were not nearly as stringent as the demands placed upon sealing devices by present space technology appplications. Thus, qualitative criteria such as visible leakage, pressure loss, and catastrophic failure, were accepted for use in seal evaluation. Also, facilities for measuring extremely small fluid flow rates were not available to many of the early seal investigators. In many cases, if seal leakage could not be detected with the equipment at hand, the seal was considered to exhibit "zero" leakage which, in reality, only indicated that the leakage path was below the minimum sensitivity of the measuring equipment.

Thus, for lack of sufficient motivation and adequate leak-measuring equipment, a background of quantitative leakage data was not built up by past investigators.

Since leakage is the prime performance criterion for any seal, this section will be devoted to development of an understanding of the fundamental leakage flow phenomena occurring in seals. This background can then be utilized in the establishment of seal design criteria, as well as prediction of leakage rates.

2. INTERFACIAL FLOW

a. Characteristics of a Surface

Seals can be generally classified into two groups, noncontact seals and contact seals. In a noncontact type of seal, a finite, though small, clearance is maintained between the surfaces forming the seal. Examples of noncontact seals are labyrinth, throttle bushings, and visco-seals. The leakage rates allowed by these seals are generally higher than the leakage rates allowed by contact-type seals and can be estimated with a fair amount of accuracy since theoretical leakage relationships for these types of seals are quite well developed. Because of the stringent leakage requirements in space systems, the majority of the seals, both static and dynamic, are likely to be contact seals.

In the contact-type seal, the surfaces forming the seal are brought into physical contact forming a barrier to fluid flow. Since leakage takes place with contact seals also, it is first necessary to understand the phenomenon by which the fluid passes through the contact interface in the leakage process in order to develop useful criteria. Since the contact of two surfaces forms the seal, a description of the nature of a seal surface is necessary for an understanding of the leakage flow phenomenon.

Any surface, no matter how smooth in appearance to the naked eye, when viewed at the microscopic level exhibits a complex three-dimensional pattern of irregularities. A profile of such a surface is shown schematically in Figure 1.

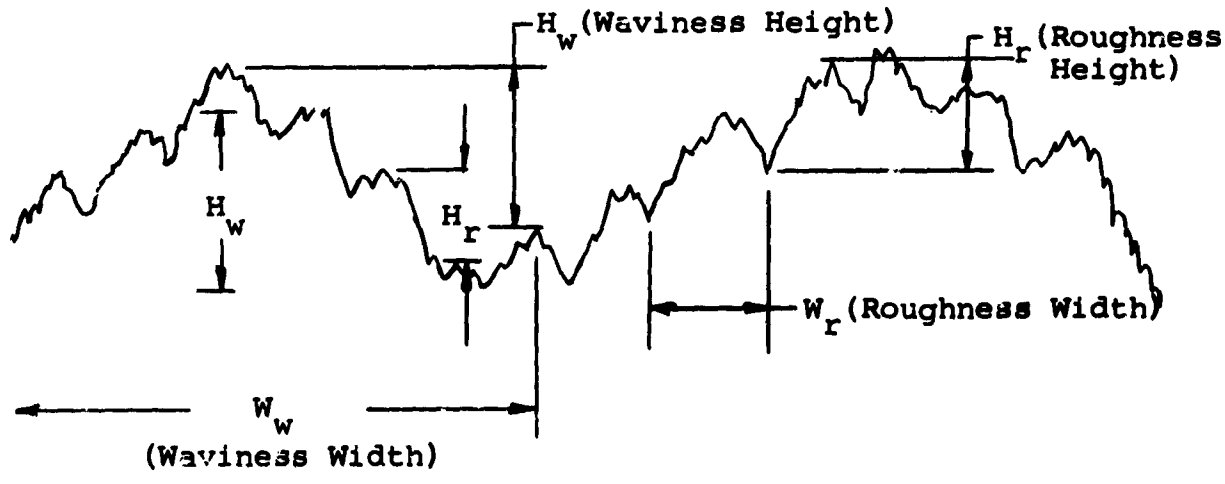

Figure 1 Schematic Representation of a Surface

Three basic patterns are usually present in a typical solid surface. A comparatively long wavelength disturbance, commonly called waviness and designated by height, H_W, and wavelength, W_W, in Figure 1. is usually present. This phenomenon in a machined surface is generally caused by a periodic disturbance in the machining operation such as runout on a lathe spindle, eccentricity on a grinding wheel, etc. Superimposed on the waviness pattern is a pattern of smaller peaks and valleys. This surface disturbance is called roughness and is designated in Figure 1 by height, H_R, and wavelength, W_R. This surface phenomenon is dependent on tool profile, feed rate, and depth of cut in machined surfaces. Still smaller peaks and valleys caused by the tearing away of material during the machining operation are superimposed on the roughness pattern.

Although the preceding discussion was concerned with machined surfaces, the same general characteristics are exhibited by most solid materials. In molded polymers the surface finish is influenced by the surface finish of the mold. Sintered materials such as carbon graphite have a porous texture.

In addition to the complex surface topography produced by surface finishing techniques, the interaction between the surfaces forming a seal interface is further complicated by other phenomena. The development of electron microscopy techniques has permitted observations of the individual crystals of materials which have shown that the molecular array is generally regular on the crystal surface. However, regions of marked defects or dislocations can be found. These dislocations cause surface irregularities even at the crystal level of most materials. Thus, it can be concluded that no solid surface is truly flat or perfectly smooth at the microscopic level. Even the best mechanically prepared surfaces show irregularities much larger than those produced by the crystal dislocations. The height of the irregularities range from a few angstroms for crystal dislocations to the range of 1×10^{-6}-in. for the best mechanically prepared surfaces.

Further complication in the interaction of contacting surfaces is introduced by the presence of contaminants on the surfaces. These contaminants can range from dust or wear particles to chemically or physically adsorbed molecular layers. The particulate contaminants such as dust tend to separate the surfaces locally and then reduce the amount of contact on the surfaces.

The chemical and physical contaminants range from layers of adsorbed oxygen and the water molecules in layers of one to several molecules thick in noble metals exposed to air to oxide layers up to 1×10^{-6}-in. thick in reactive metals. These oxide layers form almost instantaneously when metals are exposed to air, and can be avoided only under strict laboratory-type inert atmospheres. The importance of the oxide layer is that it can retard surface deformation. With most metals the oxide is

usually harder and more brittle than the base metal. Thus, the hard case of oxide retards surface deformation at the microscopic level.

From the preceding discussion it is seen that the surface of a solid material is a complex, three-dimensional pattern of peaks and valleys which are dependent on the finishing process and the material itself. Particulate and chemical contaminants on the surface influence and complicate the nature of the contact between two surfaces.

At this point, the contact of two surfaces forming a sealing interface can be considered.

b. Description of the Interface

When two surfaces are brought into contact under light loading, contact takes place first at the highest peaks or surface asperities. The asperities deform elastically and plastically until the load is supported. At this point, the surfaces are in contact at only a small number of locations. Many void spaces or areas of no material contact are present.

As the load is increased further, elastic and plastic deformation of the asperities occurs and more asperities come into contact. This process of deformation at the microscopic level is shown schematically in Figure 2. As the deformation and number of asperities in contact increases, the number and size of the void spaces decreases.

Fluid leakage occurs when the fluid passes through the complex leakage path formed by the interconnection of void spaces in the seal interface. Thus, the fundamental requirement of interfacial sealing can be deduced. That is, in order to achieve sealing, substantial deformation of one or both surfaces at the asperity level is necessary to reduce the size and number of voids in the interface. Methods of achieving this deformation and factors influencing the degree of deformation necessary to achieve adequate sealing can now be considered.

3. FACTORS AFFECTING INTERFACE LEAKAGE

a. Surface Deformation

The deformation of asperities that occurs at the contact interface is either elastic or plastic and is dependent on the net contact load applied to the sealing surface. As the deformation increases, the magnitude of the interface voids (possible leakage paths) decreases. Thus, the relationship between asperity deformation and contact load exerts a profound influence on seal leakage. This relationship is complicated by the irregular nature of real solid surfaces.

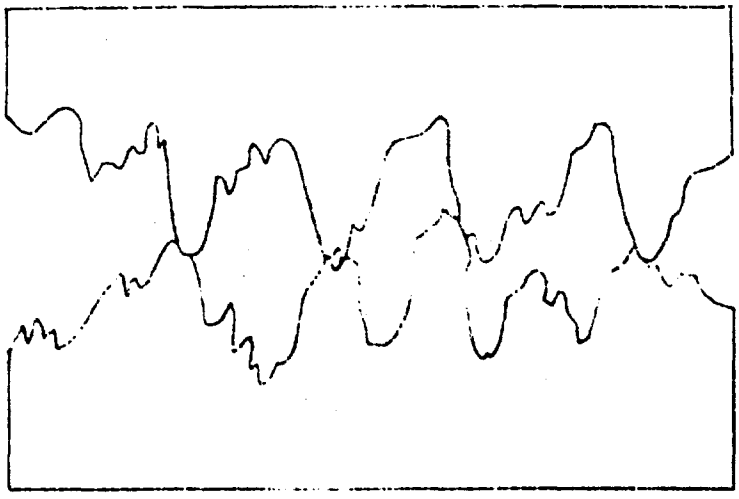

a) Light Contact Load

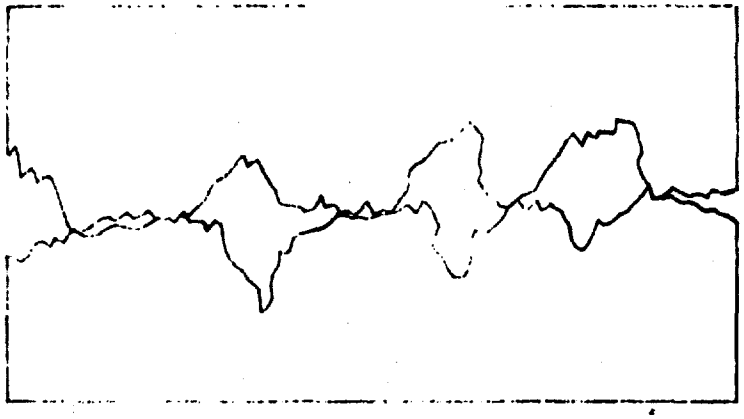

b) Increased Contact Load

Figure 2 Schematic of Two Surfaces in Contact Under Load

The magnitude of the effect which modes of deformation have on seal leakage is dependent on the seal material. All metals with relatively rough surfaces may undergo elastic and plastic deformation as well as combinations of both. Plastic materials behave similarly to lead in that subsurface yielding and permanent deformation predominate. Rubber materials form a sealing interface elastically.

The theoretical approaches to the problem of deformation are discussed in Section IV.

b. Material Properties

The ability to deform easily is one of the most important properties of seal materials. Resilience is almost equally important. Elastic recovery of the bulk material during reductions in contact load is important in maintaining interface contact, as pointed out in the discussion on the hysteresis phenomenon. When used within their chemical and environmental limitations, elastomers are ideal seal materials.

Chemical compatibility and environmental degradation problems often prevent the use of elastomer materials in aerospace sealing applications. In order to approach the conformability and resilience requirements for good interface contact in sealing applications, the seal and component designer has been forced to consider other materials. Often composite-type seals are developed utilizing a deformable material as the contact interface and a resilient supporting structure. Soft metals plated onto more resilient metals are also frequently used in seal applications. The seal material for a particular application is often a compromise between the desired conformability and resilience properties, the chemical and environmental degradation resistance, and the required sealing contact stress. The effects of environment on materials are treated separately in Section V.

. INTERSTITIAL FLOW

The flow of fluid through controlled clearance spaces such as between a bushing and shaft is defined as interstitial flow. The flow regime may be laminar or turbulent, but molecular flow cannot be attained. Thus, the applicability of this phenomenon to spacecraft sealing because of the inherent prohibitive leakage values is rather limited. However, flow through interstices can be predicted with a fair degree of accuracy. The theory of fluid flow in narrow spaces is rather well developed, and a wealth of experimental data is published and available to supply the necessary empirical coefficients.

The flow passage is usually annular, although such other configurations as the clearance between two flat plates or between two disks are occasionally encountered. The two surfaces

that form the flow passage may be in motion or stationary with respect to each other. Depending on whether the flow regime is laminar or turbulent, motion of the boundaries may have an effect on the leakage flow. In summary, the three factors that affect flow through a gap are:

- flow path geometry
- motion of the boundaries
- flow regime

5. PERMEATION

Gases can permeate solid walls of metals, polymers, or elastomers by a molecular diffusion process. The rate of permeation flow is very slow compared to leak rates encountered in interfacial or interstitial sealing mechanisms. Permeation flow can be readily measured by a mass-spectrometer leak detector. To achieve the ultimate in leaktightness, especially in space stations and other space vehicles of long voyage duration, and to make accurate predictions as well as measurements of leakage, the possibility of flow through solid walls and solid gaskets must be considered.

The process whereby gases pass through sound solid membranes is described by Norton (Ref. 1) in the following manner:

- The gas on the high-pressure side is first adsorbed and dissolved in an external surface layer on the membrane surface. Surface pretreatment is important here.
- The gas diffuses through the "solid" driven by the concentration gradient according to Fick's Law. The diffusion of the gas may be as atoms of a dissociated molecule if the membrane is metallic or as molecules if the membrane is a polymer.
- When the gas reaches the low-pressure side of the membrane, it undergoes a transition from a dissolved state to an absorbed state and is desorbed at the surface passing into the surroundings. Again, surface pretreatment may be important.

The over-all steady-state process described above and depicted on Figure 3 is termed "permeation," and the speed of the process is controlled by the slowest of the above steps.

Permeation equations detailing the magnitude of leakage flow due to the permeation process are given in Section IV.

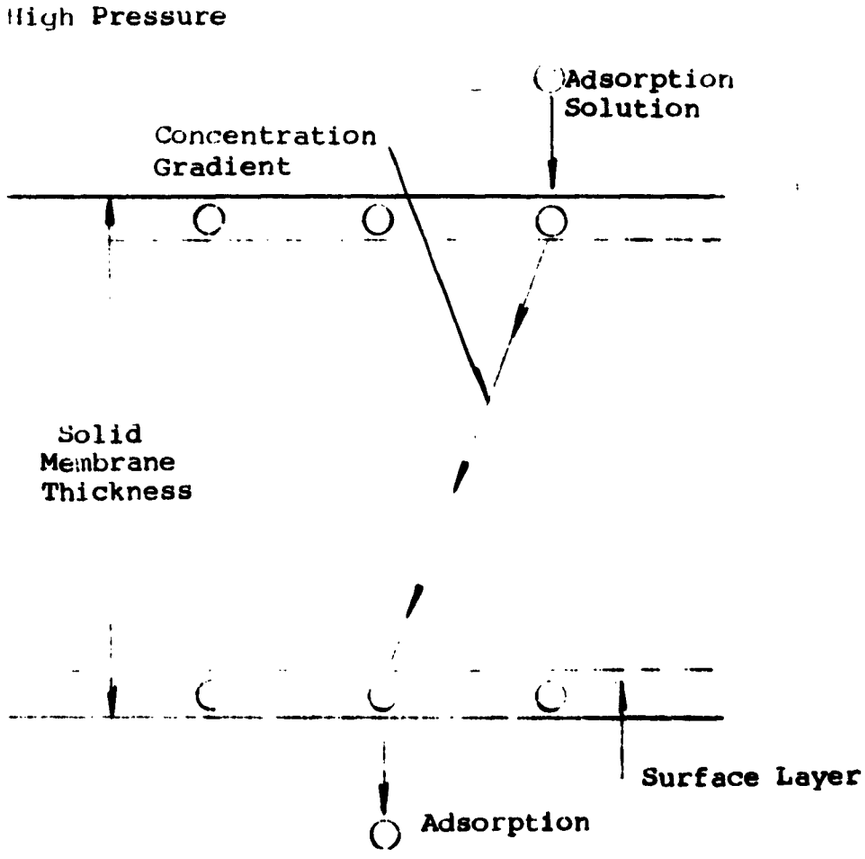

Figure 3 Permeation of Gas Through a Solid Membrane

SECTION III

SEAL CLASSIFICATION

1. INTRODUCTION

Spacecraft and space station seals can be classified in many manners. One classification system is by the mechanism of sealing involved. Another is based on the application of the seal. With these two systems, either the sealing mechanism encountered while selecting a seal for a specific design function, or the seal application which may be known can be directly looked for under a particular heading. Both systems, therefore, were included in this section so that the aerospace vehicle designer can readily obtain useful and meaningful data as to what seal to employ where.

The functional categories and sealing methods which apply to spacecraft and space station sealing with approximate sealed opening dimensions are shown on Table I. Permanent structural sealing methods such as welding, brazing, soldering, etc., are not categorized and not considered to be a sealing method but rather a structural process. Table I, furthermore, is a summary of the classification categories and sealing methods and can be used as a quick reference guide.

2. CLASSIFICATION OF SEALS BY SEALING MECHANISM

A seal can be defined as a device which minimizes the interchange of fluid from one region to another. The device refers to the interstice or interface formed by the surfaces of two materials. Interstitial seals are generated by two surfaces that are not in contact but produce a very small clearance for leakage flow. Interface seals are generated by the surfaces of two materials in contact. Hermetic seals are classified as a separate type. However, the sealing mechanism consists of a permanent interface.

a. Interfacial Seals - Static

The category of interfacial seals can be subdivided on the basis of the type of contact occurring between the materials forming the interface. Interfaces may be classified as:

- Separable
- Semipermanent
- Permanent

Separable interface seals may be defined as seals formed by the surfaces of two materials that can be separated readily without application of an external force as compared to the permanent interface seal. The latter are exemplified by weldments, diffusion bonds, and certain adhesive bonds in which a substantial force is required to form a separation at the interface. In addition, the topography of the interface is changed considerably during separation. Semipermanent interface seals require a minimum of external force to obtain separation, and the surfaces forming the interface are not changed appreciably. These seals are exemplified by adhesive or molten metal interfaces. In the latter case, heat is applied to the interface to soften or liquify one of the interface materials permitting easy separation of surfaces.

The technical definition of a seal refers only to the interface of two materials; however, in general use, the definition is extended to include a structural member which possesses two or more interfaces. To clarify the distinction between the two definitions, a schematic representation of various types of interfaces are shown on Figure 4. Figure 4(a) and (b) represent seals described by the technical definition. Figure 4(c) and (d) depict several sealing interfaces formed by an intermediate structure where the sealing interfaces and structure are viewed as one seal, defined by the general usage of the term "seal." A seal is, therefore, defined as a device composed of a structural element possessing two or more interfaces.

The important aspects of an interface are the macroscopic geometry, microscopic topography, and material properties. Each of these factors combined with the forces acting at the interface determines the size of the leakage paths and, consequently, the leakage. The interrelationship between the factors is determined by the modes of material deformation under load. The two types of deformation occurring are:

- elastic deformation
- plastic deformation

The distinction between the two is whether the deformation is permanent.

Elastic deformation of materials forming an interface is typically produced by metallic materials under light loads and rubber materials. If metallic surfaces are substantially rough, a large leakage path is produced. The application of a light load results in little change in the leakage path. When the topography of metallic surfaces is very flat, elastic deformation may provide a very small leakage path. A characteristic of an elastic interface is its susceptibility to changes in interface forces. An increase in force produces a decrease in leakage path, and a relaxation in force results in a corresponding increase in leakage path.

Table I

Classification of Spacecraft and Space Station Seals Summary Table

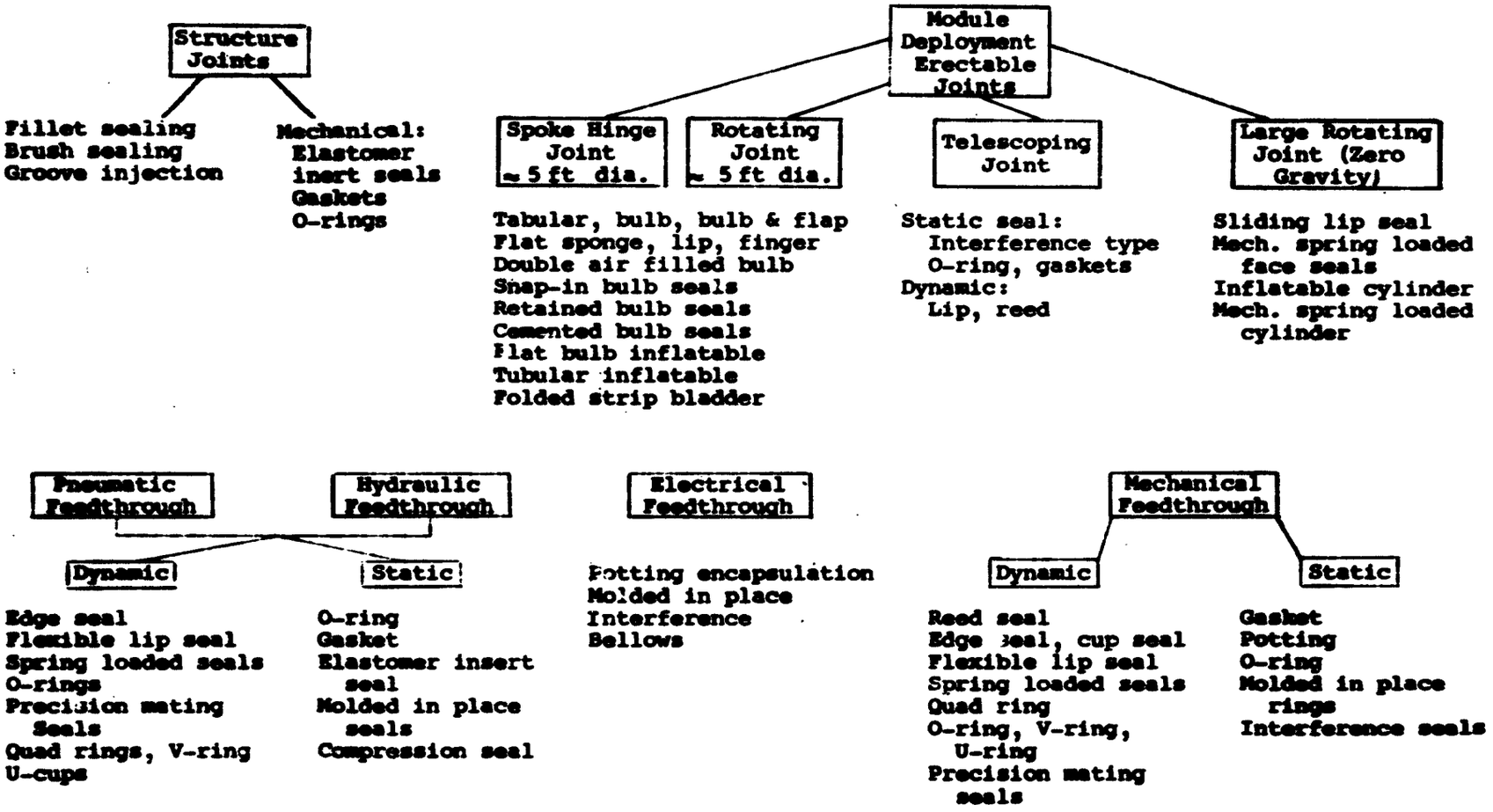

Air Locks
Exit Hatches
≈2½-20 ft dia.

Inward Opening

Bumper seal
O-ring
Diaphragm seal
Closed cell sponge and lip seal
Multi-striker seal

Outward Opening

Cemented inflatable seal
Retained inflatable seal
Diaphragm inflatable seal
Large inflatable seal
Rubber stops

Internal Access Doors
3 ft x 4 ft

Inflated diaphragm seal
Elastomer & fabric material seal
Bumper seals
Multi-striker seals
O-ring

Fuel Transfer Ports

O-ring
Molded in place elastomers
Bellows connector
Spring actuated seal

Docking Transfer Ports
≈2½ ft dia.

Closed cell sponge filled seal
Tubular shape bladder seal
Inflatable fabric and rubber seal
Cemented in place elastomer seal
Air filled fabric and rubber tubular bulb seal

Observation Ports
≈ 1 ft dia.

Indium seal
Hoop tension ring
Organically bonded
Platinum/fused silica

Fuel Lines

Same as hydraulic feedthroughs

Fuel Tanks

Gaskets
Molded in place seals
O-rings

Valves

Bellows
O-ring
Edge seal
Labyrinth seal
Precision mating seals
Interference fit seals

Faying Surface

Flexible type
Adhesives
Flexible sealant

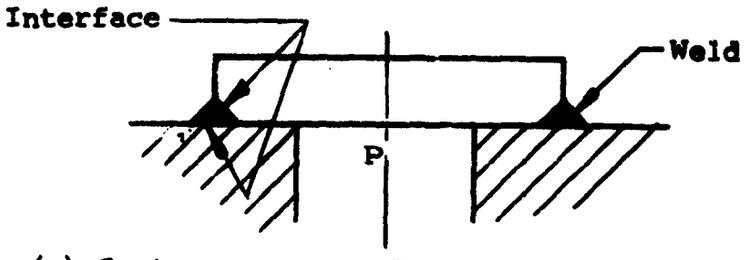

(a) Semipermanent or Permanent Interface

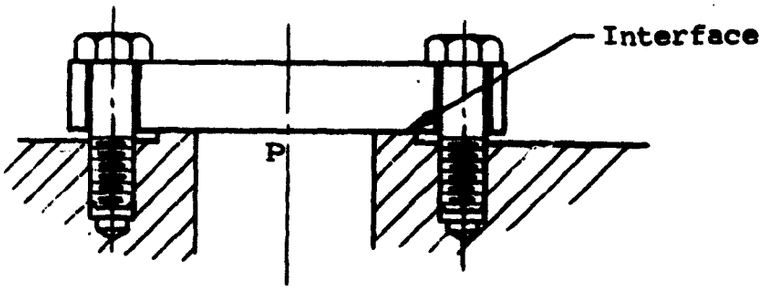

(b) Single Separable Interface

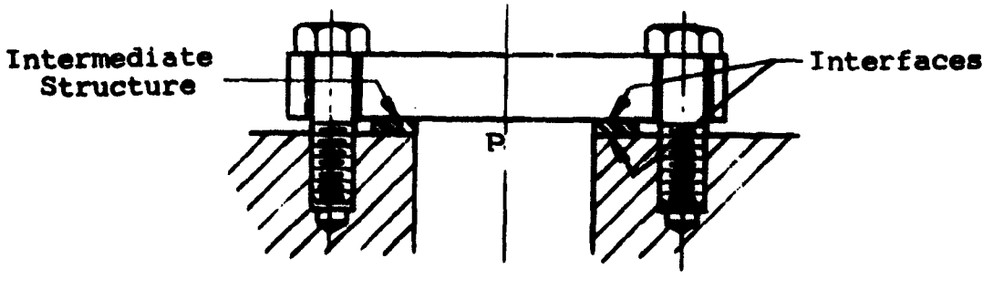

(c) Two Separable Interfaces Formed by an Intermediate Structure

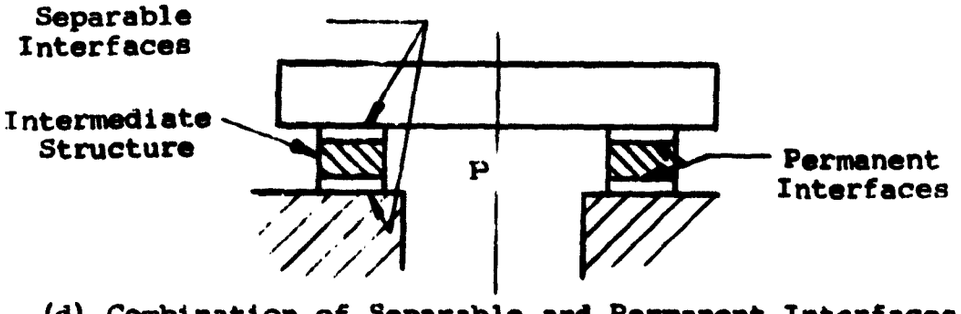

(d) Combination of Separable and Permanent Interfaces Formed by an Intermediate Structure

Figure 4 Types of Interface Construction

Plastic deformation of materials forming an interface is typically produced by metallic materials, as well as, plastic and other nonmetallic materials under substantial loads. If the mating surfaces are rough, a minimum leakage path can only be achieved by plastically displacing material on the microscopic surface of the materials in contact. The size of the leakage path is determined by the maximum force acting at the interface. A relaxation of load does not produce a corresponding change in the leakage path.

The characteristic of the seal shape to tolerate increased deformation is defined as seal resiliency. The beneficial effect of resiliency is to provide and maintain interface contact when motion of the interfaces occurs. The movement of the interface may be due to thermal warpage or to pressure deformation of one or more interface surfaces.

The application of sealed fluid pressure to a seal produces additional deformation effects on a seal structure. Ring seals, for example, deform radially, tending to decrease the cross section of the seal ring. If the effect of applied pressure tends to deform the seal and maintain interface contact, the seal is defined as a pressure energized seal. If fluid pressure produces no substantial change in cross-sectional deformation and an increase in force at the interface occurs, the seal is defined as a nonpressure-energized seal. The ability of a seal to deform and maintain interface contact under fluid pressure is particularly beneficial when the mating interface surfaces deform. Figure 5 compares nonpressure-energized and pressure energized seal cross sections.

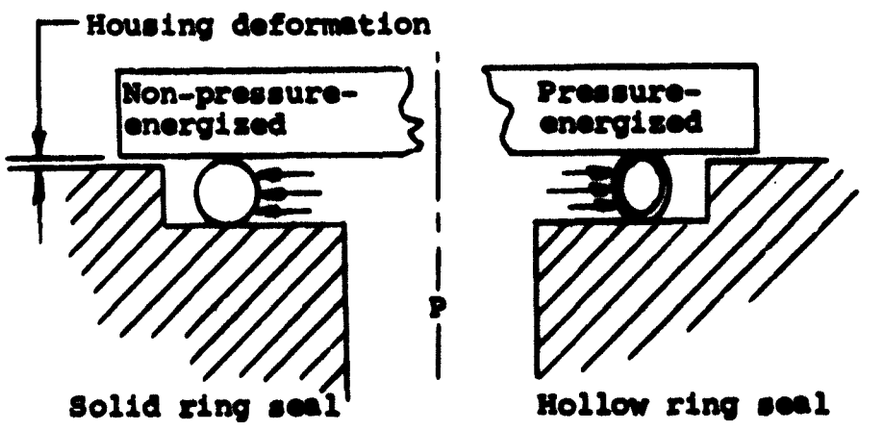

Figure 5 Comparison of Deformation Characteristics of a Non-pressure-Energized and Pressure-Energized Seal

Another classification factor is the materials of construction. A seal may be composed of one or more materials. When two or more materials are used, the softer material is used to form the interface surface. If the materials are metals, the seal is defined as a metallic seal. Seals composed of a rubber, plastic, or other material in conjunction with a metal are termed as combination seals. Seals constructed of plastics, rubber, or other nonmetallic materials singularly or in combination are defined as nonmetallic seals.

b. Interfacial Seals -- Dynamic

(1) Sliding Seals

In the following discussion, the basic classification of sliding seals is described using typical seals to illustrate the "sealing action." Additional examples of the seals described are presented in the Appendix.

Sliding seals can be broadly classed on the basis of materials of construction and use. A distinction is made between metals and nonmetals, but no further differentiation is attempted. Sliding seals are used to seal between surfaces that can be moved relative to each other. The sealing elements are most commonly circular, and seal dynamically at an inner or outer surface as typically described by a rod and piston seal. No distinction is made between uses, since most seals can be used in either application.

Conforming seals are continuous elements such as uninterrupted circular rings in which sealing surfaces are urged into contact by resistance of the seal structure to deformation or externally applied forces. Precision mating seals are discontinuous elements with sealing interfaces brought into contact largely by precise geometrical mating of surfaces. Bellows and diaphragm seals are formed by elastically deforming a material. This type seal does not possess a rubbing interface but certain designs do include one or more static interfaces.

Interface contact loads are produced by the applied pressure and any radial and axial mechanical preload induced by interference of the seal with surrounding parts or by such external means as adjustment nuts. Seals which rely solely on radial interference are classed as radially preloaded seals. Other seals subjected to axial loads usually transfer part of the axial load to the radial contact surface. These seals are classed as radial and axial preload seals. Table II lists the various categories of sliding seals. Figure 6 depicts some typical sliding seals.

Table II

Classes of Sliding Seals

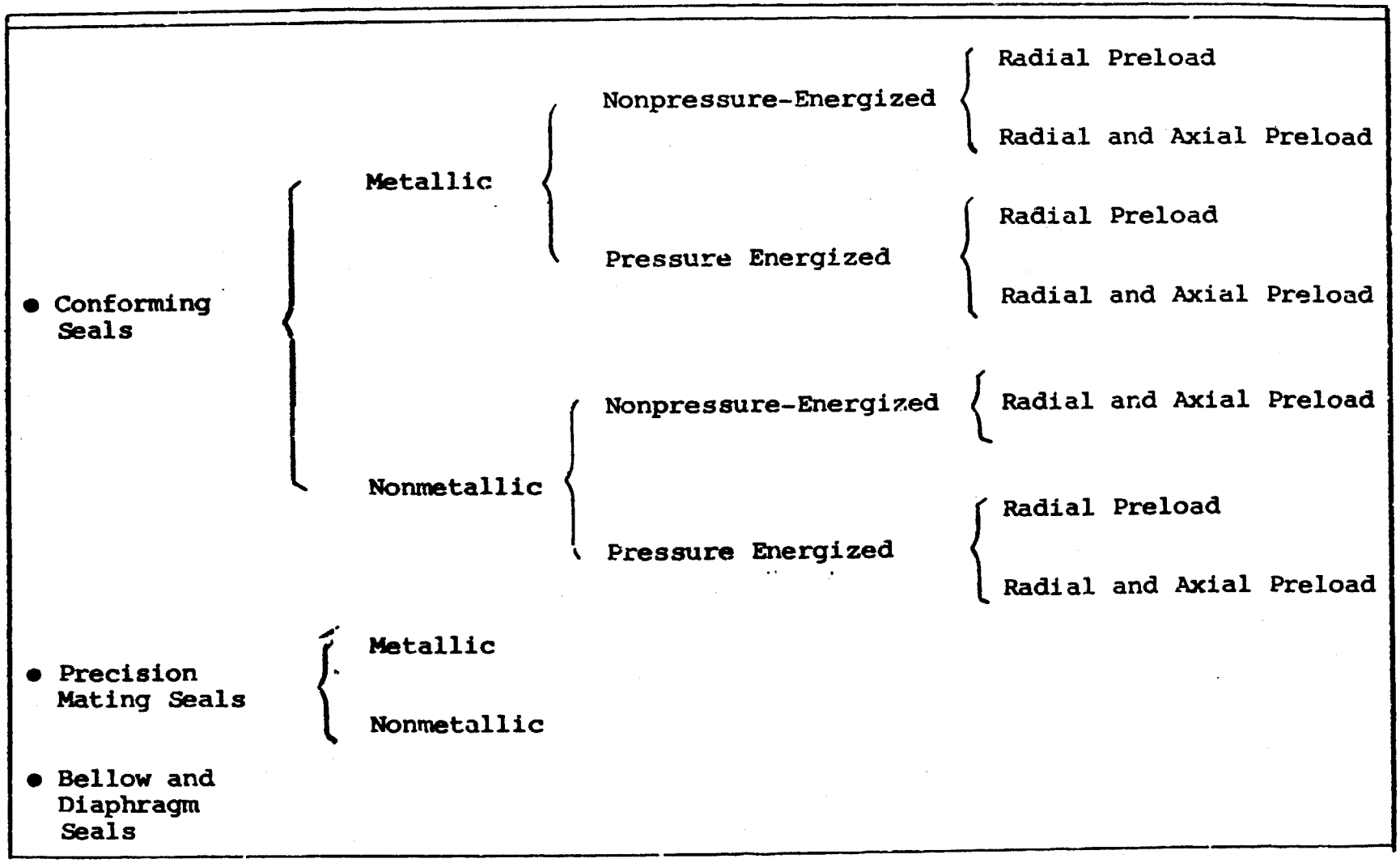

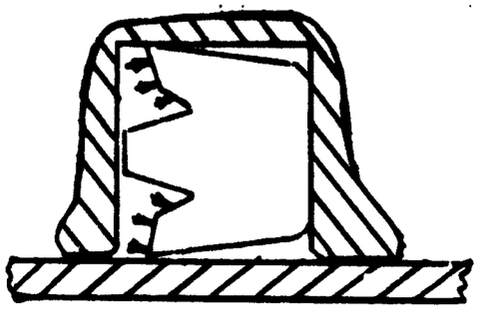

a. A nonmetallic ring having considerable resiliency produces radial interference with the shaft.

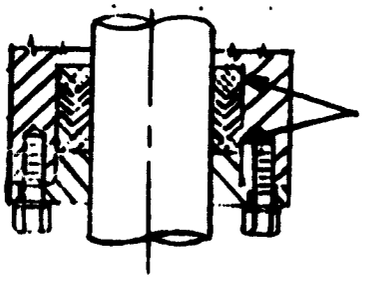

b. Nonmetallic seal rings having initial radial interference are additionally urged into contact with the shaft by an external retainer.

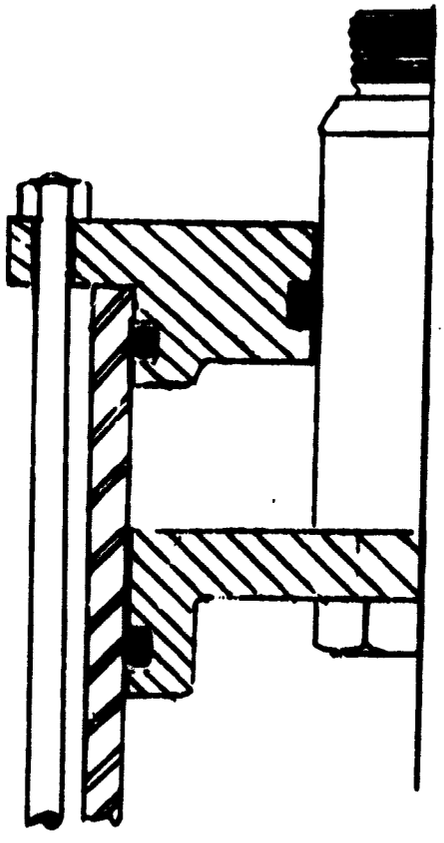

c. The O-ring is subjected to radial interference. If the seal groove is sufficiently narrow, additional axial loads are imposed on the seal.

Figure 6 Sliding Seals

(2) Rotating Seals

The classification of interfacial rotating seals is based on the construction features of the seals. Two subclassifications are axial and radial seals, depending upon the orientation of the interface subjected to relative motion. Axial seals are commonly called face or mechanical seals. Figure 7(a) shows a typical face seal. Radial seals were further classified as lip, packing, and circumferential split ring seals. Lip seals, as typically shown on Figure 7(b), are commonly made from plastic or rubber materials. A typical identification of these seals is the relatively flexible leg which is urged radially against a rotating shaft.

Another class of sliding seals identified as precision mating seals may be used as rotating seals. Quite often, however, these seals, when used in rotary applications, are called circumferential split ring seals. Figure 7(c) shows a typical seal in this classification. The last type of interfacial seal is the stuffing box or packing seal shown on Figure 7(d). The details of packings were not considered in this study. Packings can be described as deformable materials, such as asbestos, metal foils, or cork, which are compressed in a groove surrounding the shaft. An external loading mechanism is necessary to maintain the material in contact with the shaft. In summary, the major classes of seals are shown in Table III.

Table III

Classes of Rotating Shaft Seals

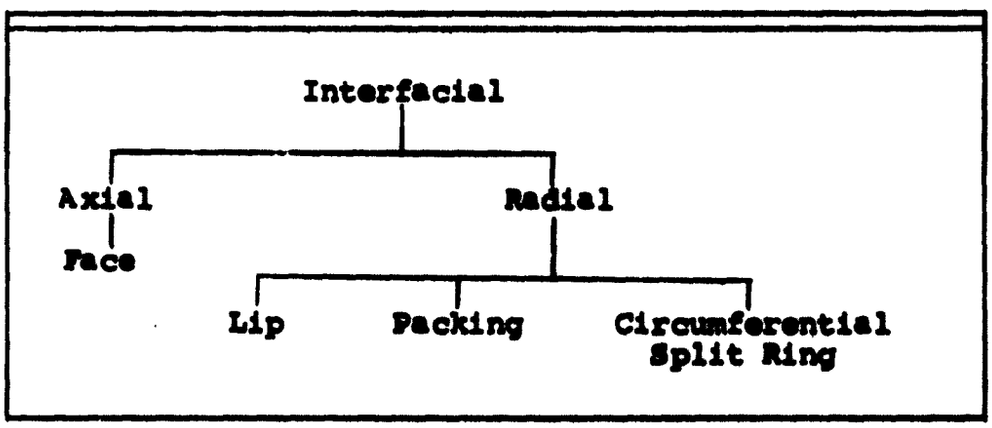

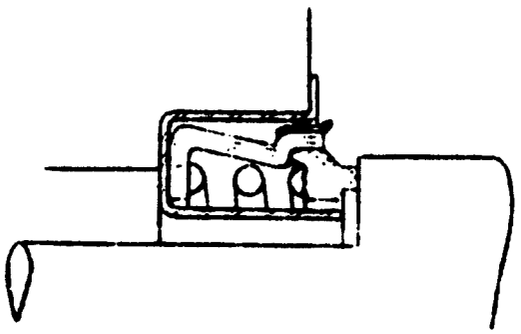

a) Face-Type Seal

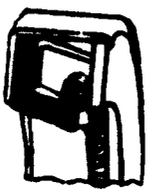

b) Lip-Type Seal

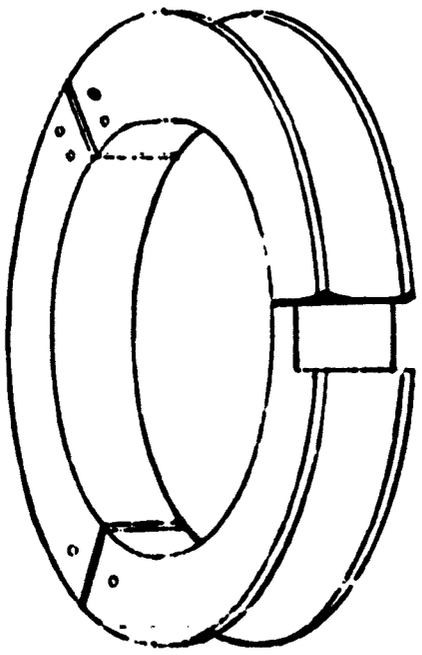

c) Circumferential Split-Ring Seal

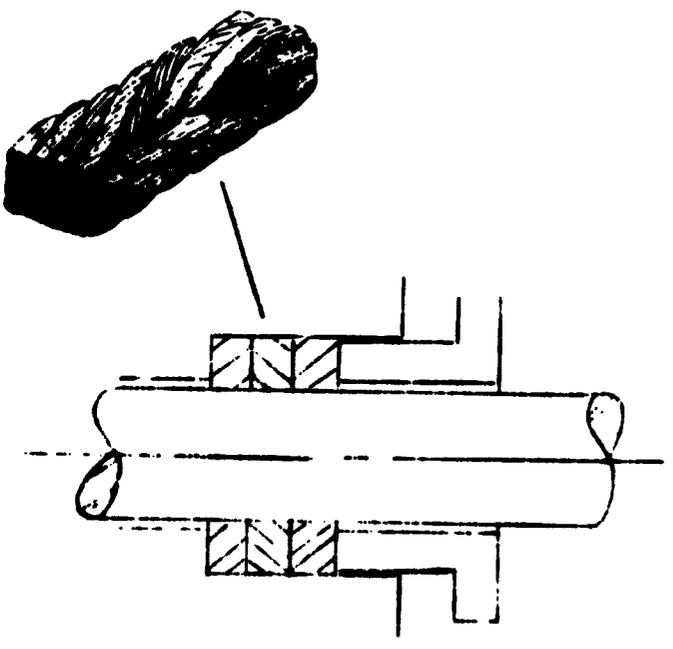

d) Packing or Stuffing Box Seal

Figure 7 Rotating Seals

c. Interstitial Seals

Interstitial seals are devices that retard the flow of leakage by controlling the clearance through which the fluid flows or by imposing external forces on the fluid. Bushings, labyrinths, and visco-seals are described in the following section to exemplify the principle. The applicability of these types of seals to spacecraft sealing, because of the leakage values encountered, is rather limited.

Before proceeding with the description of specific seal types, consideration should be given to their over-all mode of operation. The function of interstitial seals is to create a pressure drop of the sealed fluid with the least possible flow, and simultaneously permit unrestricted relative motion between moving parts. Interstitial seals are able to maintain a pressure differential between the interior of a machine and its surrounding environment by throttling the escaping fluid. Unlike interfacial seals, no contact of moving parts is intended. An advantage is that friction is minimized. However, to throttle fluid, it is necessary to have some flow. Therefore, it is impossible to completely eliminate leakage. It can only be minimized.

Since rubbing between moving members is kept to a minimum, all the problems inherent with friction and wear are eliminated. Excellent durability and reliability are characteristic of these seals.

When fluid throttling is accomplished by the sudden irreversible acceleration and deceleration of the fluid, the seal is referred to as a labyrinth-type seal. This seal configuration is frequently used in applications such as steam and gas turbines and centrifugal compressors. They are reliable and efficient at medium and low pressures. The labyrinth is seldom used with liquids.

If throttling of the fluid is accomplished by viscous friction losses through a small but essentially constant cross-sectional area gap, the seal is called a bushing-type seal. If the bushing is free to follow the shaft in its radial motion, it is called a floating bushing. Often, the bushing is constructed of several segments. These seals are commonly referred to as floating ring seals.

The viscous seal is a device which pumps a viscous fluid against a sealed fluid by the sole effect of the viscosity and motion between two surfaces in close proximity. The fluid pumped is a liquid while the sealed fluid can be liquid or gas.

(1) Bushing Seals

The bushing seal, as the name implies, consists essentially of a close fitting stationary sleeve surrounding the rotating shaft. Fluid seeps through the small annular gap existing between the shaft and the sleeve. Leakage is minimized by the throttling effect of the small passage that forces the fluid to flow at a high velocity with the consequent high pressure drop created by fluid viscous friction. Because the sealing mechanism is based on energy dissipation by viscous friction, this type of seal is suitable for sealing liquids, but is seldom used with gases unless a relatively large leakage rate is tolerable. Basically, there are two types of bushing seals: fixed and floating. These types are depicted on Figures 8 and 9 respectively.

(2) Labyrinth Seals

Controlled clearance seals are used in applications where rubbing is not desired and where some leakage is tolerable. Clearance seals are used to control the leakage of both liquids and gases. Seals for liquids usually rely on throttling the fluid through a narrow and relatively long annular gap with a minimum of leakage. Seals for compressible fluids, usually called labyrinths because of their peculiar shapes, rely on successive accelerations and decelerations of the fluid by alternatively flowing through narrow and wide gaps to dissipate the pressure energy and reduce the leakage flow. The dissipation of pressure energy is caused by the purposely "inefficient" accelaration and deceleration of the fluid stream with the consequent high pressure losses. Labyrinth seals are preferred in high-speed rotating machinery such as compressors and turbines because of their inherent simplicity and reliability. This is easy to understand when the poor lubricating properties of superheated vapors and gases are considered. A well designed labyrinth requires practically no maintenance and, barring an anomalous situation where rubbing and, therefore, wear can take place, should have an indefinite life. Even if part of the labyrinth is worn away, nothing worse than an increase in leakage will take place. The higher leakage allowed by labyrinths, compared with contact seals, must be weighed against these advantages.

Although there are countless versions or designs of labyrinth seals, all work on the same principles and differ only in details and refinements. The simplest type of labyrinth consists of a series of adequately spaced blades with the edges a short distance away from the mating surface. The blades can be either stationary on the housing or rotating with the shaft. This type of seal (illustrated in Figure 10) is called straight or straight-through labyrinth.

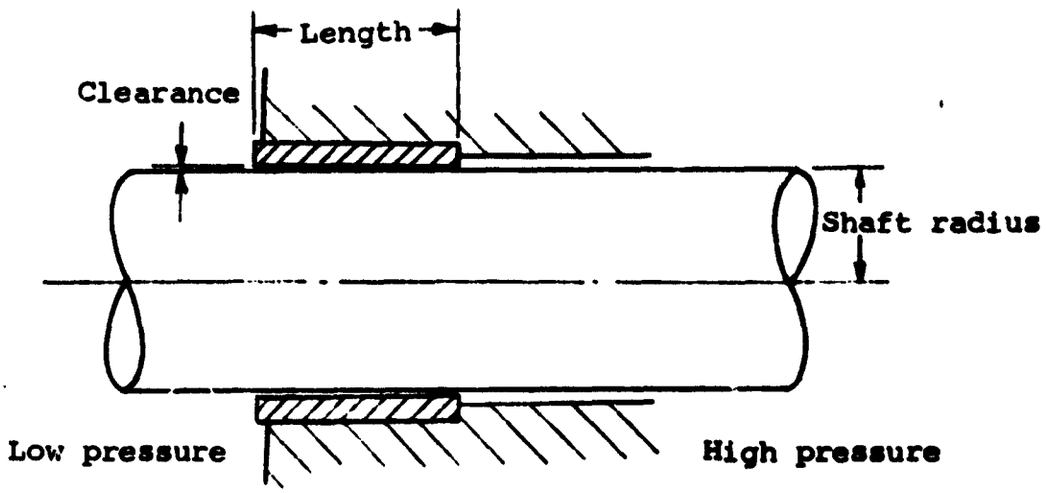

Figure 8 Fixed Bushing Seal

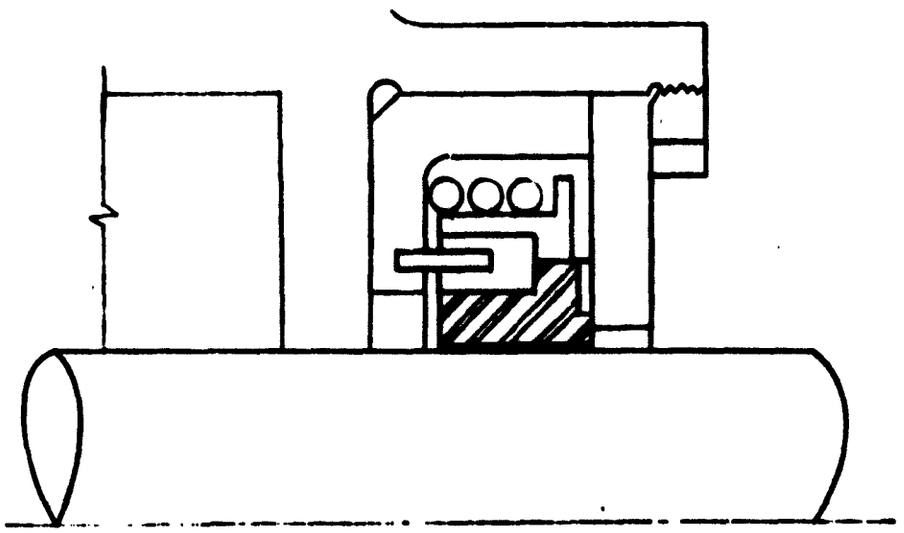

Figure 9 Floating Bushing Seal

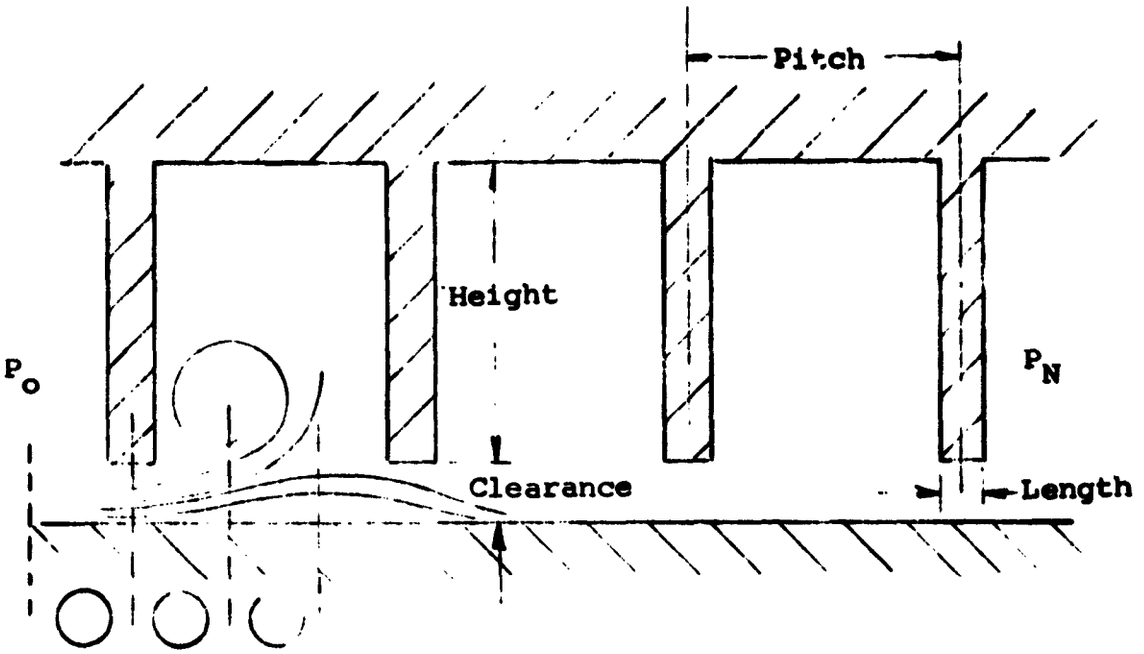

Figure 10 Straight Labyrinth

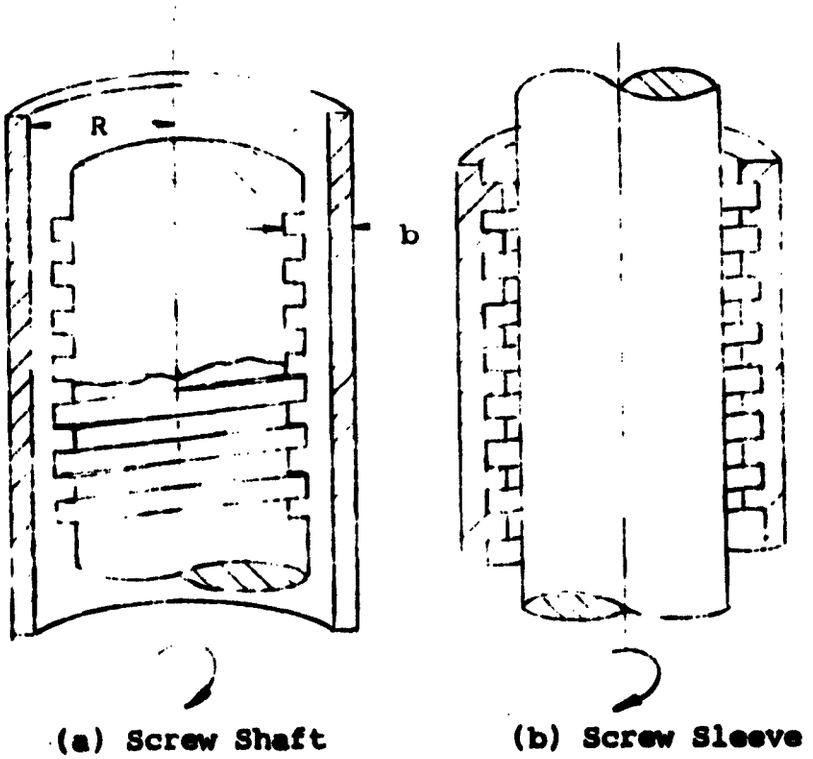

(a) Screw Shaft (b) Screw Sleeve

Figure 11 Two Types of Visco Pumps

(3) Viscous Seals

The screw, viscosity, or spiral-groove seal is device capable of moving a viscous fluid against a pressure ad in close proximity (Figure 11).

As a fluid pump, the visco pump has limited use nce the flow rate is rather small and the efficiency very or. By using two such pumps, one against the other on the me shaft, however, it is possible to create a pressure gra- ent with practically no fluid flow that could be used to event leakage of a second fluid through the clearance around e shaft (Figure 12). This type of seal is particularly use- l for containment of gases, in which case a secondary fluid used to generate the pressure. When used in this applica- on, the device is known as a visco seal, although other names, ch as threaded seal and spiral groove seal, are found in the terature.

Among the main characteristics of this seal is e fact that it becomes ineffective at low or zero shaft speed. nce it is basically a dynamic seal, other methods of sealing r stationary conditions must be provided. This is one of its ggest shortcomings. On the other hand its main advantage es in the fact that there is no contact between the shaft and e stationary sleeve and, therefore, no wear. Thus, long seal fe can be expected. This feature, combined with the inherent w leakage past the seal (theoretically only that due to dif- sion through the secondary fluid) makes this seal very attrac- ve for critical applications where complexity can be tolerated.

d. Hermetic Seals

(1) Basic Considerations

A hermetic seal may be defined as a device which rmits the transmission of power without the use of interfa- al or interstitial sealing.

The method of joining the "feedthrough" to the rent structure is normally a technique of such proven relia- lity that any leakage is due to diffusion. Welding, brazing, d other bonding methods are conventionally used to effect rmetic seals and thus leakage rates are reduced to a minimum tainable value.

Hermetic seals, although attractive from the akage standpoint, have other characteristics which have mited their applicability to all sealing problems. Torque d speed limitations, demountability, ease of repair, lack of sitive drive, and fragility are some of the most pertinent awbacks. Brief discussions of the hermetic seals listed in ble IV are given below. Since all of these devices are

either commercially available or must be specially designed for a particular application, no attempt was made to develop design criteria. Rather, it is only intended to inform the reader of their general characteristics so that their potential applicability may be judged and, if appropriate, further information can be obtained from tbe referenced sources.

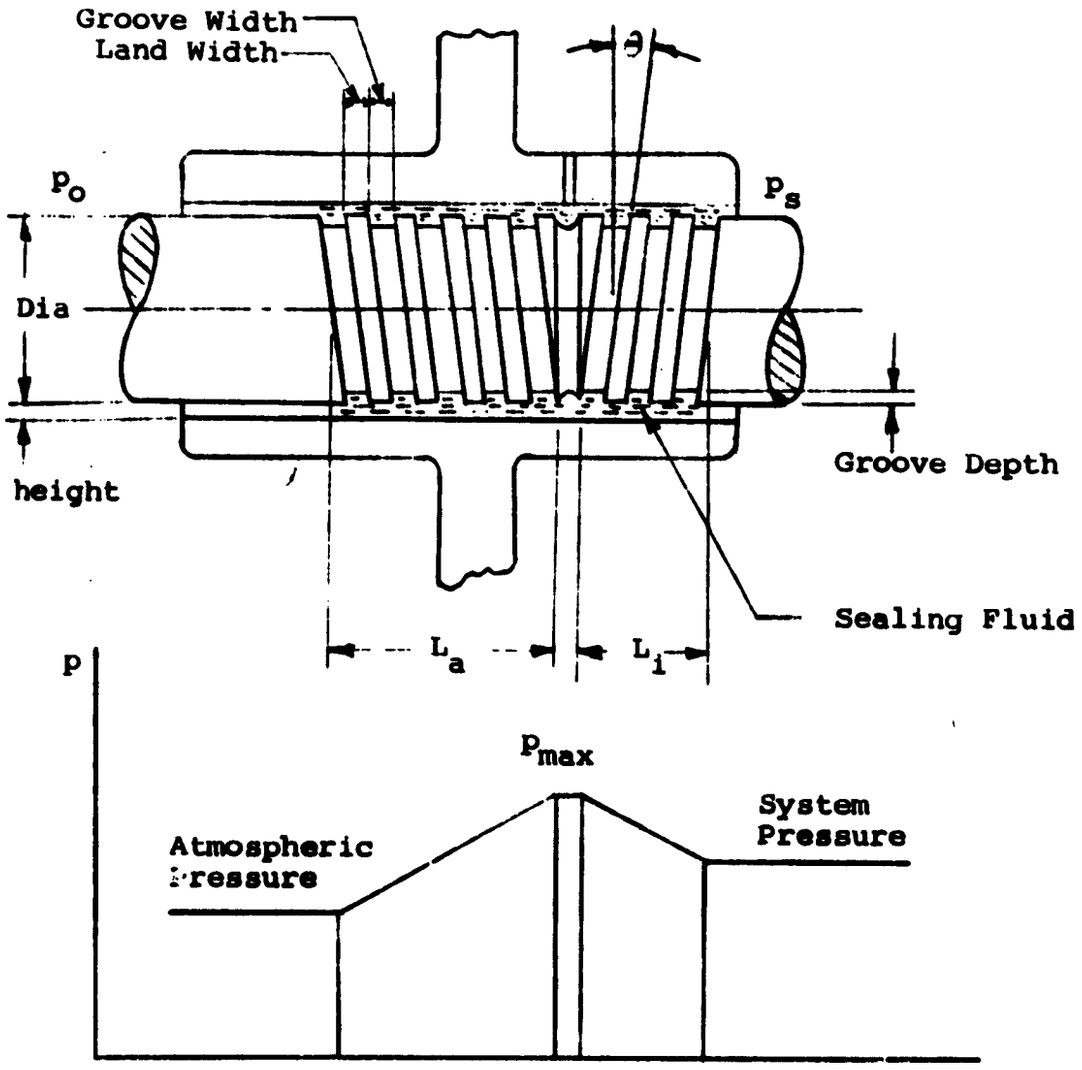

Pressure Distribution within the Seal

Figure 12 Visco Seal Formed by Two Shaft-Screw Visco Pumps Working Against Each Other

Table IV

Hermetic Seals

Dynamic	Static
Permanent magnetic coupling	Ceramic or glass
Electromagnetic coupling	Potted Seals
Electrostatic coupling	
Harmonic drive*	
Wobble plate	
Bellows	
Flexure devices	

*Manufactured by United Shoe Machinery Corporation, Beverly, Massachusetts

(2) State of Development and General Characteristics of Hermetic Seals

(a) Dynamic Hermetic Seals

Permanent Magnet Coupling

A hermetic permanent magnet coupling (Figure 13) can be designed for either axial or rotational motion with either axially or radially aligned magnets. The magnets are, in either case, separated by a thin, nonmagnetic material which is, preferably, also nonconductive. Typical magnetic drives are available commercially (Ref. 2) which can transmit 8 kg-cm of torque at rotational speeds of up to 750 rpm. Magnetic drives have an inherent advantage of being able to withstand fairly high temperatures (720°C). An inherent disadvantage is that when one pole slips past another, the hysteresis effect may permanently lower the magnetization of both poles.

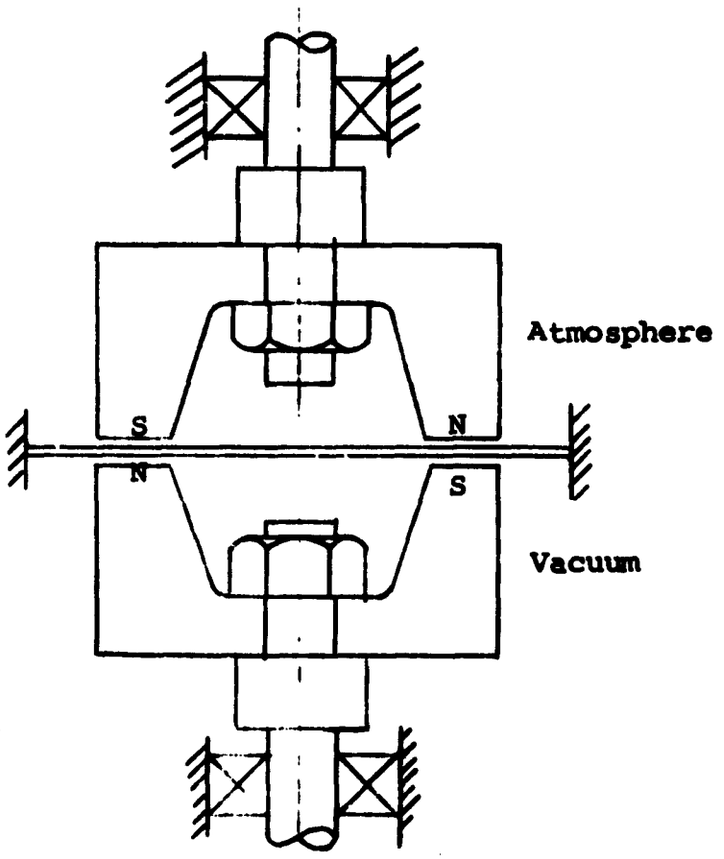

Figure 13 Axial Magnetic Coupling

If a conducting material, such as 304 Stainless Steel is used to separate the magnets and to form the hermetic seal, the development of eddy currents places an upper limit on the speed that can be used. Speeds of 3000 rpm and higher have been used in bearing tests. If, on the other hand, a nonconducting material, such as ceramic, is used for the hermetic seal, the joining of the ceramic to the space ship structure material may pose an exceedingly difficult problem.

Electromagnetic Coupling

Electromagnetic drives (Figure 14) in the form of "canned" motors can be used in many applications. Normally, the rotor is in the vacuum environment and the stator outside. With nonsynchronous drives, heat is developed in the rotor which is proportional to the produce of slip times stator rotational power. With synchronous drives no heat is developed in the rotor. This is the more desirable condition because in vacuum the only means of dissipating heat is by radiation. Unfortunately, at the temperatures where heat transfer by radiation is effective, special high-temperature insulation may be required, and outgassing becomes a problem. The speed and power limits are the normal induction motor limitations. The efficiency is less due to the larger air gap which is needed to accomodate the can thickness. An analysis of magnetic and electromagnetic drive capabilities has been performed and is presented in Reference 3.

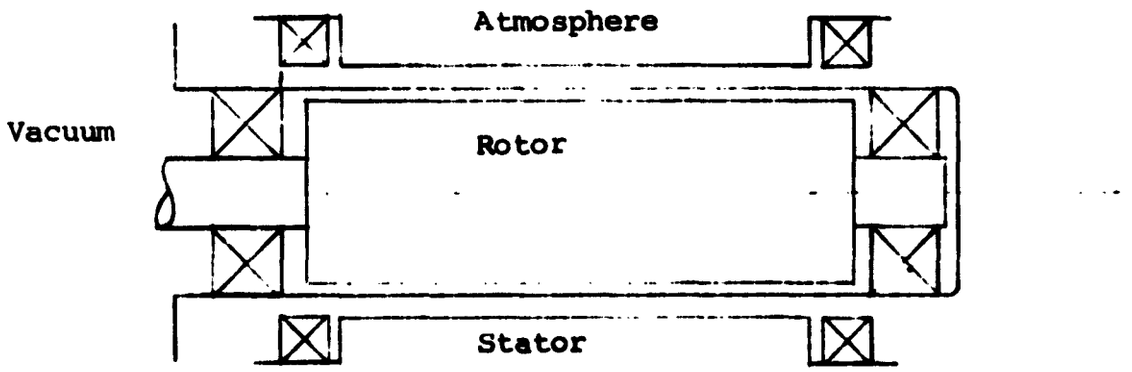

Figure 14 Electromagnetic Coupling

Electrostatic Coupling

It is possible to couple through a vacuum interface using electric fields instead of electromagnetic fields for rotational applications. This method is shown on Figure 15. The torque which can be transmitted is limited primarily by the electric field which can be supported in the vacuum. For a small coupling, perhaps 3 inches in diameter, fields approaching 80 kv/mm should be possible without breakdown in the vacuum (Ref. 6). It appears that for an applied voltage of about 100 kv and a field strength of 80 kv/mm, a 3-inch coupling would transmit 2000 gm-cm of torque at 25,000 rpm, 0.5 kw of power. Reference 7 discusses the capabilities of this technique in greater detail.

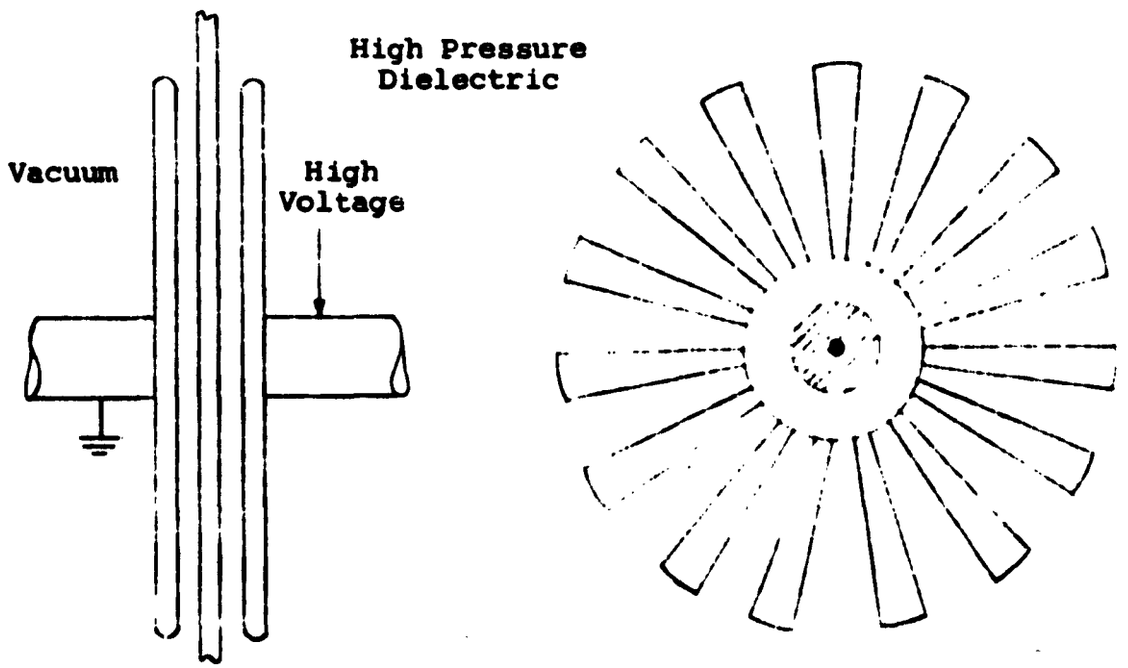

Figure 15 Axial Field Electrostatic Coupling

Harmonic Drive

The harmonic drive (Ref. 5) shown on Figure 6 (developed by United Shoe Machinery Corporation) has been dapted for transmission of linear or rotational motion across vacuum-pressure interface. This is a unique system where the ontrolled deflection of one or more parts for the transmission f motion through a sealed wall is utilized. The effective se of the harmonic drive in vacuum requires the use of lubriation in vacuum with its inherent problems.

Wobble Plate and Bellows Coupling

The wobble plate, or Thiel coupling, opertes by flexing a diaphragm. Figure 17, which depicts this oupling, also shows that both the shaft on the vacuum side nd the shaft on the pressure side of the interface require two adially loaded bearings and a thrust bearing. If the offset r cam angle is small, the deflection of the diaphragm is small, ut the thrust bearing load is large. Large membrane deflecions would severely limit the fatigue life; thus, heavy thrust earing loads would impose a severe vacuum bearing lubrication roblem. A bellows seal (shown on Figure 18) has essentially he same disadvantages as the wobble plate seal. Satisfactory pplications with rotational speeds of up to 50 rpm have been xperienced, however.

(b) Static Seals

Ceramic and Glass Hermetic Seals

Ceramic and glass hermetic seals are quite imilar in all respects except the temperature range and thermal hock to which they can be subjected. Either seal is made by hemically bonding the ceramic or glass material to an appropriate metal. In some cases, the seal is made in stages. Metal A s bonded to the ceramic or glass, and Metal B is joined to etal A by welding, brazing, or soldering. The choice of bonding technique would be indicated by the temperature limits to hich the seal is exposed.

Ceramic and glass hermetic seals are commerially available on an off-the-shelf basis from a wide range of uppliers. A well-made ceramic seal is expected to be leakight to less than 10^{-9} std cc/sec of helium. Actually, the eal is much better than that, but the standard leak test is ade with a helium sensitive mass spectrometer whose sensitivity imit is approximately 10^{-9} std cc/sec.

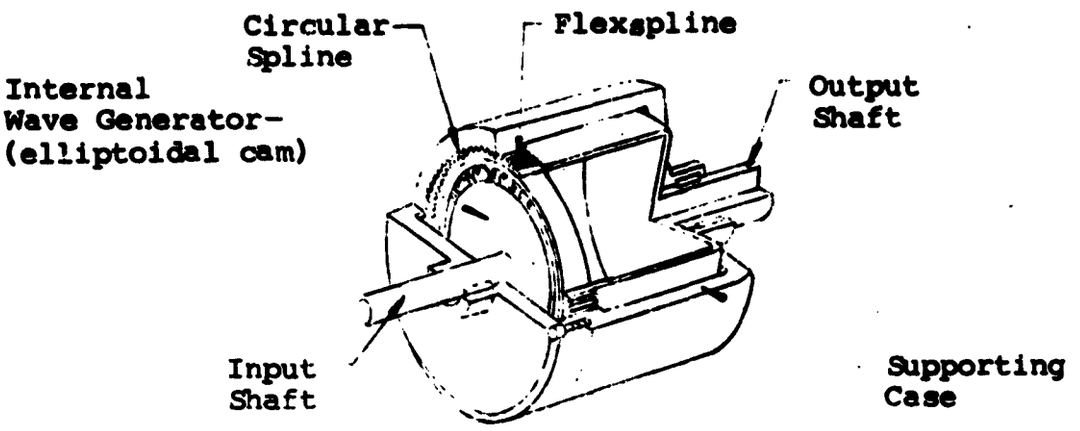

Figure 16 Harmonic Drive

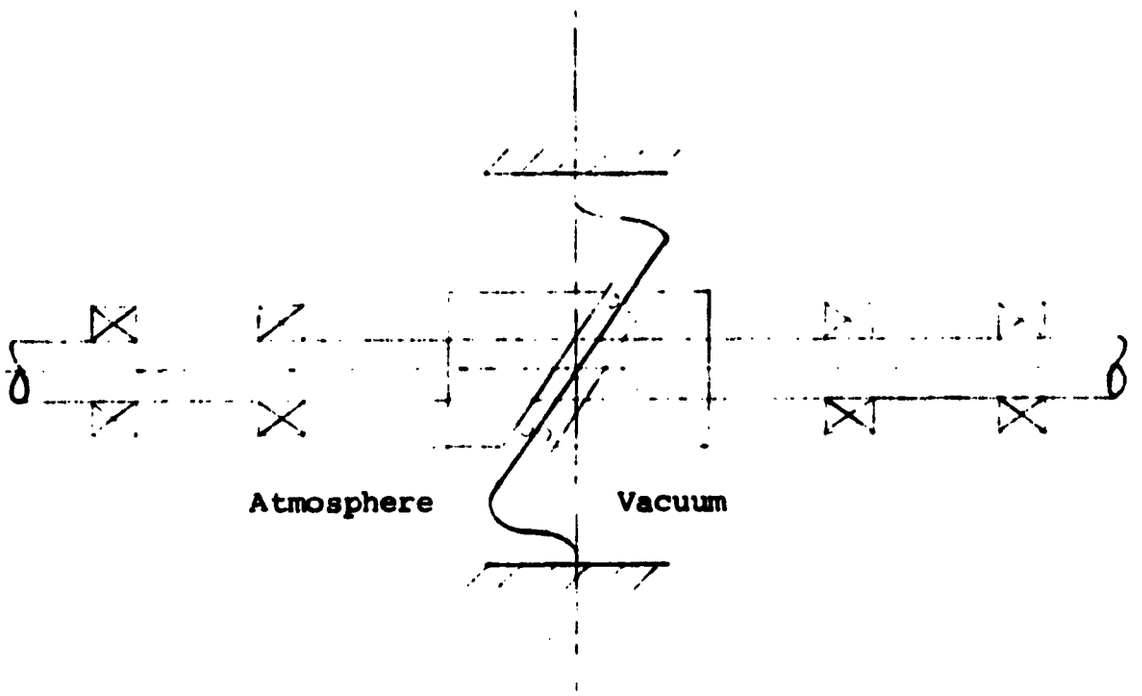

Figure 17 Wobble Plate (Thiel Coupling) Drive

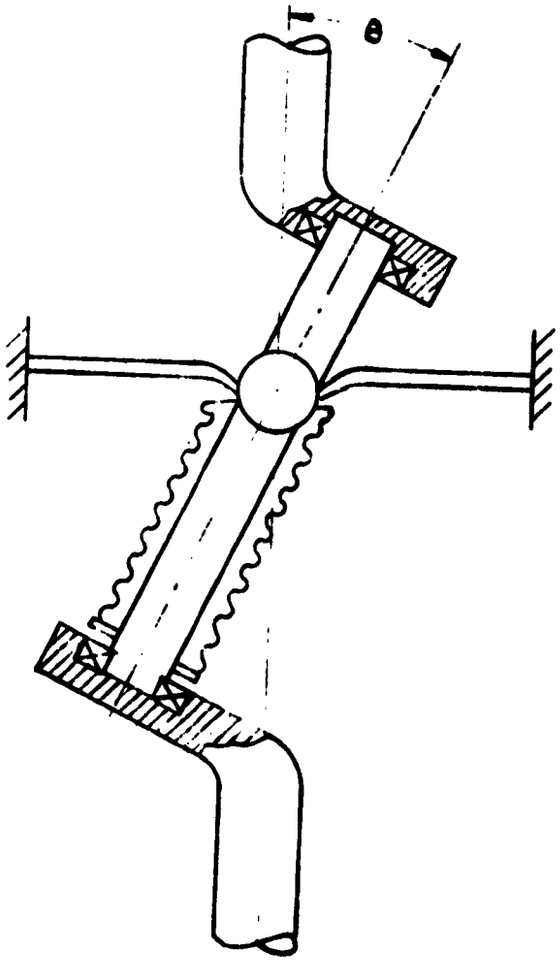

Figure 18 Bellows Seal

The choice of the seal is dictated by the service required. Multi-pin feedthroughs are available for instrumentation leads with 5 amperes as the rated maximum current per lead. Very high current feedthroughs are available, but they require the conductor to be cooled as it passes through the seal. Hermetically sealed ceramic to sapphire windows are available which can be used to observe operation of equipment at cryogenic temperatures. Ceramic hermetic seals are further used to pass fluids from cryogenic temperatures up to higher temperatures. The temperature limitations for hermetic ceramic seals are from -200°C to +500°C. For a glass seal, the temperature limits are more restrictive, i.e., from -65°C to +250°C.

(c) Potted Seals

Potted seals (see Figure 19) are used quite extensively for instrumentation feedthroughs in vacuum laboratories when a system bake-out is not required. Usually the potting takes place after a feedthrough leak has been located. However, in a pinch, a completely potted seal can be and has been used. For a space application, it would be more likely that potting would be used as a repair technique.

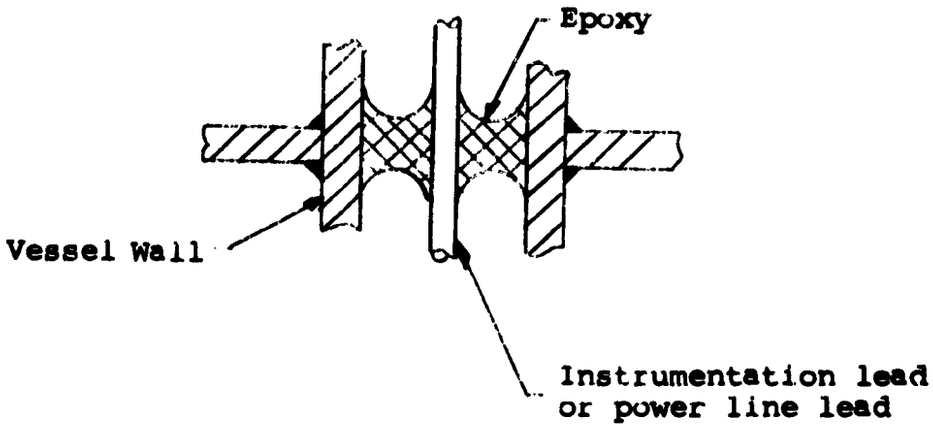

Figure 19 Potted Seal

e. Adhesives and Sealants

(1) Adhesives

The materials usually encountered in spacecraft systems are mostly metals together with some elastomers and plastic materials. Therefore, the adhesives used in spacecraft systems would be those that can successfully bond metals, plastics, and elastomers to each other or to themselves.

Adhesives capable of bonding these materials with a reasonable strength include:

- epoxides
- phenolics
- isocyanates (urethanes)
- neoprene rubber base
- polysulfide elastomer base
- silicone elastomer base
- nitrile rubber base
- butyl rubber base
- ceramics
- hot melts (phenoxy, phenol-formaldehyde, polyvinyl acetate, polyethylene, etc.

Of these adhesives, only the epoxides, phenolics, socyanates, cyanoacrylates, and ceramics polymerize or set after ire into hard and rigid solids, more or less infusiable and nsoluble. The hold melts, as the name indicates, soften up at gher temperatures and are limited in application to a certain mperature range. Some of the elastomers, such as silicone se, have surprisingly high thermal resistance but, in general, astomers tend to soften or deteriorate rather quickly with mperature.

Because no one adhesive has the required properes to bond all materials of interest or to give the best perrmance for all possible conditions, more than one adhesive is ten combined to obtain a system combining the properties or aracteristics of the individual constituents. For instance, e rigid, highly cross-linked and temperature resisting struc- re of phenolics is combined with the more elastic structure of astomers to yield a phenolic-elastomer capable of higher de- rmation, good resistance to shock loads, and a relatively high ermal resistance. This is an improvement over both individual nponents, i.e., the rigid and somewhat brittle phenolic, or the e elastomer with its low temperature resistance.

The properties of adhesives can be modified in y ways, as by the addition of 1) dilutents to decrease vis- ity, 2) fillers to increase viscosity and decrease shrinkage, plasticizers and flexibilizers to increase elasticity of the d, or 4) resinous modifiers to alter the basic chemical

character of the adhesive base. The proper combination of these different constituents to obtain the best adhesive system for a given application is usually referred to as formulation.

The best adhesive for a particular application cannot be determined solely from the standpoint of physical properties of the adhesive. Many other characteristics, of which cure is probably the most important, must be taken into consideration. With the exception of hot melts and ceramics, all adhesives set by polymerization; and this reaction must be induced by heat or the presence of the proper catalyst. The time required for the reaction to be completed, and the application of heat when needed, constitutes the cure.

It can be seen that if a relatively large structure is to be bonded, and the strongest bond can be obtained with an adhesive that required high temperature cure, it may be very difficult or impractical to heat the whole structure to the required temperature. In that case, a room-temperature curing adhesive may be indicated.

(2) Sealants

Sealants are used to make structural joints leaktight, and/or electrically insulated. Because they must adhere to the surfaces they seal, they have common characteristics with adhesives. Actually, the same chemical species are used many times in both applications; the only difference being the function (i.e., if the main purpose is to support a load, it would be termed an adhesive; if to fill a void or close an interstice,it would be called a sealant).

Since the load supporting requirements in a sealant are usually small or totally lacking, strength is a property that can be sacrificed to obtain other, more desirable characteristics. This actually increases the freedom in selecting and using adhesive materials for sealing applications.

Sealants that may have possible applications in the aerospace field parallel the list of adhesives previously considered. The most important ones are:

- epoxides
- phenolics
- silicones
- polysulfides
- isocyanates
- nitriles
- neoprene
- ceramics

Since, in general, sealants will be in contact :h fluids, one of the most important considerations in .ecting the proper material for a given application is chemi- . compatibility. Useable temperature range is probably next importance; and practical considerations such as cure, han- .ng and surface preparation, physical strength, aging, toxicity, meability, and, in some cases, color and odor must also be :en into consideration.

It is difficult to generalize about the chemical istance of sealants. Since there are many polymer systems l compounding ingredients available for making a wide variety sealants, there is a sealant and a method of sealing to sat- y almost every need. Chemical resistance depends not only the nature of the material, but also on surface erosion :e and permeation, and on temperature. Furthermore, chemical :ects can be of two types: irreversible chemical attack and :lling in water or solvent.

In general, epoxides, phenolics, polyethylenes, l dense glazed ceramics are considered chemically resistant. ng the rubbers, neoprene and butyl are resistant by virtue their low permeability, and silicone because of its hydro- bic nature.

In order of decreasing heat resistance, sealants be listed as:

- ceramics
- silicones
- phenolics
- epoxy
- organic rubber

amics are the only system for severe temperatures above 0°F. Silicones can probably go up to 600°F, while phenolic- rile-epoxy combinations have been reported useable up to -600°F for short times. Epoxides are usually limited to -500°F.

Low temperatures can also introduce severe blems since polymeric materials in general tend to stiffen embrittle with low temperatures. Silicones and polyurethanes form rather well at low temperatures.

Table V lists some typical properties and pro- sing conditions for elastomeric sealants. Typical present ospace applications of sealants are sealing of propellant: ks, coatings, door and hatch seals, and other cabin and khead seals. Methods of application vary from hand spraying, shing, troweling, etc., to pressure gun application and simply ll and drain."

Properties and Processing Characteristics of Elastomeric Sealants

Mechanical Properties

Material	Adhesion lb-in.	Shrinkage percent	Elongation percent (ASTM D 412)	T.S. psi	Shear Strength psi	Abrasion Resistance
Butyl	---	0.0-3.0	600-800	2500-3000	150-200	Good
Chlorosulfonated polyethylene	15-100	10.0-20.0	75-125	500-600	40-100	Excellent
Fluoroelastomer	---	3.0	150-325	1200	125-175	Good-Excellent
Neoprene	50-75	---	200-350	1000-1500	---	Excellent
Polysulfide	7-50	1.0-3.0	150-500	50-125	125-175	Fair-Good
Silicone	20-40	0.2-0.6	50-150	400-750	250-350	Fair-Good
Urethane	18-30	0.1	250-600	100-3000	125-350	Excellent

Environmental and Electrical Properties

Material	Temperature Range F	Aging Properties	Weatherability	Chemical Resistance				Dielectric Strength v/mm	Voltage Resistance ohm-cm
				Alkalis	Acids	Solvents	Water		
Butyl	-80 to 300	Good	Good	Good	Good	Poor	Good	250-600	10^{16}
Chlorosulfonated polyethylene	-45 to 300	Excellent	Excellent	Excellent	Good-Excellent	Fair	Good-Excellent	300-600	10^{11}
Fluoroelastomer	-65 to 450	Excellent	Excellent	Poor	Excellent	Good	Excellent	300-450	10^{11}
Neoprene	-45 to 300	Good-Excellent	Good	Fair-Good	Good	Fair	Good-Excellent	300-600	10^{11}
Polysulfide	-60 to 275	Good	Good	Fair	Fair	Good	Good	250-350	10^{11}-10^{12}
Silicone	-60 to 700	Good-Excellent	Excellent	Poor-Fair	Fair-Good	Poor	Good-Excellent	400-600	10^{14}-10^{15}
Urethane	-60 to 300	Good	Good	Fair	Poor	Fair-Good	Good	---	---

Processing Characteristics

	Available Forms	Method of Application	Curing Conditions
Butyl	One component solvent types, tapes, contact bonding	Calking gun, spread coating, trowel, putty knife	Room temperature, long time for complete cure
Chlorosulfonated polyethylene	One and two component systems with solvent	Calking gun, brush, spatula, spread coating	Room temperature, 1-14 days
Fluoroelastomer	One and two component	Calking gun, spatula, brush, spread coating	Room temperature, 24 hours
Neoprene	One and two component	Brush, calking gun, spread coating	Room temperature, 7-14 days, cures by solvent evaporation
Polysulfide	One and two component cans and prepacked cartridges	Calking gun, brush, trowel, putty knife, spread coating	Room and elevated temperature
Silicone	One or two component liquids in tubes, prepacked cartridge cans	Calking gun and tubes, spatula, putty knife	Cures at room or elevated temperature by chemical reaction
Urethane	Two component liquids cured by chemical reaction	Calking gun, brush, trowel, putty knife	Room or elevated temperature

Most of these applications are of a more or less manent nature; i.e., the parts being sealed are seldom, if :, taken apart. Modern sealants are rarely used in appli- ions where the seal is taken apart frequently or occasion- . This is probably due to the rather high physical strength ost modern sealants which would make disassembly difficult.

Most gasket and pipe compounds consist simply ighly filled unsaturated oils which are quite different, ically speaking, from the sealants considered here.

CLASSIFICATION OF SEALS BY APPLICATION

a. Structural Joint Sealing

The sealing of the initial structure to eliminate problem of possible loss of gases or water vapor from a e vehicle presents a serious design problem. The more lex the vehicle design, the greater number of possible age sources exist. The sealing methods which may be oyed for structural sealing are listed and described in following paragraphs.

(1) Faying Surface Sealing

This method involves the application of the ing media such as flexible tape, adhesives, and flexible ants in between the faying surface areas as shown in Figure).

(2) Fillet Sealing

Fillet sealing consists of the application of ling compound such as polysulfide, silicone, or polyure- over the joints and seams inside the pressure vehicle assembly of the joint has been completed. This method own on Figure 20(b).

(3) Brush Sealing

Brush sealing consists of the application of shable sealant such as silicone over welds, fasteners, illets along joints after completed assembly of the joints. e 20(c) depicts brush sealing utilized in conjunction a film barrier.

(4) Film Barrier Sealing

This sealing method is used in conjunction with methods, as shown on Figure 20(c). Materials which de excellent gas retention properties and are commercially able as films are Aclar, Mylar, Saran, and Tedlar.

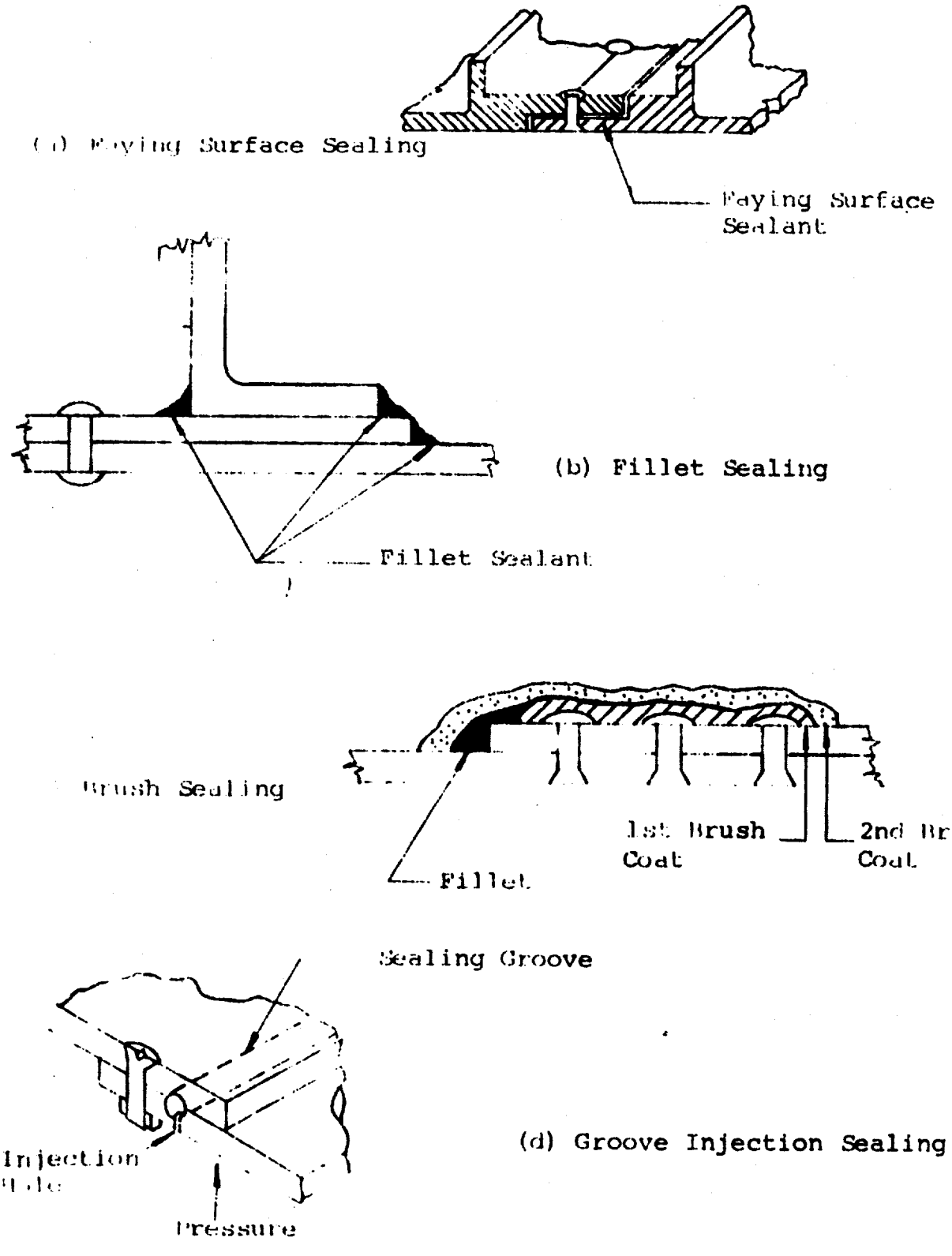

Figure 20 Structural Joint Sealing Methods

(5) Groove Injection Sealing

This sealing method involves the use of a high-pressure gun which injects elastomeric-type putty sealant into grooves located in the interior skin layer at the joints of an assembly. The joints must be designed with grooves running down each joint into which the sealant can flow, as shown in Figure 20(d).

(6) Mechanical Sealing

(a) Gaskets (Fig. 89-97)

These seals may be of a metallic or non-metallic material and are nonpressure-energized seals. They must have an externally applied contact load to attain proper contact stress for sealing. Dimensional changes due to environmental conditions greatly affect the seal choice. Variations due to environmental conditions are discussed in Section VI.

(b) Elastomeric Seals

Molded in Place (Fig. 8.)

In this seal design, the elastomeric material is vulcanized to the metallic structure. Sealing is accomplished when the elastomer is compressed on installation.

b. Feedthroughs

Communication, plumbing, and power systems will have cables, lines, and nonmoving or moving shafts which extend through the pressure wall. These items will require the use of static or dynamic seals of composite materials, metallic materials, or elastomeric materials.

(1) Electrical Feedthroughs (Fig. 89)

(a) Potting-Encapsulation

Electrical feedthrough cables exhibit leakage not only around the periphery of the cable but also through individual strands and between the wire and insulation. Thus, this sealing method must close both leakage paths. Typical materials which may be utilized are polysulfides, polyurethanes, and silicone compounds.

(b) Mechanical Seals (Fig. 90 and 91)

Mechanical seals do not appear adequate in electrical feedthroughs due to the leakage between the individual wire strands and the insulation. However, if the leakage level is tolerable, the following seals are useable: bellows pressure seal and packing gland-type seal.

(2) Mechanical Feedthroughs

Shafts and linkages necessary for transmitting motion through the pressure hull requires seals of dynamic and static nature. However, static sealing of such items as pivot shafts, stand-offs, etc., may be accomplished by structural methods such as welding, hand soldering, etc. Furthermore, sealing methods utilized on hydraulic and pneumatic feedthroughs are applicable. Therefore, only dynamic seals will be condidered.

(a) Sliding-Type Seals (Fig. 92-95)

Wide variations in construction features are exhibited by sliding seals. The variations in contruction are directly related to the principles of operation. To classify sliding seals, it is necessary to differentiate seals on the basis of configuration and principle of operation. The basic categories of sliding seals are 1) conforming (non-metallic and metallic), 2) precision mating, and 3) interference. Each basic group of seals is presented separately.

(b) Rotary-Type Seals (Fig. 96 and 97)

The classification of rotating shaft seals is based upon contruction features following the procedures used in classifying sliding seals. The materials of construction, performance, and environmental limitations are briefly presented.

Interfacial rotating shaft seals can be identified as radial or axial types, depending on the orientation. The basic categories of rotating shaft seals are 1) axial seals (mechanical face seals), and 2) radial seals (circumferential split ring seals and circumferential lip-type seals).

(3) Hydraulic and Pneumatic Feedthroughs (Fig. 98-100)

Hydraulic and pneumatic lines are necessary to transfer the fluid media through the pressure hull. Since these lines must be removable or repairable in many instances, they cannot be sealed structurally (welding, fillet sealing, hand soldering, etc.). Furthermore, the lines are more readily installed if they terminate at the pressure hull, and the feedthrough is accomplished with a fitting. The nonpressure-energized seal must have an externally applied contact load to attain proper contact stress for sealing.

c. Module Deployment Seals (Fig. 101)

Deployment of modules from launch position to orbital position requires seals designed to function for a limited period of time. This period of time is normally less than 72 hours. The seals must be designed to retain pressure until the interior surface of the module mating joints have been welded in the fixed orbital positions. Some deployment seals, however, are of a dynamic nature and are required to retain pressure for the life or duration of the orbital mission. The sealing methods employed on the various joints, with the specific joint being the category heading, are discussed in the following paragraphs.

(1) Spoke Hinge Joint Seals

These seals are required to seal between the tubular module sections after deployment of the mating modules. The area being sealed is the same as two flat surfaces being pressed together.

(2) Rotating Joint Seals

These seals will be required to seal off the mating joints formed by adjacent modules after deployment if the module spokes are rotated into orbital position. To prevent damage during launch and deployment, these seals must be recessed into the structure; and, therefore, they must be of an inflatable type to produce the necessary sealing contact stress.

(3) Large Rotating Joint Seals

Sealing for this type joint becomes a requirement when space station designs include a zero gravity module (motionless with respect to the large rotating space station). Passage of personnel between the two separate pressurized sections, while one is rotating with respect to the other, presents a difficult sealing problem.

(4) Telescoping Deployment Seals

This type of seal is required if the spokes of the space station are to be telescopically deployed into orbital position. The seal must perform after deployment which means it is of the static type. Pressure between the telescoped sections must be retained for the life of the station. Therefore, only seals compatible with the space environment are applicable. The joint could be seam welded after deployment to eliminate any leakage. However, these joints are not readily accessible. Seals should be selected so as to take advantage of the cold welding effect which will exist; thereby, leakage which may exist after deployment will disappear after approximately 48 hours.

d. Air Locks--Exit Hatches

To permit personnel and equipment transfer as well as emergency exits from the spacecraft or space station, it is necessary to provide them with air locks and exit hatches. The air locks allow personnel to enter or exit from the station environment without subjecting the environment to the ambient one. The doors or exit hatches of the inward opening type are more easily sealed than outward opening ones because of the simulated atmospheric conditions (pressure) in the cabin. The size of opening varies from 2½-to 17½-feet in diameter. It can be seen that with an internal cabin pressure of 7 psi, the latching mechanism to hold an outward opening hatch must be rather substantial. Inward opening hatches take advantage of the sealing action which the outward pressurization force provides. This permits the use of simplified noninflatable seals. Quick opening emergency escape exits and other outward opening hatches require special seal configurations to provide good sealing characteristics.

(1) Inward Opening Exit Hatches (Fig. 102)

These seals are generally of the pressure energized type. Initial contact stress is attained by the compression of the elastomer or deformation of seal structure by the closing of the hatch. Further contact stress and conformability is attained when the initial sealing phase (closing of door) has occurred and a pressure differential exists.

(2) Outward Opening Exit Hatches (Fig. 103)

These seals are of the inflatable type and require a latching mechanism for holding the exit hatch in place. Initial and final contact stress are attained by the doors deforming the inflated elastomer tube or bladder.

e. Docking Transfer Ports (Fig. 104)

To enable personnel transfer between a logistic vehicle and a space station, docking transfer ports and their respective seals in conjunction with air locks are required. The seal will prevent leakage between the mating surfaces of the two vehicles during the personnel transfer period. At other times, the exit doors (inward openings) will be closed and the docking port seal is in an unpressurized state. The seals, therefore, are generally of an inflatable nature and are not energized until the vehicles have been hatched together. The necessary contact stress to effect sealing is attained by inflating the bulb or tubular shape seal to the necessary pressure level. Close cut sponge filled tubular shape seals may be used if the inflating procedure is not possible. However, the seal is subjected to damage during the maneuvering and latching phase.

f. Internal Access Doors (Fig. 105)

Internal access door seals required by space station designs have both inward and outward opening requirements. The sealing function is necessary for short durations of time, mainly during transfer of personnel or equipment between pressure chambers. The door designs are such that two locking positions are effected by the latching mechanism, one for ordinary closing with gas transfer between equally pressurized chambers, and a second position which compresses or energizes the seal when leakage must be minimized.

g. Observation Ports (Fig. 106-110)

Psychological, as well as, physical needs for glazed observation ports in aerospace vehicles are well established. Sealing methods for the windows are of the static variety and can be structural. That is, the window can be sealed by faying surface and fillet-type sealing methods. However, great temperature variations such as from -100°F to 1000°F may be encountered by the ports during supersonic, hypersonic, or re-entry flight conditions. Therefore, sealing methods which can cope with this problem are necessary. The schemes are such that the necessary contact stress to effect sealing does not shatter the silica window material.

h. Fuel Transfer Ports (Fig. 111)

To enable fluid transfer between logistic vehicles and space stations, fluid transfer ports are required. These ports consist of connections, one member of which is rigidly mounted (screwed, welded, cemented) into the pressure hull; the other member is attached to the logistic vehicle fluid line. The connectors are designed so that each member is sealed separately. Upon separation, spillage or leakage of fluid or gas is restricted to a minimum. The sealing is of a static nature and initial contact stress is normally attained by spring loading. After separation (when seal is energized), the fluid pressure in the line or tank increases the sealing action.

i. Fuel Tanks

The various fuels necessary in spacecraft and space stations for altitude control, environmental control, etc., require storage tanks which are compatible with the fluid and fluid induced environment. The construction of the tanks can be such that structural sealing methods such as brazing, welding, or cementing are utilized. However, cleaning or filling ports necessitate the use of removable cover plates.

These plates require the use of gasket-type nonmetallic or metallic static seals. The seals are generally of the compressive nonpressure-energized type. Contact stress is attained by the initial load imposed on the gasket by the damping force between cover plate and tank body.

j. Valves (Fig. 112)

Valves of many sorts are utilized on a spacecraft or space station system. They range from on-off type manually operated ones to torque motor actuated electrohydraulic servo valves. The sealing problem in all designs, however, is very similar. Static seals to prevent external leakage past mounting surfaces (if manifold mounted), cross-port leakage, and leakage between connectors and body are necessary. Dynamic seals of the sliding and rotary type are necessary to restrict leakage past control stems between valve housing bore and spool or poppet controlled ports. Internal leakage in most control valves is only minimized, because cross-port leakage is not always detrimental to system performance. Therefore, precision mating type seals are usable. On-off or metering valves of the globe, gate, or needle variety require careful design of the valve seat and stem packing. In valve assemblies where a spool or inner cylinder may have a multiplicity of ports each demanding isolation from the other, it is necessary to provide diametral static sealing. This type of seal must be capable of sealing on both inside and outside diameter.

k. Bladders (Fig. 113 and 114)

Bladders which are utilized as pliable storage tanks can be vulcanized or bonded structurally. The sealing problem encountered is at the place of connection between bladder and filling or removal port. Sealing at the junction can also be effected with a structural method such as molding a metallic tube or collar in place, or cementing or bonding the same in place. The connection from a fluid or gas line can then be made by utilizing an appropriate threaded or flange-type connector. However, in some cases, the foregoing is not applicable or necessary; and a simple change arrangement with the bladder material acting as the seal is appropriate.

SECTION IV

ANALYTICAL TECHNIQUES

1. INTRODUCTION

The development of analytical techniques for predicting seal leakage or performance first requires the definition of the leakage path in terms of the forces and material properties involved. Fulfillment of this objective will then permit the use of theoretical fluid flow equations which combine the characteristics of leakage path with fluid properties to yield the desired analytical leakage prediction method. However, few seal designs are simple enough to permit the application of basic theoretical concepts. The random distribution of the void spaces at the interface comprising the leakage path require a great deal of judgment in applying the appropriate theoretical concept. Thus, empirical data must provide the information necessary to close the existing gaps in understanding the theoretical concepts.

This section presents the analytical techniques available for determining leakage flow. The basic theoretical fluid flow equations, delineation of flow regimes, and a theoretical method for describing the flow passage are presented. The seal and seal housing or cover structural effects on the leakage path are discussed in the form of a structure analysis approach.

2. FLOW CONDUCTANCE PARAMETER CONCEPT

From the discussion of Section II, it can be seen that because of the irregular nature of real surfaces complete contact of two separable surfaces is virtually impossible. Thus, there will always be a void in the interface whose random inter-connections create leakage paths across the seal interface. The previous discussions pointed out quantitatively the requirements on load, contact stress, surface topography, and material properties necessary to achieve good sealing. These parameters must now be combined with fluid properties, fluid flow phenomena, and environmental conditions of the sealed fluid in order to develop techniques for the quantitative analysis and prediction of fluid leakage.

The major difficulty encountered in attempting to analyze flow through an interface is the application of the laws of fluid mechanics to the interface flow. In all the fluid flow equations, some characteristic flow path dimension must be known. As can be seen from the discussion of surface characteristics, the flow paths formed by the contact of two surfaces are irregular and random. There may be a few large paths or many small paths. This random nature of the leakage paths makes the determination of a characteristic leakage path dimension directly from the surface characteristics difficult. Statistical methods of

defining surface dimensions are cumbersome to apply and largely unsubstantiated.

The only conclusive fact that can be stated about the interface is that it does present a resistance to flow. The electrical analog of voltage potential, current, and resistance can be utilized at this point to develop an approach to the sealing problem. If the undefined leakage path is represented by a damped conductance factor, C, the leakage flow rate Q would be analogous to electrical current; and the pressure difference ΔP across the seal would be analogous to the voltage in an electrical system. Thus, a relation for leakage flow rate can be stated as

$$Q = C\Delta P$$

If accurate leakage measuring techniques are available, the factor C can be determined experimentally. Thus, a single parameter can be used to describe the interface leakage path.

If any number of surfaces similarly prepared and with similar topographical characteristics of roughness and waviness are brought into contact under identical loading conditions, the surface deformation should be similar in all cases for the same materials. While the locations of asperities and void space vary randomly in each of the interface combinations due to the extremely large number of asperities and voids involved, it seems intuitively correct to assume that over-all effect of the interface deformation would be the same for surfaces of similar surface topography and identical material combinations and loading conditions. A statistical averaging process is inherent in the physical contact and deformation process. If this assumption is correct, then a series of experiments in which factors such as load, surface topography, fluid properties, etc., are controlled and leakage is accurately measured should yield a useful parameter which describes the leakage path. In order to determine the validity of the initial assumption that topographically similar surfaces under identical loading and environmental conditions will exhibit the same flow resistance, certain basic questions must be answered analytically.

1. Will surfaces of a given material under identical loading conditions and with similar initial topography yield the same leakage parameter?

2. What are the effects of stress?

3. What are the effects of fluid properties and pressure?

4. What are the effects of macroscopic interface geometry (seal diameter, width, etc.)?

5. What are the effects of seal material?

In order to answer these questions, the lumped parameter concept must be modified. A modeling technique utilizing a theoretical flow equation and known parameters has been used. Experimental results are then used to check the validity of the initial assumptions. Extensive work has been done along these lines at IITRI. The use of this approach is demonstrated using the equations of laminar flow. The equation for isothermal compressible laminar flow between two flat annular surfaces with a uniform separation is given by

$$W = \rho_o Q_o = \frac{\pi \rho_o (P_2^2 - P_1^2) h^3}{12 \mu P_o \ln r_2/r_1} \qquad (1)$$

where

h = uniform separation height (height of the flow path)
P_o = pressure at standard conditions
P_1 = exit fluid pressure
P_2 = inlet fluid pressure
Q_o = volume flow rate at standard conditions
r_2, r_1 = outside and inside radii of the annular surfaces
W = weight rate of flow
μ = absolute viscosity
ρ_o = fluid density at standard conditions

The use of other flow equations will be shown separately. When the terms of the equation are rearranged, the uniform separation can be expressed as

$$h^3 = \frac{12 P_o \mu \ln r_2/r_1 W}{\pi \rho_o (P_2^2 - P_1^2)} \qquad (2)$$

In the case of a contact interface, it is not geometrically significant to speak of a uniform separation. A new term (h^3) is defined as the conductance parameter. The conductance parameter can be determined experimentally from equation (1) if the leakage flow rate W is known. This modeling technique was used to establish the answers to basic questions and thus establish the validity and usefulness of the conductance parameter.

The development of the conductance parameter approach to seal leakage investigation has been carried out at IITRI on other programs (Ref. 9 and 10). The major results that will be discussed here illustrate the validity of the approach.

First, in order to determine if topographically similar surfaces under identical loading and environmental conditions offer the same resistance to flow, a large number of experiments were performed on metal gaskets and flanges at various ranges of surface finish.

It was found experimentally that the conductance parameter (h^3) versus contact stress relationship was quite similar for gaskets of the same initial surface finish. Some typical results for aluminum gaskets are shown in Figure 21. Average results for aluminum and steel gaskets in given surface roughness groups are shown in Figure 22.

The results of this portion of the study show that seal surfaces of similar initial topography exhibit the same resistance to flow under the same conditions of loading and environment to a high degree of agreement. Thus, the relationship between the conductance parameter (h^3) and the contact is quite similar for seals of the same initial topography.

The conductance parameter decreases with increasing contact stress. Thus, it appears that the conductance parameter does truly represent the flow path resulting from the complex interconnections of the voids of the interface and, therefore, is representative of a physical interface condition.

Since the surface deformation and the initial topography determine the actual leakage path, the fluid properties and pressure should not change the value of the conductance parameter if the contact stress does not change. This is true in the case of metallic interfaces, because fluid pressure and properties usually will not alter the interface deformation. Therefore, if the conductance parameter is truly representative of the actual flow path, the relation between (h^3) and the contact stress will not be affected by pressure or fluid properties.

Thus, the validity of the conductance parameter concept for describing the leakage in interfacial seals has been established by

- similar relationships for conductance parameter (h^3) versus contact stress for gaskets of the same initial surface finish
- the decrease in conductance parameter for increase in contact stress
- fluid properties and pressure not changing the value of the conductance parameter

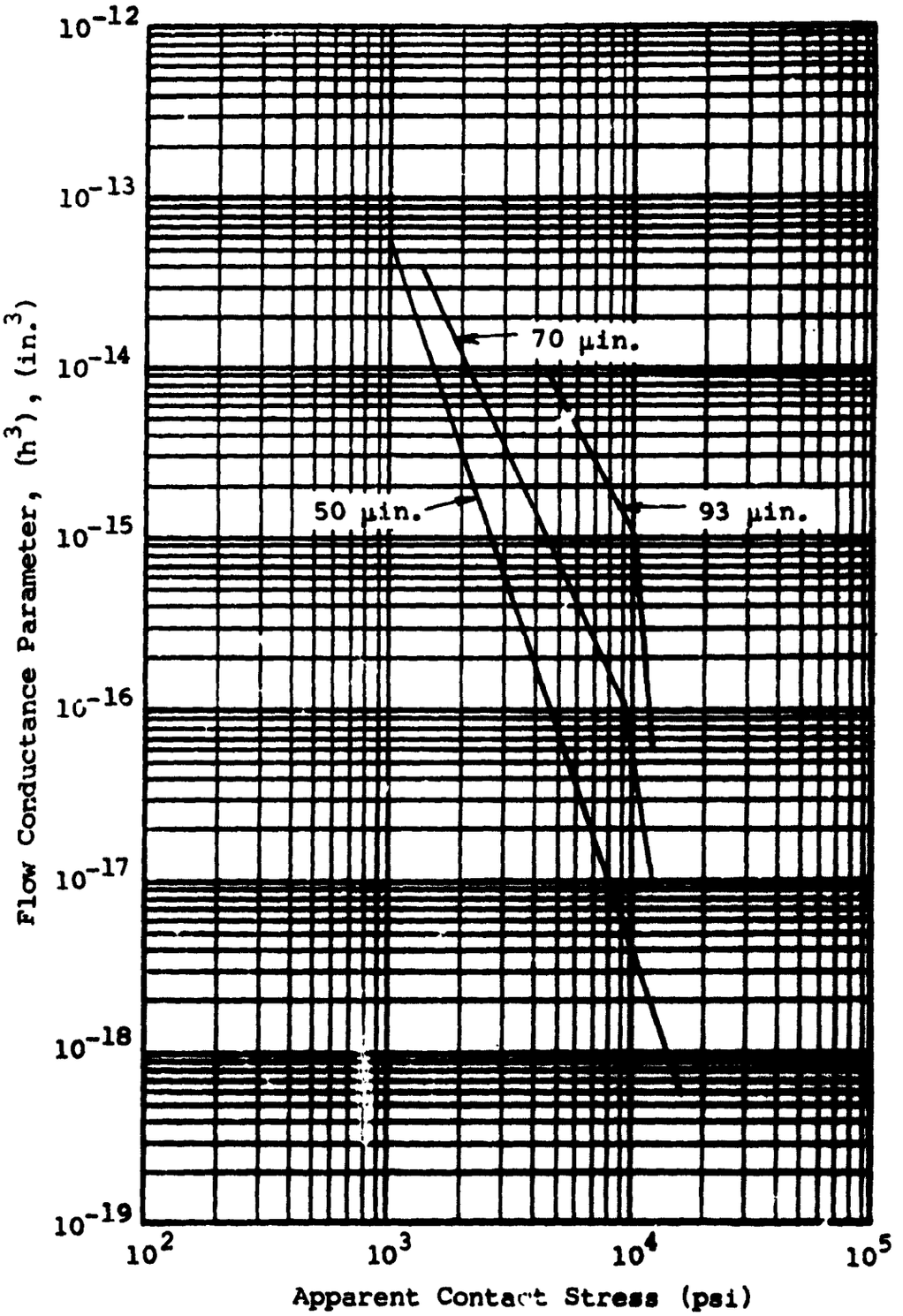

Figure 21 Flow Conductance Parameter as a Function of Contact Stress for Turned Aluminum Gaskets with an Interface Roughness of 50-100 µin. (Helium, 7.5 Atmospheres Pressure, 80°F) (Ref. 9)

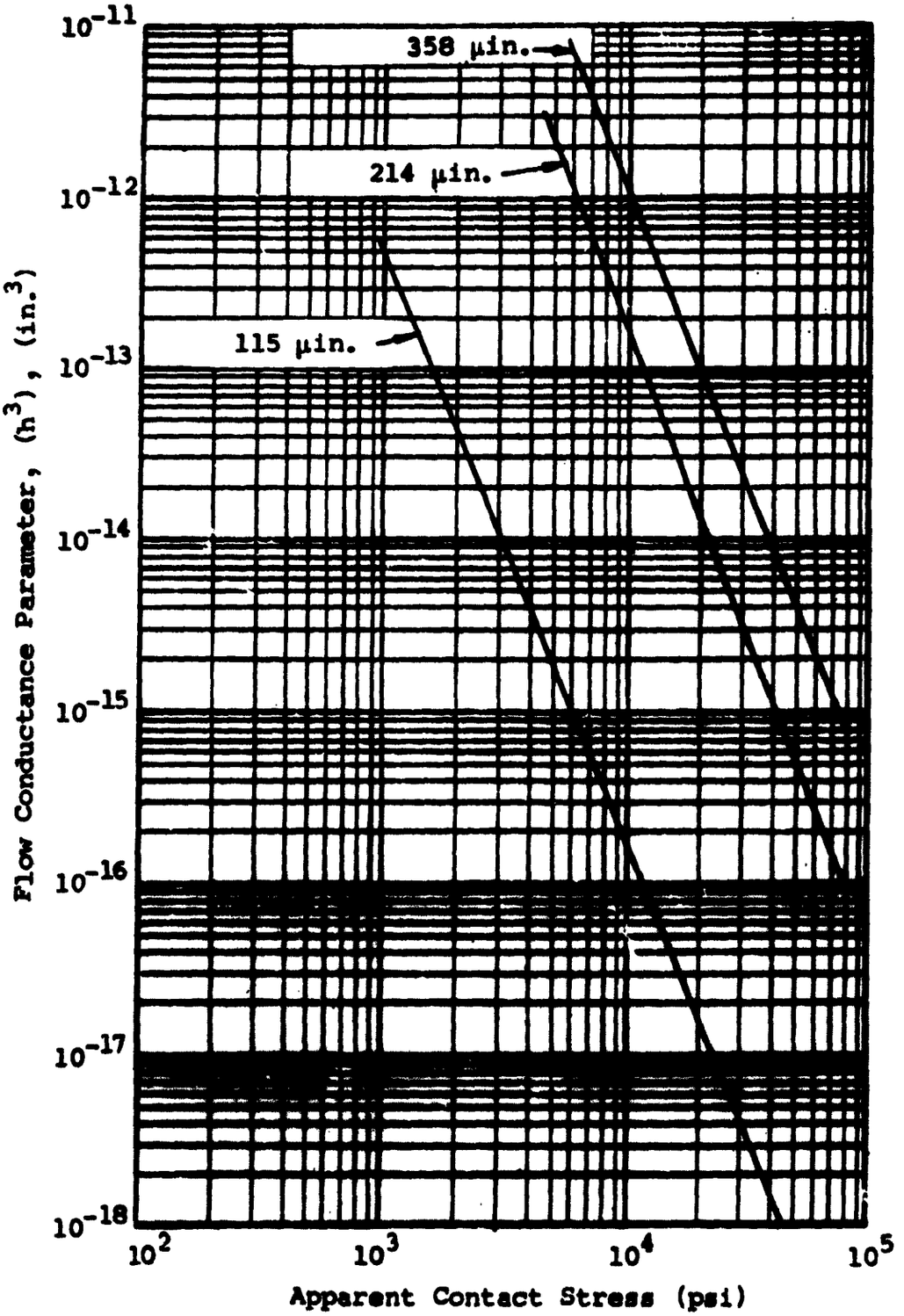

Figure 22 Average Flow Conductance as a Function of Contact Stress for Steel Gaskets; Average Interface Roughness for all Gaskets is Shown as a Parameter (Ref. 9)

3. LEAKAGE FLOW ANALYSIS

To analytically describe or predict leakage flow, it is necessary to realize the basic laws of fluid mechanics governing the flow of fluids. These principles are presented in the following discussion with particular emphasis placed on flow of fluid in very small passages, or channels. Furthermore, guide lines for estimating the flow regime are presented. Some of the theoretical concepts can be used for comparative purposes only because of their limitations due to the assumptions made in obtaining a solution. More encompassing assumptions, however, quite often render the problem unsolvable. The assumptions necessary for arriving at solutions for leakage flow through geometrically defined small channels are presented. Conversion of calculated leakage units and time units to other units are facilitated by conversion tables.

References 9 through 22 are suggested as sources for supplementary information. Derivations of the various flow equations are contained in these references along with definitions of the flow regimes.

a. Delineation of Flow Regimes

Fluid flowing steadily past a stationary wall generates a velocity gradient in the fluid normal to the direction of flow due to the particles next to the wall adhering to it. The retarding force exerted by the boundary on the fluid depends on both the velocity gradient at the boundary and the viscosity of the fluid. For Reynolds numbers less than 2000,

$$N_{Re} = \rho VD/\mu \qquad (3)$$

where

D = passage diameter
V = average velocity
ρ = density
μ = viscosity of the fluid

The flow in a passage is not turbulent so that the path followed by each particle is a smooth curve called a streamline. This type of flow is designated as laminar or viscous flow.

In many cases of leakage flow, the flow is laminar and may be analyzed as such. However, for larger Reynolds numbers, the flow may consist of random lateral motions superimposed on the main forward motion. The flow no longer consists of steady streamlines and is called turbulent flow. Under these conditions, the relationship between shear stress and velocity gradient is very complex; and no exact theory exists to describe it. However, considerable empirical information is available which permits

close approximation of the flow. It is most convenient to define the shear stress as $\tau = f\rho(V^2/2)$, where f is the friction factor. The friction factor is a function of the Reynolds number, wall roughness, and distance from the channel or pipe inlet.

In both laminar and turbulent flow, collisions between molecules occur more frequently than collisions of molecules with the channel wall. The coefficient of viscosity reflects the influence of intermolecular interactions. When the pressure of a fluid is sufficiently reduced, the mean free path of the molecule, λ, becomes large compared to a characteristic dimension, h, of the channel. When the fluid molecules collide more often with the wall than with each other, the flow is termed free-molecular flow.

A summary of the various flow regimes along with their identification is presented in Table VI. Flow concepts based on frictionless conditions are presented in the following discussion. The applicability of the concepts using frictionless and other assumptions depends on complex factors and must be determined from discussions contained in other sections of this report.

Table VI

Definition of Flow Regimes

$N_{RE} > 2200$	Turbulent flow
$1800 < N_{RE} < 2200$	Mixed flow
$N_{RE} < 1000, \frac{\lambda}{h} < 1.00$	Laminar flow
$0.01 < \frac{\lambda}{h} < 1.00$	Transition flow
$\frac{\lambda}{h} > 1.00$	Molecular flow
Not defined	Diffusion flow

b. Flow of Gases Through Solids-Permeation

The process by which gases pass through sound solid membranes is described in Section II. The general equations for describing this mechanism of diffusion as given by Reference 1 are:

Molecular Diffusion:

$$Q = KDA \frac{(P_2 - P_1)}{L} \tag{4}$$

Atomic Diffusion:

$$Q \sim \sqrt{P_2} - \sqrt{P_1} \text{ or for } P_1 = O_{abs}$$

$$Q = Q_e \frac{P_2}{P_e} \tag{5}$$

where

A = area of leakage

D = diffusion coefficient

K = solubility

L = thickness of the wall

P_1 = exit pressure

P_2 = inlet pressure

P_e = experimental pressure difference usually P_o

Q = volume rate of flow at any pressure difference $(P_2 - P_1)$

Q_e = flow rate at pressure P_e, determined by experiment

The general rules in applying the formulas for various materials are outlined in Table VI.

Table VII

Summary of the Nature of Gas Permeation

Metals
None of the rare gases will permeate any metal
Hydrogen permeates most metals, especially iron
Oxygen permeates silver
Hydrogen through iron by corrosion electrolysis
Flow rates vary as $\sqrt{P}$ (atomic diffusion)
Very small halogen gas leakage through metal (Ref. 11).
Polymers
All gases permeate all polymers
Water rate apt to be high
All rates vary as pressure (molecular diffusion)
Permeation rate varies exponentially with temperature

A permeation rate, Z, may be defined as a conductance factor for molecular and atomic diffusion. The permeation rate is an experimentally determined value and often expressed in the units.

$$Z = \frac{cm^3 - mm}{sec - cm^2 - torr}$$

For molecular diffusion,

$$Z = \frac{ZA(P_2 - P_1)}{L} \qquad (6)$$

For atomic diffusion,

$$Q = Q_e \sqrt{\frac{P_2}{P_e}}$$

where

$$Q_e = \frac{ZA(P_e)}{L} \qquad (7)$$

Thus,

$$Q = \frac{ZA(P_e)}{L} \sqrt{\frac{P_2}{P_e}} \qquad (8)$$

In these formulas, the units of measurement must be:

P in torr = 10^{-6} mm Hg

A in cm^2

L in mm

Q in cm^3/sec

Permeation rate is converted into common engineering units using the factor

$$Z \times 131.2 = cc/sec \times in./(psi)in.^2$$

where the units of measurement may be given;

P in psia

A in $in.^2$

L in in.

Q in cm^3/sec

In general, very little permeation rate data are available for cases other than those shown in Table VIII and Fig. 23. Permeation rates for gas and material combinations were obtained from References 1, 11, 12, and 13.

The permeation rates for rubber, shown in Table VIII, are typical experimental values obtained from the literature. Considerable variation of permeation between elastomer materials may be expected because of the molecular structure of the filler materials and processing variations.

Table VIII

Air Permeabilities at Various Temperatures
Various Elastomers

Elastomer	Permeability x 10^7				
	75°F	176°F	250°F	350°F	400°F
Natural	0.49	4.4	7.1	20.7	26.2
SBR	0.25	2.9	4.7	15.4	---
Neoprene	0.09-0.10	0.98-1.7	2.6-3.0	7.3	---
Butyl	0.02	0.32-0.46	1.3-1.8	5.6-6.1	10.0
Nitrile	0.13	0.8	2.2	6.6	---
Thiokol	0.02	0.37	1.6	melted	---
Hypalon	0.72	0.73	2.3	6.2	---
Polyurethane (polyester type)	0.05	0.97	3.1	7.1	melted
Silicone	11.00-33.00	35.00-47.00	---	69.0-113.0	74.0
Fluorocarbon	1.5	9.6	24.0	49.0	---
Vyram	0.007	0.24	0.56	5.1	---
Kel-F 3700	---	0.8	3.4	15.6	---
Viton A	---	0.88	3.6	14.6	---
Acrylon EA-5	0.16	1.5	3.7	10.2	---
Hycar 4021	0.19	1.8	4.8	9.4	---
Methacrylate	---	---	---	---	16.3
Adiprene C	---	2.3	3.8	16.6	---
Carboxyl	---	2.4-2.6	2.3-6.2	7.1-14.0	---

Permeability is expressed in cubic centimeters of air (corrected to STP conditions) per second which would permeate through one square centimeter of vulcanizate one centimeter thick ($cc/sec/cm^2/cm$) with one atmosphere of pressure difference.

WADC Report TR 56-331, "Gas Permeability Properties of Elastomers," Part II, Section VI.

Figu

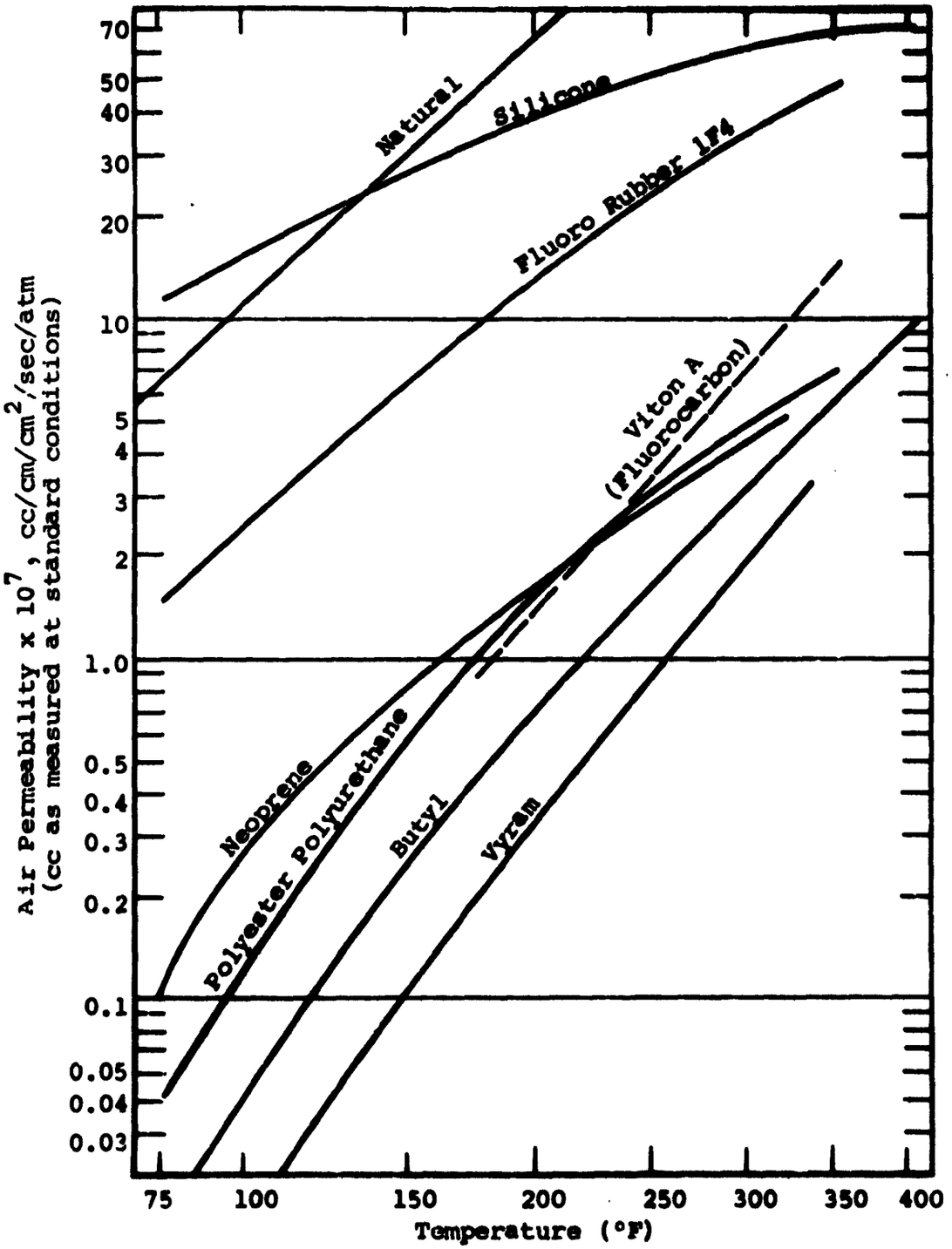

WADC Report TR 56-331, "Gas Permeability Properties of Elastomers" Part II, Section VI.

Figure 23 Air Permeabilities of Elastomers at Elevated Temperatures

Table IX

Permeation Rates of Gases at Temperatures Between 20° and 30°C

$$\left(\frac{cm^3 - mm(STP)}{sec - cm^2 - torr}\right)$$

	Nitrogen	Hydrogen	Oxygen	Helium	Air
Rubber	1.3×10^{-9}			8.6×10^{-10}	$4.2 \times .0^{-10}$
Neoprene	1.4×10^{-10}	1.3×10^{-9}		7.8×10^{-10}	
Aluminum		1.1×10^{-12}			
Silver			9.4×10^{-19}		
Nickel		1.5×10^{-12}			
Steel		8.0×10^{-13}			
Iron	1.5×10^{-20}	1.4×10^{-10}			

To show the method of estimating molecular and atomic diffusion flow, the following example is presented:

Given: A circular rubber ring seal with a rectangular cross section with the dimensions:

Outside diameter, D_o = 2.00 in.

Inside diameter, D_i = 1.75 in.

Thickness, t = 0.10 in.

Helium is sealed at P_2 = 14.7 psi inside seal and P_1 = 0 psi external. Temperature is 68°F.

Calculate: Leakage rate in cubic centimeters per second. The material selected is rubber, and the contact stress is such that the leakage mechanism is molecular. From Table IX, the diffusion rate is 8.6×10^{-10} cm^3-mm (STP)/sec-cm^2-torr. When the units are converted,

$$Z = 1.13 \times 10^{-7} \quad \frac{cm^3}{sec} \quad \frac{in.}{(psi)\ in.^2} \text{ (STP)}$$

The volume rate of flow may be calculated from the formula for molecular diffusion (Eq. 6).

$$Q = \frac{Z\ A\ (P_2 - P_1)}{L}$$

$$Q = \frac{1.13\ (10^{-7})\ \pi\ D_o T\ \ (P_2 - P_1)}{\frac{D_o - D_i}{2}}$$

$$Q = \frac{1.13\ (10^{-7})\ (\pi \times 2 \times 0.10)\ (14.7)}{0.125}$$

$$Q = 8.4 \times 10^{-6}\ \ cm^3/sec\ (STP)$$

Correction of permeation rate for other temperature conditions may be accomplished using the procedures described in Reference 11.

c. Molecular Flow Through Long Channels

Clearance spaces in the same order of magnitude as the molecular free path require considerations to be given to the collisions of the molecules with the wall. Knudsen (Ref.11) introduced a method of analysis to the problem based on the kinetic theory of gases. For a long tube, the equation deduced by Knudsen is:

$$W = \frac{4}{3} \frac{\rho}{p} \frac{v_a}{\int_o^L \frac{H}{A_p^2}\, dl} (P_2 - P_1) \qquad (9)$$

where

A_p = cross section of channel

H = perimeter of channel

L = channel length

M = molecular weight of gas

W = weight rate of flow

ν_a = mean molecular speed = $\sqrt{\frac{8\ RT}{\pi M}}$

From the kinetic theory of gases, the mean molecular free path is:

$$\lambda \cong \frac{1}{0.31}\sqrt{\frac{\pi}{8}}\ \frac{\mu}{P}\sqrt{\frac{RT}{M}} \qquad (10)$$

Substituting this equation into the leakage equation we obtain:

$$W = 1.064\ \frac{\rho \bar{\lambda} \bar{P}(P_2 - P_1)}{L \rho \mu \int_o \frac{H}{A_p^2}\ dl} \qquad (11)$$

where $\bar{\lambda}$ is defined as the mean free path at a mean pressure $\bar{P}$ $= \frac{P_2 + P_1}{2}$

For a rectangular channel having width w and height h

$$H = 2(w + h)$$

The weight rate of flow is:

$$W = 0.532\ \frac{\lambda P(P_2 - P_1)wh^2}{R_o T \mu L} \qquad (12)$$

To utilise the preceding formula, the properties of fluids and equations of state must be known.

d. Comparison of Theoretical Leakage Equations for Compressible Flow

Selection or determination of the applicable leakage flow equation requires comparison of typical calculated results with assumptions made in the analysis. To demonstrate this comparison process when applied to one-dimensional flow equations, a channel having the geometrical properties of channel height, h, channel length, L, and width, w, is assumed.

Case I - Isothermal Laminar Flow

Infinite heat transfer is assumed.

$$W = \frac{wh^3}{24\, R_o\, T\, \mu\, L} \quad (P_2^2 - P_1^2) \tag{13}$$

Case II - Isothermal Laminar Flow with Inertia

Infinite heat transfer is assumed. An approximation for laminar flow in included in the analysis to obtain a solution when inertia is considered.

$$\frac{2W^2 h}{gw} \ell_n \frac{P_1}{P_2} = - \frac{wh^3}{R_o T} \quad (P_2^2 - P_1^2) + 24\, W\, \mu\, L \tag{14}$$

Case III - Transition Flow

Infinite heat transfer is assumed. Molecular flow correction factor is included.

$$W = \frac{wh^3 (P_2^2 - P_1^2)}{24\, R_o\, T\, \mu\, L} \quad (1 + 5\ 75\, \frac{\bar{\lambda}}{h}) \tag{15}$$

Case IV - Adiabatic Frictionless Flow

No heat transfer is assumed.

$$W = wh \sqrt{\frac{2kg}{R_o(k-1)}} \left(\frac{P_2}{\sqrt{T_2}}\right) \left(\frac{P_1}{P_2}\right)^{\frac{1}{k}} \sqrt{1 - \left(\frac{P_1}{P_2}\right)^{\frac{k-1}{k}}} \tag{16}$$

If the ratio of P_2/P_1 is much greater than the critical pressure ratio, then the weight rate of flow is given

$$W = wh \left(\frac{2}{k+1}\right)^{\frac{1}{k-1}} \sqrt{\frac{2\, gk}{R_o(k+1)}} \left(\frac{P_2}{\sqrt{T_2}}\right) \tag{17}$$

Before final selection of the appropriate flow equation, other factors must be considered. The most important one is the affect of turbulence and wall roughness. Since the Reynolds number is an indication of the flow regime, determining its value is necessary.

In summary, the final choice of the applicable flow equation requires sample calculations, past experience, and experimental correlation if available. Figure 24 depicts the approximate ranges of applicability for the various equations. The unshaded area represents the flow regime during which momentum effects due to acceleration predominate.

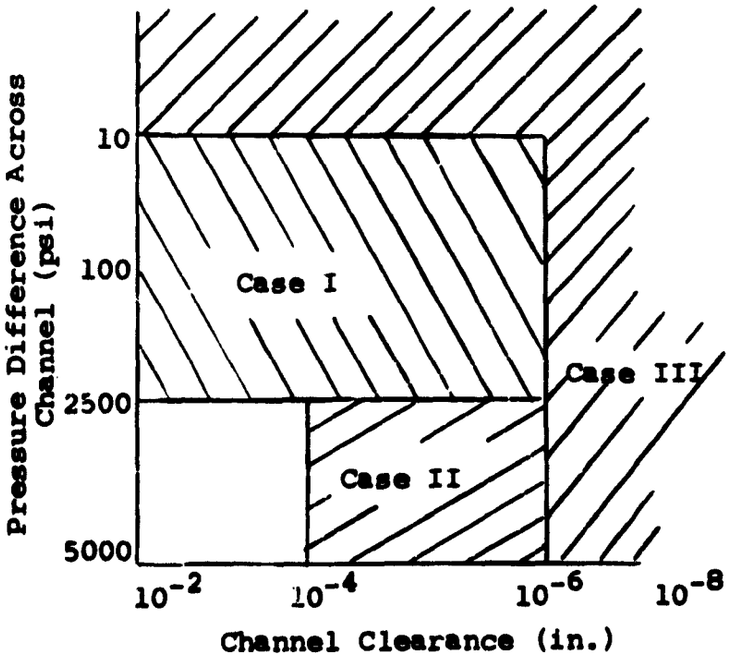

Figure 24 Approximate Applicability Range for the Theoretical Equations

For the weight rate of flow in the transition range between laminar and molecular flow, an empirical relationship has been determined where:

$$W = W_{laminar} + \psi W_{molecular}$$

For a single gas, ψ is equal to 0.9 and is dependent upon the gas properties and clearance dimensions. Combining the free molecular and viscous flow equations for uniform channel flow, the transition flow rate may be defined. Thus,

$$W = \frac{wh^3(P_2^2 - P_1^2)P}{12R_oT\mu L} + \frac{0.532P(P_2^2 - P_1^2)wh^2}{R_o\mu L} \qquad (18)$$

Rearranging terms,

$$W = \frac{wh^3(P_2^2 - P_1^2)}{24R_oT\mu L}\ (1+5.75T/h) \qquad (19)$$

A comparison of molecular and viscous flow shows that:

$$\frac{W_{free\ molecular}}{W_{laminar}} = 6.38\,\bar{\lambda}/h$$

where $\bar{\lambda}/h$ is the Knudsen number.

e. Conversion Tables

Conversion factors for leakage values and time units into applicable or more readily usable values are easily obtained by the use of tables. Table X presents leakage value conversion factors for the units most frequently encountered; Table XI contains time unit conversion factors.

Table X

Leakage Conversions

To Convert Multiply	Std. cm^3/sec	Std. ft^3/yr	Std. $in.^3/min$	Std. ft^3/min	Std. ft^3/hr	Std. cm^3/min	Std. cm^3/hr	$\mu l/hr$	$\mu ft/hr$
Std. cm^3/sec	1	1.112×10^3	3.51	2.117×10^{-3}	0.127	60	3500	2.736×10^6	9.66×10^4
Std. ft^3/yr	8.99×10^{-4}	1	3.29×10^{-3}	1.90×10^{-6}	1.14×10^{-4}	5.39×10^{-2}	3.24	2.56×10^3	86.8
Std. $in.^3/min$	0.277	3.04×10^2	1	5.79×10^{-4}	3.474×10^{-2}	16.4	9.84×10^2	7.58×10^5	2.68×10^4
Std. ft^3/min	4.72×10^2	5.26×10^5	1.73×10^5	1	60	2.83×10^4	1.7×10^6	1.29×10^9	4.56×10^7
Std. ft^3/hr	7.87	8.77×10^5	2.88×10^3	1.67×10^2	1	4.72×10^2	2.83×10^4	2.15×10^7	7.6×10^5
Std. cm^3/min	1.67×10^{-2}	1.86×10^3	6.1×10^{-2}	3.53×10^{-5}	2.12×10^{-3}	1	60	4.57×10^4	1.61×10^3
Std. cm^3/hr	2.78×10^{-4}	0.309	1.02×10^{-3}	5.88×10^{-7}	3.53×10^{-5}	1.67×10^2	1	7.61×10^2	26.85
$\mu l/hr$	36.5×10^{-7}	3.91×10^{-4}	1.32×10^{-6}	7.75×10^{-10}	4.65×10^{-8}	2.19×10^5	1.31×10^{-3}	1	3.53×10^{-2}
$\mu ft^3/hr$	1.63×10^{-5}	1.15×10^{-2}	3.73×10^{-5}	2.19×10^{-8}	1.32×10^{-6}	6.21×10^{-4}	3.72×10^{-2}	28.33	1

Table XI

Table XI

Time Conversion Table

To Convert Multiply	Seconds	Minutes	Hours	Days	Weeks	Months	Years
Seconds	1	60	3.6×10^{3}	8.6×10^{4}	6.1×10^{5}	2.6×10^{6}	3.1×10^{7}
Minutes	1.7×10^{-2}	1	60	1.4×10^{3}	1.0×10^{4}	4.3×10^{4}	5.2×10^{5}
Hours	2.8×10^{-4}	1.7×10^{-2}	1	24	1.7×10^{2}	7.2×10^{2}	8.8×10^{3}
Days	1.2×10^{-5}	6.9×10^{-4}	4.2×10^{-2}	1	7	30	3.7×10^{2}
Weeks	1.6×10^{-6}	9.8×10^{-5}	5.9×10^{-3}	0.14	1	4.3	52
Months	3.8×10^{-7}	2.3×10^{-5}	1.4×10^{-3}	3.3×10^{-2}	0.23	1	12
Years	3.2×10^{-8}	1.9×10^{-6}	1.1×10^{-4}	2.8×10^{-3}	1.9×10^{-2}	0.83	1

4. LOAD AND DEFORMATION

To understand the phenomena of seal, housing, and cover deformation due to compression, one can simplify the model for inspection in order to gain insight into the events taking place. In this section, the phenomenon of seal deformation is described in terms of classical elastic-plastic material behavior. The information obtained from such an undertaking will not yield quantitative results extremely close to experimental observations. However, a better understanding of the experimental observations is achieved. The magnitude of the deformation or conformability problem for rubber alone, when nonlinear material property variations and generalizations in the analytical approach are considered, is easily seen. Thus, generalized equations enabling optimization of seal leakage based on deformation are not presented because of the limited duration and scope of program. The experimental results are presented in Section VI.

a. Deformation

The elastic and plastic deformation occurring at the interface is dependent on the net contact load applied to the sealing surfaces. An increase in deformation or conformability produces a decrease in interface voids (possible leakage paths). Thus, the relationship between deformation or conformability and applied contact load influences the seal leakage profoundly.

In seals formed by metal to metal contact, several modes of deformation generally take place. A graphic illustration of the effect of deformation on seal leakage is experienced by the behavior of a flat circular gasket pressed between two flat flanges. The behavior of the seal in the various regimes of deformation is shown in Figure 25. These results were obtained for an aluminum gasket approximately 2-1/4-in. inside diameter and 1/8-in. square cross section. The sealed fluid was nitrogen gas at two atmospheres pressure differential. The load is expressed in terms of apparent contact stress which is defined as the net contact load divided by the geometric contact area.

The leakage characteristic curve indicates that rate of change of leakage with a change in apparent contact stress varies with the magnitude of the stress. For low stress values, leakage changes slightly. As the stress increases, the leakage decreases at an increasing rate. A sudden decrease in stress results in a slowly increasing leakage rate until a significantly lower stress value is reached. At this time, a rapid increase in leakage occurs. A subsequent increase in stress up to the maximum value reached prior to reversal produces identical leakage-stress characteristics. Increasing the stress further decreases the leakage. This process can be divided into four

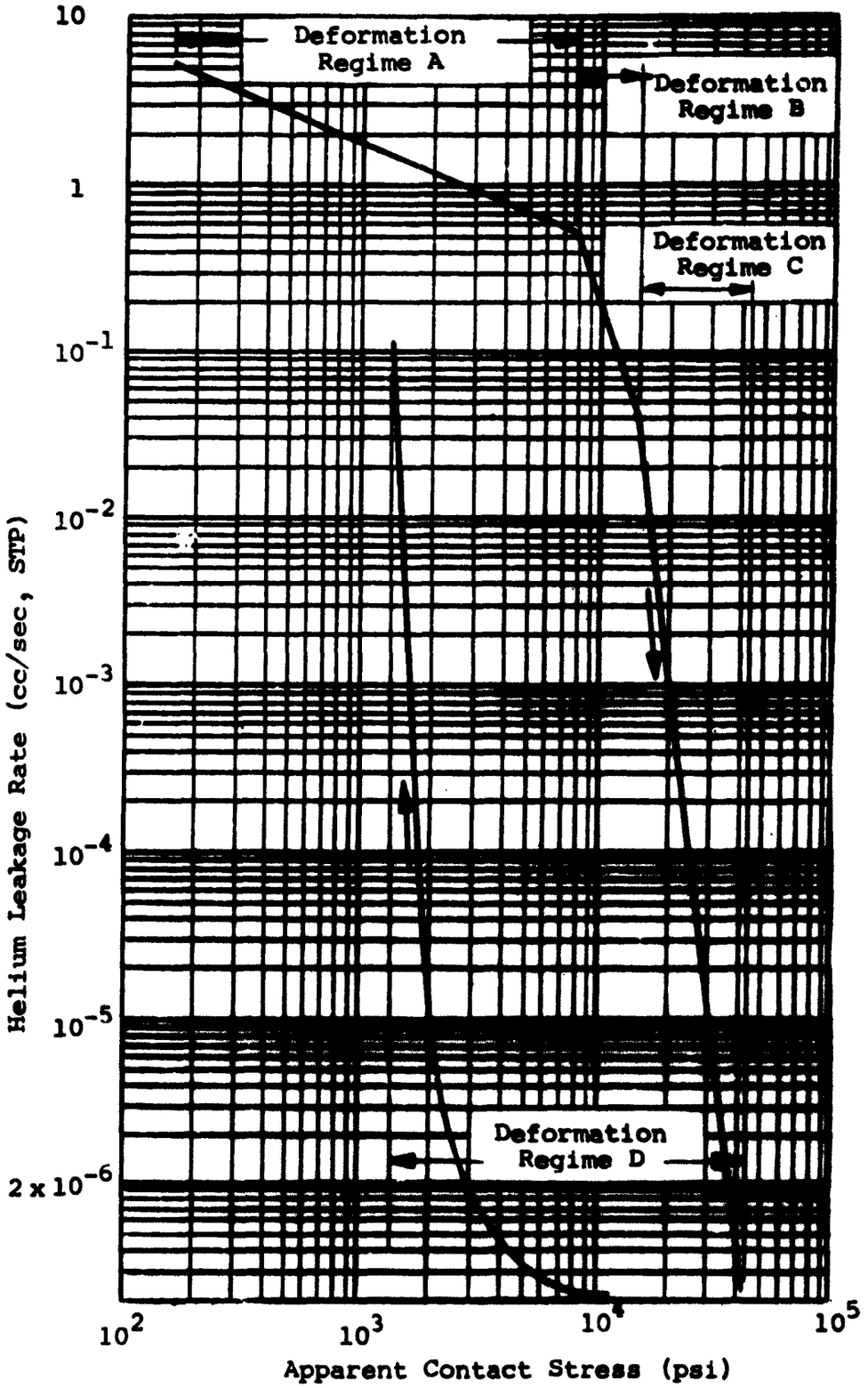

Figure 25 Leakage-Contact Stress Characteristics of an Aluminum Gasket Pressed between Steel Flanges

distinct regimes where the leakage versus stress characteristics change abruptly. These regimes are identified by a letter designation in Figure 25.

Regime A represents the contact and deformation of prominent surface projections. Surface waviness and nonplanar contact surfaces, such as may occur with a gasket whose surfaces are slightly warped (as shown in Figure 26), are also deformed in this regime. The mode of deformation in this regime is both elastic and plastic with the elastic effects predominating.

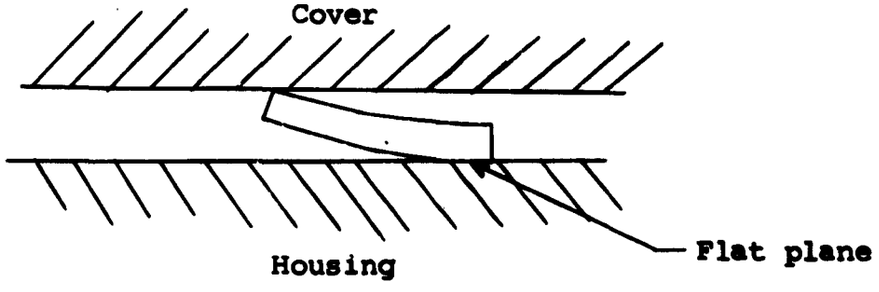

Figure 26 Exaggerated View of a Warped Gasket

Regime B represents the deformation of a large number of surface asperities. The plastic and elastic deformations are approximately equal in effect although the larger prominent projections deform plastically. The effect of the permanent deformation is observable by the fact that the leakage-stress relation for a reduction in stress in this regime does not follow the same curve as the leakage-stress relation for increasing stress.

Regime C is characterized by sub-surface yielding of the seal material. Macroscopic sliding occurs and more asperities come into contact. Because the surface projections can reorient themselves readily due to sub-surface yielding, a greater degree of surface conformability is achieved. A reversal of applied stress in this region shows little change in leakage until a significant stress decrease occurs.

Regime D represents the effects of load on stress reduction. The characteristics of the leakage curve in this region are indicative of the degree of plastic or permanent deformation. The general characteristics of this region are defined as hysteresis effects.

The phenomenon of hysteresis can be related to the effects of plastic deformation at the interface. As the surfaces that compose the sealing interface are brought into contact, the contact takes place first at the highest surface asperities. Thus, the actual contact area is quite small, and the local contact stress at the points of contact is high. The local contact stress may be high enough to cause plastic deformation of the asperities even though the average contact stress is still in the elastic range. The deformation may be partially plastic and partially elastic, while the bulk of the seal material will still be elastically deformed. The effect of deformation of the asperities is to reduce the size of the actual leakage paths and, therefore, reduce the leakage rate.

When the contact load is reduced, there will be a certain amount of elastic recovery of the deformed material. The plastically deformed portions of the interface will remain in exactly the same contact relationship until elastic recovery of the surrounding material brings the plastically deformed areas out of contact. The elastic deformation of the bulk materials, in a sense, spring load the areas of plastic deformation. Thus, when the load is reduced, the area of contact does not decrease proportionally. Therefore, large increases in leakage rate will not occur until sufficient elastic recovery has occurred to bring some of the areas of plastic deformation out of contact. Figure 27 schematically depicts the effects of deformation and recovery.

The magnitude of the effect of any of these modes of deformation is dependent on the seal material. All metals with relatively rough interface surfaces generally undergo the four modes of deformation. Lead exhibits characteristics of Regimes C and D predominantly, while steel exhibits all four regimes somewhat equally. Plastic materials behave similarly to lead. Rubber possesses no noticeable hysteresis effects and, therefore, forms a sealing interface elastically.

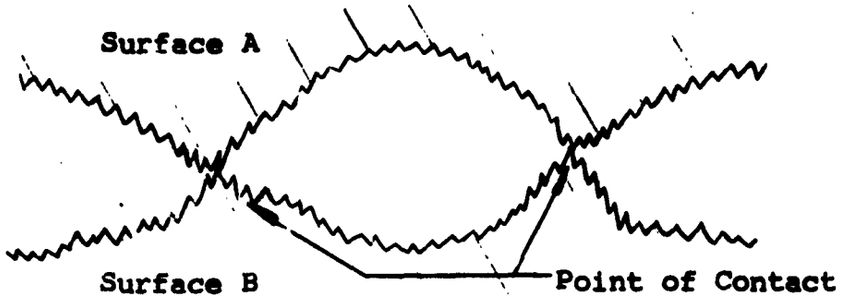

a) Contact of Unloaded Surfaces

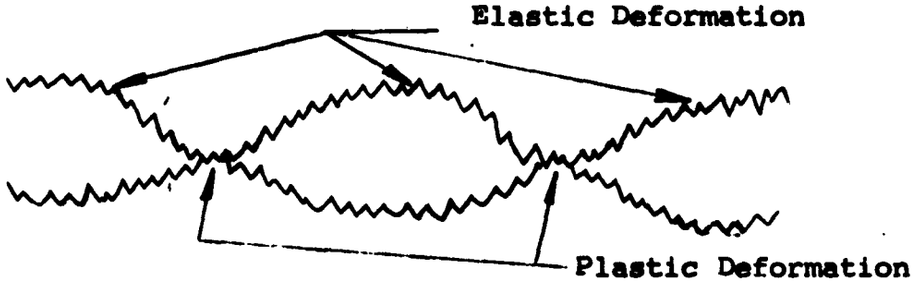

b) Contact at Loaded Surfaces

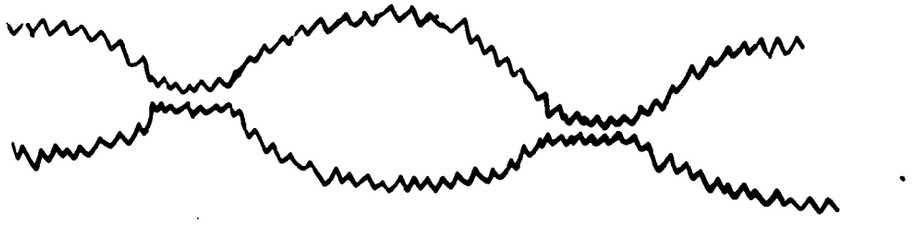

c) Partial Recovery Due to a Decrease in Load

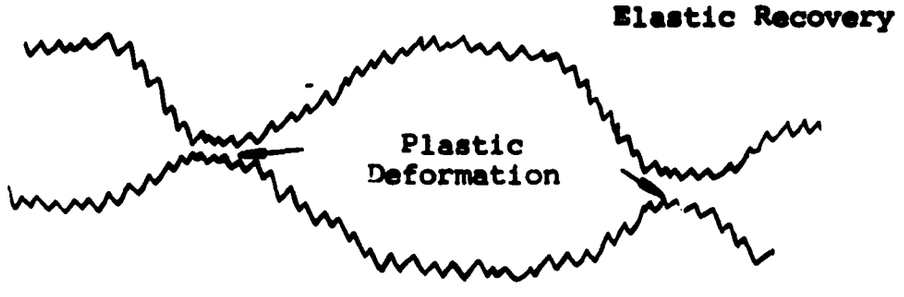

d) Sufficient Elastic Recovery to Cause Loss of Contact of Plastically Deformed Areas

Figure 27 Effects of Loading on the Material Deformation at and near Points of Contact on a Seal Interface

(1) Metal to Metal Interface

Theoretical approaches to the problem of deformation fall into two general classifications. One approach investigates the deformation of various shaped geometrical forms. The solution to the elastic deformation problem of such forms developed by Boussinesq and Hertz (Ref. 23) provides a means for determing the stress at points a considerable distance from the point of contact. The problem is shown schematically in Figure 28 with the solution obtained at point x. The local stress σ_x is given by Ref. 24 as:

$$\sigma_x = \frac{2F \cos \theta}{\pi r} \qquad (20)$$

where

F = load/unit contact length

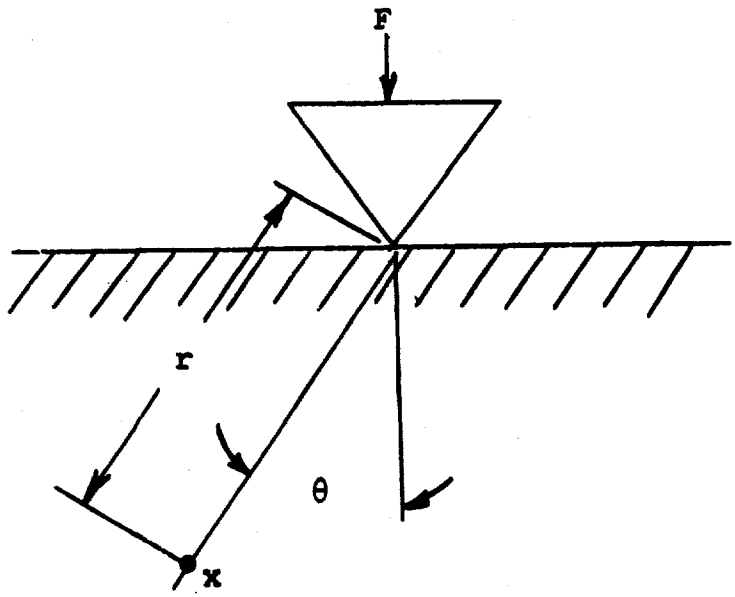

Figure 28 Rigid Knife Edge on Semi Infinite Plate

For most problems concerning contact, the stress and deformation in the immediate vicinity of the contact must be known. Solutions to the preceding problem and others of variable geometry have been obtained (Ref. 25, 26 and 27). A classical solution for a cylinder mating on a flat plate (Figure 29) is given (Ref. 28) as

$$a = 1.6 \sqrt{FD \left[\frac{1-Y_1^2}{E_1} + \frac{1-Y_2^2}{E_2} \right]} \qquad (21)$$

where

a = area of contact per unit length

E = Young's modulus

Y = Poisson's ratio

$$\sigma_a = 0.798 \sqrt{\frac{F}{D \left[\frac{1-Y_1^2}{E_1} + \frac{1-Y_2^2}{E_2} \right]}} \qquad (22)$$

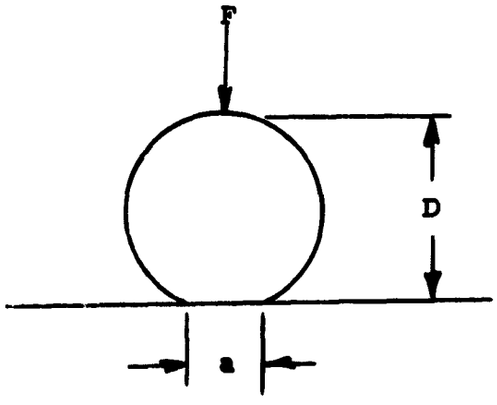

Figure 29 Cylinder Pressed Against a Flat Plate

These analyses assume smooth contact surfaces and the given relationships for the apparent contact area only.

Thus, while the theories describing surface contact which have been discussed may be adequate to calculate contact area, the results of this work are not directly applicable to the sealing problem. In sealing considerations, the magnitude and distribution of the areas of noncontact are of primary importance. Even if the various theories were accurate to within a few per cent of predicting the real contact area, the areas of noncontact still may be large enough to cause substantial leakage. Analytical expressions for these areas of noncontact have not yet been developed. The major difficulty is the randomness of the void spaces and their interconnections.

(2) Plastic to Metal Interface

The sealing interface formed by a plastic-seal and a metallic cover or housing is a function of the soft seal material properties due to the relative rigidity between the two materials. The material properties affecting leakage are the mechanical properties governing deformations necessary for sealing at the interface and the chemical properties affecting permeation. Thus, the interface formed is a function of the visco elastic properties of the plastic seal. The yield stress of the plastic which is indicative of the gross deformations attainable for given load conditions is the most meaningful parameter for determining surface asperity deformation. The yield stress for plastic materials is a pronounced function of temperature, strain rate, nature of loading (compressing tension), and the directional properties of the material. Furthermore, the roughness of the mating surfaces, friction and plane strain loading affect the gross deformations. The yield stress of the seal is higher for the rougher mating surfaces. This effect is less pronounced for teflon, probably due to its very low coefficient of friction. Yield stresses for various plastic materials are shown in Table XII.

Table XII

Plastic Material 0.2 Percent Yield Stress (Ref. 35)

Gasket Material	Strain Rate (0.001 in./min)	0.2 percent Yield Stress (psi)
KEL-F-81	50	7250
KEL-F-81	20	6750
Saran	100	7200
Saran	50	6400
Saran	20	5650
Saran	2	4850
Teflon-FEP	100	3275
Teflon-FEP	50	3600
Teflon-FEP	20	3750
Teflon-TFE	100	2500
Teflon-TFE	50	2525
Teflon-TFE	20	2375

(3) Rubber to Metal Interface

The deformation or conformability characteristics of an elastomer material govern its sealing ability. These characteristics are primarily a function of the rubber material properties. The mechanics of deformation of rubber-like materials is, in general, extremely complicated. The durometer system is the only general approach at classifying the mechanical behavior of rubber. This system provides a basis for comparison of the stiffness of one rubber with respect to another. Relating this information to other types of materials is not possible. The stiffness of each elastomer decreases with decreasing durometer value. However, rubber-like materials have a very low stiffness in relation to metal and plastic materials. Thus, the deformation and compliance at the interface will occur at a correspondingly low contact stress level. An example of the influence of contact stress on leakage for aluminum, teflon, and rubber gasket type seals are shown in Figure 30. The seal dimensions were 2-1/2-in. OD and 2-1/4-in. ID. It can be noted from this figure that the contact stress necessary to achieve the same deformation or conformability and, thus, leakage is one order of magnitude higher than rubber for plastic materials and two to three orders of magnitude for metallic materials. Furthermore, at higher contact stresses, the flattening of the curves can be seen indicating the region where permeation becomes predominant.

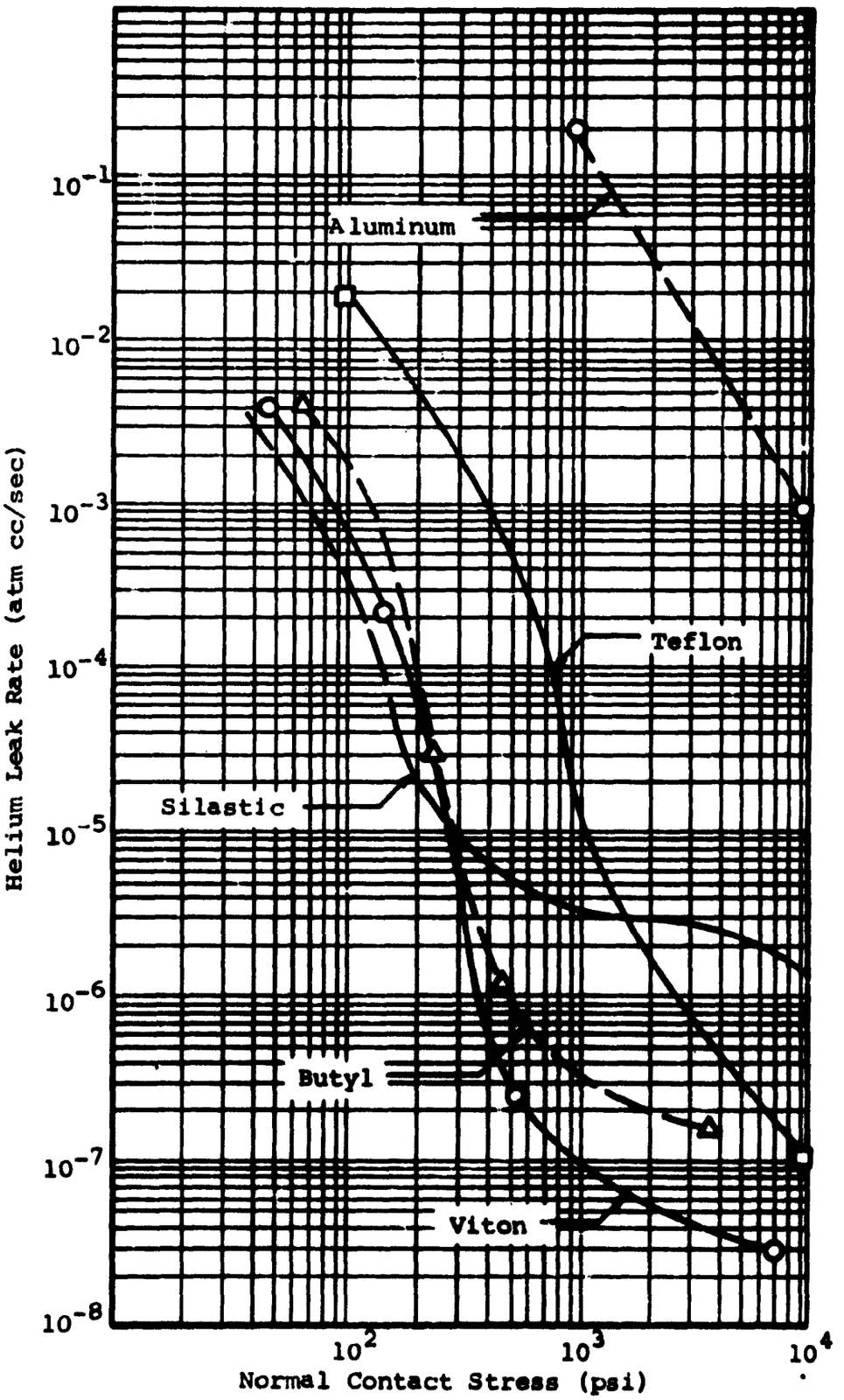

Figure 30 Leakage Characteristics of Various Materials

The method of analysis that defines the effects of material properties and loading with respect to leakage performance is presented in Section IV.6. This method employs simple theoretical considerations uniquely combined with empirical data obtained from the verification tests. The format of the analysis is general and may be applied to many elastomer seal configurations.

b. Relation of Deformation and Surface Conditions

To obtain an insight into the relationship between surface conditions such as roughness, waviness, as well as lay and the surface deformation process, an explanation of the surface inspection techniques and the constituents of a surface topography is appropriate.

(1) Surface Inspection Techniques

A great deal of disagreement exists concerning the instrumentation and methods available for describing, inspecting, or evaluating a surface. Three methods of surface evaluation employing three types of instrumentation are discussed in the following paragraphs. It is not intended to suggest that these methods and instruments are the optimum ones. These three methods are:

- Stylus instrument for roughness and waviness measurement. This instrument records the surface topography in a single plane normal to the surface.
- Optical flat for over-all waviness. The optical flat provides a three-dimensional view of large surface irregularities and is limited to flat and fairly reflective surfaces.
- Interferometer for microscopic measurements of surface topography. The interferometer provides a three-dimensional view of small surface irregularities.

Each of the preceding instruments may be used independently. However, in many cases, it is beneficial to use all three since they complement and compensate each other.

The stylus instrument for roughness and waviness measurement is based on the displacement of a tracer point that lightly touches the inspection surface and is moved by the surface irregularities. Such instruments measure one or more

surface characteristics depending on the maximum frequency commercially available. They differ somewhat in construction details but produce essentially the same results. Therefore, the description of such an instrument is limited to one used to obtain surface characteristics data for the flanges employed during the verification phase of this program. This inspection instrument is manufactured by the Micrometrical Manufacturing Company and is sold under the trade name "Proficorder."

A 0.0005-in. radius diamond stylus is moved mechanically across the surface in a nearly perfect plane. The stylus is connected to a differential transformer which converts the up and down stylus motion due to the surface imperfections into an electrical signal proportional to this motion. The tracing speed is 0.0005 in./sec, and the maximum length of trace is 2-1/2-in. Representation of the surface is obtained on chart paper and produced by a recorder which receives and amplifies the electrical output signal of the differential transformer. Figure 31 shows a typical trace obtained.

The amplitude sensitivity is shown as 25×10^{-6}-in. per division. Other selections available are 5-, 100-, 250-, and 1000-μin. per division. Since the reference surface of the instrument is an optical flat, all variations of the surface measured are referenced to it. The instrument is capable of producing a read-out showing only roughness and waviness, or both. Figure 31 shows a trace of waviness and roughness. Since the Proficorder is capable of measuring waviness only, it can record disturbances with a wavelength up to the maximum traversing distance. Accuracy of measurement is claimed to be 3×10^{-6} in.

In addition to flat surface measurements, the Proficorder is equipped with a rotating stylus attachment for measuring roundness of concave or convex curved surfaces. The stylus reference is a precision spindle which rotates about its center within 3×10^{-6} in. The instrument is capable of recording roughness and variations from a true circle (out of roundness) with the output displayed on a polar chart. Diameters of surfaces up to 8 in. may be evaluated.

Optical flats are circular transparent disks usually made of fused quartz or pyrex. They are fabricated in at least four grades which correspond to the accuracy of the surface. Typical grades are:

Reference	1×10^{-6} in.
Master	2×10^{-6} in.
Working	4×10^{-6} in.
Commercial	8×10^{-6} in.

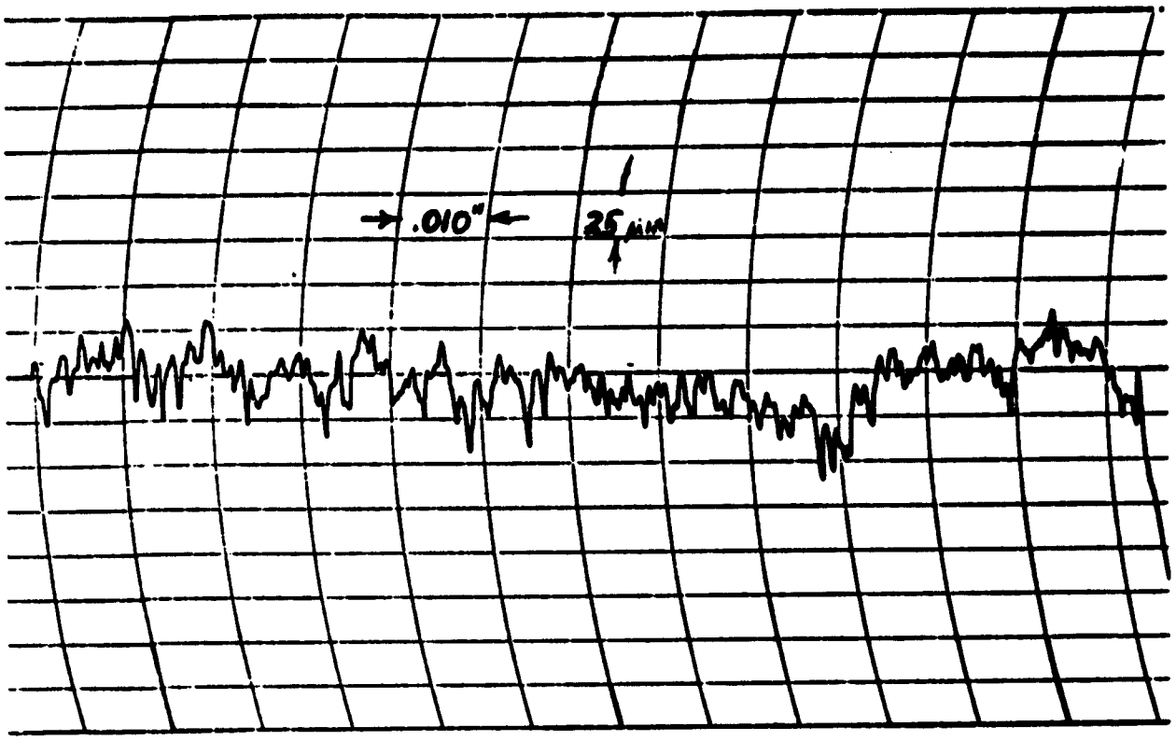

a) Surface Roughness Trace

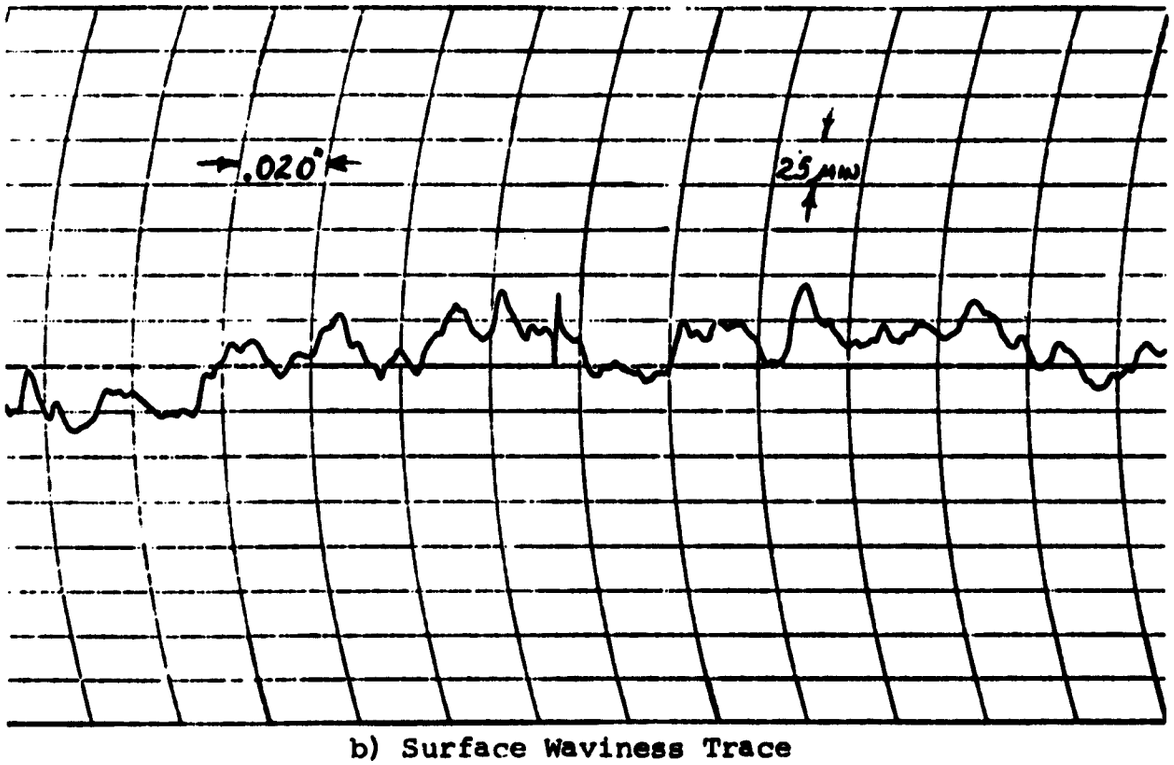

b) Surface Waviness Trace

Figure 31 Proficorder Surface Characterization Traces

Flats having diameters exceeding 24 in. are commercially available. When an optical flat is placed on a comparatively flat surface and a monochromatic light source is used for illumination, a series of bands appear. The bands are caused by light wave interference resulting from variations in the air gap existing between the flat and mating surface. When an optical flat is placed on a fairly flat reflective surface, part of the incident light is reflected from the optical flat and part of the light is reflected on the surface of the object. A wave phase difference occurs when the reflected beams recombine. This phase difference is due to the difference in the distance traveled by the light reflected from the optical flat and the light reflected from the surface of the object. When the difference in distance traveled is equal to one-half the wavelength of the light, the light beams reflected from the optical flat and the object surface cancel each other and a dark area is produced. Thus, a series of dark bands occur at integral multiples equal to one-half the wavelength of the monochromatic light. The optical flat can be thought of as carrying a number of section planes parallel to it. These section planes are assumed to intersect the surface being inspected. If these planes are separated by half a wavelength of the light, they will trace a series of contour lines (interference bands). The separation between successive bands is equal to 1.2 times the wavelength of the light. Thus, a light band corresponds to approximately 10μin. The interference pattern obtained for a perfectly flat surface would correspond to the one shown on Figure 32.

The interferometer surface evaluation instrument, in principle, operates much like the optical flat. The variation lies in the fact that the interferometer shows surface imperfections on a microscopic scale. The operating principle involves splitting of the monochromatic light beam. One portion is directed to and reflected from the viewed surface while the other portion is reflected to the surface by a mirror located at a known distance and angle with respect to the surface. When a light wave from each portion reaches the surface in plase, a bright band appears. Complete phase difference is indicated by a dark band. The distance between adjacent "like" bands is approximately 1×10^{-5} in. and is equivalent to one-half the wavelength of the thallium light source employed. Figure 33 shows a typical photomicrograph with an interferometer. The field of view is approximately 0.002 in. to the inch.

(2) Topographical Identification of Surfaces

The random topographic patterns comprising a surface appear at first glance to be unintelligible. However, these patterns can be classified in a manner which separates them by their respective wavelengths. As can be seen from Figure 34, this is possible; because the irregularities are

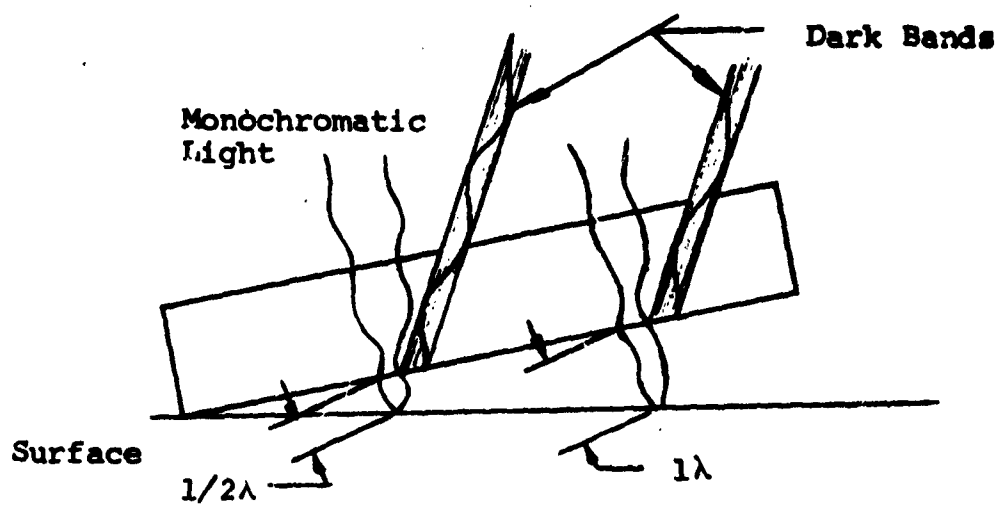

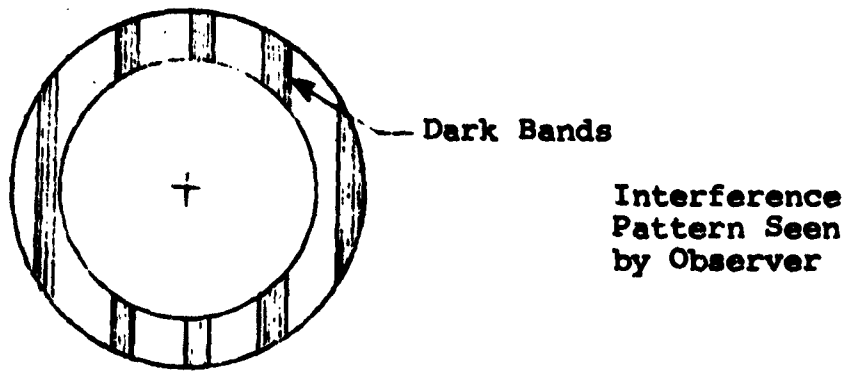

Figure 32 Interference Bands for a Perfectly Flat Surface

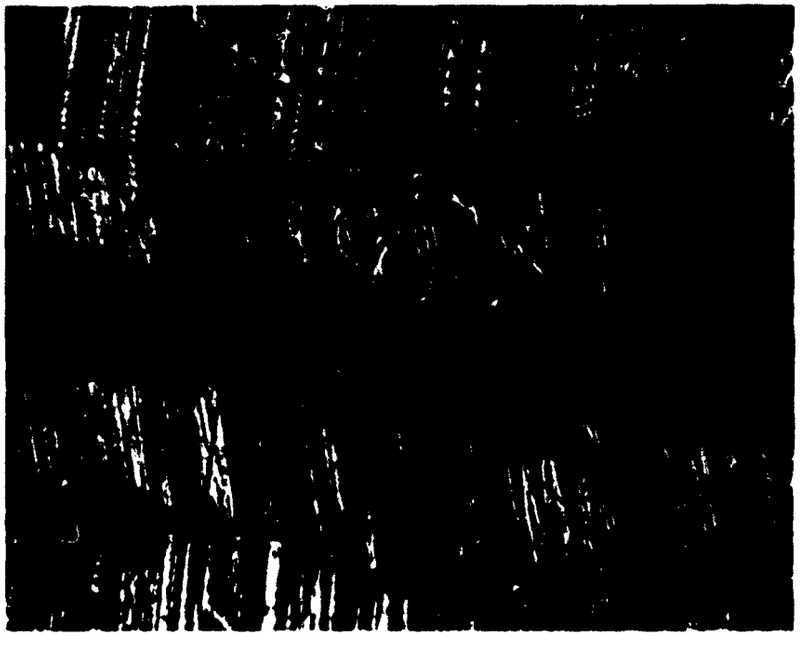

Figure 33 Interference Microscope Picture of Scratch on Test Flange Surface

a) Total Surface

b) Errors of Form

c) Waviness

d) Roughness

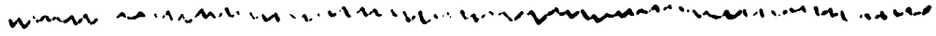

e) Material Rupture

Figure 34 Constituents of a Surface Topography

actually periodic in nature even though the waveform is complicated and difficult to interpret.

The irregularities consisting of the longest wavelength (Figure 34b) are described as errors of form. These are due to flexure of the machine or work piece, or by errors caused by the machine bearings and slideways. Superimposed on this waveform is the next shorter wavelength shown on Figure 34c. This irregularity is generally caused by component vibration or by poor truing of the cutting or grinding tool. Surface roughness is the next shorter wavelength (Figure 34d) and is caused by successive grooves or scratch marks. The shortest wavelength depicted on Figure 34c is superimposed on the roughness and results from irregularities within each groove or scratch. These are caused by rupturing of the material during chip formation.

These characteristics are broadly classified by designating them as either surface roughness or waviness. Roughness takes into account the finer irregularities caused by the cutting tool and the machine tool feed. Waviness is the wider spaced irregularity resulting from machine or work deflections, vibrations, etc. To distinguish between these two characteristics, a roughness-width cutoff is defined which specifies the maximum width (in.) of surface irregularities to be included in the measurement of roughness height. Random irregularities, called flaws, such as scratches, holes, burrs, or cracks, are present in addition to the foregoing surface characteristics. These occur at one place or at relatively infrequent intervals on a surface.

In general, the character of a surface depends upon the proper use of the machine, the particular cutting apparatus, the direction of the cut, the feed rate and cutting tool shape, the crystalline structure or chemical bond of the material, the elastic and plastic material deformations occurring during machining, and the mechanism of material removal.

An insight into the general relationship existing between machining process and surface character is obtained by considering a simple theoretical relationship which exists between tool radius, feed rate and surface finish. As the cutting tool is uniformly fed across the work piece, a scalloped surface is produced as shown in Figure 35.

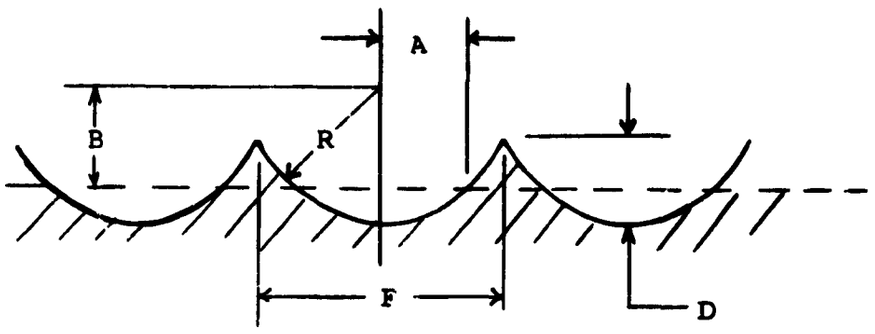

Figure 35 Geometry of a Scalloped Surface

Knowing the feed rate and the cutting tool tip or end radius, geometric relationships yield,

$$A = \sqrt{R^2 - B^2} \tag{23}$$

$$B = \sqrt{R^2 - \frac{F}{4}} + \frac{R^2}{F} \sin^{-1} \frac{F}{2R} \tag{24}$$

where

D = depth of scallop (in.)

F = feed per cut (in.)

R = tool radius (in.)

Using the feed per cut, F, and the tool end radius, R, the depth of scallop or surface finish can be predicted from,

$$RMS = \left\{ R^2 - \frac{F^2}{12} - \frac{1}{F^2} \left[\left(R^2 - \frac{F^2}{4} \right)^{\frac{1}{2}} + R^2 \sin^{-1} \frac{F}{2R} \right]^2 \right\}^{\frac{1}{2}} \tag{25}$$

$$AA = 2 \frac{R^2}{F} \sin^{-1} \frac{A}{R} - \frac{2AB}{F} \tag{26}$$

RMS is the root mean square deviation from a mean line generally given in micro-inches, and AA is the arithmetic average deviation from a mean line usually in micro-inches.

Equations 25 and 26 theoretically describe the surface topography and indicate that to obtain smooth or low roughness value surfaces, large tool end radii and small feed per cut rates are necessary.

(3) Effect of Surface Finish

The amount of deformation necessary to achieve a desired degree of sealing depends on the initial magnitude and distribution of voids comprising the leakage path. Thus, the initial topography or surface finish of the interface surfaces is an extremely important consideration in contact sealing.

At this point, several general observations can be made concerning sealing interfaces:

- In order to achieve sealing with minimum contact load, the amount of initial surface deformation necessary should be kept to a minimum. Therefore, the contact surfaces should be as smooth as possible.

- To achieve good surface conformity, one of the contacting materials should be easily deformed.

Since metallic materials are relatively rigid as compared to nonmetallic substances such as plastic and rubber materials, the influence of the initial topography on the required contact stress for sealing with metal-to-metal interfaces is extremely important.

Extensive work has been done, and is still in progress, to determine if an optimum surface topography for sealing exists (Ref. 9). The results of this study to date indicate that for metallic surfaces the best are the smoothest, flattest or roundest surfaces which can be produced. An example of the influence of initial surface topography on the contact stress required for sealing is shown for turned aluminum sealing surfaces in Figure 36 (Ref. 10). The total roughness parameter shown in Figure 36 is the sum of the peak-to-valley surface roughness of the flange and gasket surfaces. The sealed fluid was helium gas at 3 atmospheres pressure differential across the seal.

Although the results of studies on metallic sealing surfaces indicate that the best sealing surfaces are those which are the smoothest and flattest possible with present surface finishing techniques, certain practical considerations limit the choice of metallic sealing surfaces. The cost of producing nearly perfect surfaces is generally prohibitive for large-scale production using present techniques. A second and perhaps more serious limitation is the effect of contaminant particles on the contact interface.

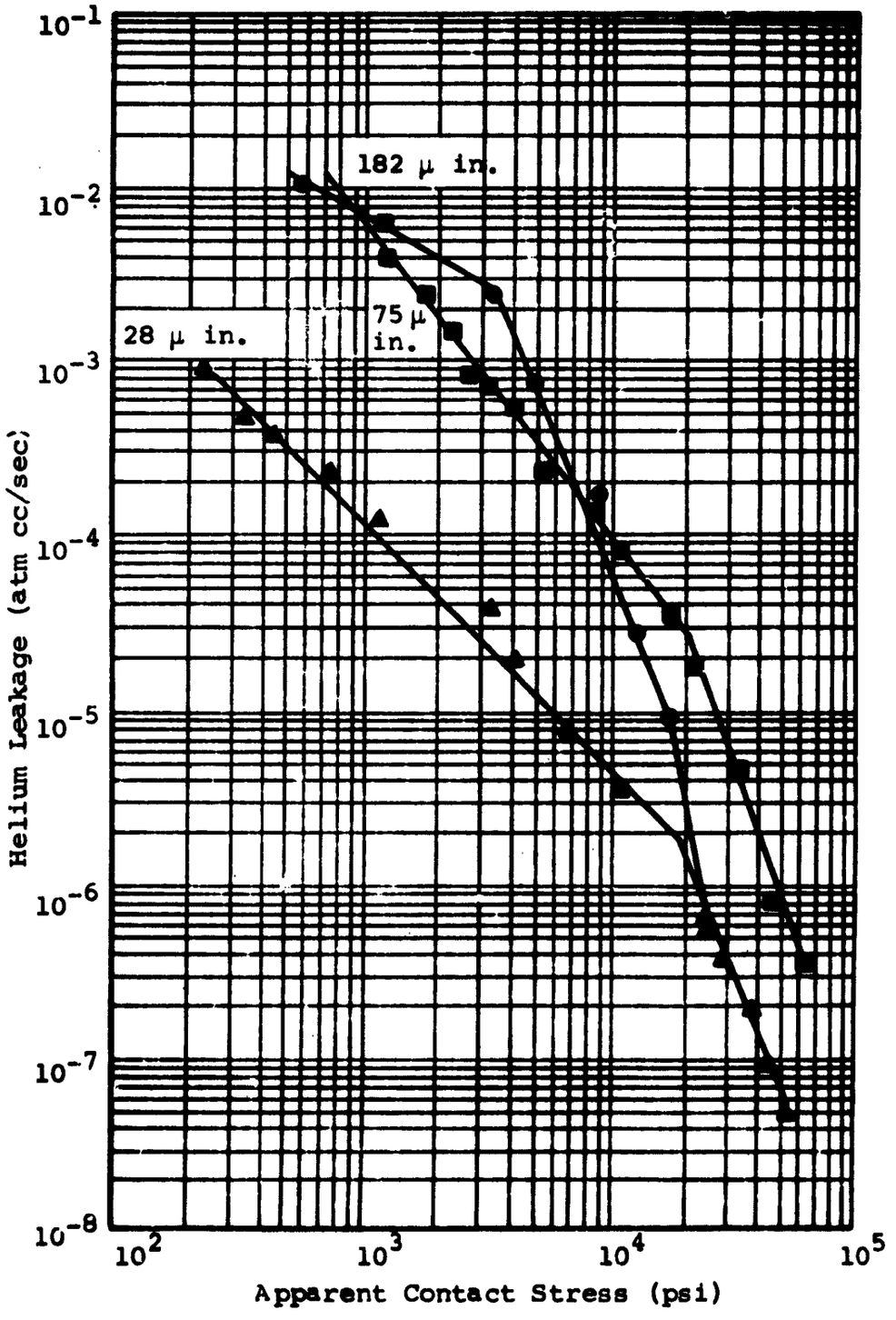

Figure 36 Comparison of Leakage for Turned Aluminum Interfaces. Total Roughness is Shown as Parameter (Ref. 10)

When the contact surfaces are smooth to less than 1 micro-inch peak to valley and flat to less than 4 microinches (less than half a light band), contaminant particles tend to separate the surfaces. Thus, the size of the leakage path will be influenced more by the size of the contaminant particles than by the roughness of the surfaces. The effect of the contaminants can be overcome by increasing the contact stress. This causes the contaminants to become imbedded in the softer surface. However, the stress required to accomplish this is usually significantly higher than the stress necessary to achieve the same degree of sealing without contaminants present. This increase in stress is often large enough to completely offset the advantages gained by using an extremely smooth surface. The cleanliness required to achieve sealing with low contact stresses (apparent contact stresses below the compressive yield point of the softer material) is difficult to achieve outside the laboratory. Either fine turned, ground, lapped, or polished surfaces using standard industrial manufacturing techniques are normally used with metallic seals.

The ability of elastomers to exhibit large elastic deformation with fairly low contact stresses makes these materials particularly attractive for use as seals. Since these materials can deform fairly easily, the effect of initial topography on the required contact stress is not as profound as in the case of metal-to-metal sealing. Figure 37 illustrates a typical leakage versus contact stress relationship for a square cross section Buna N gasket confined in a close fitting groove (Ref. 10).

A comparison of Figure 36 and Figure 37 shows that much higher stresses are necessary to achieve sealing with metal surfaces. Also, the influence of initial surface topography on the contact stress is smaller in the case of the elastomer in contact with a metallic surface. When elastomers are used as dynamic seals, smooth surfaces are required in order to reduce friction and wear.

(4) Effect of Surface Lay

The direction of surface lay irregularities resulting from a material removal process has an influential effect on leakage. In the case of turned surfaces, the deformation of asperities is localized and oriented to produce an almost continuous barrier normal to leakage flow. When the direction of lay or two interface surfaces is not the same, the deformation of asperities is localized, but not oriented, to produce an uninterrupted barrier normal to leakage flow. The case of parallel lay orientation produces a uniform barrier, but it is not normal to the leakage flow at all locations in the interface. For optimum sealing, therefore, the lay of mating surfaces should be oriented in the same direction and normal to the direction of leakage flow. This effect is

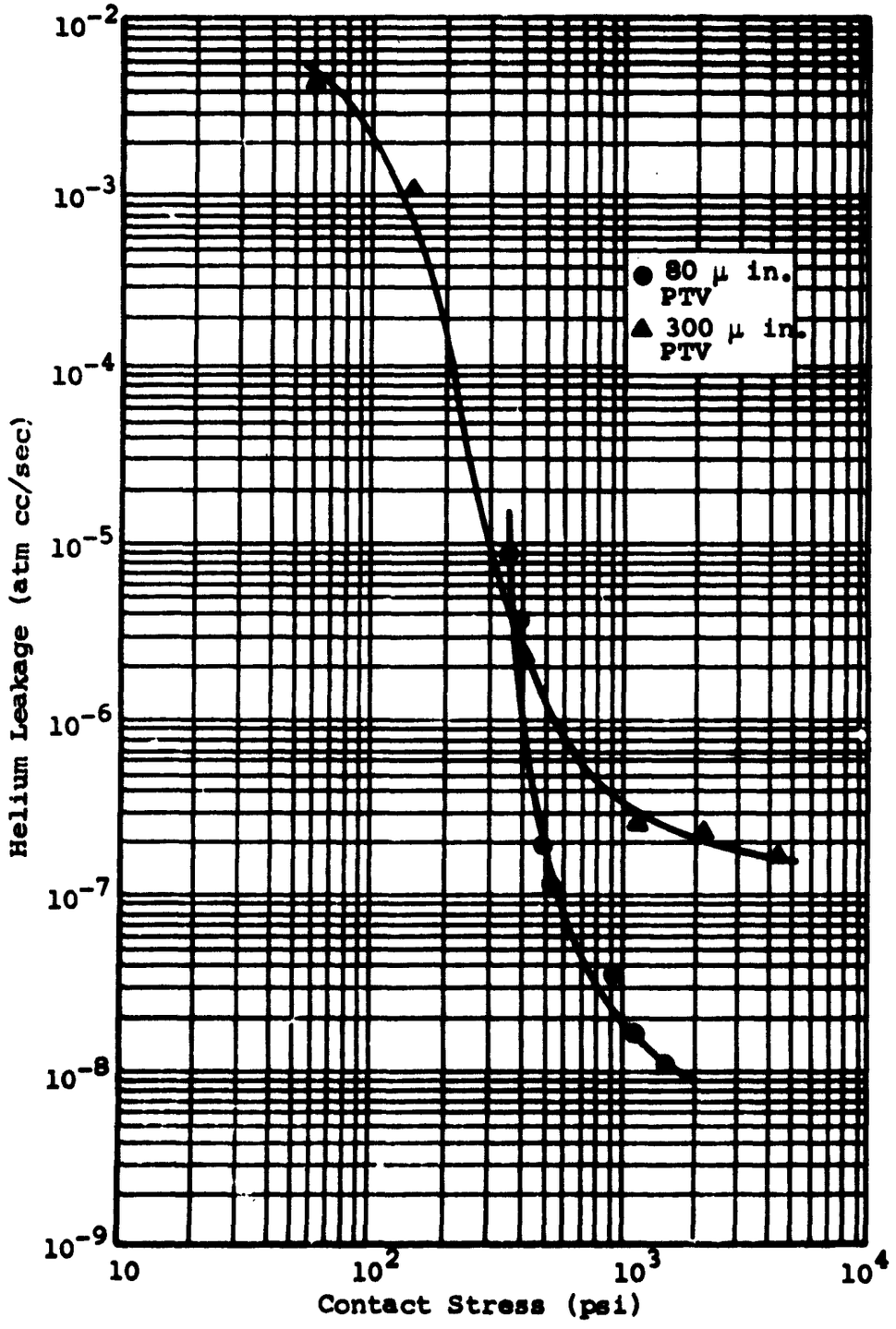

Figure 37 Leakage Characteristics of Confined Buna N Gasket (Ref. 10)

predominant in metal to metal interface seals. In elastomer or plastic to metal interface seals, the effects of material properties related to surface condition conformability are more influential than surface lay.

c. Relation of Deformation and Material Properties

The effect of material properties on deformation has been identified as influential in the previous discussions. The specific material properties were identified as hardness, yield strength, oxide and other contaminant layers, and strain hardening. Experiments were conducted on previous seal investigations (Ref. 9 and 10) to determine the effects of material properties. These tests consisted of a series of leakage experiments using materials having a wide range of properties but essentially the same surface finish.

The principal properties investigated were hardness and yield strength. Since both properties describe the resistance of a material to deform, either property could be used to describe the material. The yield strength is defined as the stress that will produce a small amount of permanent deformation (generally, a strain equal to 0.01 or 0.2 per cent of the gage length of a specimen). The geometry of the specimen is usually standardized since the degree of strain is significantly affected by the geometry. To develop criteria for any geometric configuration, a material property should be independent of the geometry. On this basis, the yield strength property was not applicable.

Material hardness, however, is independent of the geometry and, therefore, is considered further. The hardness of a material is a measure of its resistance to permanent or plastic deformation. The instrumentation used for hardness measurement is readily available. The Brinell hardness measurement test is the most commonly used method of hardness measurement for metals and plastics. The Brinell hardness test consists of indenting a surface with a 10-mm diameter steel ball with a load between 500 and 3000 kg, depending on the softness of the material. The load is applied for a standard time, usually 30 seconds, and the diameter of the indentation measured with a low power microscope. The Brinell hardness number (BHN) is expressed as the load, P, divided by the surface area of the indentation:

$$BHN = \frac{P}{\left(\pi \frac{D}{2}\right)\left(D - \sqrt{D^2 - d^2}\right)} \qquad (27)$$

where

P = applied load, kg

D = diameter of ball, mm

d = diameter of indentation, mm.

The Brinell hardness test has several deficiencies that limit the interpretation of results. Foremost is the requirement for geometrical similarity of the indentation diameter and ball diameter for any applied load. This condition is not adhered to in general engineering practice. Another deficiency is the error in measuring the impression diameter caused by elastic recovery and ill-defined edges.

An improved method consists of using a hardness value suggested by Meyer based on the projected area of contact (Ref 31). The mean contact stress between the surface of the indenter and indentation is given as the Meyer hardness and is equal to the load divided by the projected area of the indentation.

$$\text{Meyer Hardness} = \sigma_m = \frac{4P}{\pi d^2} \tag{28}$$

Meyer hardness is reportedly less sensitive to applied load than Brinell hardness. For a cold-worked material, the Meyer hardness is essentially constant and independent of load, while the Brinell hardness decreases as the load increases (Ref. 31). For an annealed material, the Meyer hardness increases continuously with increasing load, whereas, the Brinell hardness first increases and then decreases.

The durometer system is the only general approach at classifying the hardness of rubber materials. This system functions on a comparative basis in that the stiffness of one rubber is compared to another. A device capable of measuring the durometer value of rubber materials is the "Shore Hardness Test."

The hardness measurement is made by pressing a blunt point into the surface of the rubber and comparing the indentation resistance to a calibrated spring. A pointer amplifies and displays the amount of spring deflection.

To employ the material hardness as a parameter in the leakage prediction process, correlation between the conductance parameter, contact stress, and hardness is necessary. Section IV.6 discusses this correlation.

5. STRUCTURAL ANALYSIS CONSIDERATION

In order to maintain interface conditions necessary for efficient sealing, a housing or supporting structure containing the seal must provide these conditions during all operational modes. Therefore, the definition of these conditions must

receive attention during any structural analysis and act as input data for housing or support structure design.

Generally, housings can be divided into several groups such as:

- fluid line connection
- covers or doors
- dynamic seal support

The structural loads which are applied, as well as, the variations in configuration differentiate the groups from each other. The structural loads which the housing is experiencing include:

- separation force due to sealed fluid pressure
- torsion and bending due to misalignment and thermal expansion
- hoop stresses due to fluid pressure

In addition to the structural loads applied to the housing, the effects of variable temperature conditions must be considered. These effects result in:

- reduced contact stress at the seal interface due to creep or relaxation
- reduced physical material properties
- increased brittleness of materials at cryogenic temperatures
- variations in thermal expansion due to material property differences in the seal and housing.

Fatigue problems due to vibration and cyclic loading must also be included in an analysis. Thus, the problem of housing design is a complex process. The final design may consist of a compromise between the conflicting limitations of strength and weight.

A generalized approach to the structural analysis of a pressure vessel cover has been undertaken by Reference 10. The approach taken was to adapt existing plate and sheet theory in order to establish relationships for the description of the elastic displacements that take place in the housing close to the seal-housing contact region.

A general cover geometry was chosen, with the restriction that the geometry must have cylindrical symmetry. The cover geometry is shown in Figure 38.

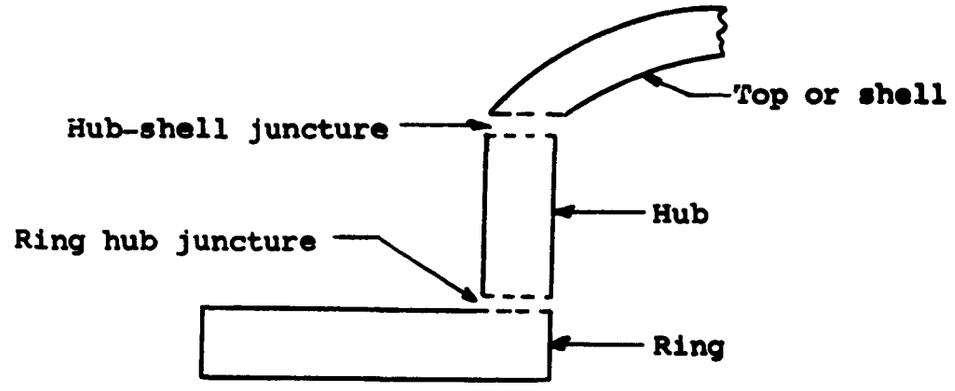

Figure 38 General Cover Geometry

Each of the cover members elastically deform when the pressure, clamping, and seal reaction forces are applied. Thus, each cover part must undergo a separate deformation analysis. The internal stresses at the junctures of the members are replaced by undetermined forces and moments to effect such an analysis. A set of simultaneous deflection equations are developed whose solution is accomplished by the use of the common boundary conditions (displacement and rotation) at the junctures. To effect a flexible analysis, one invariant boundary condition is assumed and the other being imposed by the fastening mechanism for which a known load-deflection curve is assumed to exist. This latter type of boundary condition requires the use of an iterative procedure since the load-deflection characteristics of the fastener must be matched by the loading and deflection properties of the cover.

The actual process of iteration is accomplished through the reaction loading system which provides a measure of convergence of the solution. In particular, an initial reaction load is chosen; this provides the loading on the fastener, such as bolts arranged along the bolt circle. The deflection of the fastener is determined from its load-deflection characteristics which then provides the necessary boundary condition on a ring. All the requirements of the cover equations are then fulfilled which makes a complete cover deformation solution possible. The reaction load is then adjusted to be compatible with these resulting deformations, and the process repeated until convergence on the reaction load and corresponding deformations is attained.

These deflection equations can be programmed for solution by a digital computer. The coding system may be Fortran II source language. The results of these solutions can be presented in tabular or graphical form. Thus, a designer can determine the elastic displacements in the vicinity of the seal for any geometry of cover meeting the restriction of cylindrical symmetry, and for the various modes of seal contact:

- total contact (i.e., flat gasket with bolt holes)
- contact within the bolt or clamping circle
- contact outside the bolt or clamping circle
- contact both within and outside the bolt or clamping circle but not total contact

These forces and the deflection results are combined with the seal structural design criteria to yield a complete structural and leakage performance analysis for the entire seal assembly.

The general approach of the foregoing discussion can be used for any cover geometry having cylindrical symmetry, simply by applying the appropriate boundary conditions. However, a simplified approach is suggested by Reference 10 to describe the relationship between cover design and deflection. The problem involved solution for small elastic deflections in thin circular flat plates employing the methods detailed in Reference 36.

Figures 39 and 40 are plots of the results obtained from this simplified approach and indicate that for a given pressure, stress level, and material, the slope at the seal location increases slightly with the radius ratio of real location from axis/outside radius of cover which is a geometry parameter. Figure 39 illustrates the behavior of the deflection parameter as the geometry parameter varies. This indicates that for a given material, pressure, and stress level, the ratio of deflection parameter/cover radius decreases with increasing geometry parameter. Since an increasing value of the geometry parameter is obtained as the cover becomes rather large, the deflection at the seal will also be larger. Thus, for a given geometry parameter, a larger cover will indicate correspondingly larger deflection.

The cover deformation analysis show deflections and slopes that are expected at the seal location. The next important criterion is the means which attaches the cover to the pressure vessel. The most frequently used scheme employs a bolt. A great deal of information is available on bolt loading, preloading, torque to load relationship for such fasteners. The general requirements which the bolt must comply with are:

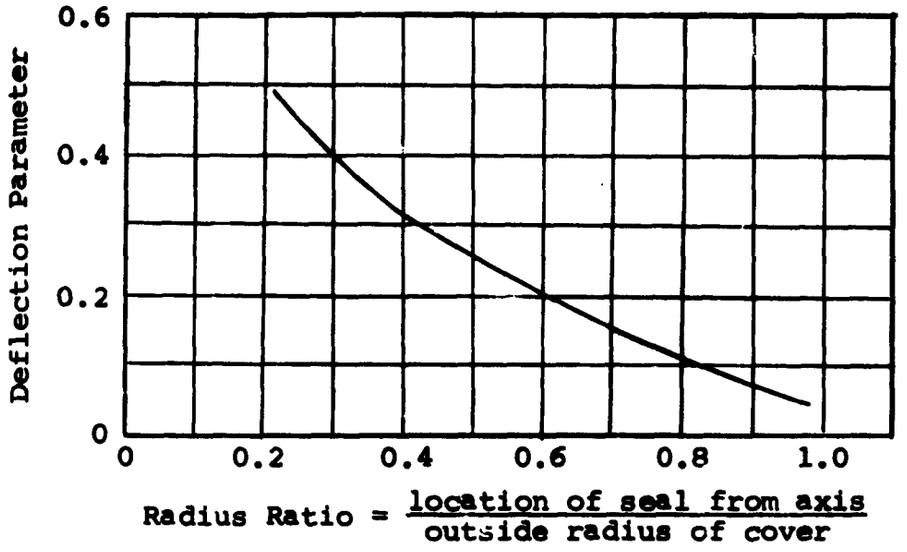

Figure 39 Deflection Parameter Versus Radius Ratio for a Flat Cover

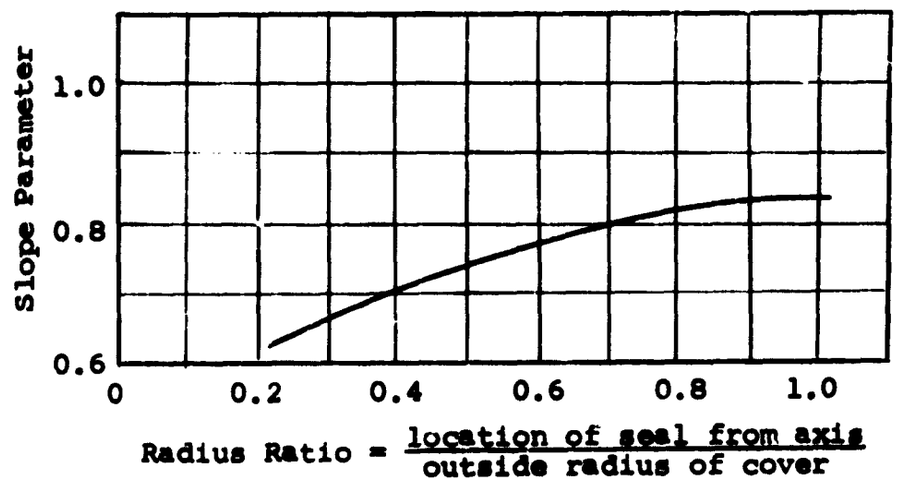

Figure 40 Slope Parameter Versus Radius Ratio for a Flat Cover

- The bolts must be capable of providing the initial contact force required by the seal.

- The bolts must be capable of withstanding the full fluid pressure force with tolerable elongation.

- The bolts and other members of the seal and housing assembly must have carefully mated thermal properties.

As indicated previously, the effects of thermal expansion of the components comprising a seal and housing assembly can exert a significant influence on the assembly's performance. The differences in expansion or contraction of the components can cause displacements equal to or greater than the deflections due to structural forces imposed on the seal assembly. Thus, minimizing the thermal expansion problem by matching material properties as closely as possible is necessary. Another method of temperature compensation can be effected by designing the seal such that sufficient elastic-deflection in the seal structure is available to maintain adequate contact force at the interface after thermal effects have occurred.

In addition to the thermal effects noted above, temperature changes have subtler influences on the seal and housing assembly in the form of physical property variations. Increasing temperature produces a decreasing modulus of elasticity. Thus, more deflection is obtained for a given applied force. Structures at high temperatures are less rigid under the same loading conditions than ones at lower temperatures. The material-yield strength at elevated temperatures must also be considered when designing a structure for operation at high temperature.

Creep, which is the slow, steady, continuous plastic deformation that occurs in most metals at elevated temperatures and at stress levels far below the materials yield strength, must be considered if long periods of operation at such temperature levels are anticipated. Quantitative data on creep are extremely limited, and little is known about the theoretical basis of the phenomenon. The creep strength is usually defined as that stress which produces a given elongation at a given temperature during a given time interval.

The available information on creep strength cannot readily be interpolated or used to find creep rates at varying conditions of stress and temperature. Often, experimental evaluation under specific conditions is necessary to evaluate the creep properties of a material.

Dynamic sealing applications require contact stresses of lower values at the interface than static sealing applications.

The seal configuration generally provides the required contact stress to effect sealing. Examples of such configurations are the lip-type sliding seal where lip deflection provides the contact stress, and the face-type rotating seal where the hydrostatic balance force and the loading springs supply the necessary force. The housing design does not directly contribute to the contact force.

The housing of dynamic seals supports the seal in a manner whereby positional relationship between the sealing contact surfaces is maintained. Some inherent motion of the moving surfaces is present in dynamic seal applications, however. This undesired and unnecessary motion is caused by:

- bearing play, eccentricity, misalignment
- side loading and variations in shaft straightness
- variations in shaft diameter and out-of-roundness

In order to compensate for this secondary motion, most dynamic contacting seals have built-in flexible supports. An example of this is the spring loaded face-type seal. The spring-loaded face has freedom to wobble slightly about a plane perpendicular to the axis of shaft rotation. Thus, the face can follow the motions of the mating seal configuration member. Hence, the designer of dynamic seal housings must consider not only those structural criteria described in the static seal housing discussion, but the additional, associated dynamic seal problems of:

- seal support flexibility
- bearing rigidity or stiffness
- part roundness and straightness
- elimination or reduction of misalignment
- special housing functions

The one major objective of all seal and housing structural design considerations is to provide and maintain the necessary interface conditions for adequate sealing during all conditions of operation. The design process for static sealing applications can be summarized as follows:

1) Operating temperature and fluid media compatibility govern the selection of seal assembly materials.

2) The material selected, with its properties, permits the calculation of a conductance parameter.

3) The necessary contact stress required for obtaining such a conductance parameter can be estimated. The applied load to effect the contact stress is used as input data in the structural analysis of the seal and housing.

4) The design of the seal and housing requires the use of iteration. The seal configuration and the initial contact load determine the initial seal deflection. The required seal load retainment is determined by the initial load and the hysteresis characteristics of the seal material. This establishes the permissible mating surface deflection opposite to the direction of seal deflection.

5) If the estimated housing deflection is greater than the allowance as determined from (4), the design must be modified. The choice of which component to modify is made by the designer after consideration of the following:

- the relative difficulty of modification on the seal or the housing
- the size limitations of the seal
- effect of manufacturing inaccuracies
- weight
- cost

The important design considerations presented illustrate a systematic procedure for seal and housing design. To achieve maximum effectiveness of available sealing techniques, seal and housing design, as well as, leakage prediction must be an integrated process.

6. DESIGN ANALYSIS

a. Design Analysis of a Rubber Seal

The low leakage levels attainable with elastomeric seals, in applications where the environmental conditions permit their use, have led to their widespread use. The state-of-the-art of these seals is well advanced as compared to static and

dynamic seals of other materials. The developmental areas which have received emphasis are structural configuration and material characteristics. The requirement for standardization due to their wide usage is the most significant factor in the establishment of design criteria for rubber seals. Criteria are normally tabulated as dimensional data based on seal shape and groove configuration. These criteria are beneficial to the designer because seal designs possessing the necessary characteristics for achieving minimum leakage are obtainable. No analytical technique for estimating the leakage value for the seal design, however, is available. The development of such techniques would advance the state-of-the-art of elastomeric sealing, as well as result in such benefits as:

- Prediction of leakage performance
- Minimization of experimental efforts to obtain relationships between seal configurations, groove dimensions, and applied load
- A method of comparison for various seal shapes

The following summarizes a method of analysis for rubber seals using theoretical, as well as, empirical considerations.

The conductance parameter concept described in Section IV.2 is dependent on, and obtained from, the geometry of the interface, interface forces, theoretical flow equations, and experimentally determined leakage values. The conductance parameter, however, must be solely dependent on the interface forces. This relationship was established from leakage experiments with subsequent calculations for determining the conductance parameter as shown on Figure 41. It was determined experimentally (Ref. 9) that the effects of fluid pressure could be neglected. A mathematical expression developed during previous work (Ref. 9, 10) for approximating the conductance parameter-stress relationship is:

$$h_x = \frac{5.7 \times 10^{-10} \quad H^{3.25}}{\sigma_x} \qquad (29)$$

where

h = conductance parameter

σ = apparent contact stress

H = rubber hardness

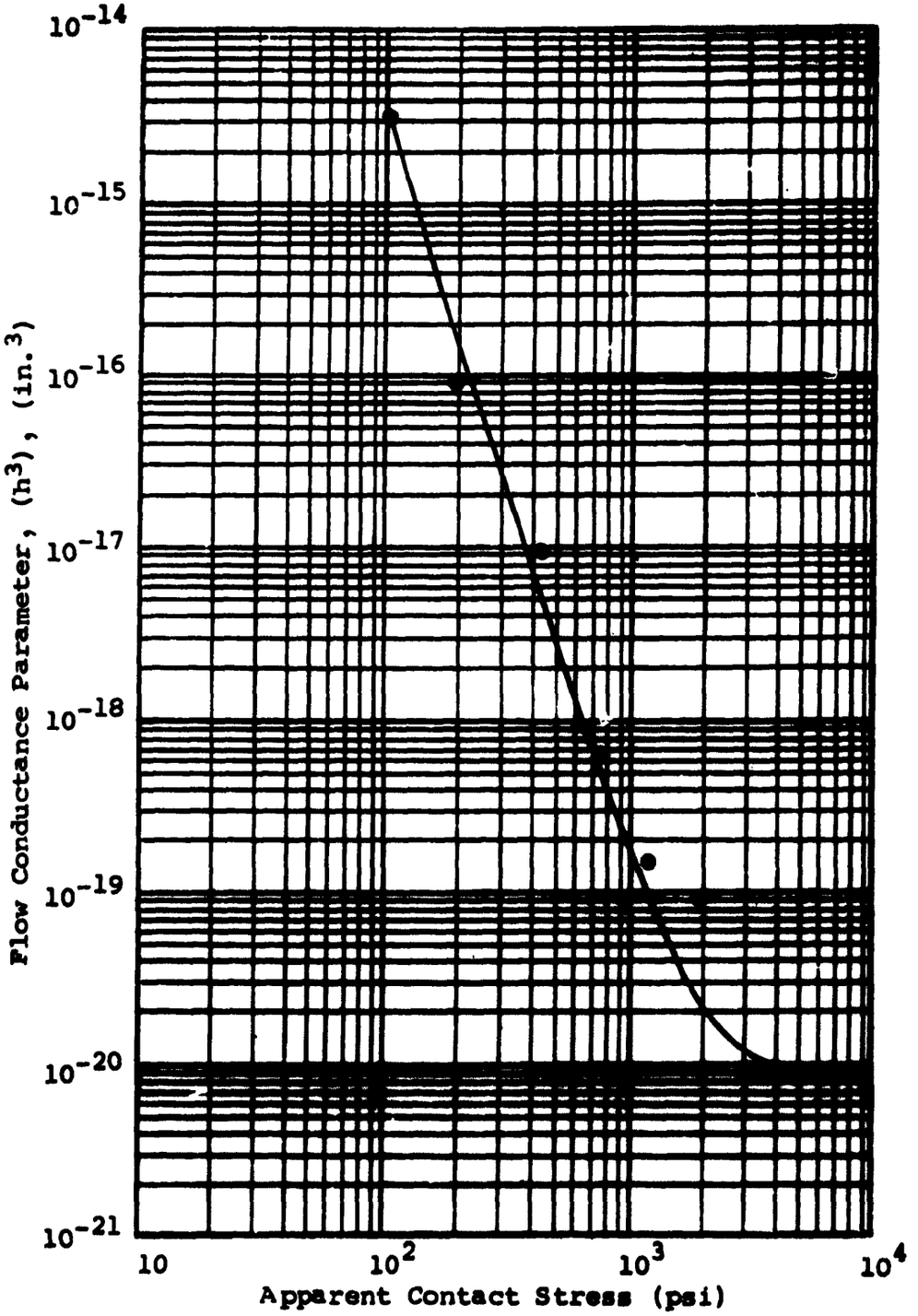

Figure 41 Flow Conductance Parameter as a Function of Contact Stress for Buna-N Gaskets with an Interface Roughness of 300 μ in. (Helium, 2 Atmospheres Pressure, 85°F) (Ref. 9)

Equation 29 was obtained by employing curve-fitting techniques and specific boundary conditions. A first approximation of the interface forces-conductance parameter relationship is obtained from an expression of the form

$$h_x = \frac{K}{\sigma_x^m}$$

where K and m are constants. It can be noted that as the contact stress approaches zero, the conductance parameter becomes infinitely large. The conductance parameter is an equivalent leakage gap clearance, and large values of conductance indicate interface separation. To alleviate this condition, which does not comply with the assumption of interface contact previously made, the limiting value of conductance is assumed equal to the solid surface peak-to-valley roughness. The expression for conductance-contact stress is then,

$$h_x = \frac{K}{a + \sigma_x} \left(\frac{H}{70}\right)^{3.25}$$

where $a = K/h_o \left(\frac{H}{70}\right)^{3.25}$ and h_o is the peak to valley roughness.

A rubber seal of rectangular cross-section is used to illustrate the procedures necessary for combining the conductance-stress relationship with a force and leakage analysis. The experimental equipment used for verification of the data is shown on Figure 42. The empirical data was obtained from Reference 9. The geometry of the flange is represented as a rectangular shaped one with no leakage past the edges. This approximation entails neglecting the curvature of the seal ring and is valid when the ring width is small compared to the diameter. The approximate geometry is depicted on Figure 43 with the forces acting on the cross-sectional element (Figure 44).

The forces imposed on the seal cross-section consist of the external load, the fluid pressure, and the contact forces between seal and flange. A summation of these forces acting on one interface yields:

$$\frac{F_N}{LX} = F - \frac{p\pi D_i^2}{4} - p_x - \sigma_x \qquad (30)$$

where

F = flange load

F_N = net normal force

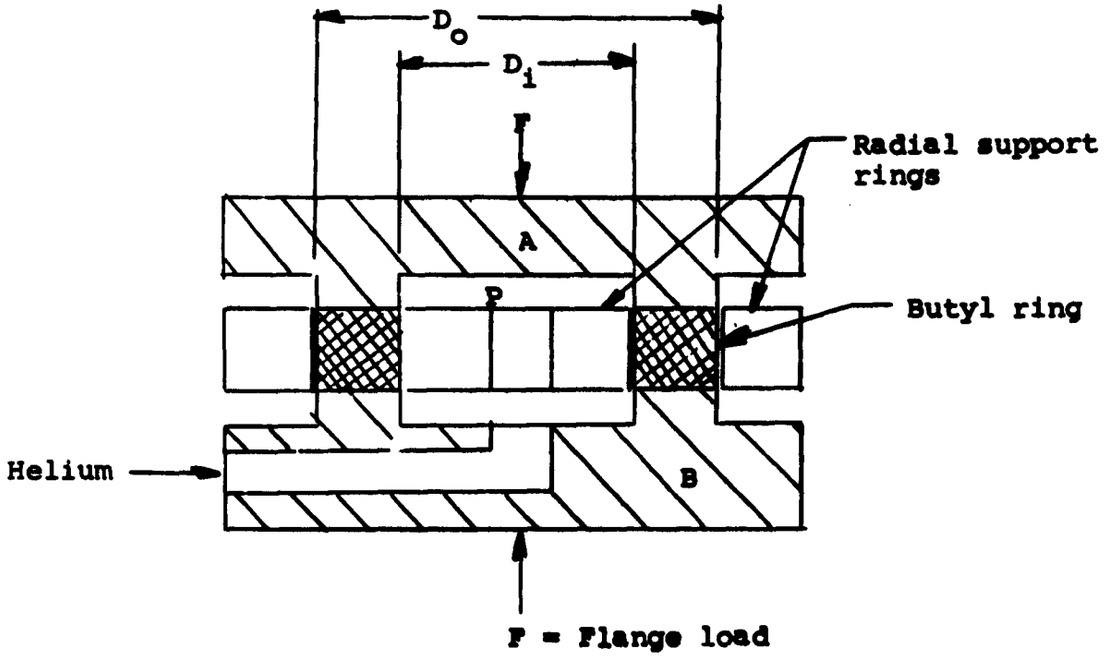

Figure 42 Experimental Apparatus for Evaluating Rubber Materials

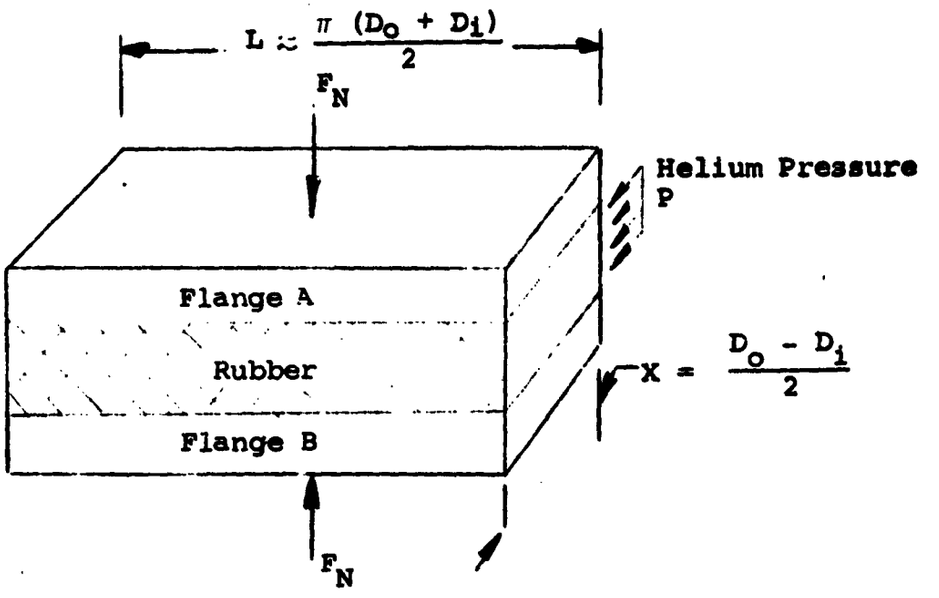

Figure 43 Approximate Geometrical Representation of the Seal Interface

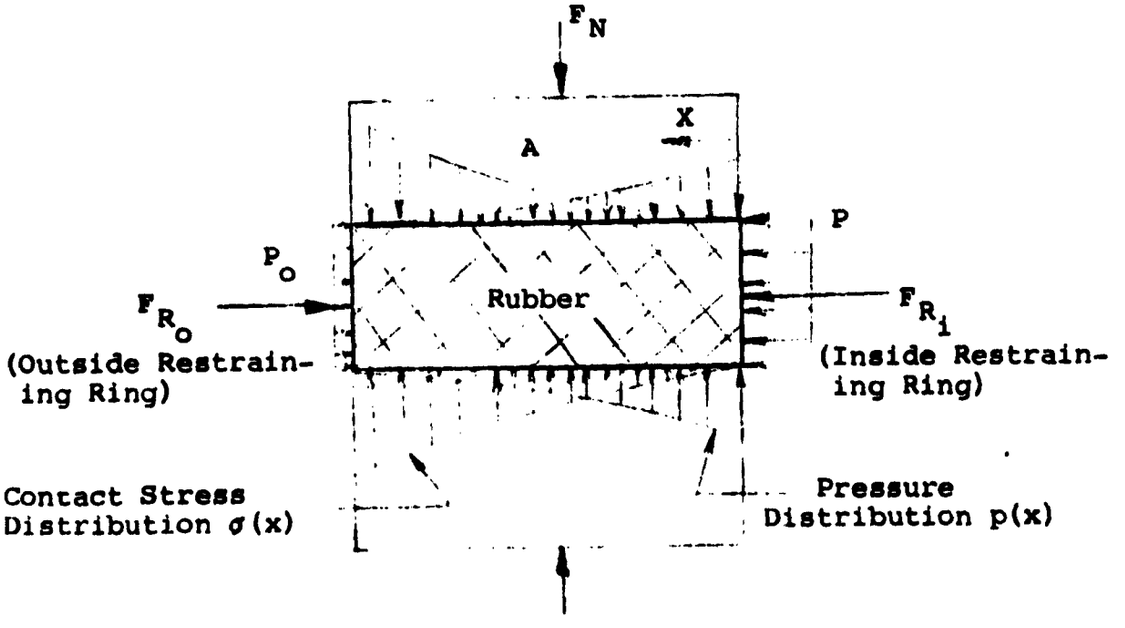

Figure 44 Pressure and Contact Forces Acting at the Interface

σ_x = contact stress at any point

p_x = fluid pressure at any point

When the conductance parameter obtained from equation 29 is introduced into the equation for weight rate of flow through two interfaces under the conditions of laminar, compressible flow results in an expression of the form,

$$W = \frac{\rho L (h_x)^3}{6\mu} \frac{dp}{dx} \tag{31}$$

Rearranging terms:

$$W \int_o^x dx = \int_{p=p}^{p=p_o} \frac{L(h_x)^3 p \, dp}{6\mu RT} \tag{32}$$

The conductance parameter-contact stress relationship was shown to be:

$$h^3 = \frac{7.1(10^{-4})}{a + \sigma} \left(\frac{H}{70}\right)^{9.75} \tag{33}$$

Combining equations 30, 32, and 33 results in

$$W = - \frac{L(1.85)(10^{-28}) \quad H^{9.75}}{X6\mu RT} \int_{p=p_1}^{p=p_o} \frac{p}{\left(a + \frac{F_N}{LX} - p\right)^3} \, dp$$

and integration yields:

$$W = \frac{L(1.85)(10^{-28}) \quad H^{9.75}}{X6\mu RT} \left[\frac{a + \frac{F_N}{LX} - 2p_o}{2\left(a + \frac{F_N}{LX} - p_o\right)^2} - \frac{a + \frac{F_N}{LX} - 2p_1}{2\left(a + \frac{F_N}{LX} - p_1\right)^2} \right] \tag{34}$$

By substitution of the physical seal, fluid, and pressure values into equation 34, the volume leakage rate at standard temperature and pressure can be determined. These properties for a butyl rubber seal for experiments conducted by Ref. 9 and 10 are:

H = 70 Shore A

h_o = 46μin. PTV

μ = 2.83×10^{-9} lb/sec/in.^{2} viscosity of helium

$X = (D_o - D_i)/2 = 0.134$ in.

D_o = 2.500 in.

D_i = 2.232 in.

$$L = \frac{\pi(D_o - D_i)}{2} = 7.42 \text{ in.}$$

$$Q_o = \frac{WRT}{P_o}$$

The pressure conditions applicable for the sealing conditions of interest to this program are,

p_1 = 14.7 psia

p_o = 0 psia

The leakage rates attainable for varying flange loads can be calculated to obtain curves similar to those shown on Figure 45.

The procedures can be applied to many different shape seal configurations and modes of flow. The appropriate force and flow relationships must be determined and combined with the conductance-stress relationship to obtain a leakage analysis. An analysis of an O-ring rubber seal is shown in Section VI.

In summary, it can be noted that the analysis requires:

- the assumption that a leakage path exists at the interface
- an empirically derived expression for the relationship between conductance parameter and contact stress
- the assumption of a mode of flow
- the empirical conductance correlation description of the deformation in an interface

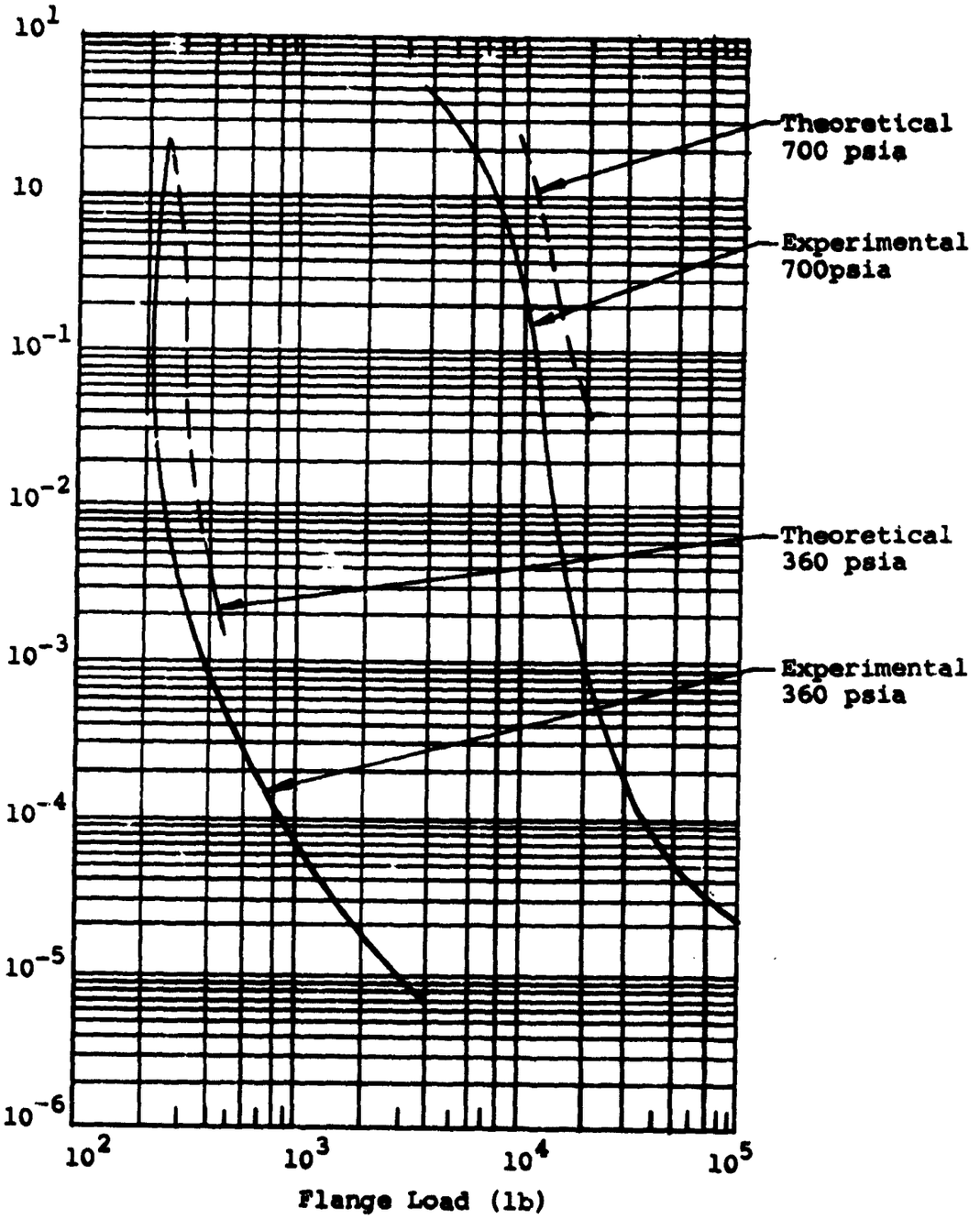

Figure 45 Theoretical and Experimental Leakage Characteristics of a Butyl Rubber Ring.

- the acceptance of the theory that both contact forces and fluid pressure can simultaneously exist at any point in the interface.

b. General Seal Design Analysis Procedure

To summarize the design analysis presented in the previous discussions, as well as, provide the designer with concise design procedures, a step by step outline for a general seal design analysis is presented.

Step 1: Calculation of Initial Load on the Seal Interface

The definition of the net seal interface load is the external load necessary to deform a seal structure a given distance. The physical properties, as well as, material properties which govern the resistance to plastic or elastic deformation establish the relationship between load and deflection.

To exemplify this, a generalized seal is presented on Figure 46 depicting the deformation occurring during initial seal installation. The forces required to deform the seal can be expressed by

$$F = F_o = K (X_i - X_o) \qquad (35)$$

where

F = flange load per unit length of mean interface circumference

F_o = initial net contact load

K = proportionality constant

X_i = initial thickness of seal

X_o = final or installed thickness of seal

In the case of the U-shaped seal depicted, the flange load is equal to the net interface force. Since both legs of the seal are uniform, the deflection per leg is,

$$\gamma_1 = \gamma_2 = \frac{F_o}{K} \text{ and}$$

$$\gamma_1 + \gamma_2 = X_i - X_o \text{ where,}$$

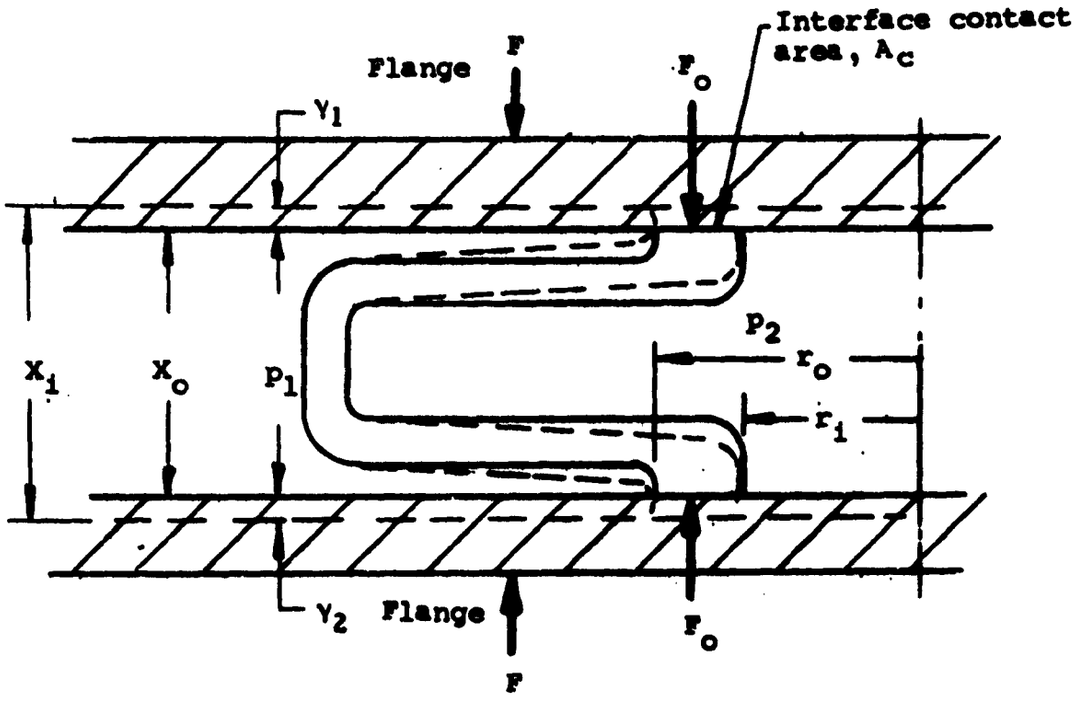

Figure Generalized Seal Example

γ_1 and γ_2 are the deflection per seal leg. The proportionality constant, K, and the leg deflections are obtained from seal structure analysis. For configurations involving plastic deformation or structures difficult to analyze, experimentally determined load-deflection characteristics can be employed to obtain values for K and γ.

Step 2: Determination of the Initial Interface Contact Stress

The concept of an apparent interface contact stress defined as the applied load divided by the apparent area of contact was discussed earlier. Uniform stress distributions for seals configurations having well defined interface surfaces parallel to the mating surface can be assumed. Interface surfaces which are nonparallel or irregular are more difficult to analyze and may require experimental determination of the contact area. For slight departures from the parallel condition, the assumption may be made that uniform stress distribution exists.

The minimum external applied load, F, must be sufficient to counteract the fluid pressure forces, thereby preventing separation of the interface surfaces. The minimum external load is determined by the maximum fluid pressure, the seal housing geometry, and the pressure gradient due to leakage at the interface.

The following example is selected to demonstrate the design considerations necessary to effect this step of the design procedure. The arrangement depicted on Figure 47 consists of a seal pressed between a flange or cover and a housing.

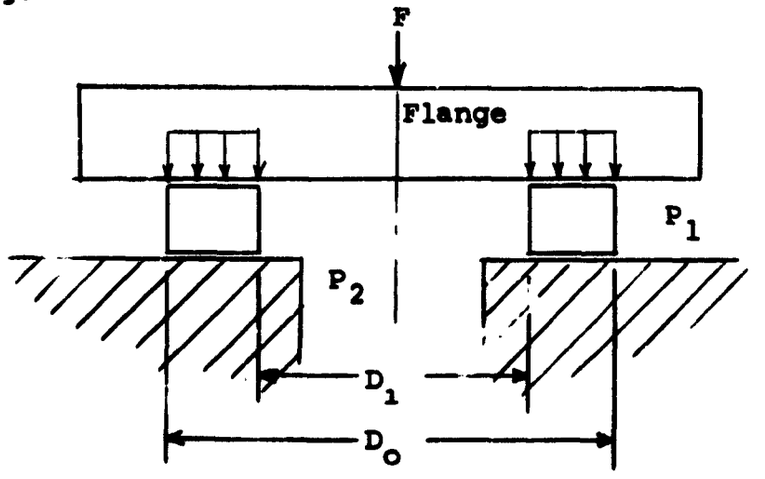

Figure 47 Uniform Pressure Gradient Acting on Gasket-Flange Assembly

The summation of forces acting at the interface result in:

$$F = (P_2-P_1)\ (\frac{\pi D_o^{\,2}}{4}) + \sigma \left[\pi \frac{(D_o^{\,2}-D_i^{\,2})}{4}\right] \tag{36}$$

Interface separation is neared as the contact stress, σ, approaches zero. Thus, the minimum flange load is:

$$F_{min} = (P_{2max} - P_1)\ (\frac{\pi D_o^{\,2}}{4}) \tag{37}$$

In the absence of fluid pressure, the initial minimum contact stress is governed by the minimum flange load,

$$\sigma_o = \frac{4F_{min}}{\pi(D_o^{\,2}-D_i^{\,2})} \quad \text{or}$$

$$\sigma_o = (P_{2max} - P_1) \left[\frac{1}{1 - \frac{D_i^{\,2}}{D_o^{\,2}}}\right] \tag{38}$$

Step 3: Calculation of Contact Stress Resulting from the Combined Effects of Initial Deformation and Fluid Pressure

Either an increase or decrease in contact stress, depending on the seal configuration, may result when fluid pressure is applied. The rectangular cross-section seal depicted on Figure 47 will exhibit a decrease in contact stress due to the radial deformation of the seal when fluid pressure is applied, while the seal shown on Figure 45 will produce an increase. The deformation considerations for the flange or housing discussed in Section IV.5 must also be considered during this step. If, however, very small flange deflections are encountered, they may be neglected. The deformation due to pressure effects is assumed to be small compared to initial installation deformation. The apparent contact stress may be stated as,

$$\sigma = \sigma_o + \sigma_s - \sigma_G \tag{39}$$

where

σ_s = stress contribution due to applied pressure on the seal structure

σ_G = stress contribution due to the pressure gradient in the interface

Since σ_s and σ_G are functions of the pressure difference across the seal interface, the definition

$$\sigma = \sigma_o + C\ (P_2 - P_1) \qquad (40)$$

is made where C is a pressure energization constant for a particular seal configuration.

Step 4: Determination of the Flow Conductance Parameter for the Seal Interface

A description of the conductance parameter appears in Section IV.2 with methods of application discussed and shown in Section IV.6a and Section VI. The method of obtaining a conductance parameter value for relatively flat surfaces can be either of the following:

Graphic, from data experimentally obtained and plotted as a function of material properties and surface characteristics. A sample of such data is shown on Figure 48. To utilize this method the contact stress, as well as, the material and surface finish properties must be known.

Approximation, from experimental data relating material hardness, apparent contact stress, and conductance parameter. A sample of such data is given on Figure 49. To effect this method, the Meyer hardness of the softer material forming the interface must be known.

The following rules established by Reference 9 and 10 must be observed in applying either of the methods:

- The surfaces composing the interface must be nearly parallel
- The softer interface material with its properties must be employed in determining the conductance value
- The sum of the peak-to-valley roughness of the mating surfaces should be applied for determining the conductance parameter when surfaces of similar hardness values are pressed together. When dissimilar hardness materials are used, the interface roughness is defined as the roughness of the harder surface.

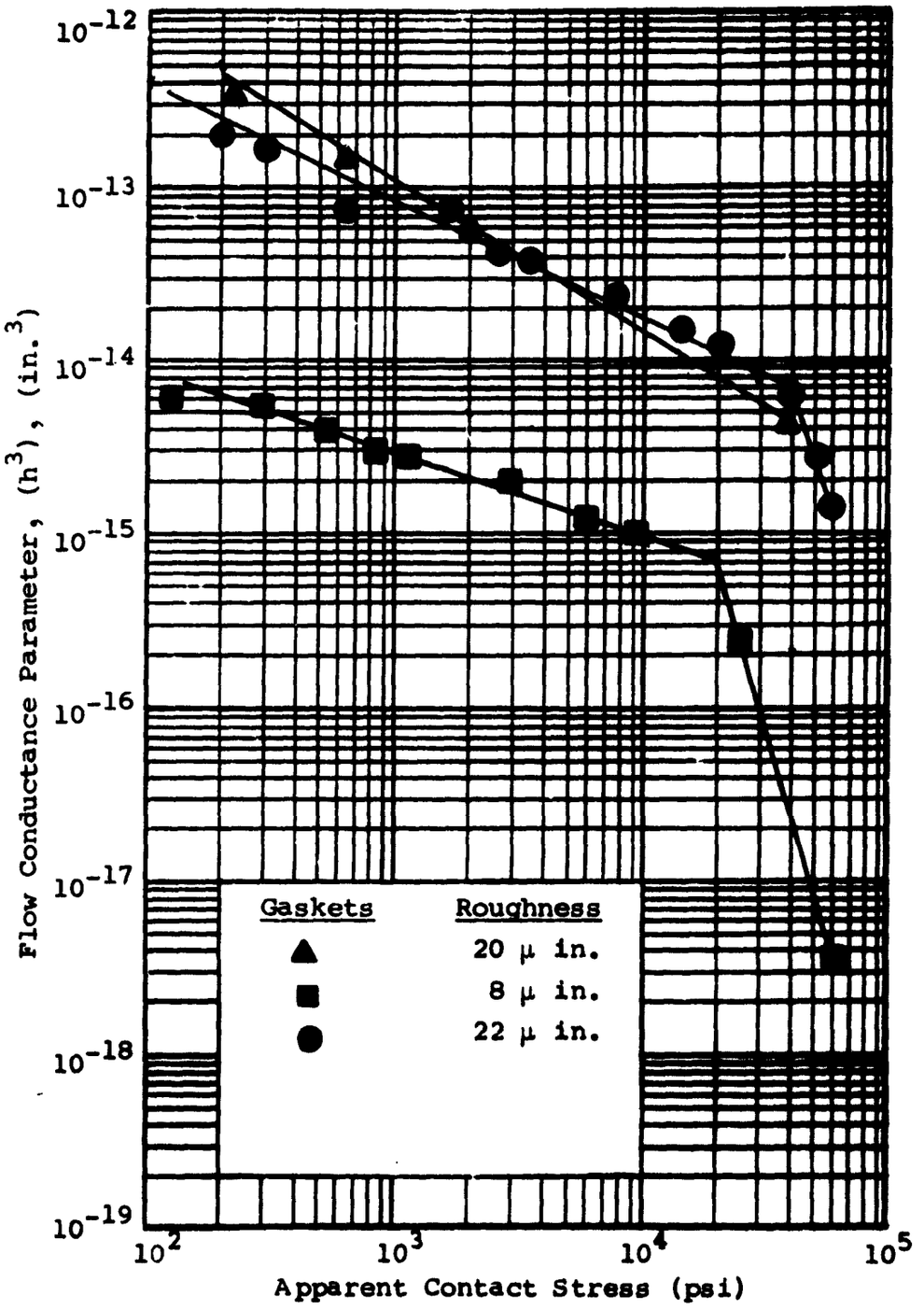

Figure 48 Average Cubed Equivalent Leakage Path Dimension as a Function of Total Interface Roughness for Lapped Steel Gaskets (Ref. 9)

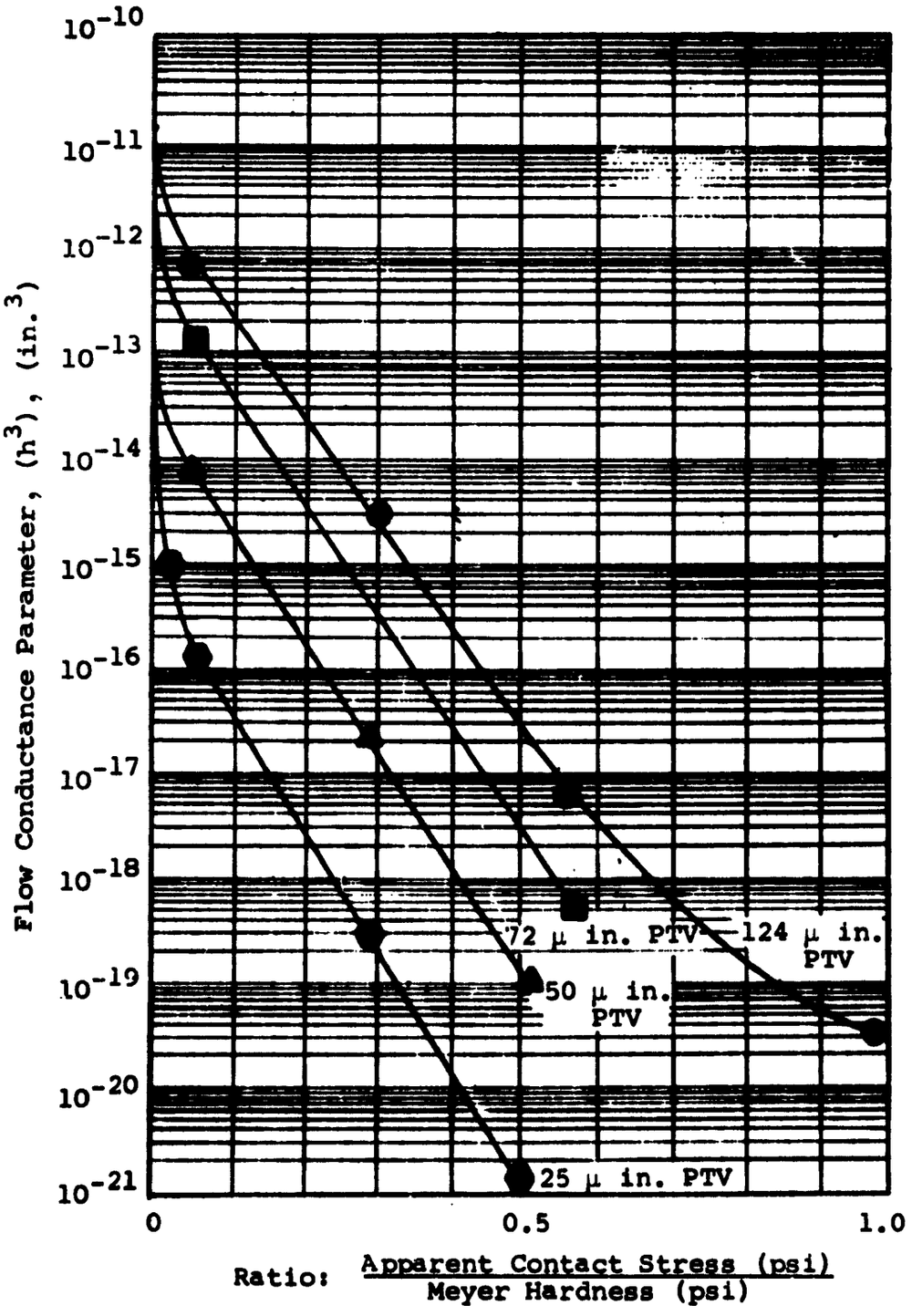

Figure 49 Approximate Relationship Between Contact Stress Hardness, and Conductance Parameter with Initial Surface Roughness Shown as a Parameter (Ref. 9)

Step 5: Calculation of Leakage

The theoretical flow equations presented in Section IV.3 along with the known parameters of sealed fluid properties, fluid pressure, and interface geometry are used to calculate leakage for each interface. These interface leakage values must be added to obtain the total leakage rate for the seal configuration.

Step 6: The Influence of Hysteresis on the Interface Conditions

Permanent or plastic-deformation of the microscopic irregularities in an interface results in a hysteresis effect when the applied load is released. The size of the leakage path is affected by the degree of plastic deformation occurring at the interface. Slowly releasing the load pressing the surfaces together results in very little change in leakage path. When the load is sufficiently reduced, elastic deformation becomes predominant in the determination of the size of the leakage path. The ensuing phenomenon is a hysteresis effect since the plastic deformation is irreversible.

For rubber to metal and plastic to metal seals, the hysteresis effect is not applicable. In these cases, the deformation is predominantly elastic or plastic. Design criteria, for the general case of metallic contact, to describe the influence of hysteresis has been developed (Ref. 9). The criteria are presented in the form of interface contact stress reduction, as a function of an arbitrary maximum stress necessary for 100 and 500 per cent increase in leakage.

Step 7: Seal Stability Criteria

To effect a satisfactory seal, it is necessary to minimize or eliminate sliding motion between the interface surfaces. Motion is normally produced by deformation of the seal housing or by radial deflection of the seal structure. This motion can be minimized by providing sufficient radial interface friction forces to counteract the forces tending to radially deform the seal structure. This will result in radial restraining forces greater than the radial deformation forces.

SECTION V

ENVIRONMENTAL EFFECTS ON SEAL MATERIALS

1. GENERAL CONSIDERATIONS

The space environment contains a broad spectrum of parameters which vary considerably in intensity with both position in space and with time. The space environment is discussed in detail in Part II Section III. It is seen that the environment consists of two parts, the natural environment, which exists in space in the absence of the spacecraft, and the induced environment, which is introduced by the presence of the spacecraft. It is the composite environment in which a seal must function and which will determine its useful life. The spacecraft not only introduces additional environmental parameters, but also may reduce the environmental exposure of a component or material through shielding. The shielding efficiency will vary with the mission profile, the environmental parameter and the material susceptibility.

It is impossible in this report to fully document the space environmental effects on all candidate seal materials, or even to tabulate the existing data from the literature. What has been done is to state general effects and to point out important interactions so that the designer may extract information from the literature pertaining to his materials and applications.

Caution must be exercised in applying data from the literature. Some data may not be pertinent because 1) the true environment may not have been adequately simulated, 2) synergistic effects of other environmental parameters may not have been considered in obtaining them, 3) extrapolations (or interpolations) may be required to the projected application, 4) pre-test or pre-usage processing may drastically alter the materials properties and susceptibility, and 5) the materials properties may vary from one manufacturer (or one lot) to another, particularly with organic materials.

2. ENVIRONMENTAL CLASSIFICATION OF SEALS

For environmental considerations, a different type of seal classification is required from that previously stated. Rather than one based on type of mechanism to be sealed, or on a particular mechanical configuration, a classification is needed which is based on degree of exposure and subsequent mechanical interaction of the sealing components. Such a classification is shown in Table XIII. It can be seen that a few classes cover most of the applications and that cross referencing to other methods of classification is easily accomplished.

Table XIII

Seal Classification Based on Environmental Exposure and Mechanical Interaction

Seal Type	Application Example
1. Dynamic Seals	
1.1 Continuous rotary motion	Rotating hub
1.2 Intermittent rotary motion	Door latching mechanisms
1.3 Linear motion - single use	Telescoping antenna
1.4 Linear motion - repeated use	Actuators
2. Static Seals	
2.1 Permanent connections - continuously made	Flanged penetrations
2.2 Long term exposure with single make	Erectable structures
2.3 Usually made - intermittently exposed	Hatches
2.4 Usually exposed - intermittently made	Docking Devices
3. Static Seals with Dynamic Make	
3.1 Long term exposure with single make	Hose connectors
3.2 Usually exposed with multiple makes	Refueling lines
3.3 Usually sealed with multiple makes	Space suit umbilical lines

Although this classification step is not essential to the design, it allows the designer to better visualize the exposure problems and to correlate his requirements with past practices (and successes).

3. SUSCEPTIBILITY OF MATERIALS TO ENVIRONMENTAL DEGRADATION

The degree to which a seal material degrades in the space environment can only be predicted through a knowledge of the mechanisms of interaction between the environment and the material. Table XIV lists the important interactions which affect the properties of most candidate materials. The important material properties which are affected by these interactions are listed in Table XV.

The environmental parameters listed are those discussed in Part II, plus "Mechanical Action." Although the mechanical action of a dynamic seal is not usually considered a part of the space environment, it must be included because of synergistic effects with other components of the environment. For a preliminary analysis, the environment may be condensed into the following headings:

a. Vacuum-Thermal
b. Thermal Radiation and Temperature Extremes
c. Ionizing and Penetrating Radiation
d. Meteoroids
e. Dynamic Influences

For quantitative statements of the environmental effects on a particular seal, the more complete listing of environmental parameters of Table XV must be used. However, the condensed list is more appropriate for the general discussion which follows.

a. Vacuum-Thermal

The major effect of vacuum on materials is one of material loss through evaporation or sublimation. Because of the temperature dependence of evaporation rates, the thermal environment must also be considered. If the vapor pressure, p_v, of the material under consideration is known, the rate of evaporation in vacuum may be calculated from

$$G = 0.0583\ p_v\ M^{\frac{1}{2}}\ T^{-\frac{1}{2}}\ \text{grams/cm}^2\ \text{sec} \qquad (41)$$

where

p_v = given in torr
M = molecular weight
T = °K

Table XIV

Interactions between Seal Materials and Environmental Parameters

Environmental Parameters	Interactions											
	Material Evaporation	Surface Desorption	Surface Sputtering	Molecular Bond Breakage	Cross-Linking	Pyrolysis	Ionization	Lattice Displacement	Thermal Expansion	Structural Deformation	Fretting and Surface Abrasion	
1. Natural Environment												
1.1 Vacuum	x	x										
1.2 Solar radiation												
1.2.1 Thermal	x					x			x			
1.2.2 Ultraviolet		x		x	x			x				
1.2.3 X-Ray				x	x		x	x				
1.2.4 Solar flares			x	x	x		x	x				
1.2.5 Solar wind			x	x	x		x	x				
1.3 Albedo & earth radiation												
1.3.1 Thermal	x											
1.3.2 Neutrons				x	x		x	x				
1.3.3 Protons			x	x	x		x	x				
1.3.4 Bremsstrahlung	x	x										
1.4 Other												
1.4.1 Cosmic radiation			x	x	x		x	x				
1.4.2 Trapped (Van Allen) radiation			x	x	x		x	x				
1.4.3 Auroral radiation			x	x	x		x	x				
1.4.4 Meteoroids										x	x	
2. Induced Environments												
2.1 Kinematic												
2.1.1 Acceleration										x		
2.1.2 Shock										x		
2.1.3 Vibration										x	x	
2.1.4 Acoustic										x	x	
2.2 Aerodynamic heating	x	x				x			x			
2.3 On-Board nuclear radiation				x	x		x	x				
2.4 Mechanical action		x								x	x	

Table XV

Materials Properties Affected
by Environmental Interactions

Material Properties Affected	Primary Induced Leakage Mode	Interactions										
		Material Evaporation	Surface Desorption	Surface Sputtering	Molecular Bond Breakage	Cross-Linking	Pyrolysis	Ionization	Lattice Displacement	Thermal Expansion	Structural Deformation	Fretting and Surface Abrasion
1. Inorganic Materials												
1.1 Tensile strength	Interfacial				x		x	x	x			
1.2 Elastic modulus	Interfacial				x		x	x	x			
1.3 Stress relaxation and creep	Interfacial				x		x	x	x			
1.4 Hardness	Interstitial, Interfacial			x	x		x	x	x			
1.5 Gas permeability	Permeation	x			x		x	x	x			
1.6 Surface finish	Interstitial	x	x	x	x		x					x
1.7 Friction	Interstitial, Interfacial		x	x	x		x			x	x	x
1.8 Distortion	Interfacial									x	x	
1.9 Fracture and cracking	Interstitial									x	x	
2. Organic Materials												
2.1 Tear strength	Interstitial	x			x	x	x					x
2.2 Resilience	Interfacial	x			x	x	x					
2.3 Gas permeability	Permeation	x		x	x	x	x					
2.4 Abrasion resistance	Interstitial	x	x	x	x	x	x					x
2.5 Oxidation stability	Interstitial, Interfacial	x	x	x	x	x	x					
2.6 Friction	Interstitial, Interfacial	x	x	x		x	x					x
2.7 Surface cracking	Interstitial	x	x	x	x	x	x					
2.8 Swelling	Interfacial, Permeation				x		x					

For metals and other inorganic materials, the most significant effect of evaporation will be disruption of surface conditions. For static seals of classes 2.2, 2.4, 3.1, and 3.2 (see Table XIII) in which a sealant surface is exposed to vacuum for an extended period, selective evaporation of high vapor pressure materials in alloys (e.g., Mg from Al alloys) may produce gross changes in surface finish which would subsequently provide poor sealing or abrasive action upon dynamic make with an elastomer. Selective evaporation from alloys used in other classes of seals could produce porosity if the exposure were sufficiently severe.

With organic materials, the effects of the vacuum-thermal environment are more severe, since vapor pressures are higher. Selective evaporation of plasticizers and other species affect almost all important material properties. Synergistic effects with other environmental parameters are sometimes beneficial, but more often detrimental to the materials.

b. Thermal Radiation and Temperature Extremes

Exposure of seal materials to space without regard to control of their temperature can cause seal degradation by several mechanisms. Exposure of organic sealants to direct sunlight can raise their temperature to the point where thermal damage occurs. Even at lesser temperatures, thermal radiation can enhance the degradation by other environmental parameters. Maximum service temperatures for some organic materials are listed in Table XVI.

Metal seals which are subjected to widely fluctuating temperatures can suffer surface damage through fretting due to thermal expansion and contraction.

c. Ionizing Radiation

The differences between ionizing radiation and penetrating radiation are vague, and they are differentiated here mainly by the depth of the influence on materials properties. Ionizing radiation here includes solar ultraviolet radiation and low energy charged particle radiation. Energy from such sources is dissipated rapidly in a material and damage is restricted to a thin surface layer.

Damage to metals by ionizing radiation will be restricted to surface roughening through erosion and sputtering. Organic materials suffer more severe consequences. The interaction of ionizing radiation breaks long-chain polymers into smaller molecules. The lighter molecules give the material a higher vapor pressure and drastically alter the physical properties. Since ionizing radiation has low penetration,

Table XVI

Maximum Service Temperature
of Sealant Materials

Material	Max Service Temp. (°F)
ELASTOMERS	
Natural	225
Styrene-butadiene (SBR)	250
Butyl	300
Nitrile (Buna-N)	300
Polysulfide	150
Neoprene	250
Silicone	600
Acrylic	450
Hypalon (chlorinated polyethylene)	250
Viton fluoroelastomer	450
PLASTICS	
Teflon TFE	500
TFE (filled)	To 500
TFE composites	To 500
KEL-F	350
Vinyl	212
Polyethylene	150

damage to seals which are usually "made" should be low, because of the shielding effects of the seal housing. Major problems are to be expected in Class 3 seals, where the material degradation will make the elastomer unable to withstand the mechanical action of the sealing process.

Penetrating radiation includes high energy charged and uncharged particles, X-rays and gamma rays, which cause damage deep within the material.

Damage to metals is caused by a disruption of the crystal lattice (Ref. 38). Electromagnetic radiation and light particles like electrons can dislodge only one or two metal atoms from their lattice sites, and the damage quickly anneals out. Energetic particles can knock out hundreds to thousands of neighboring lattice atoms, affecting the metals' physical properties. However, anticipated doses for realistic periods in space will produce negligible damage to most metals.

For organic materials, the damage caused by penetrating radiation is similar to that caused by ionizing radiation, except that the damage extends through the bulk of the material. Gas can be generated within the material which, together with the bond breakage, can cause swelling. When an energetic particle is absorbed by a material, secondary radiation can be produced within it. Thus, even though the damage by primary charged particles may be restricted to the surface layer, the resulting secondary neutrons and gamma rays may penetrate deeply into the structure.

The radiation damage to organic materials is roughly proportional to the amount of energy absorbed. Radiation stability data for organic seal materials are listed in Table XVII.

d. Meteoroids

The primary damage mechanism by meteoroids will be erosion and roughening of exposed sealing surfaces, for both organic and inorganic materials. Fluxes of meteoroids large enough to cause gross physical damage are negligibly low. Small meteoroids ($<10^{-12}$ grams) have high flux rates, but carry sufficient energy to produce only localized damage.

e. Dynamic Influences

The influence of the dynamic environment (such as vibration and acceleration) must be considered on an individual basis. Since the period of greatest dose will occur during the launch and injection phases, when doses of other environmental parameters will be low, synergistic effects can be ignored. The only dynamic influence of significance will be the motion

involved in the sealing process. If the seal is to be operated after long periods of exposure to space, the degradation of materials properties may be sufficient to cause failure under the stresses imposed by the mechanical action.

Table XVII

Dose Levels for Significant Property Changes in Organic Seal Materials (Ref. 38)

Total Ionization Dose (rads)	Materials
10^4 - 10^5	Teflon
10^5 - 10^6	Silicone rubber, acrylic rubber
10^6 - 10^7	Butyl rubber, nylon, neoprene, Buna-N (nitrile), styrene butadiene (SBR)
10^7 - 10^8	Polyethylene, Kel-F, polyvinyl chloride, natural rubber, Viton-A
10^8 - 10^9	Epoxy, polyurethane, polystyrene

4. SHIELDING TECHNIQUES

In many cases, action can be taken in the design phase to reduce the environmental dose seen by critical components and materials. To reduce material loss by evaporation from exposed surfaces, the partial pressure of the evaporant must be raised to a significant portion of its vapor pressure. This amounts to virtual hermetic sealing. The best method for reducing material loss is to reduce the amount of the exposed surface of the critical material to a minimum. Temperature extremes may be avoided by providing a high thermally conductive path to the spacecraft structure. The seal will assume the temperature of the structure Direct exposure of black organic materials to solar radiation should be avoided because their low thermal conductivity may support large temperature gradients (permitting a high surface temperature). Because of the damaging solar ultraviolet radiation, these materials should not be exposed to it also.

Ionizing radiation is easily shielded out because of its low penetration. Penetrating radiation may be attenuated, but not eliminated by shielding with heavy metals. For most metals, the attenuation is proportional to the weight of metal to be traverse (Ref. 38). Approximate attenuation values given in Reference 38 for one gram per sq cm of metal are shown below:

Protons	
High energy, Bev	10^{-1}
Low energy, Kev	10^{-5}
Electrons, up to few Mev	10^{-10}
Cosmic ray protons	
Bremmstrahlung	nil to 10^{-1}

Meteoroids may be shielded out by the same techniques used for radiation shielding. Figure 50 shows the effectiveness of aluminum shielding of varying thickness.

In all cases, the successful operation of seals in spacecraft requires careful consideration of protection from the damaging influences of the environment.

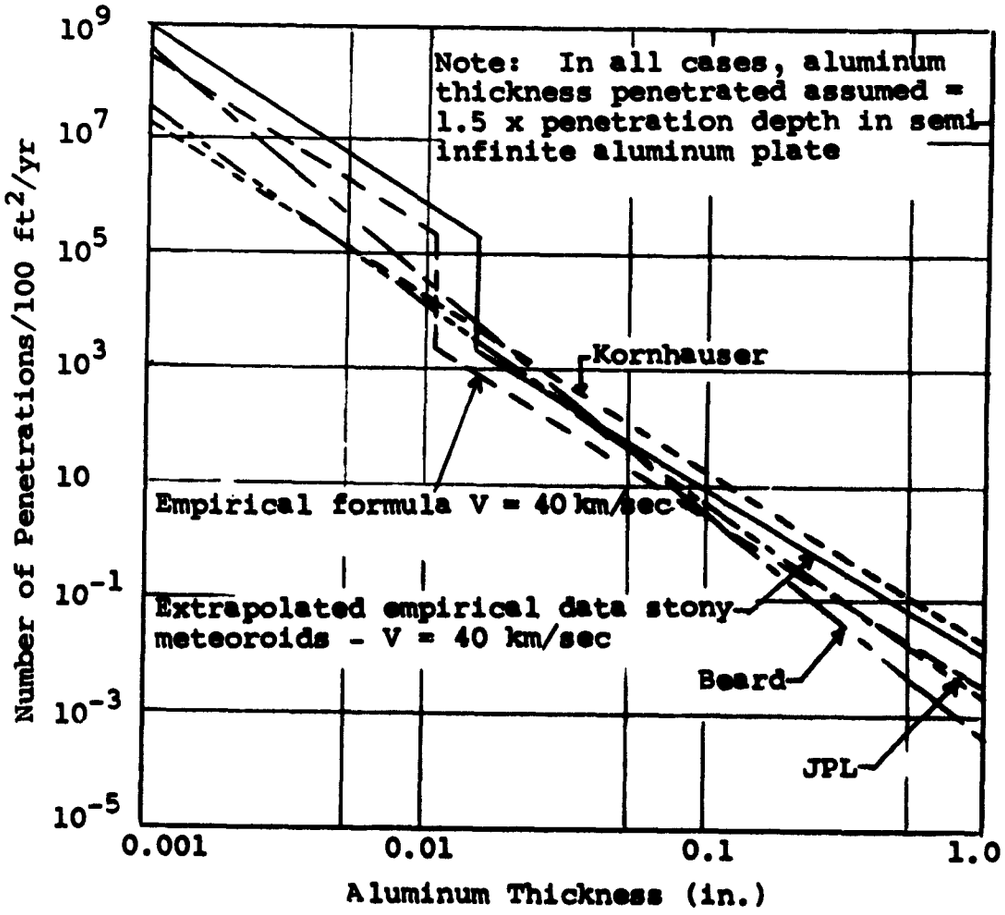

Figure 50 Estimates of Meteoroid Penetration in Aluminum

SECTION VI

EXPERIMENTAL DATA

1. EXPERIMENTAL EQUIPMENT

The objectives of the experiments conducted were to obtain leakage rate data, conformability to surface flaws, and effect of material hardness data for seal interfaces composed of various elastomer materials and steel flanges under varied load conditions. The basic equipment consisted of a flange loading device, leakage collection apparatus, load measuring instrumentation, and leakage rate measurement instrumentation.

The general assembly of the test apparatus is depicted in Figure 51. The assembly is comprised of a circular, rectangular cross-section elastomer seal pressed between two flanges to form two interface surfaces. An adjustable clamping load is applied to the flanges by a hydraulic press and gas is introduced in the center of the gasket. Leakage of gas past the interfaces is measured by several techniques described later in the discussion.

To attain compressive stresses greater than the compressive yield stress, it is necessary to prevent lateral deformation of the gasket under compressive load. The gasket is radially supported by an inner and outer ring restricting radial displacement (Figure 51). The maximum clearances between the inner ring and gasket inside diameter and between the outer ring and gasket outside diameter are each approximately 0.004 in. The inner and outer rings both have outside diameter-to-inside diameter ratios large enough that the radial deformation is very small. The small clearances also minimize extrusion of the seal material under high stresses.

The leakage collection ring was used to channel the leakage past the seal to the measuring instrument. The cross-sectional view of the apparatus (Fig. 51) illustrates the operation of the collection assembly.

The contact stress at the seal interface was indicated previously to be one of the most important variables influencing leakage. Therefore a controllable means of applying and varying contact load is necessary. A hydraulic press was utilized for this purpose. The load is simply regulated by varying the pressure of the fluid in the press actuator. The hydraulic press as shown on Figure 52 is in plastic for contaminant control. The clamping load applied by the press was measured by a strain gauge load cell. It was made up of a complete four-arm strain-gauge bridge arranged for bending compensation and hardened spherical end caps to approximate point loading. The load cell was placed between the anvil of the hydraulic press and the upper gasket flange as shown on Figure 53.

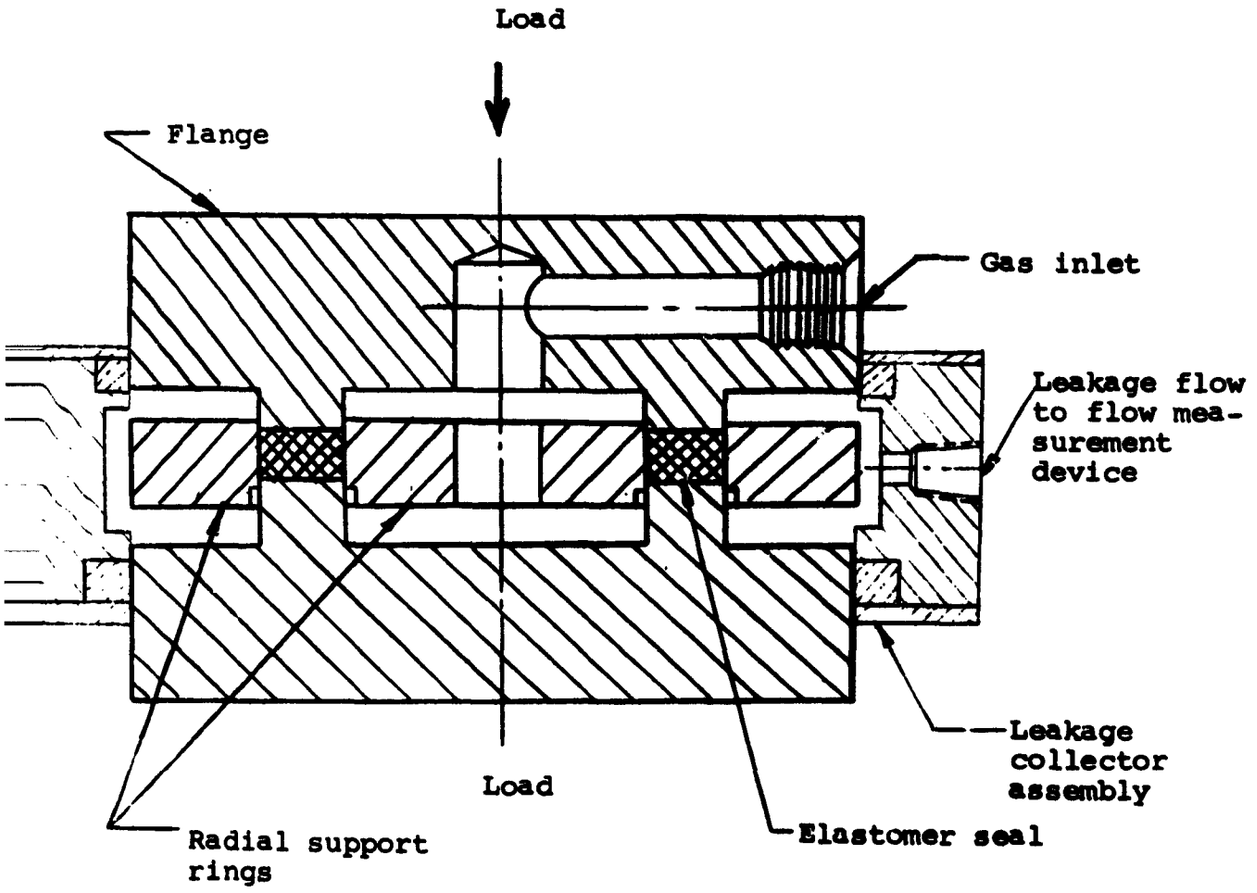

Figure 51 Confined Seal Test Apparatus

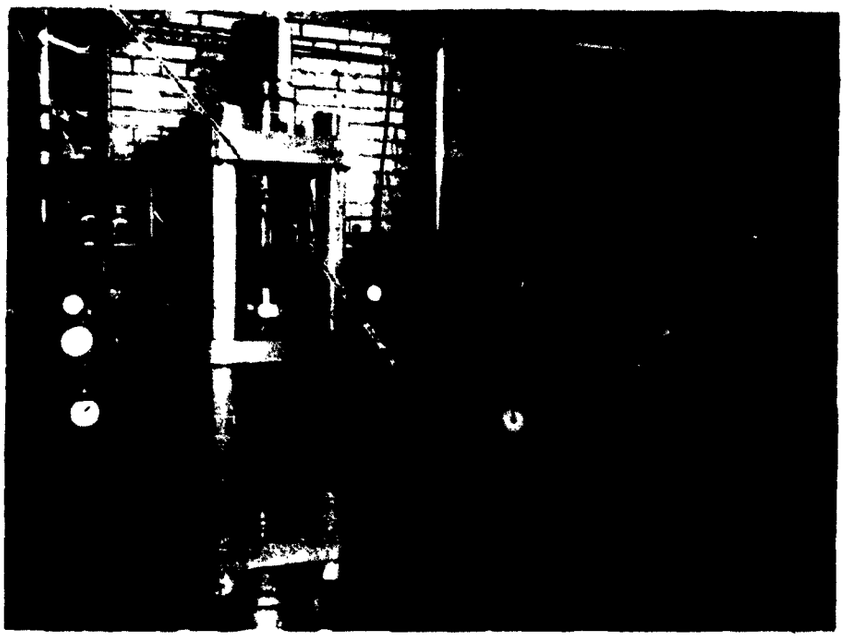

Figure 52 Hydraulic Press for Static Seal Evaluation with Leak Detection Equipment

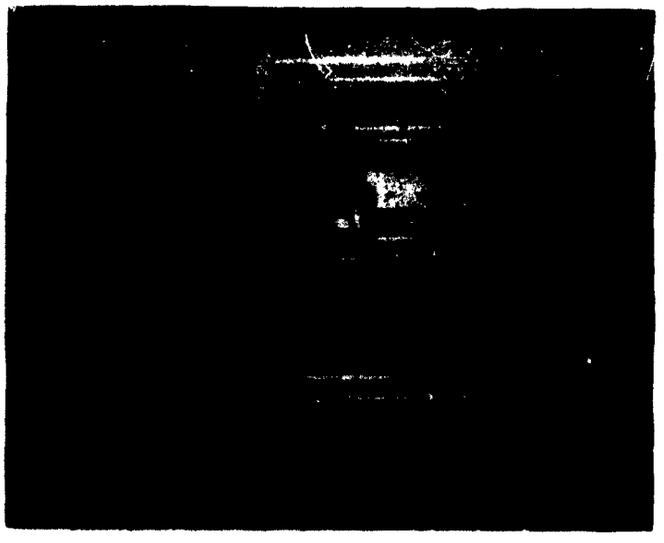

Figure 53 Static Seal Experimental Apparatus Installed in Hydraulic Press

The measurement of leakage rates under various conditions is the most important part of the experimental program. Because of the wide range of leakage rates encountered during the tests, no one measuring device or technique was applicable. The following discussion presents the basic devices used for leakage measurement and their range of applicability.

Rotameter flow meters were used to measure leakage rates in the range from 0.1- to 120-atmospheric cc/sec. Two rotameters were connected in parallel to the downstream side of the seal configuration. A large capacity rotameter (1- to 120-atmospheric cc/sec) and a small capacity rotameter (0.1- to 1.2-atmospheric cc/sec) were used. The flow was then directed to one or the other rotameter by valves. The rotameters were calibrated to determine flow rate as a function of float position.

The mercury bubble leakmeter developed during other sealing investigations at IITRI (Ref. 9) was employed to measure leakage rates lower than those suitable for use with the rotameters and too high for a mass spectrometer. This flow meter is shown schematically in Figure 54. A glass capillary tube is mounted on modified high-pressure fittings. By proper valving, the capillary tube is directly connected between a constant pressure gas source and the seal chamber. As leakage occurs in the seal chamber, the pressure of the gas in the volume between the mercury slug and the seal chamber tends to drop. Since the pressure on the upstream side of the bubble is held constant, the bubble will move in the direction of the leakage flow. The pressure is maintained constant throughout this process by a pressure regulator at the pressure source. A pressure drop of less than 0.5 psi is necessary to start the bubble in motion. The entire process is a positive displacement constant pressure process. Since the capillary tube is connected directly between the pressure source and the seal chamber, the leakage flow rate into the seal chamber at system pressure is measured.

The flow rate is obtained by timing the movement of the mercury bubble over a given distance. If the inside diameter of the tube is considered constant, then, a given distance traveled by the mercury bubble corresponds to a given displaced volume. Valving is arranged so that when a measurement is desired, the glass capillary is directly connected from the pressure source to the seal chamber. To stop the movement of the mercury bubble, the flow is diverted to a parallel flow path from the pressure source to the seal chamber. Resetting the bubble to its original position is accomplished by a bleed valve on the upstream side of the mercury bubble.

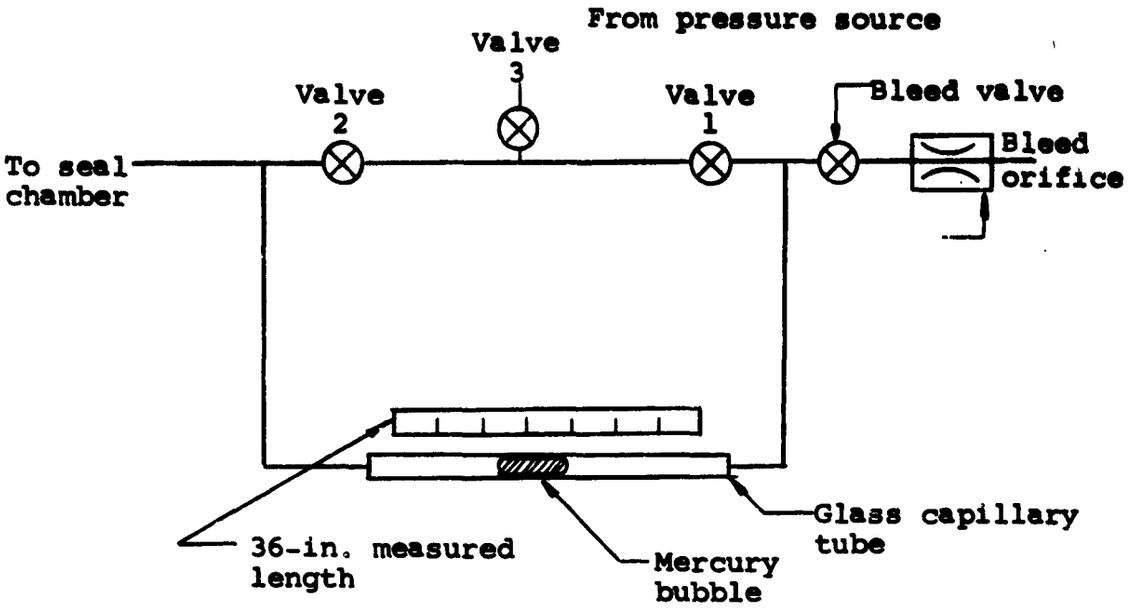

Figure 54 Valve System for Mercury Bubble Leakmeter

The nature of the operation of this device places an upper and lower limit on the leakage rates that can be measured. The length of the tubes used in this device is 47 in. The maximum measured length for leak rate determination is 36 in. The length of tube beyond 36 in. allows the operator time to manipulate the valves, necessary to stop the bubble movement before the bubble can escape from the capillary tube and be lost in the piping leading to the seal chamber. In making a leakage rate measurement, the operator closes the valve that starts the bubble movement. When the bubble reaches the beginning of the measured length or any other convenient stopping point, the operator stops the timer and opens the valve to stop bubble movement. The maximim leakage rate measurable by this method is limited by the reaction time of the operator. A bubble travel of 36 in. in one sec is approximately the fastest movement that can be timed consistently. For a calibration factor of 0.022 cc/in., this produces a volumetric leakage rate of 0.79 cc/sec. Thus, the upper limit on leakage measurement, set by operator reaction time, is approximately 8×10^{-1} cc/sec. Even if automatic devices could be used to overcome operator limitations the upper limit of leakage rate could not be extended much further since, for very high leakage rates, the rapid acceleration of the mercury bubble from rest causes the bubble to break up. Experience has shown that a leakage rate corresponding to a bubble movement of one inch in 10 minutes is the lowest leakage rate that can be measured with this device. For a calibration factor of 0.022 cc/in., the volumetric leakage rate is 3.6×10^{-5} cc/sec. The practical limit is closer to 1×10^{-4} cc/sec.

A helium mass spectrometer was used to detect and measure leakage rates of 10^{-5} atmospheric cc/sec and less. A helium leak detector manufactured by Consolidated Electrodynamics Corporation was used for these extremely low leakage rates. This instrument has a measurement range of from 1×10^{-5} atmospheric cc of helium per sec to approximately 1×10^{-9} atmospheric cc of helium per sec. The instrument is calibrated using a standard leak supplied by the manufacturer.

To use the helium leak detector, a sealed collector ring must be placed around the outside, or atmosphere side, of the seal configuration. When the collector ring is installed, the system is evacuated by a mechanical vacuum pump. Thus, leakage takes place from the high pressure side of the seal into a vacuum. The volume between the outside of the seal and the mass spectrometer is evacuated to a pressure of approximately 2 to 3 microns of mercury. The leakage flow of helium enters the mass spectrometer and the flow rate is read out and converted into atmospheric cc of helium per sec using the calibration factor determined from the standard leak.

2. EXPERIMENTAL PROCEDURES

a. Deformation Visualization of Rubber Seal

The objectives of this test procedure were to determine the shape which a rubber O-ring assumes upon being compressed. A test arrangement consisting of two finely machined plates and guideposts as shown in Figure 55 was employed to deform segments of and entire O-rings. The test procedure for segments of rings consisted of:

- placing ring between plates
- centering plate arrangement beneath the ram of the loading press
- compressing O-ring segment by varying the applied load in discreet increments (approximately 10 lb/in.)
- photographing the O-ring cross-section shape at each increment.

The procedure for an intact O-ring was identical to the segment with the exception of the photographing process. Since the cross-sectional shape was not viewable, a model was made of a portion of the ring while in the compressed state. The load was released upon hardening of the mold material, and a photograph was taken of the cross-section as it appeared on the mold. The purpose of the intact O-ring tests was to determine whether any end effects were present in the segmented ring tests due to the different stress distribution.

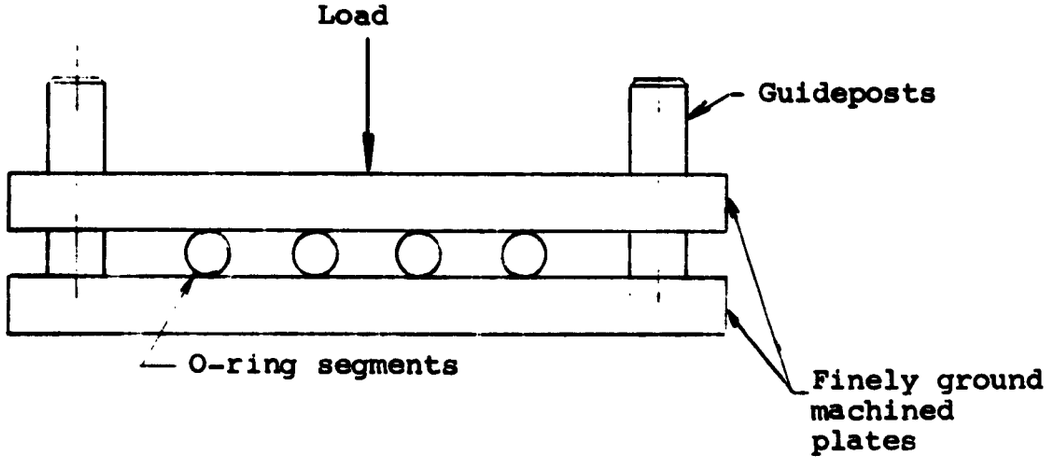

Figure 55 · Test Arrangement for Visualization of Rubber Seal Deformation

b. Conformability of Rubber Seals to Surface Flaws

The flanges depicted in Figure 56 were manufactured to simulate surface flaws at the flange and seal interface. The flanges were cleaned in an ultrasonic bath of a suitable solvent, usually acetone, to eliminate contaminant particles and their effect on leakage. The parts were stored in clean bags until ready for use. It should be emphasized that the contaminant particles referred to are foreign particles such as dust and oil. No attempt was made to remove surface contaminants such as oxide films and embedded machining particles.

The rubber seal was tested for its hardness using the Shore hardness tester. The flanges were inspected for surface roughness and waviness with the "Proficorder" instrument. The flaws were measured and their shape identified on a "shadowgraph" instrument. This device simply projects an amplified image of the cross-section contour on a screen. The screen is graduated in such a manner that numerical interpretation of the image is possible.

The rectangular cross-section rubber seals were then installed between a set of flanges (one containing a flaw, the other plain) and the leakage collector ring secured around the flange periphery. The entire assembly was placed in the hydraulic press. A minimum force was applied to the flanges by the loading equipment. Because the magnitude of the load was slightly higher than the net effect of sealed gas pressure on the seal, a minimum net contact stress was assured. The sealed gas pressure was maintained constant during each test. Leakage was measured with the appropriate range instrument corresponding to incremental changes in flange load.

The loading procedures are to increase the flange force in increments, allowing leakage phenomenon to stabilize with subsequent leakage measurements taken after stabilization. Leak rate measurements were obtained using helium gas at pressures between three and one-half and four atmospheres as the sealed fluid.

3. EXPERIMENTAL RESULTS

a. Deformation of Rubber Seal

Tests were conducted to observe the shape which a rubber O-ring assumes upon being deformed. The information was obtained from O-ring segments made of Buna-N material with a Shore A hardness of 85 and 65 durometer. The ring cross-section diameter was 0.262 in.

The purpose of these experiments was to establish the validity of the deformation analysis for an elastic body in the

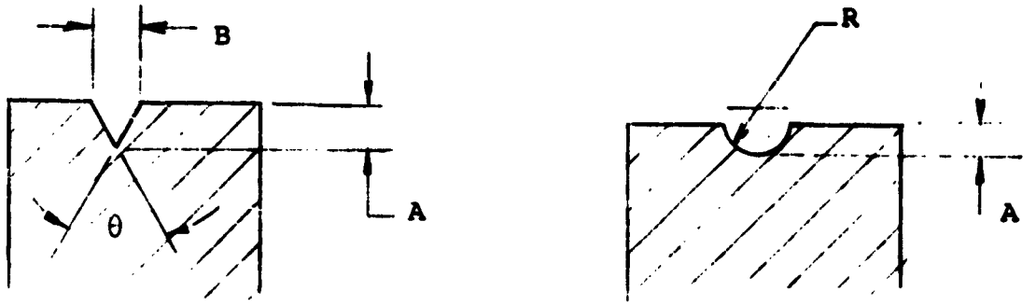

Flange Number	A	B	θ
3	0.002	0.0010	30°
6	0.004	0.0035	45°
1	0.004	0.0045	60°
2	0.004	0.0020	30°
8	0.006	0.0035	30°
4	0.001	0.0006	30°

Flange Number	R	A
7	0.031	0.004
5	0.062	0.004

Marks are perpendicular to machining marks, which are concentric with flange diameters.

Figure 56 Surface Irregularity Simulation Flanges

form of a cylinder applied to an O-ring (Fig. 29). This analysis was not intended to yield precise deformation data, but rather approximate deflection versus applied load and contact width versus applied load information. The analysis from equation (28) states,

$$a = 1.6\sqrt{FD\left[\frac{1 - y_1^2}{E_1} + \frac{1 - y_2^2}{E_2}\right]} \qquad (42)$$

where

a = contact width, in.

F = applied load, lb/in.

D = cross-section diameter, in.

E_1 = modulus of elasticity of cylinder

E_2 = modulus of elasticity of plate

y = Poisson's ratio

The total deflection (compression) is given as:

$$\Delta D = 4p\left(\frac{1 - y_1^2}{\pi E_1}\right)\left(1/3 + \ln\frac{2D}{b}\right) \qquad (43)$$

where,

ΔD = deflection, in.

The load-deflection, and load-contact stress data obtained from the two O-rings tested is shown in Figures 57 and 58.

Application of the foregoing theoretical deflection equation and subsequent comparison with the experimental values is not directly possible. The modulus of elasticity of rubber is non-linear; thus, no one value can be selected. The procedure followed was to arbitrarily select a contact width and load value from the experimental information and apply them to the equation. The calculated values of deflection and contact width were then compared. These results are shown graphically in Figures 59, 60, 61 and 62. From these figures, it may be noted that the experimental and calculated curves do not coincide, and that selection of a higher modulus of elasticity value will result in a smaller deviation. Additional calculations using the new, assumed value for E yields the corrected curves.

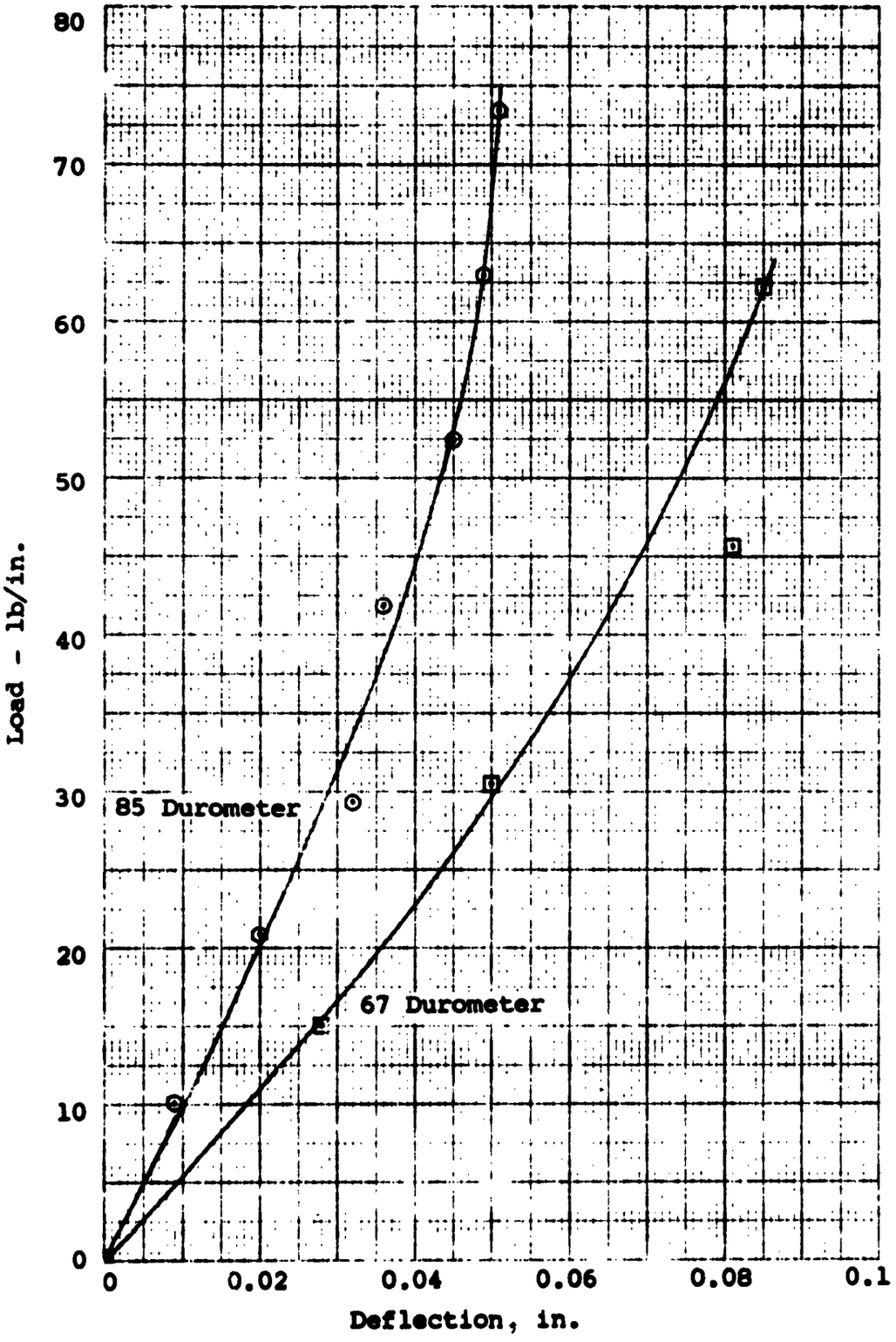

Figure 57 Load Versus Deflection

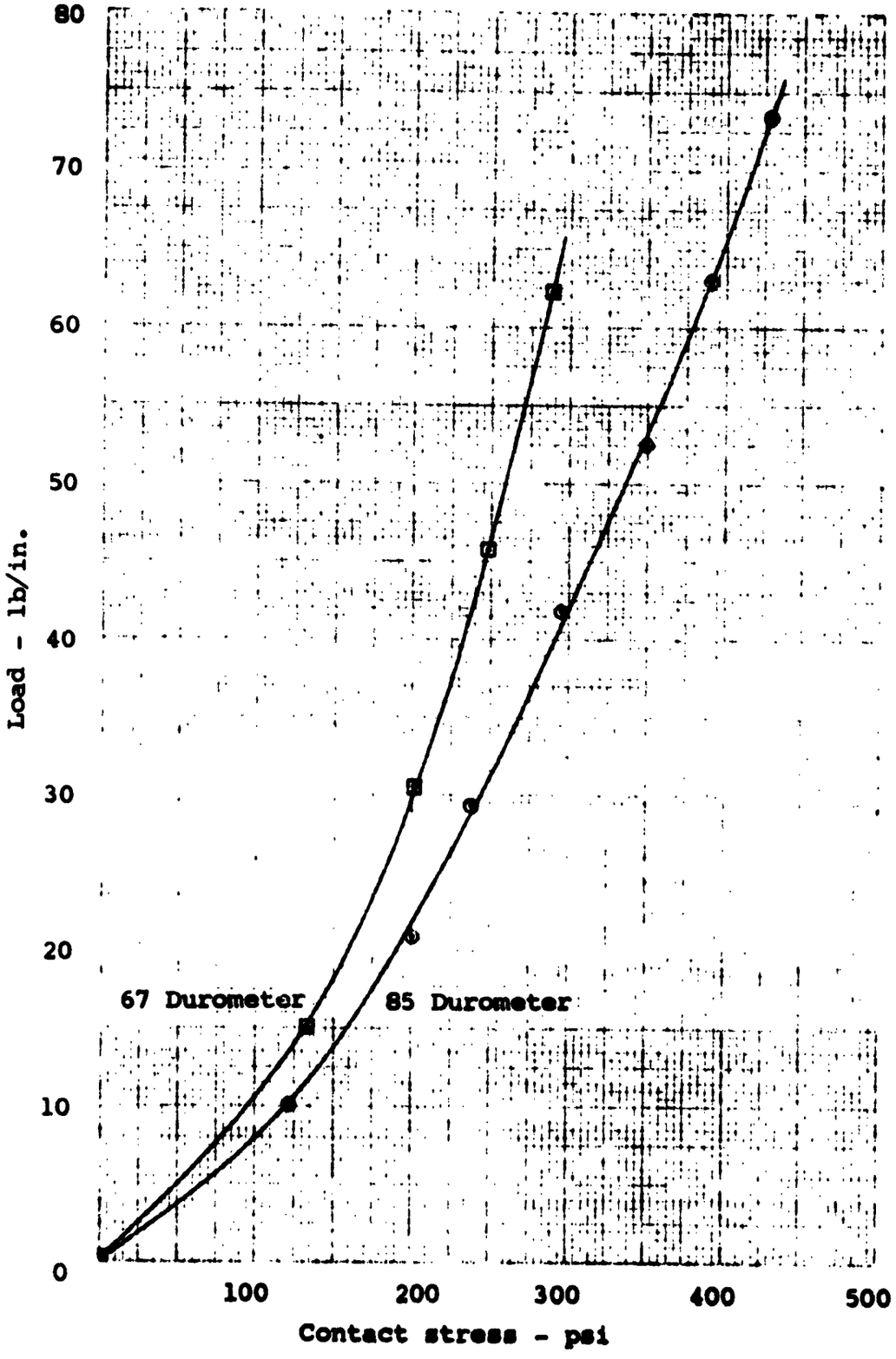

Figure 58 Load Versus Contact Stress

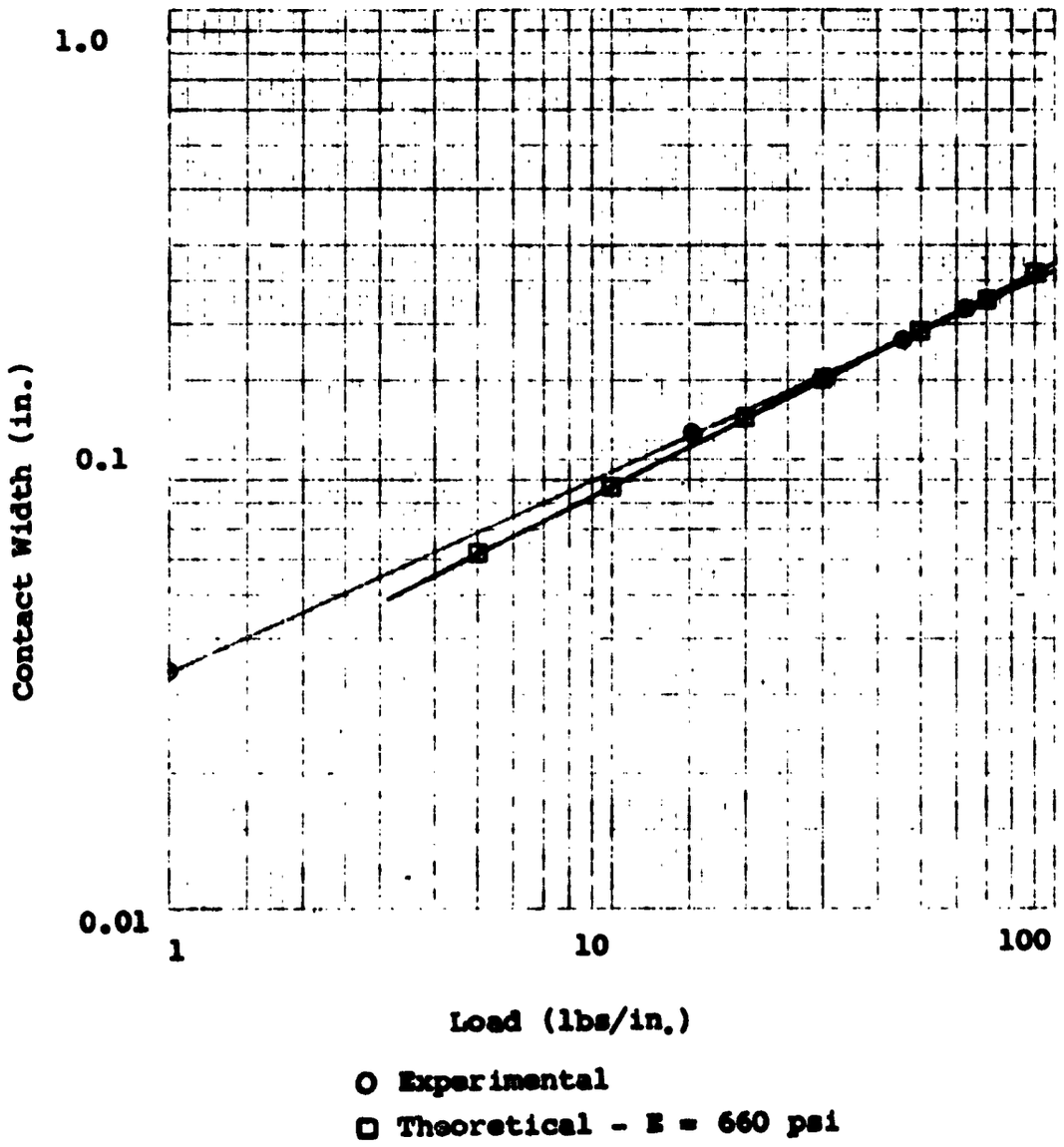

Figure 59 Experimental and Theoretical Load-Contact Width Curves for 67 Durometer O-Ring

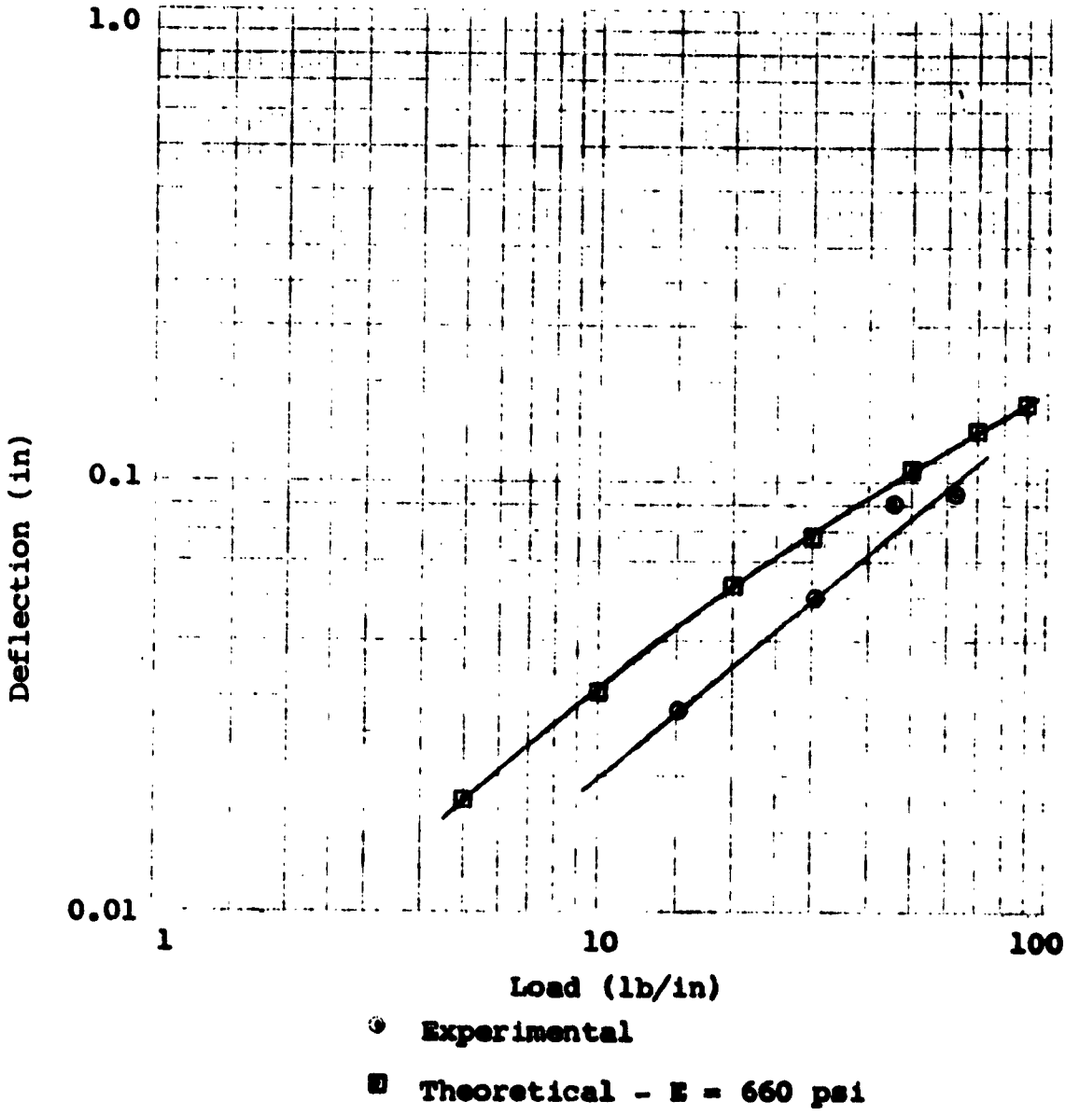

Figure 60 Experimental and Theoretical Load-Deflection Curves for 67 Durometer O-Ring

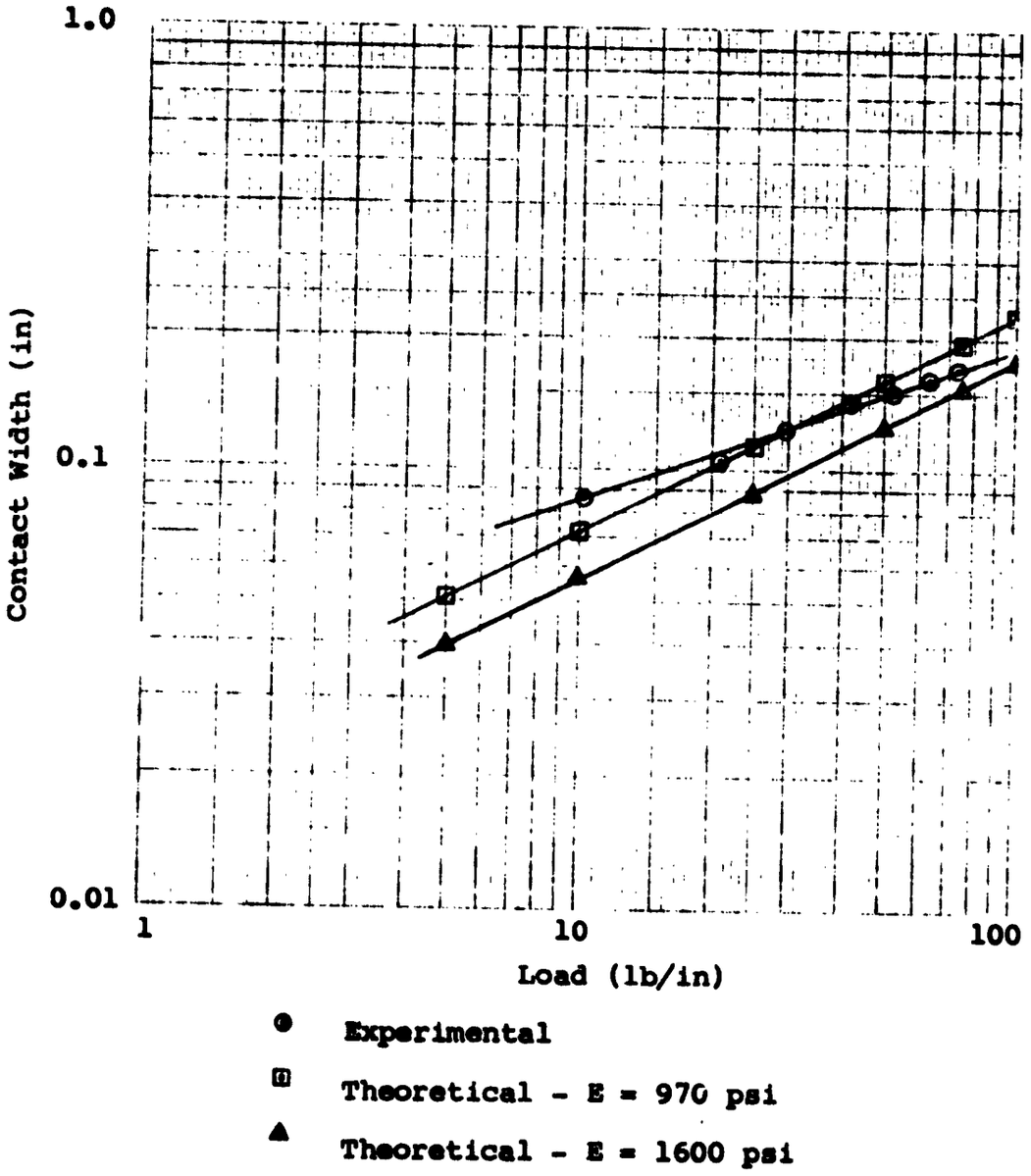

Figure 61 Experimental and Theoretical Load-Contact Width Curves for 85 Durometer O-Ring

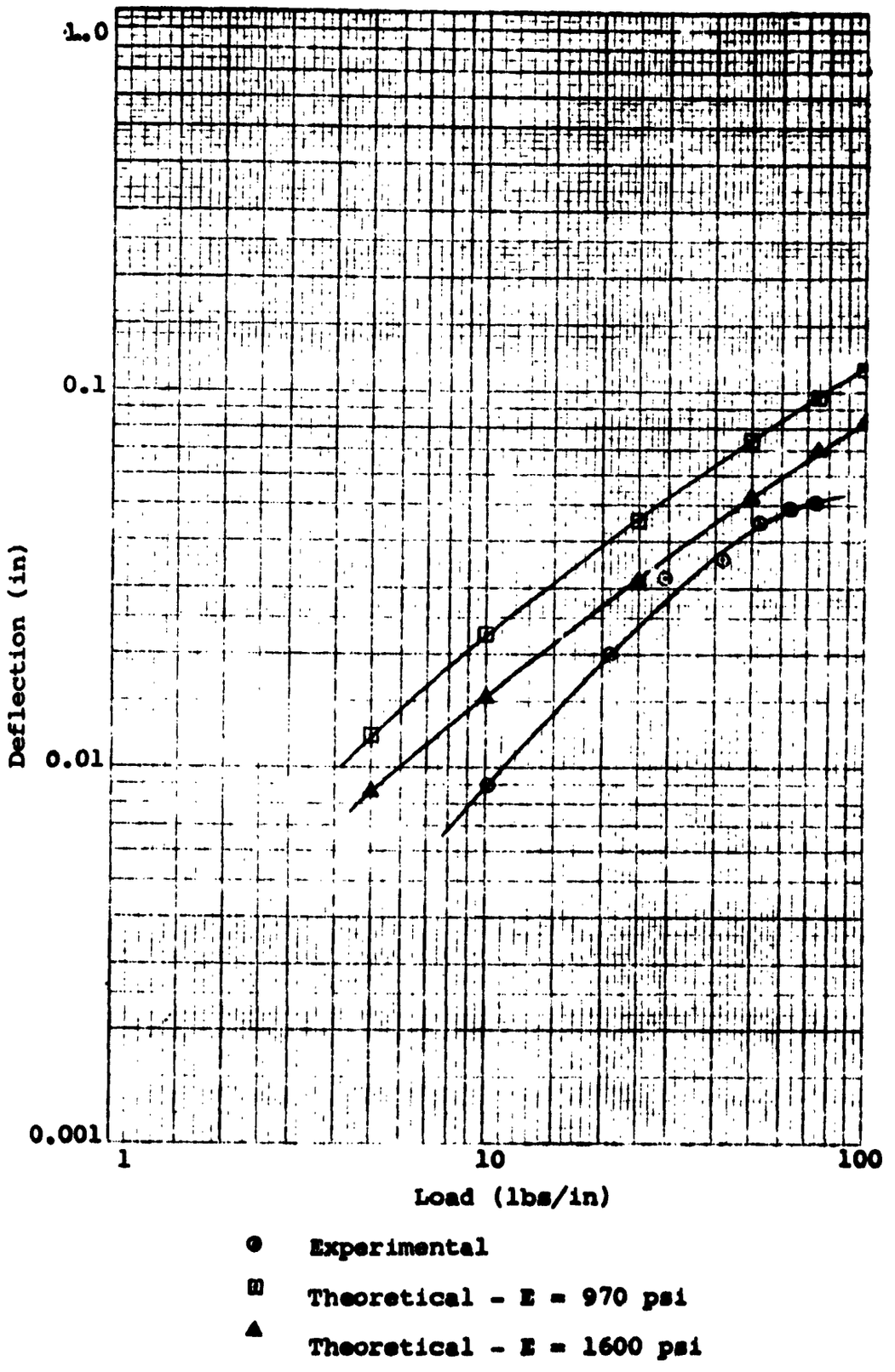

Figure 62 Experimental and Theoretical Load-Deflection Curves for 85 Durometer O-Ring

The analysis is intended to yield only approximate data. The significance of the proximity of the information lies in the fact that a parabolic stress distribution across the ring interface may be assumed. Application of this assumption to the contaminant particle size toleration level leads to the conclusion that the size is not a sole function of contact width. It is assumed, generally, that the contact width at the interface determines the maximum size particle tolerable for minimum leakage. As long as the particle is smaller in length or diameter than the contact width, it is "swallowed" up. If a parabolic stress distribution exists, however, the decrease in contact stress when the particle is located at the center of the contact surface is considerable. Since the conductance parameter and consequently leakage are proportionally affected by contact stress, an intolerable increase in leakage will result. The maximum particle size tolerable is governed by the maximum reduction in contact stress yielding desired leakage level (Fig. 63).

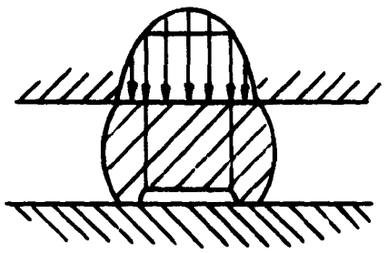

Figure 63 Contaminant Particle Effect on Contact Stress Reduction

An analysis of the deformation process of a rubber O-ring with considerations given to the change in shape, as well as, nonlinearity of modulus of elasticity is suggested for future study. Such an analysis will enable a designer to attain a better insight into the deformation phenomenon, as well as, permit more accurate application of the leakage prediction process.

To gain an insight to the change in O-ring shape with compression, visualization experiments were conducted. These tests simply consisted of photographing the cross-sectional shape of the deformed ring. These results are shown in Figures 64 and 65. The significant observation that can be made from these figures is the fact that the ring cross-section does not assume a shape consisting of two semi-circles and a rectangle but rather of two segments of circles and a rectangle. Thus, deflection calculations and contact width calculations based on the semi-circle, rectangle geometrical relationships do not appear valid as shown in Figure 66.

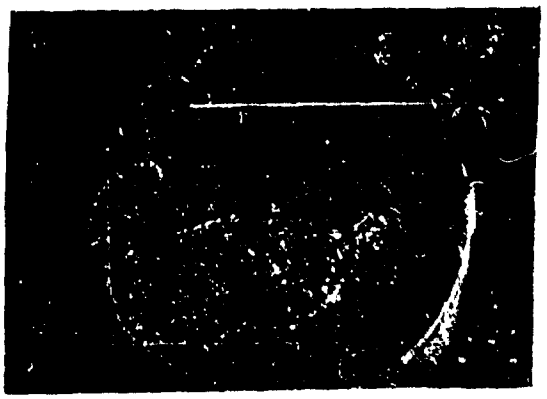

a) 0% deflection

b) 10.8% deflection

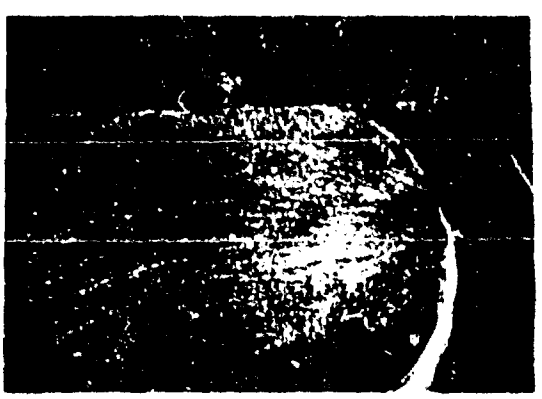

c) 19.2% deflection

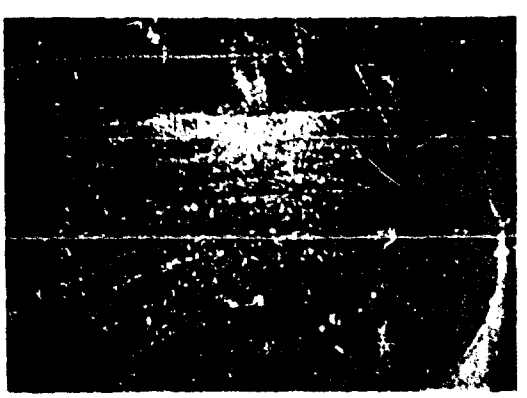

d) 31.1% deflection

Figure 64 O-ring Segment Deformation (67 Durometer Ring)

a) 0% deflection

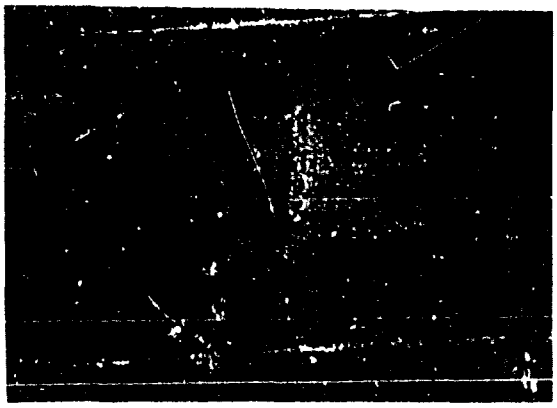

b) 7.64% deflection

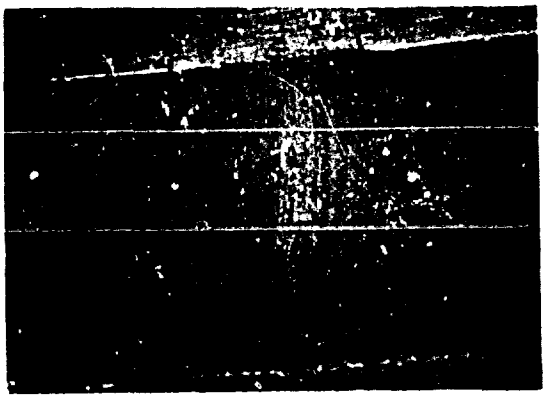

c) 13.75% deflection

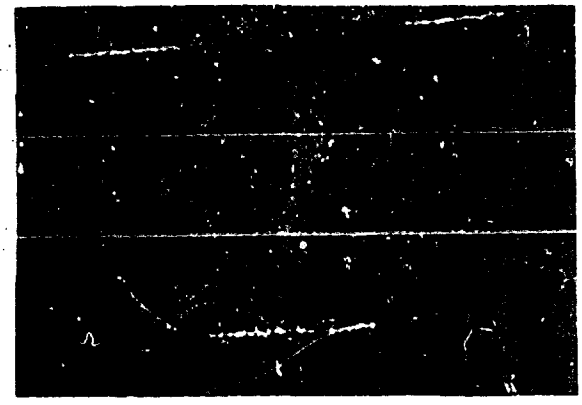

d) 20.6% deflection

Figure 65 O-ring Segment Deformation (85 Durometer Ring)

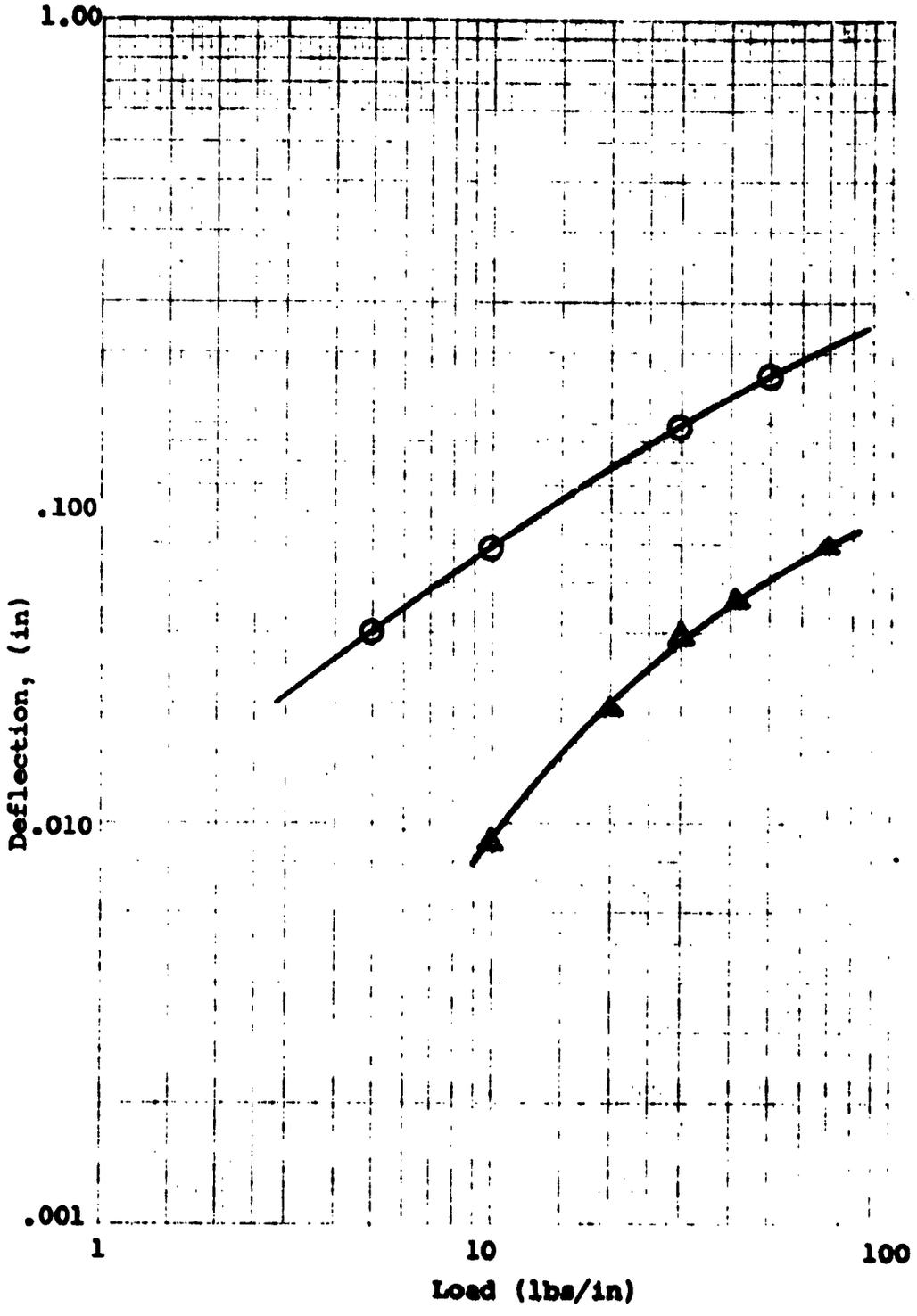

Figure 66 Experimentally and Geometrically Calculated Load Versus Deflection

b. Conformability of Rubber Seals to Surface Flaws

The flanges with the surface imperfection geometries described in Figure 56 were used to obtain leakage versus contact stress data for various hardness rubber seals. Prior to installation in the seal test fixture (Fig. 51), the flanges were inspected. The photomicrographs of the flaw zone, surface roughness, and surface waviness traces are shown in Figures 67 to 72.

The flanges were further inspected on the "shadowgraph" instrument to obtain physical dimensions of the flaw, as well as, an image of the contour. These results are shown in Figures 73 and 74.

The foregoing inspection process yielded sufficient data to identify the surface characteristics and flaws. The flanges were then installed in the test apparatus. Seals which had been previously tested for their hardness were installed and tested with helium gas as the pressurization media. The internal pressure was 50 psi. The leakage data obtained is shown on Figures 75, 76 and 77, with contact stress as the other variable.

The observations which can be made upon reviewing the leakage data are:

The shape of the flaw greatly affects the leakage rate attainable at a given stress level. For example, from Figure 75, it can be seen that the leakage rate at 100 psi contact stress for flanges 4 and 2 are 4×10^{-5} and 40 atm. cc/sec, respectively. The narrow and deep grooves (width to depth ratio of approximately two) generally exhibited greater leakage rates as may be expected.

The effect of rubber hardness is significant in conformability to surface imperfections. As can be seen from Figure 77, the 35 and 90 durometer seals when tested with flange number 5 exhibited leakage rates at 200 psi contact stress of 3×10^{-6} and 1 atm. cc/sec. respectively. Of more significance, however, is the fact that the hardness appeared to affect leakage in a discreet manner. The rubber hardness number raised to a power, the value of which for a specific material (Buna-N) is 3.25, is determined by plotting hardness versus contact stress (Fig. 78). This relationship between contact stress and hardness when applied to the conductance parameter prediction technique enables the designer to calculate

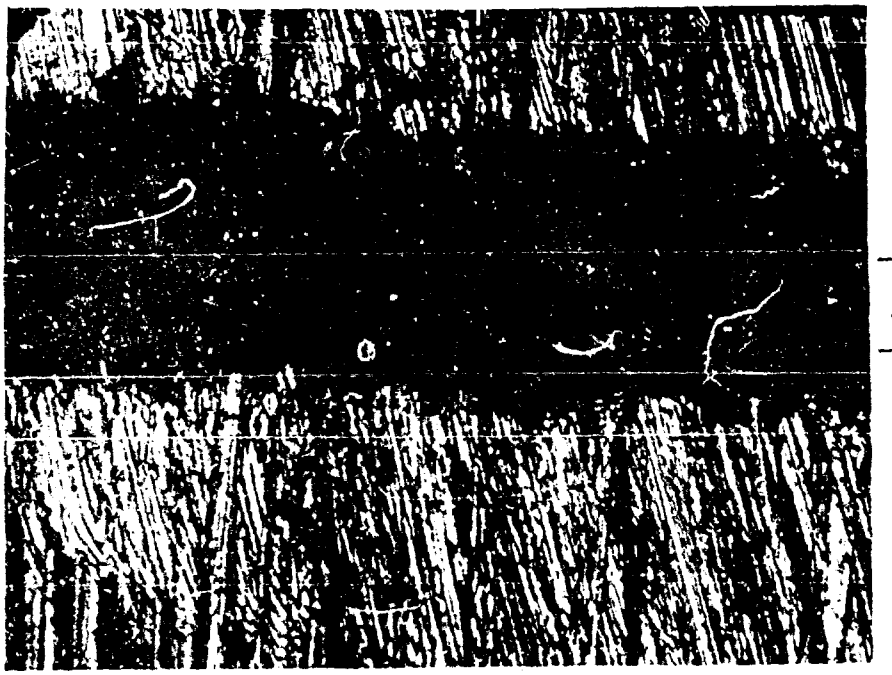

Photomicrograph

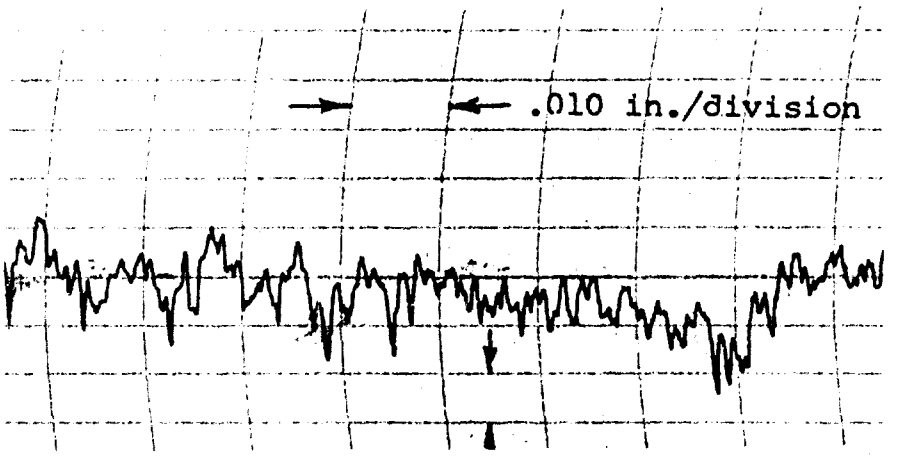

25μin./division
Typical Proficorder Trace

Figure 67 Surface Inspection Results - Flange No. 1

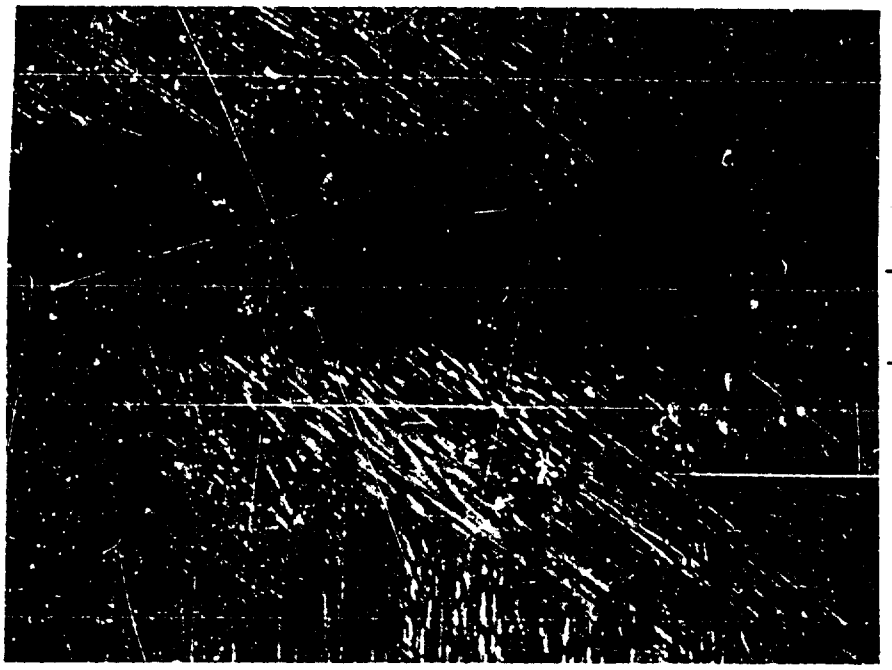

Photomicrograph

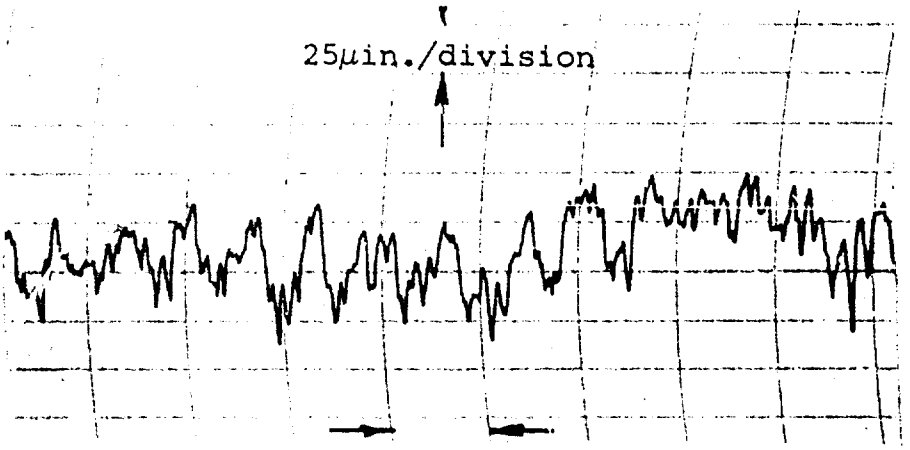

.010 in./division

Typical Proficorder Trace

Figure 68 Surface Inspection Results - Flange No. 2

Photomicrograph

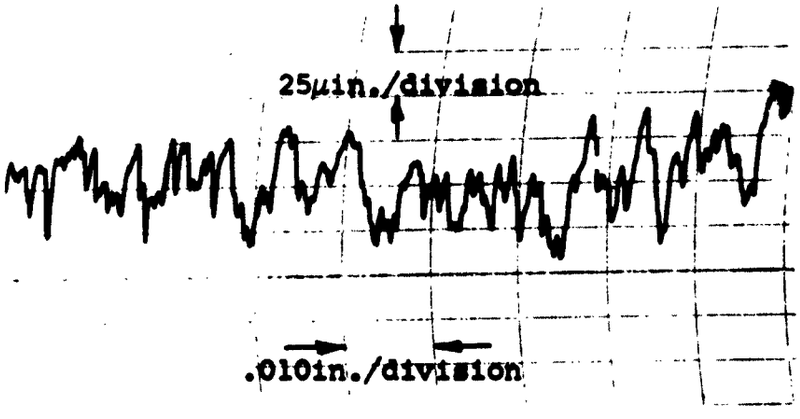

Typical Proficorder Trace

Figure 69 Surface Inspection Results - Flange No. 4

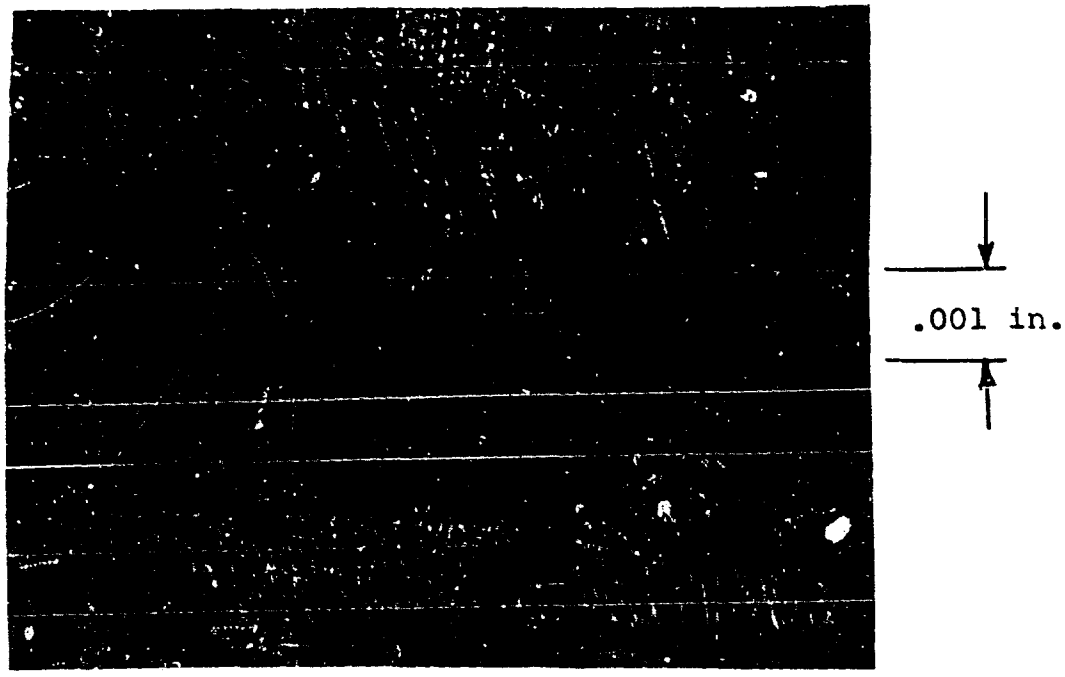

Photomicrograph

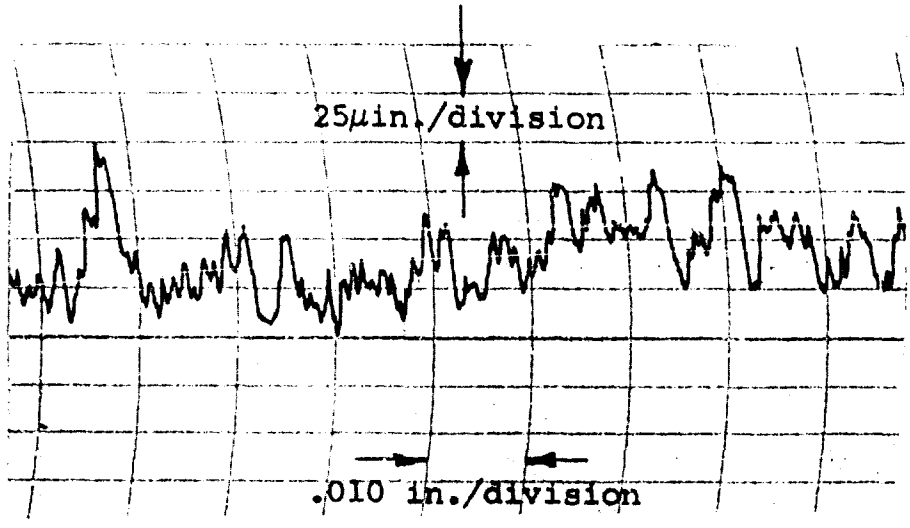

Typical Proficorder Trace

Figure 70 Surface Inspection Results - Flange No. 6

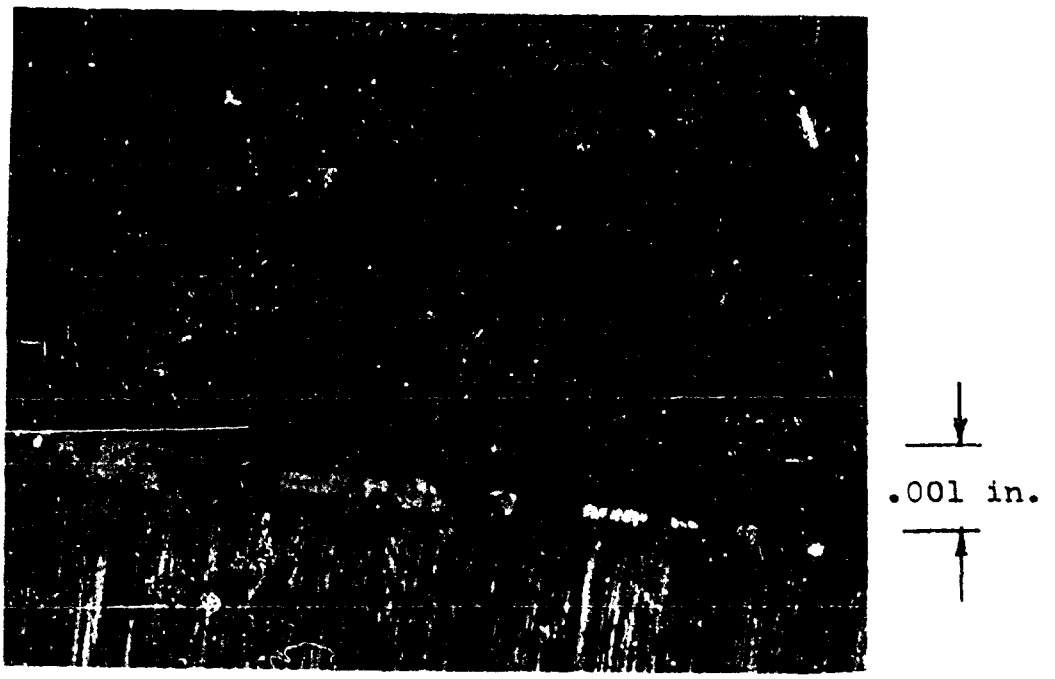

Photomicrograph

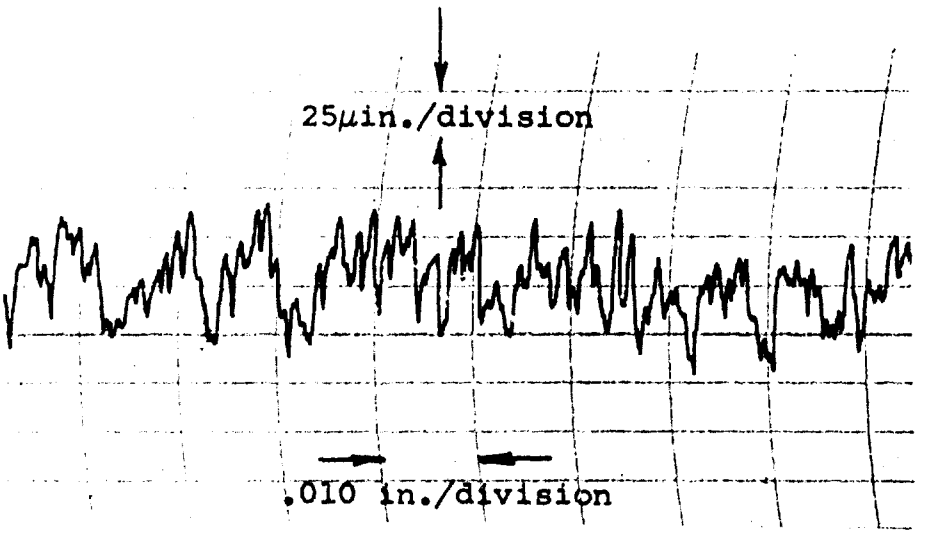

Typical Proficorder Trace

Figure 71 Surface Inspection Results - Flange No. 8

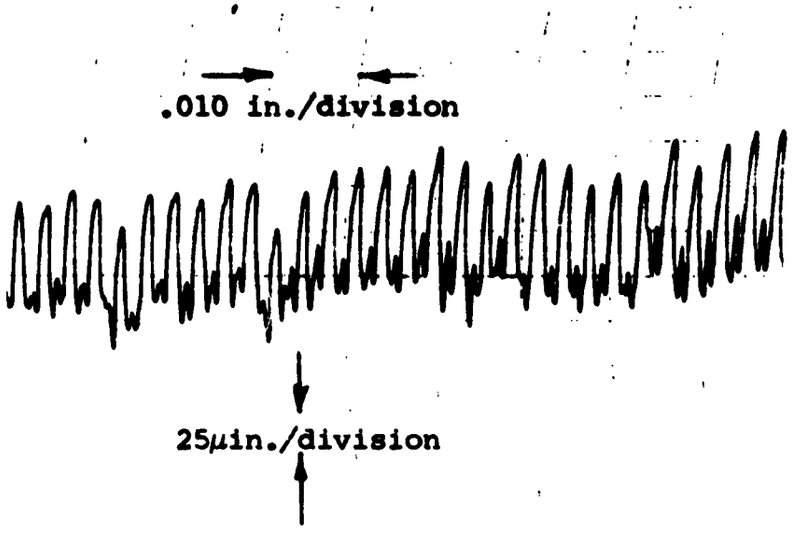

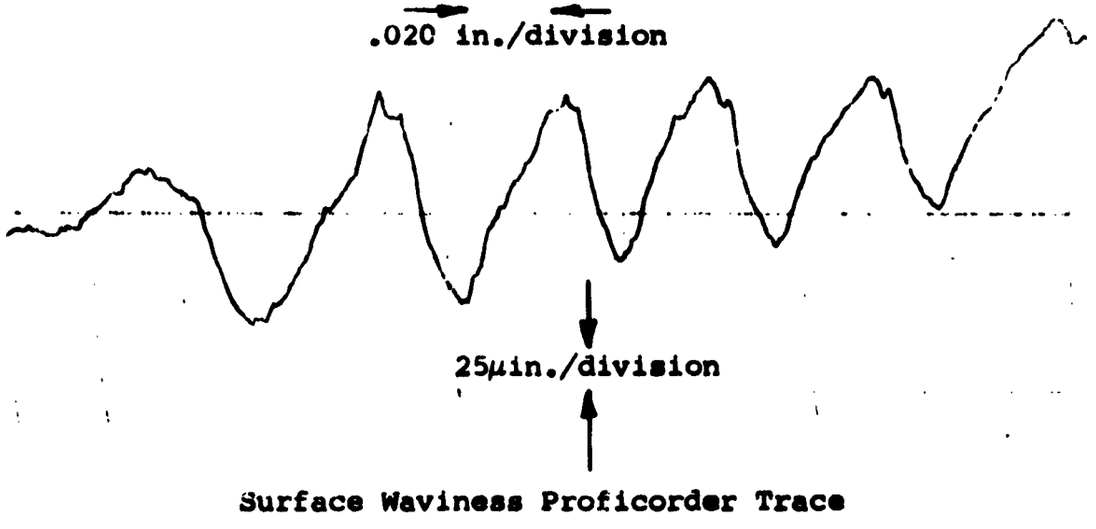

Figure 72 Surface Inspection Results of Top Flange (no flaws)

Flange No.

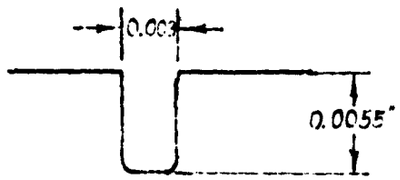

1

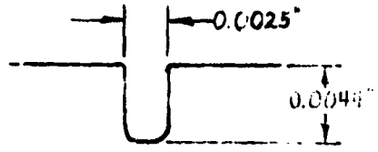

2

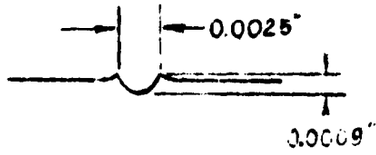

3

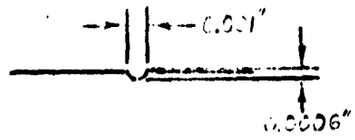

4

Figure 73 Test Results of Flange Flaw Cross-Section

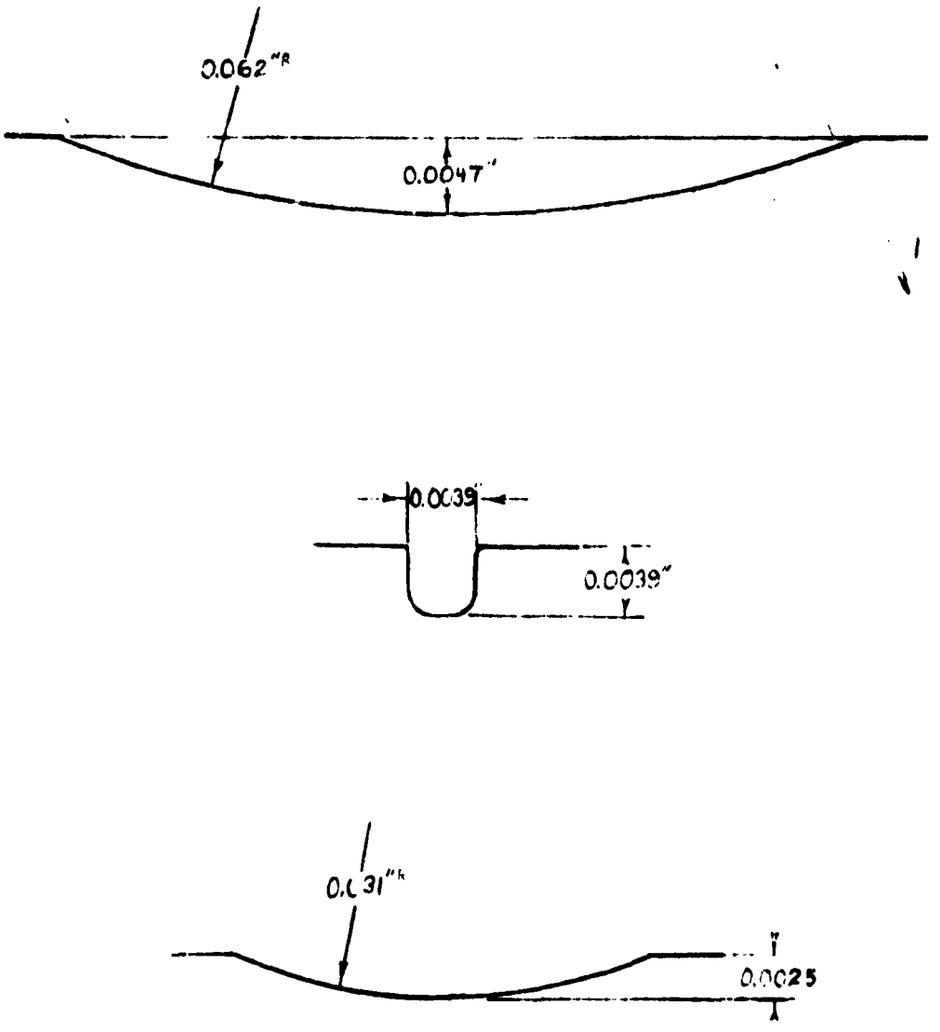

Figure 74 Test Results of Flange Flaw Cross-Section

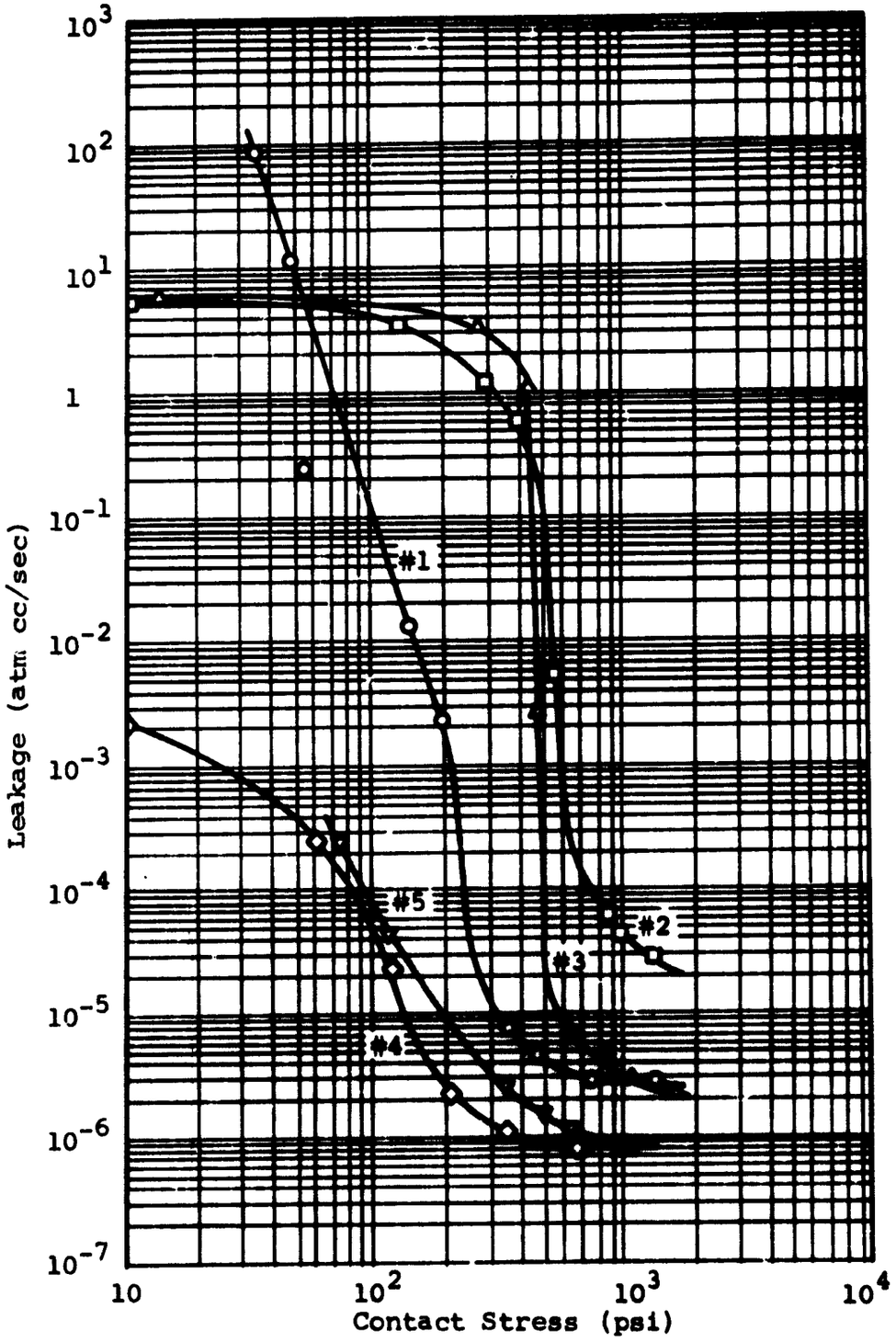

Figure 75 Leakage Versus Contact Stress for Various Flanges - Durometer = 50 Shore A

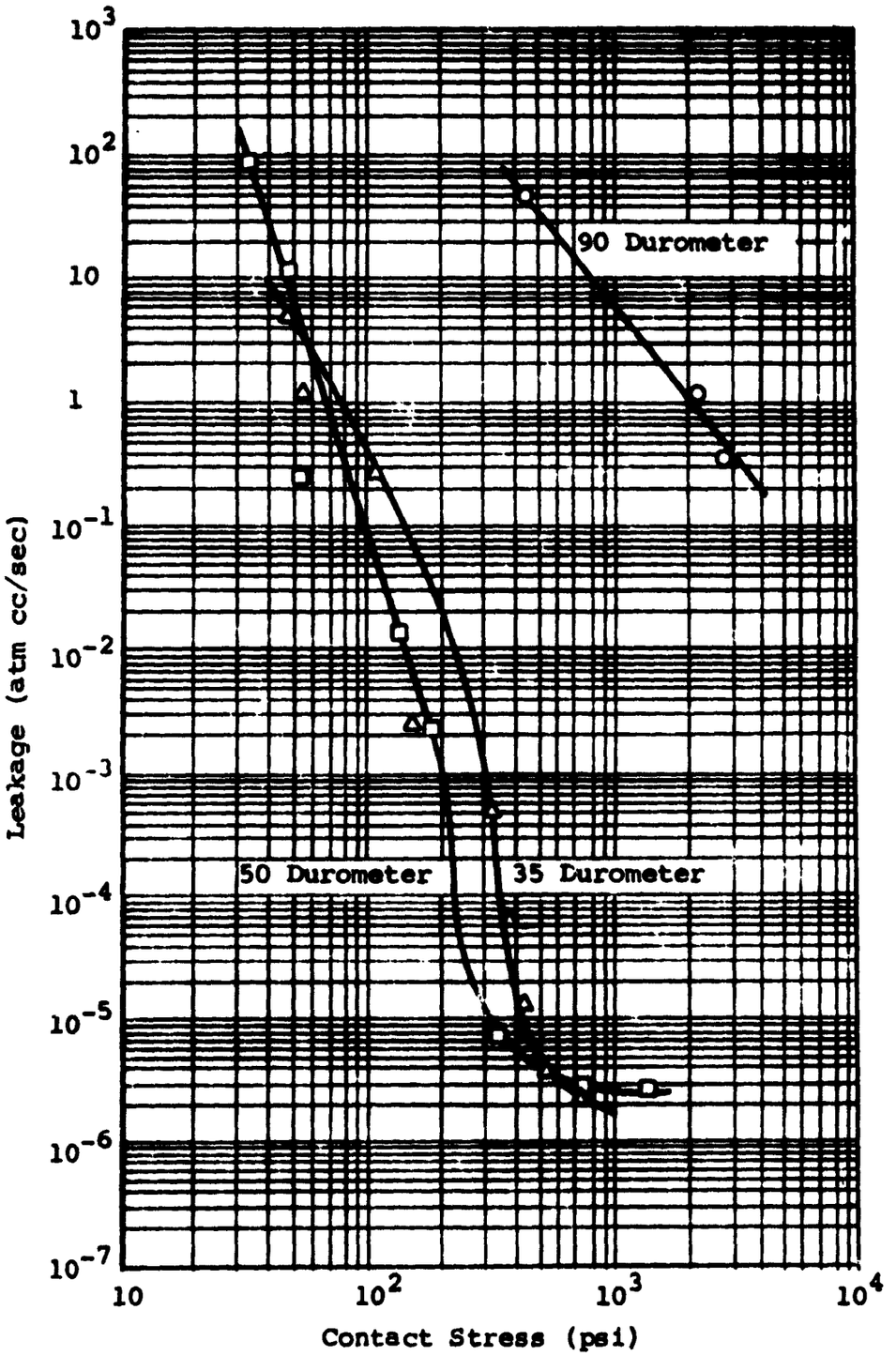

Figure 76 Leakage Versus Contact Stress for Various Hardness Rubber Seals (Flange No. 1)

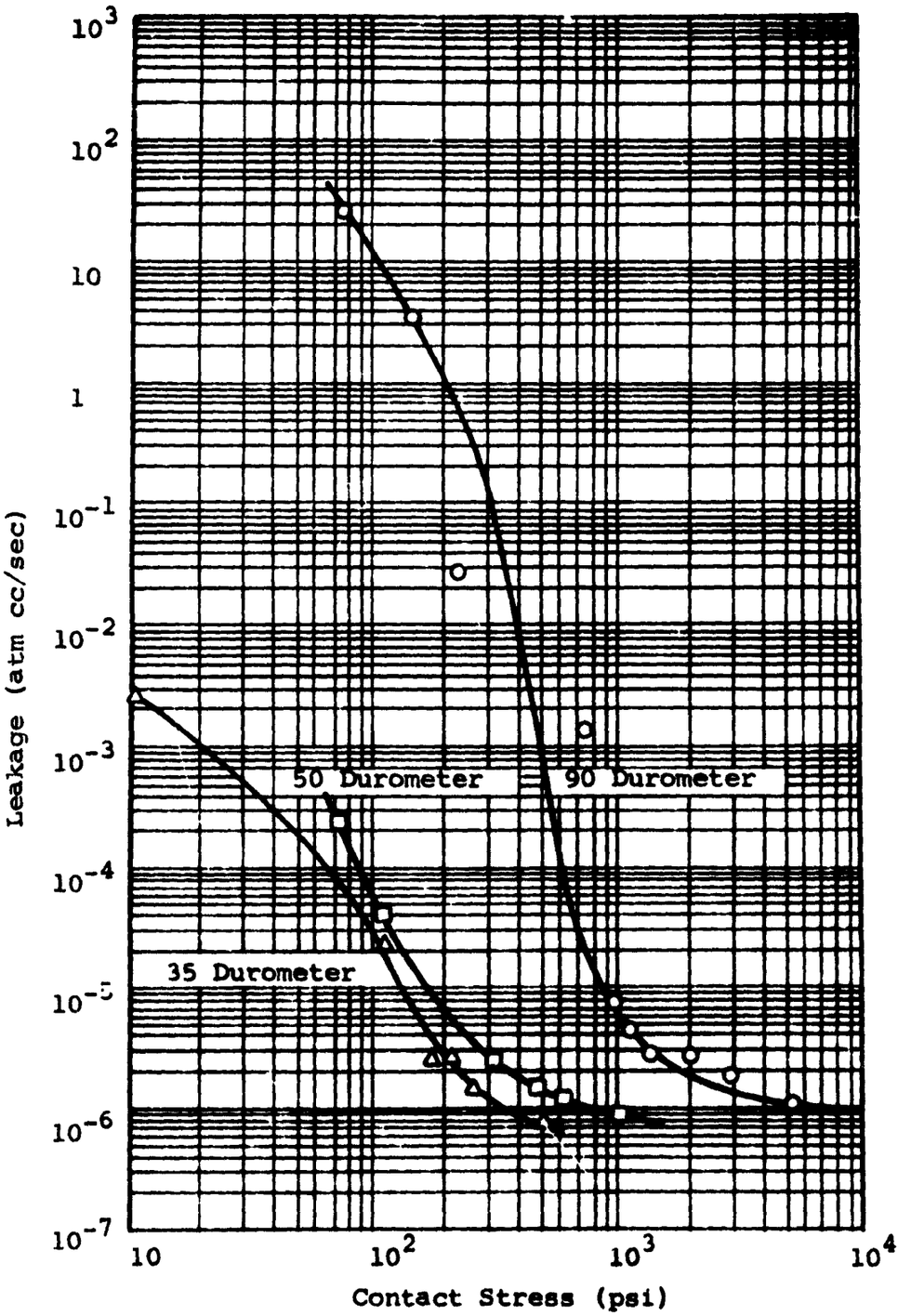

Figure 77 Leakage Versus Contact Stress for Various Hardness Rubber Seals (Flange No. 5)

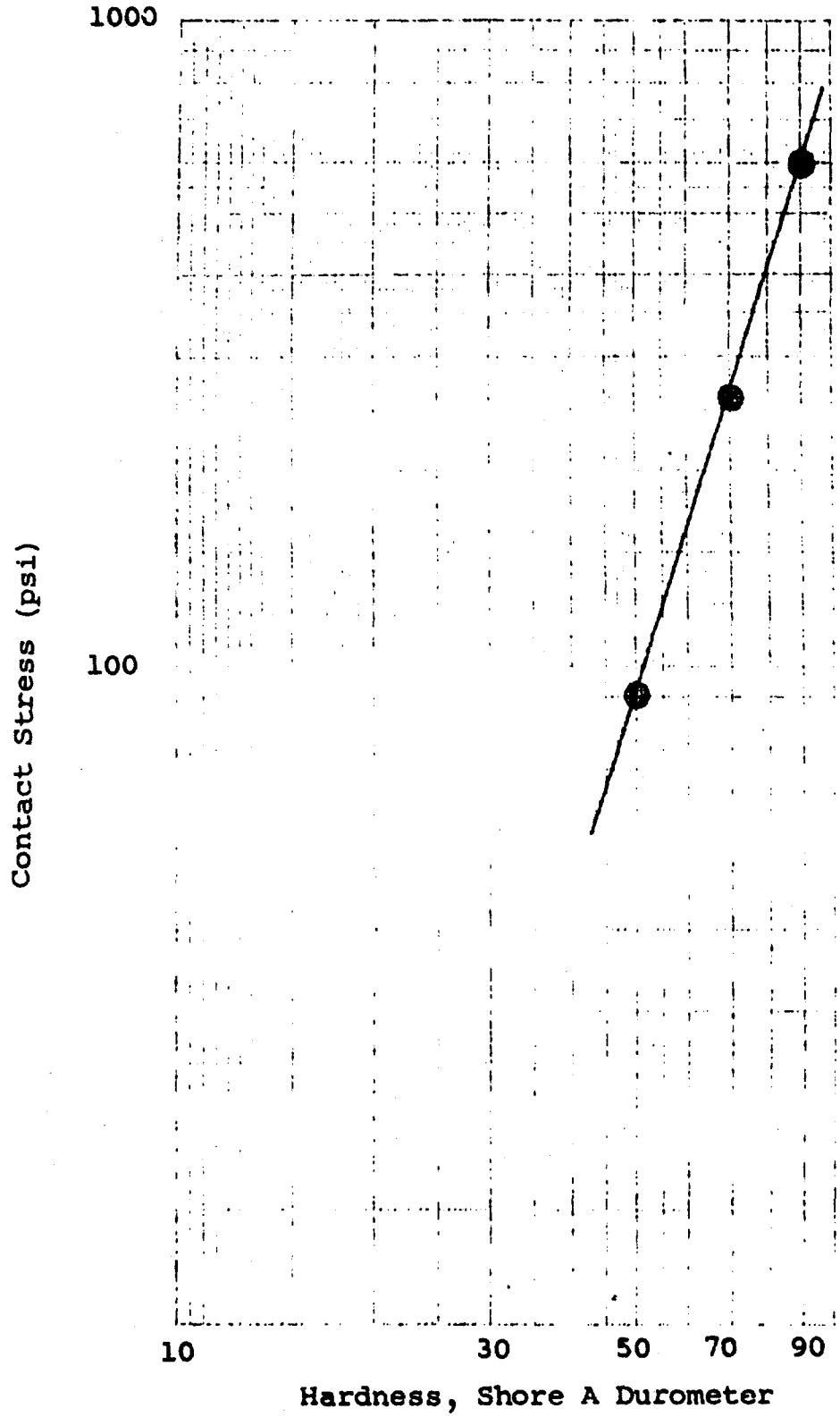

Figure 78 Durometer Hardness Versus Contact Stress for Buna-N Rings

leakage. The technique will have to be verified for other materials before its reliability can be determined.

The flange and gasket combinations were rather sensitive to applied load. Leakage decreased very rapidly for a rather small increase in load (five order of magnitude decrease in leakage for one order increase in contact stress).

The test results indicate that a repair method for scratches on the flange surface is smoothing and widening of the flaw. The elastomer seal conforms to this type imperfection readily. Imperfections such as a burr or foreign particle must be removed from the flange. If the particles are embedded in the rubber, the seal must be replaced.

The experiments conducted were mainly tailored to study the effects of material properties on conformability. They were all conducted in static seals. The effect of contaminants, surface imperfections, along with friction and wear encountered with relative velocity between the seal interfaces, were not considered. The particle generation process coincident with wear, as well as, the particle size generated or formed by particle adhesion and the effect of these parameters on spacecraft seals are suggested for future studies.

4. LEAKAGE VERIFICATION DEMONSTRATION

A leakage verification demonstration shown on Figures 79 and 80 was designed and manufactured to demonstrate the design criteria. This model consists of the following components:

- upper chamber which rotates
- pivoted cover
- lower stationary chamber which contains the drive motor
- pivoted arm assemblies
- upper and lower outer shell
- stand

The various locations which require seals are:

- feedthroughs

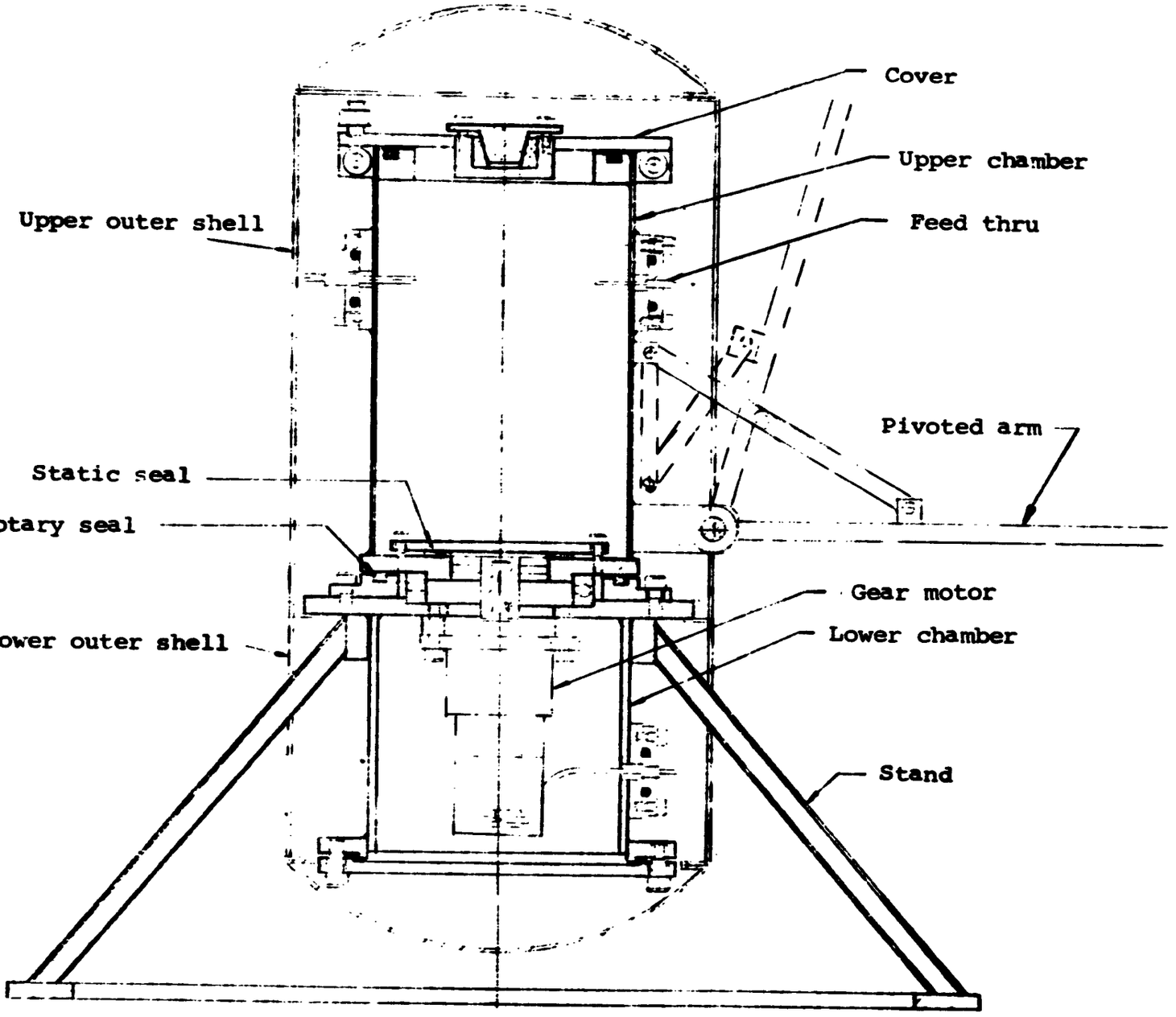

Figure 79 Leakage Verification Demonstrator

a) Cover Removed

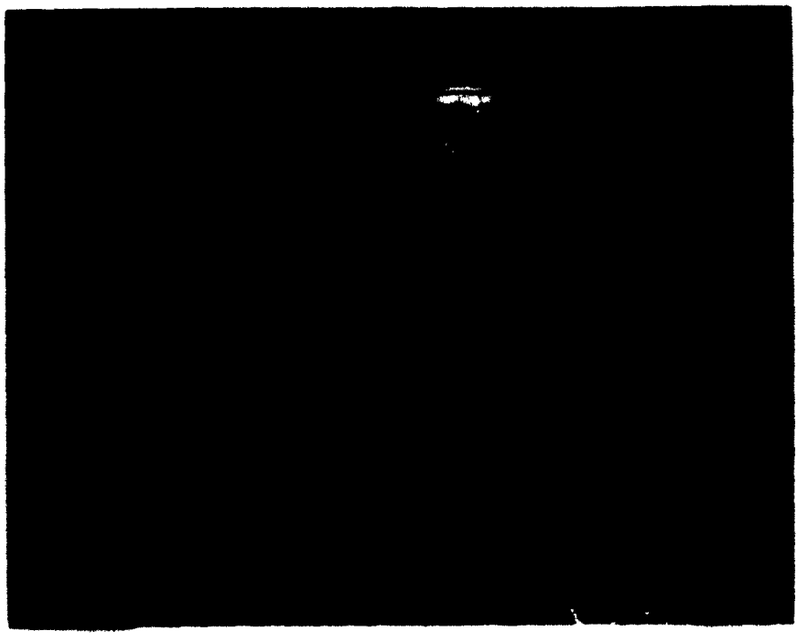

b) Cover in Place

Figure 80 Photograph of Leakage Verification Demonstrator

- pivoted cover
- rotary dynamic seal between chambers
- access cover to lower chamber

The seals selected for each location were state-of-the-art commercial seals. Interchangeability was foremost in mind so that more than one type of seal was applicable to any particular location. The specific seals chosen are depicted in Figure 81.

The size of the model is approximately 30 in. in diameter by 28 in. in height so that it can be accommodated in an existing vacuum chamber capable of 10^{-7} mm Hg pressure, or lower. Furthermore, the model is designed so that leakage measurements can be made on a single seal by blanking off all other sealed openings utilizing standard vacuum seals where contact stress can be increased to a level such that leakage is in the permeation region. The chambers are of welded construction. The entire assembly was pressurized with helium gas to an internal pressure of 30 psi and checked for leaks. Thus, leakage past the feedthroughs and the vacuum seals was determined to be negligible.

The leakage prediction for the Buna-N O-ring (cover) is accomplished by employing the deformation and hardness relationship data obtained from the visualization experiments. The conductance parameter is obtained from equation 33,

$$h = \frac{7.1 \times 10^{-4}}{15.4 + \sigma}$$

where

h = conductance parameter

σ = contact stress, psi

The forces acting at the interfaces are expressed by,

$$\sigma + p = \frac{F_N}{a}$$

where

p = pressure forces, psi

F_N = net applied load, lb

a = contact width, in.

"Omniseal" - spring preloaded, Teflon material seal, manufactured by Reid Enterprises, Inc.

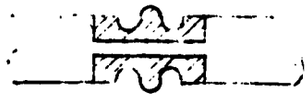

"Gask-O-Seal" - Buna N rubber molded in place seal, manufactured by Parker Seal Co.

Buna N rubber "O"-Ring

V-Cup Seal - Teflon V-shaped seal with aluminum loading rings

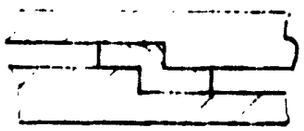

Interference or Stepped Seal, Copper Gasket, Indium Gasket

Figure 81 Leakage Verification Demonstrator Seals

The pressure forces acting on the interface, however, can be neglected because of their magnitude when compared to the net contact stress. Thus,

$$\sigma = \frac{F_N}{a}$$

As indicated by equation 20,

$$a = 1.6 \sqrt{\frac{F_N \, D(.75)}{E}}$$

Substituting these expressions into equation (33),

$$h = \frac{7.1 \times 10^{-4}}{15.4 + \dfrac{\sqrt{F_N}}{1.6 \sqrt{\dfrac{F_N (D)(.75)}{E}}}} \tag{44}$$

where,

D = ring cross-section diameter, (.25 in.)

E = modulus of elasticity (900 psi)

$$h = \frac{7.1 \times 10^{-4}}{15.4 + \sqrt{F_N}\,(43.3)}$$

The volume leakage rate can be calculated

$$Q = \frac{\pi D_R \, (P_1^{\,2} - P_2^{\,2}) \, h^3}{24 \mu \, a \, P_o} \tag{45}$$

where,

D_R = O-ring diameter (7 in.)

P_1 = internal pressure (28.7 psi)

P_2 = external pressure (14.7 psi)

P_o = ambient pressure (14.7 psi)

μ = viscosity of air (2.83×10^{-9} lb sec/in.^{2})

$$Q = \frac{23.4}{\sqrt{F_N}} \left[\frac{1}{(15.4 + 43.3\sqrt{F_N})^3} \right]$$

The results obtained for F_N equal to 1, 4, 9, and 16 lb are shown in Figure 82 compared to experimental data obtained from the demonstrator.

The predicted leakage values in the very low contact stress regions (1 to 3 psi) do not correspond very adequately. This can be attributed to the sensitivity of the load measuring device and the seal friction in the loading apparatus. These factors prohibit sensing load variations of two or three lb which substantially affect leakage values.

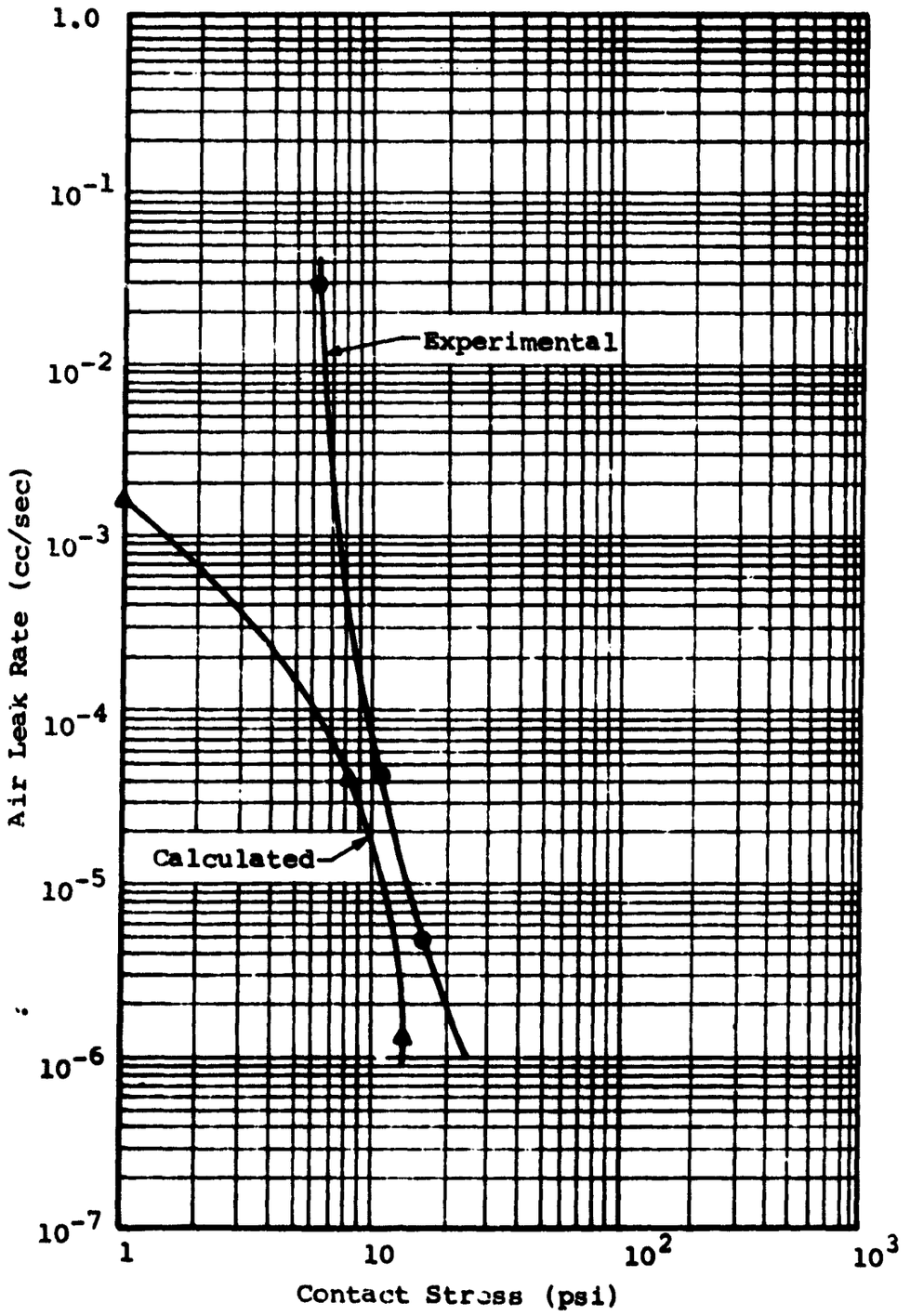

Figure 82 Experimental Verification of Leakage Prediction

SECTION VII

CONCLUSIONS AND RECOMMENDATIONS

The analysis of the leakage flow phenomena and the development of practical design techniques for controlling or predicting leakage resulted in the following conclusions and recommendations.

1. CONCLUSIONS

When two surfaces are pressed together, such as a flange and seal, a leakage path at the interface is formed by the interconnection of void spaces. The size of the void spaces determines the leakage rate and must be minimized by either producing mating surfaces having minimum topographical imperfections in terms of roughness and waviness, or by applying sufficient load to the surfaces to elastically and/or plastically deform them to conform to each other. When the mating surfaces are precisely and finely machined, a minimum load is required to attain conformability and low leakage.

Seal leakage can be predicted if the sealing interface topography is known. The topography, however, is determined by inspection and not by prediction. Empirical techniques based on the conductance parameter concept (Ref. 9), therefore, were found to be a useful method of describing the resistance to leakage flow afforded by the surfaces in contact. This conductance concept is analogous to a hypothetical uniform clearance obtained from theoretical flow equations.

The hardness of rubber materials can be empirically correlated to leakage rates since conformability or elastic deformation is a function of leakage rate. A theoretical basis for this correlation, however, still needs to be established.

Leakage rates of gases and liquids of 10^{-6} cc/sec, and lower, in static seals were shown to be attainable by elastically or plastically deforming the material to conform to the microscopic surface topography of the mating surface. Plastic deformation to the extent necessary for such leakage in dynamic seals is not practical if relative motion is to occur at the interface. Aside from elastically deformable rubber materials, elastic deformation of the surface topography of materials is not feasible. The performance of dynamic seals is governed by the degree of initial interface mating and the effects of rubbing contact.

The most important criterion, leakage performance, was not obtainable in the majority of cases and, therefore, could not be used as a means of seal classification. The classification of seals by sealing mechanism, as well as application, adequately covers the basic types of seals and provides the designer with an insight into their innovations and features.

It is not possible to give a generally applicable structural analysis of seals and seal housings. The many structural configurations which exist necessitate an individual analysis. Only one typical structure, therefore, was analyzed to demonstrate the relationship between structural effects and leakage, and to indicate a method of approach.

Elastomer sealing, generally, is an optimum method. The elastomer deforms nearly entirely elastically, and conformability is achieved at relatively low contact stress values. The initial mating flange surface finish does not affect the leakage level attainable. When environmental conditions permit their use, elastomers should be employed.

Plastic seals or gaskets may be used where low contact stress is necessary and some leakage can be tolerated. The increase in contact stress necessary to achieve approximately the same leakage values as with rubber seals is one order of magnitude. To achieve a leakage rate of 10^{-4} atm/cc/sec with rubber requires 10^{2} psi contact stress, while with plastic and aluminum, it requires 10^{3} and 10^{4} psi, respectively. Plastics, however, have limited application when used alone as seal materials due to their cold flow and permeability characteristics. Plastics bonded to metals or other materials in thin layers are generally more appropriate seal material arrangements.

Metallic seals, because of the high loads necessary to achieve conformability, should be employed only where the environment necessitates their use. When metallic seals are used, structural seal geometries which promote plastic deformation between the mating surfaces are recommended for static applications.

2. RECOMMENDATIONS

As a result of these studies, several areas requiring further investigation were uncovered. Areas where additional design information would be beneficial also emerged.

Conformability of rubber materials, and the deformation process involved, need to be further investigated to attain an analytical correlation between leakage and material properties. If the data, furthermore, could be related to contamination tolerance, the effect of contaminant particles on the interface deformation process as well as the change in contact stress due to the presence of particles would be more fully understood.

The general housing and cover analyses could be conducted to a level where weight versus contact stress and leakage are optimized. The iterative process necessary to attain this data can be computerized, and a family of design curves generated to enable the designer to optimize the cover or housing dimensions with leakage as the controlling element. This general approach to the housing or cover structural deformation problem could be extended to cover many of the typical cases to be found in pressurized spacecraft components.

Methods of fabrication for seal components and inspection techniques available for determining the accuracy of the fabrication process could be investigated. The size of the seal encountered in spacecraft designs may require excessive loads to achieve sufficient deflections of the seal to achieve circumferential sealing. Since the relative slenderness necessary in spacecraft components due to weight optimization may create warping problems after the part is removed from the machine fixture, tolerance variations other than those caused by machining process inaccuracies may have to investigated.

An analysis of the O-ring deformation process could be conducted which includes the change in ring shape, as well as, the non-linear modulus of elasticity of rubber. Such an analysis should yield design criteria applicable to any rubber material and result in an improvement over the empirical and analytical deformation approximation methods discussed in Section IV. This would provide an insight into the fundamental reasons for the success of an O-ring as a seal. The susceptibility to contamination and contaminant particle location relative to the interface boundaries can be determined, and the maximum tolerable particle size can be predicted. Similar analysis could be carried out for other cross-sectional shapes of elastomeric seals.

The leakage prediction techniques can be modified to include the effects of material degradation. Studies to determine the effect of space environment on material properties affecting the leakage mechanism should be conducted. Such parameters as hardness change, compression set, weight and size loss should be related to leakage or contact stress, with environment exposure time as the variable.

The influence of rubbing contact on topographical changes of dynamic sealing surfaces could be investigated. If the influence of wear can be satisfactorily described and design criteria generated, an attempt could be made to include all forces acting on the fluid and seal in an over-all theoretical analysis.

APPENDIX

The various seal configurations and sealing methods shown in the following figures are representative of the many possible techniques either being used or being studied for possible application to future spacecraft.

Although an analysis of each of the various designs was outside the scope of the study, it was considered worthwhile to present a selection of typical seals from the literature. Many of the seal configurations are old art or can be obtained from several sources; other special shapes are unique to a particular manufacturer. Design concepts for spacecraft seals which have been taken primarily from references are acknowledged.

In spite of the endless variety of seals, one can be encouraged by noting that one or more of the basic mechanisms of sealing as discussed in this report are applicable to each seal. Judicious use of the suggested analytical and experimental techniques will enable proper evaluation of any seal configuration.

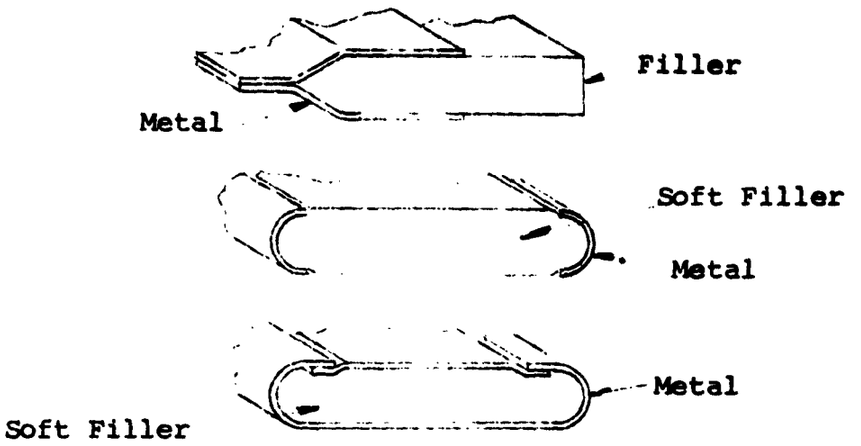

Figure 83 Composite Gaskets of Jacketed Type

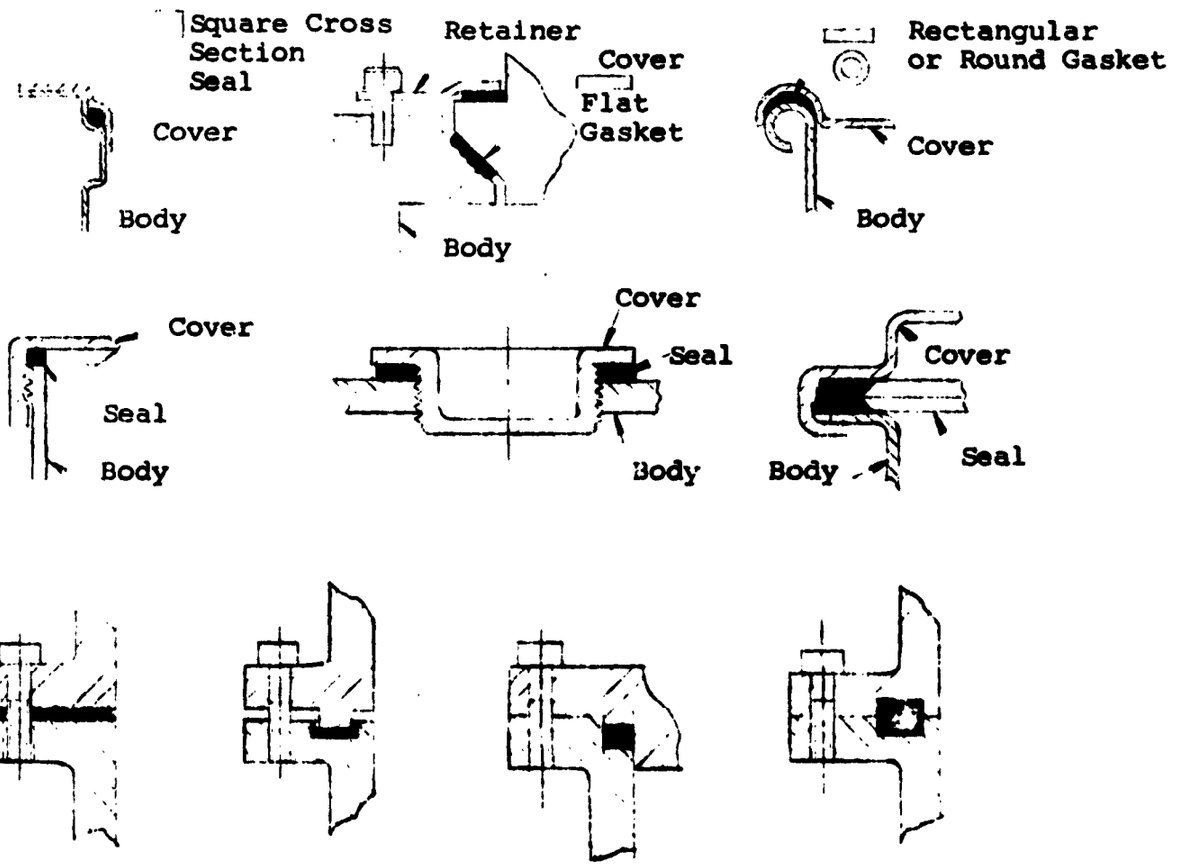

Figure 84 Typical Gasket Type Joints

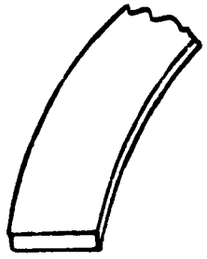

Flat Elastomer Strip

(a)

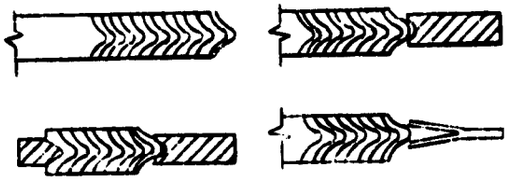

General Purpose
Flange Gasket
Spiral Laminated
Asbestos, Metal,
Elastomer

(b)

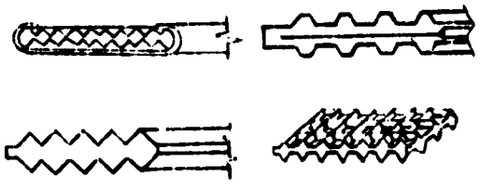

General Purpose
Flange Gasket
Metal Case
Filler, Asbestos or
Elastomer

(c)

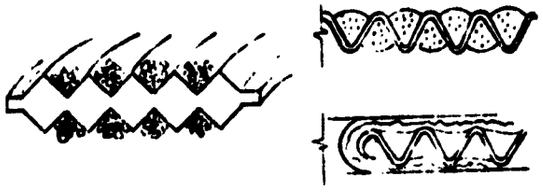

Flange Gasket
Corrugated, Metal
Reinforced
External Covering,
Asbestos, Elastomer

(d)

Figure 85 Gasket Configurations

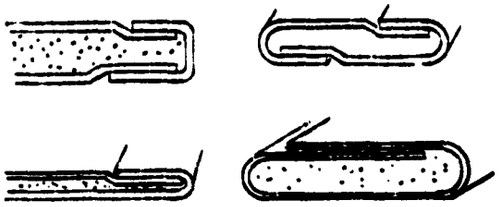

General Purpose
Flange Gasket
Metal Jacket
Filler, Soft Metal,
Elastomer, Asbestos

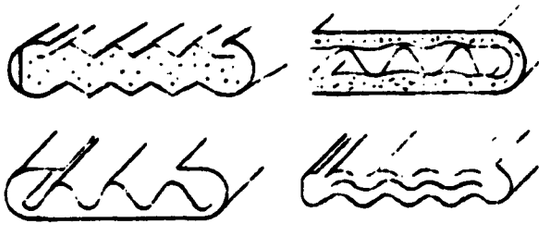

General Purpose
Flange Gasket
Metal Jacket
Filler, Soft Metal,
Elastomer, Asbestos

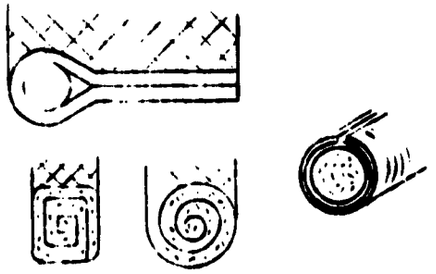

General Purpose
Flange Gasket
Metal or Elastomer Jacket
Filler, Soft Metal,
Elastomer, Asbestos

Figure 85 Gasket Configurations (Cont.)

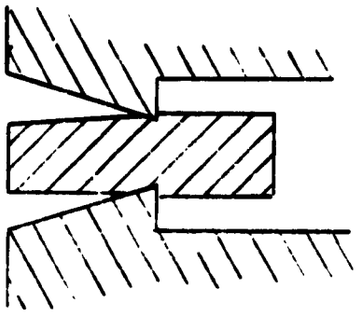

Gasket
Soft Metal
Two Shaped Flange

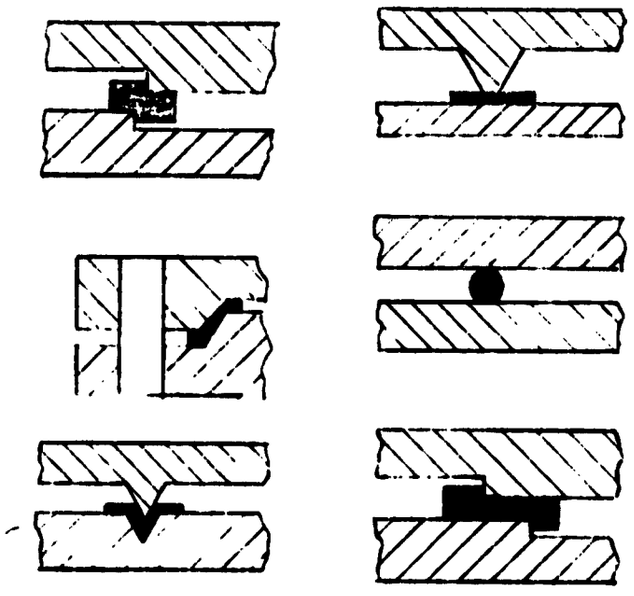

Gaskets
Soft Metal
Plastic Deformation
or Interference Seal

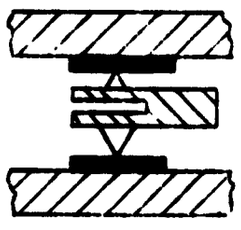

Gasket
Soft Metal
Median member provides
resiliency and spring-
type loading

Figure 86 Cryogenic Type Gasket Seals

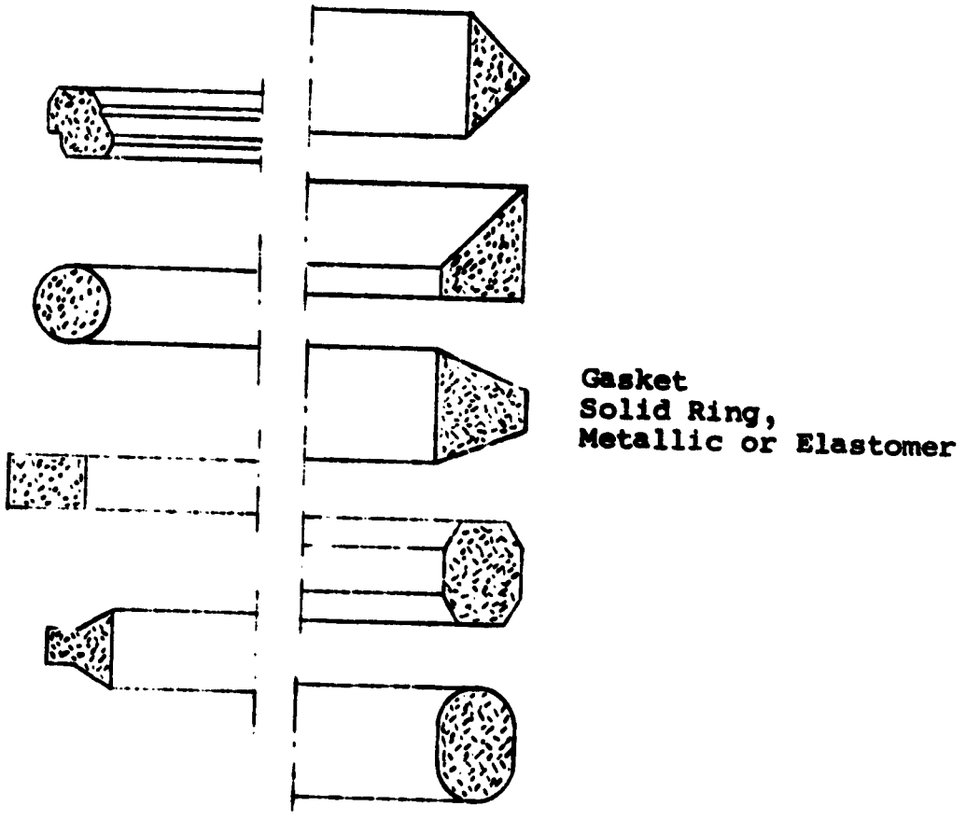

Figure 87 Metallic Gasket Ring Shapes

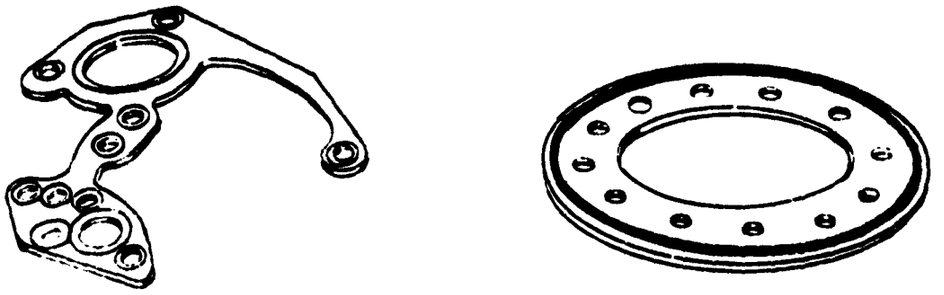

Figure 88 Configurations of Molded-In-Place Elastomeric Seals

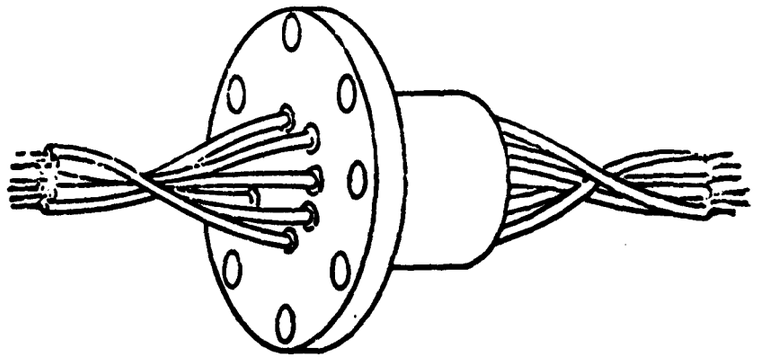

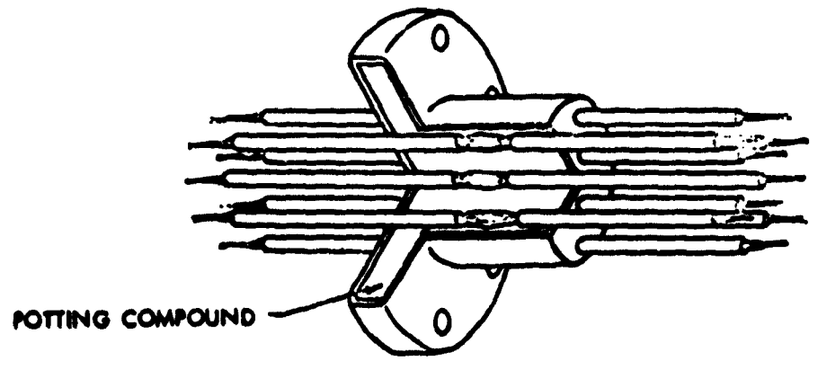

Figure 89 Typical Insulated Wire Seal and Potting Concept

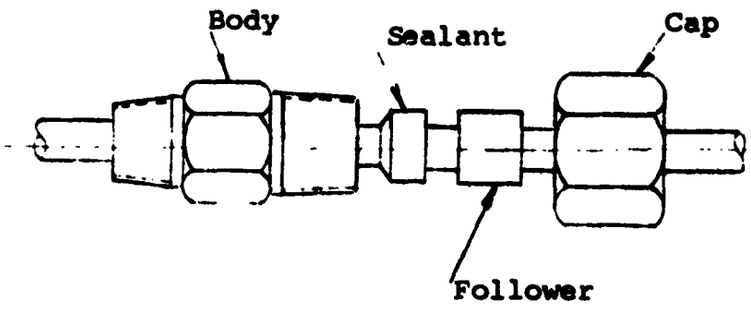

Figure 90 Packing Gland Type Seal

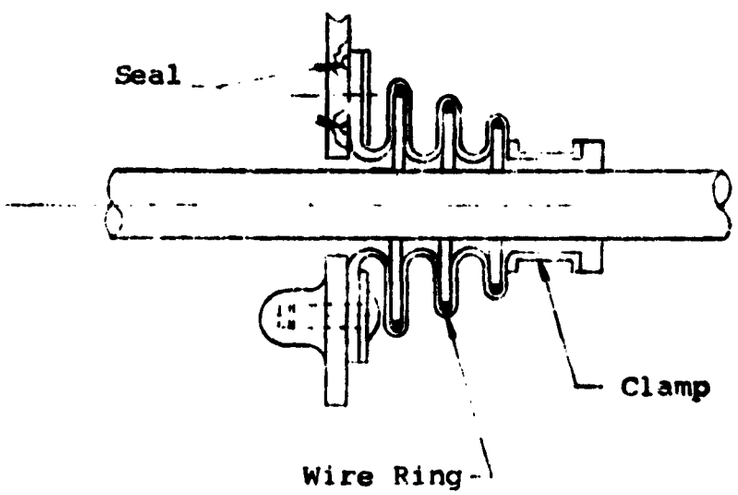

Figure 91 Bellows Pressure Seal

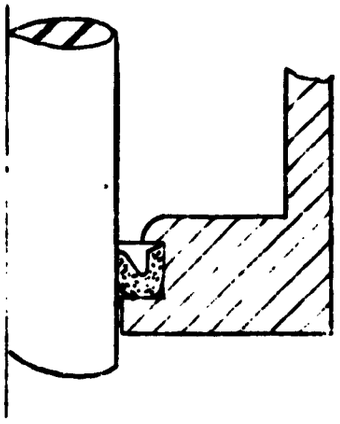

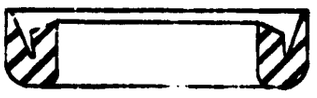

Flexible Lip
Pressure Actuated

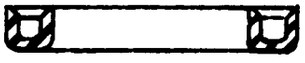

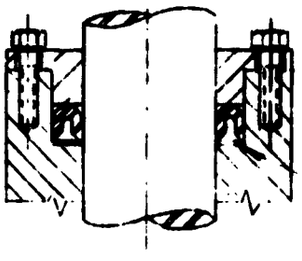

Retaining
Ring

U Cup
Flexible Lip
Pressure Actuated
Metal Retainer Ring
Usually Used to
Prevent Seal Motion

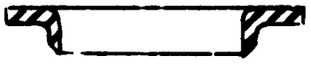

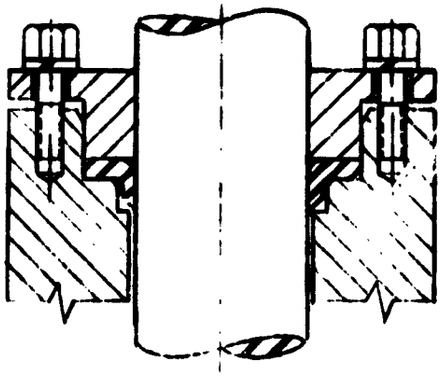

Hat Cup
Flexible Lip
Pressure Actuated
Held in Position
by Flanges

Figure 92 Nonmetallic Conforming Sliding Seals

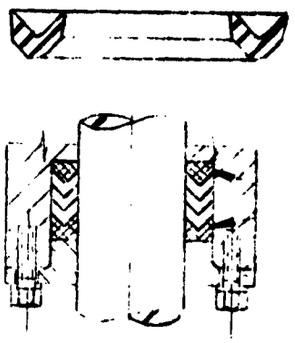

V Cup
Flexible Lip
Retainer Pressure Actuated
Rings Used with Retainer Rings

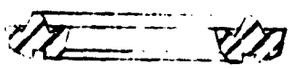

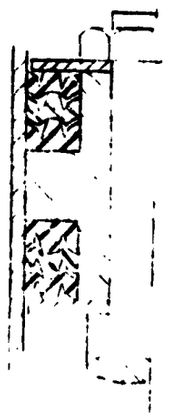

W Ring
Flexible Lip
Pressure Actuated

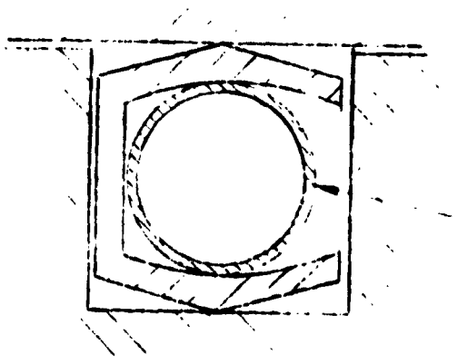

Spring

Teflon Seal
Pressure Actuated
Spring Loaded

__gure 92 Nonmetallic Conforming Sliding Seals (Cont.)

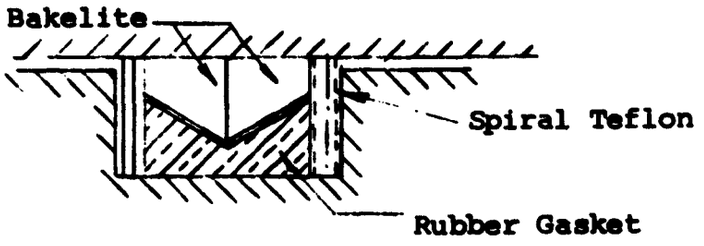

Segmented Bakelite Wedge Pressure Loaded by Rubber Gasket

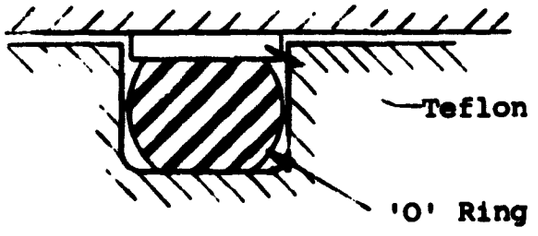

Teflon Ring Pressure Loaded by 'O' Ring

Figure 92 Nonmetallic Conforming Sliding Seals (Cont.)

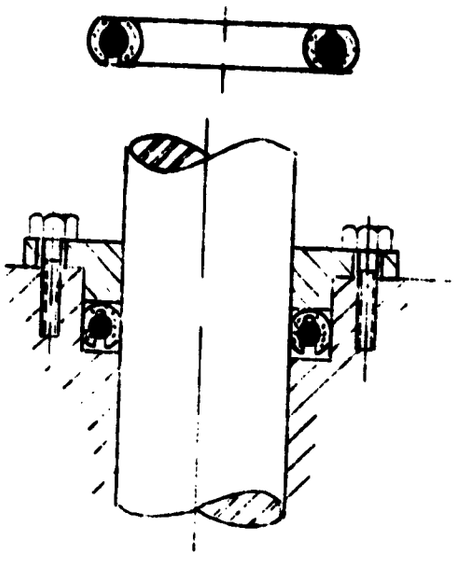

Teflon Seal Surface
Pressure Actuated
Spring Loaded
or Pressure Loaded
With O Ring

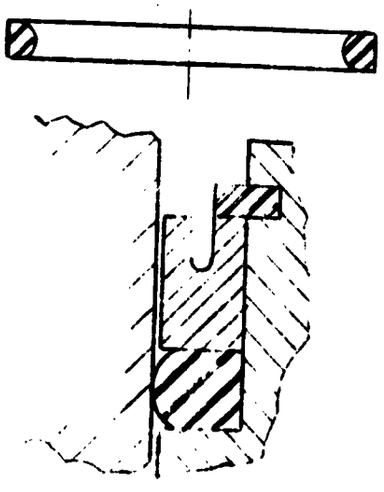

D Ring
Initial Compression
Pressure Actuated

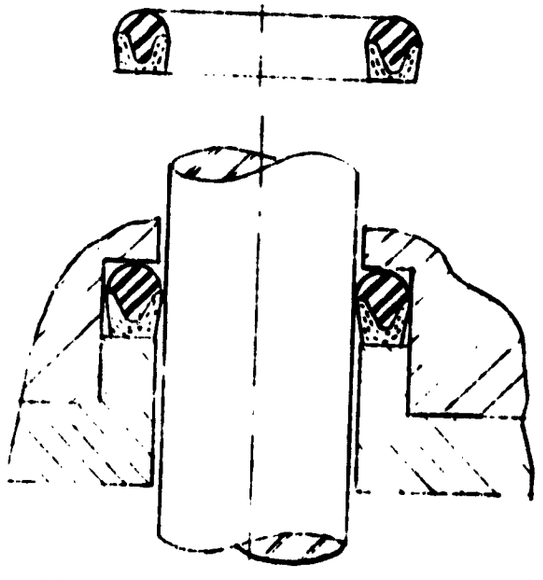

Rubber Seal Surface
Fabric Reinforcing
Jacket
Pressure Actuated

Figure 92 Nonmetallic Conforming Sliding Seals (Concluded)

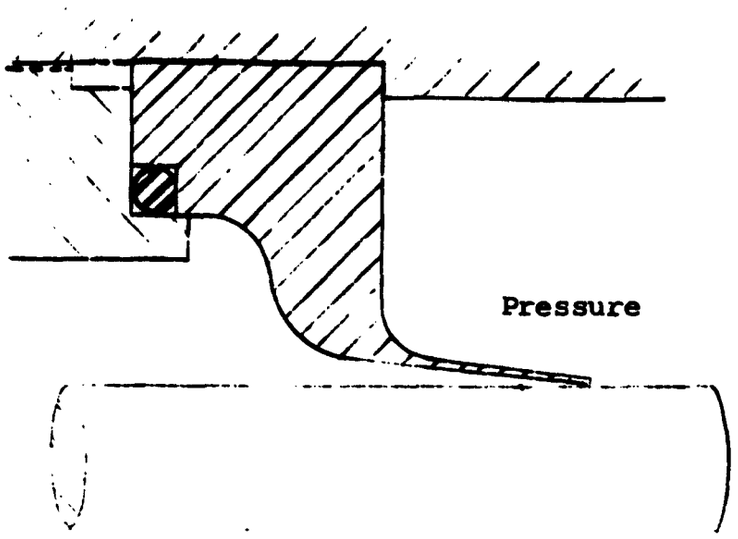

Flexible Reed
Reed Deflects to Conform to Shaft Because of Initial Interference

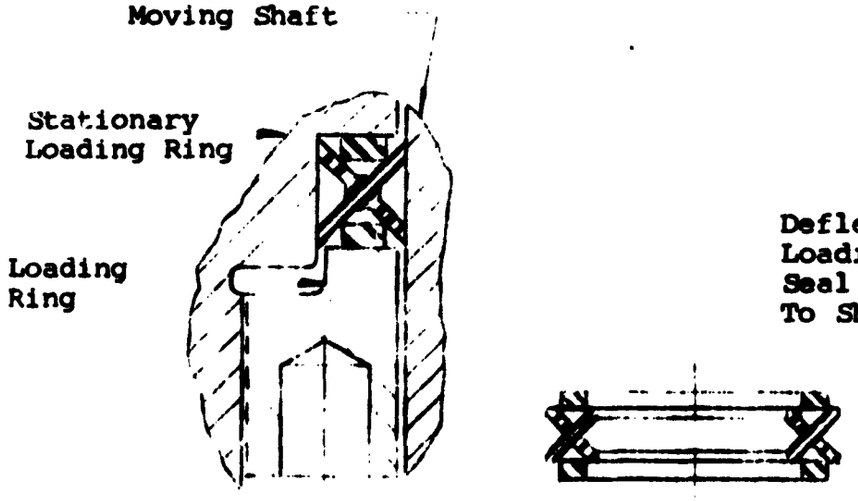

Deflection Caused by Loading Ring Forces Seal Legs to Conform To Shaft

Figure 93 Metallic Conforming Sliding Seals

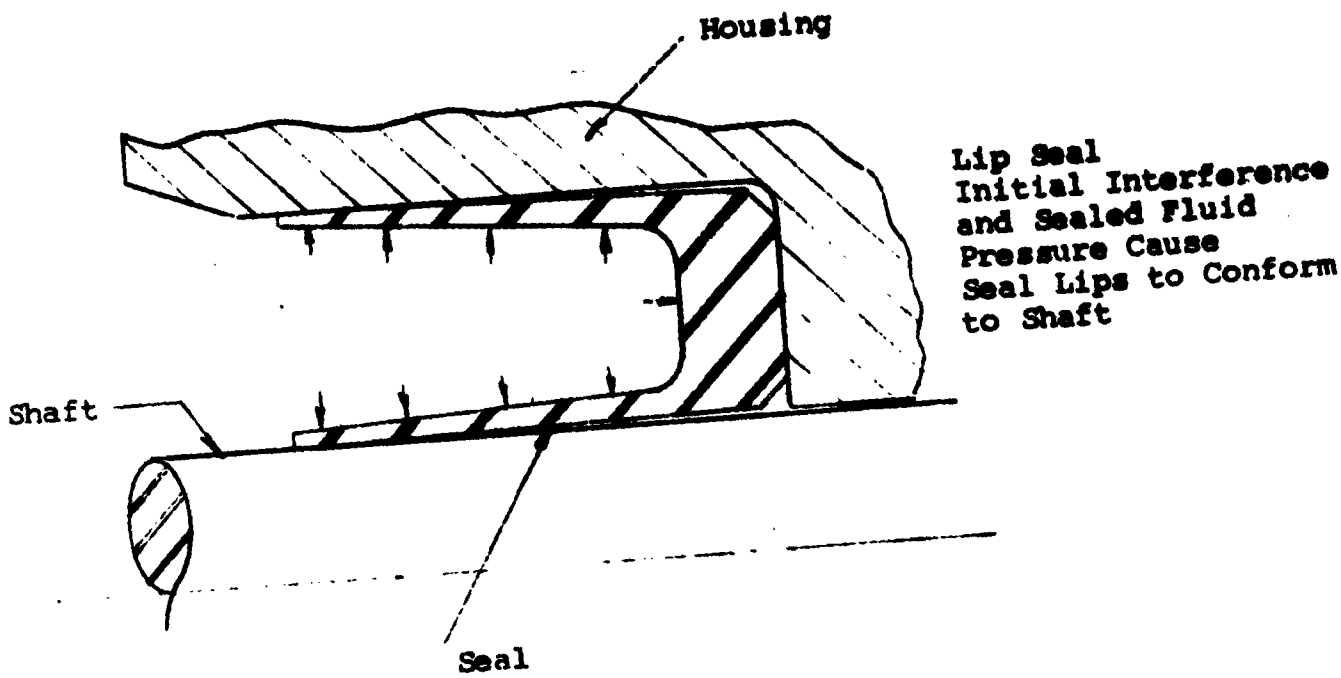

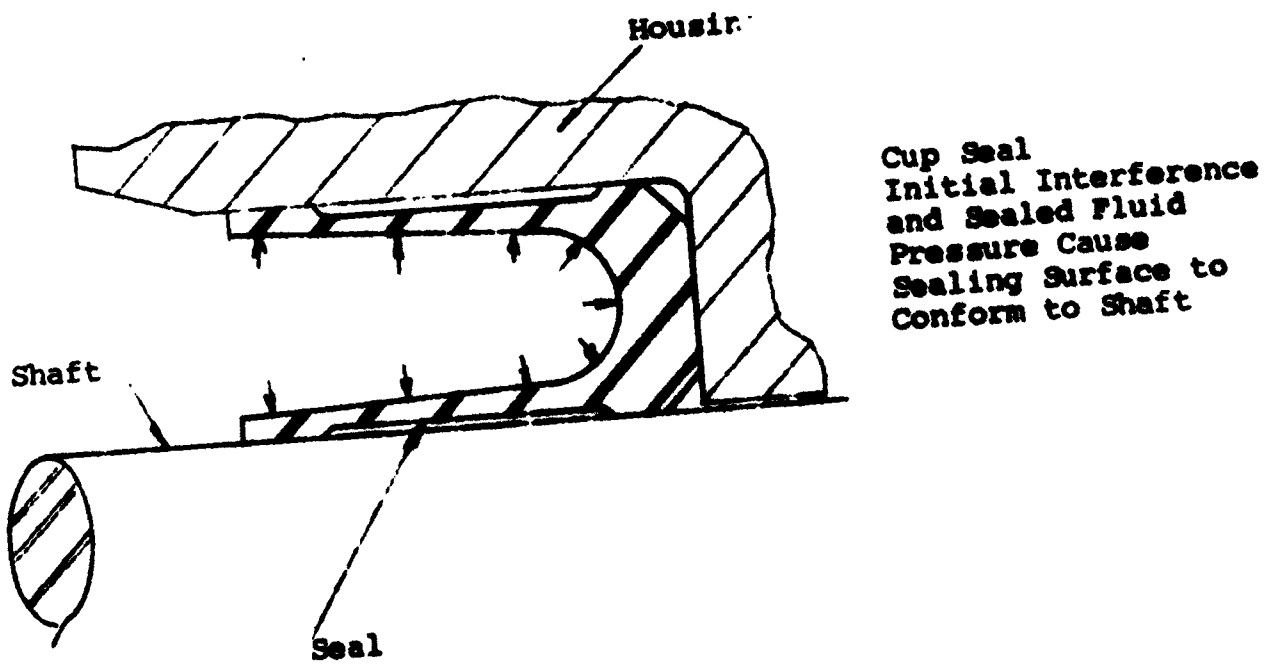

Figure 93 Metallic Conforming Sliding Seals (Continued)

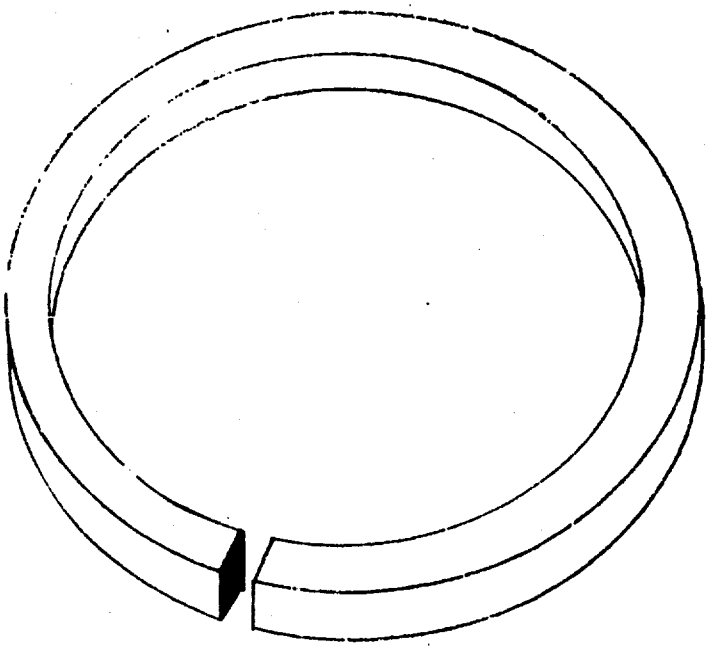

Split Piston Ring
Various Gap Configurations are Available
Used as Either Bore or Rod Seal

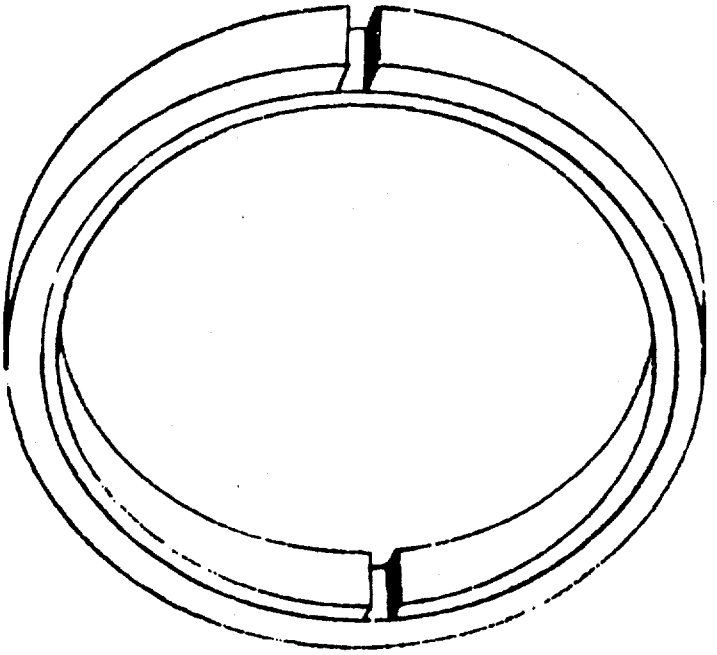

Double Piston Ring
One Ring Acts to Spring Load, the Other
Gaps Staggered to Improve Sealing

Figure 94 Precision Mating Seals

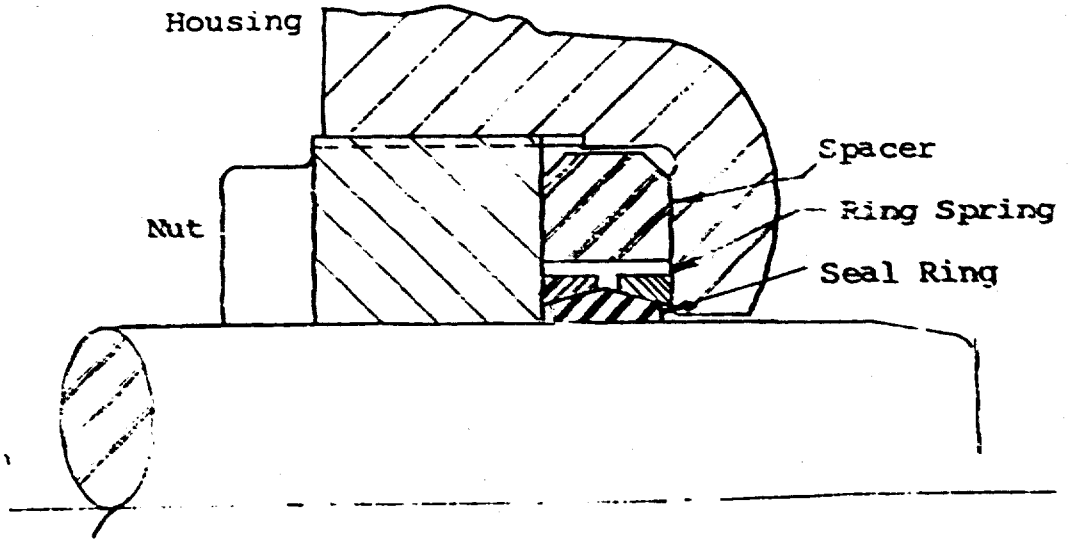

Ring Spring Seal: Hoop tension in spring caused by nut forcing spring up the tapered seal ring, creates high contact stress at sliding interface

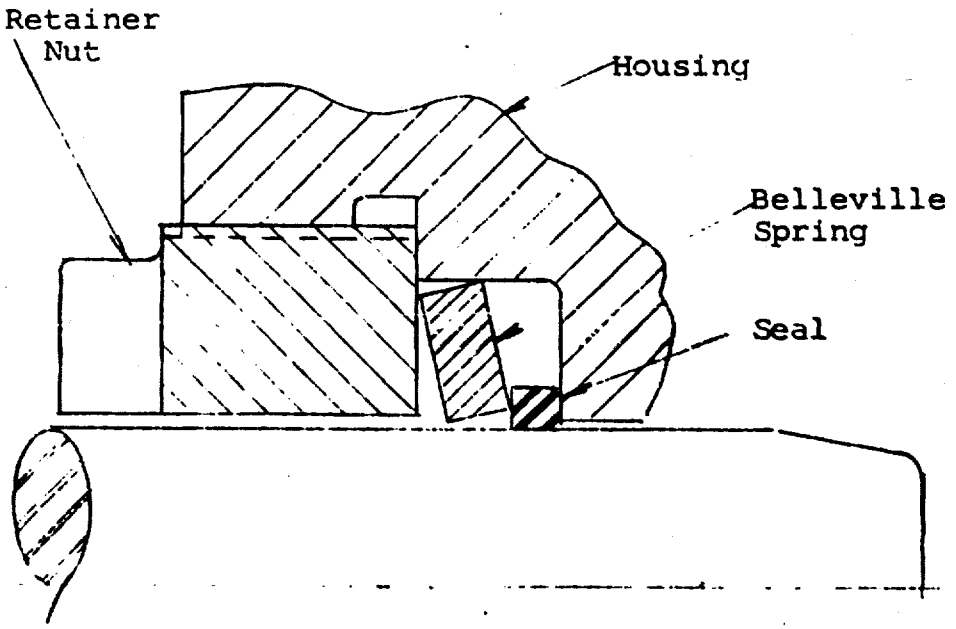

Interference Ring Seal: Interference fit causes high contact stress at sliding interface

Belleville Spring: Holds seal in place

Figure 95 Interference Type Sliding Seals

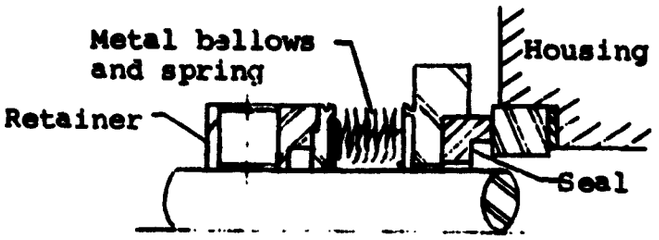

Rotating Assembly
Metal bellow replaces static seal, provides spring loading, suitable for high and very low temperatures, corrosive environments

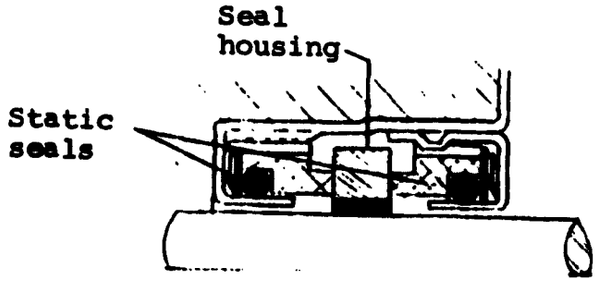

Cartridge Seal
Utilized construction allows simple assembly

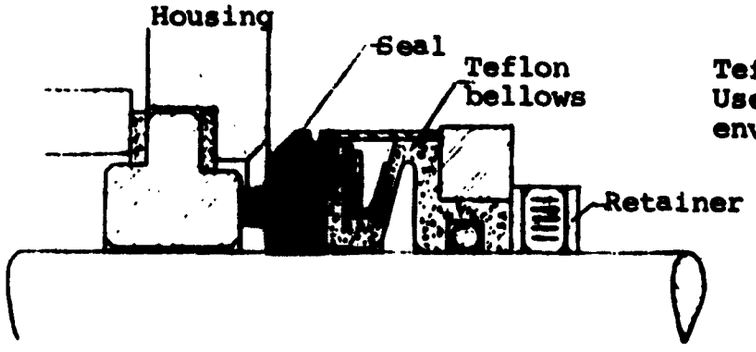

Teflon Bellows
Used in corrosive environments

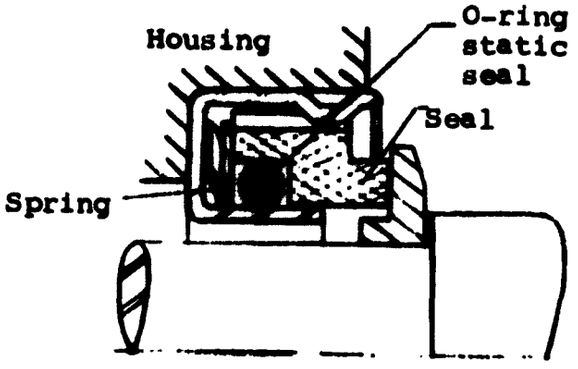

O-ring Static Seal
Stationary Assembly
Temperature and compatibility limited by O-ring material

Figure 96 Mechanical Face Seals - Rotating Shafts

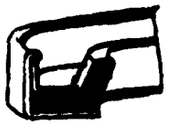

Cased Type Single Lip
Non spring loaded,
used for low surface speed
and low pressure

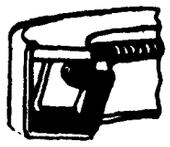

Cased, Single Lip
Spring loaded
contact stress supplemented
spring force
various spring types used

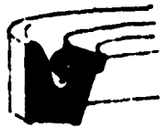

Bonded, Single Lip
Spring loaded
sealing element bonded
to case

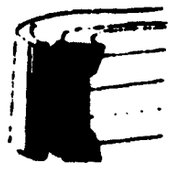

Bonded, Multiple Lip
Spring loaded
opposed lip

Figure 97 Lip Type Rotary Seals

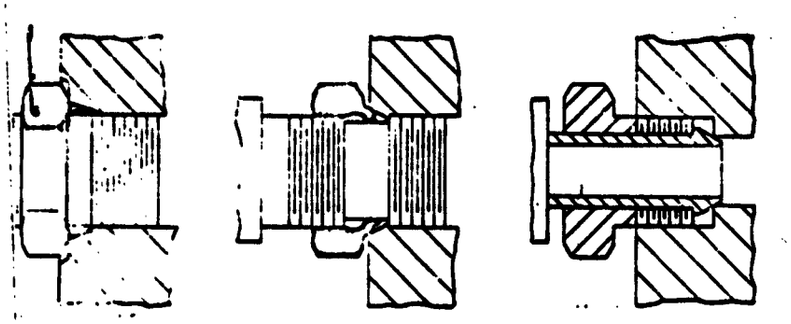

Straight Thread O-ring seal

Metal to Metal

Metal to Metal

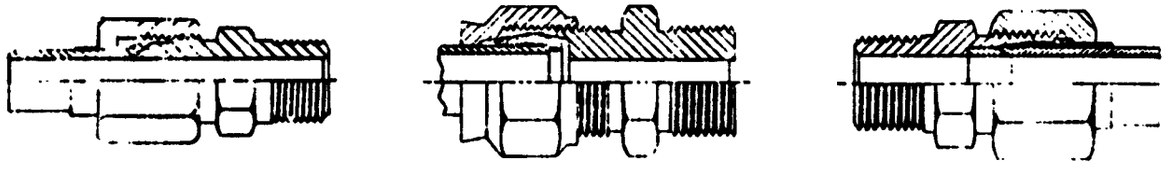

Three piece flared fitting

Butt joint

Self-flaring fitting

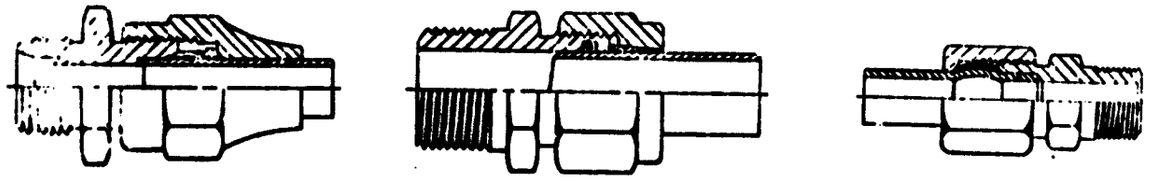

"Bite" type flareless fittings

O-ring type fitting

Compression fitting

Figure 98 Tubing Connections

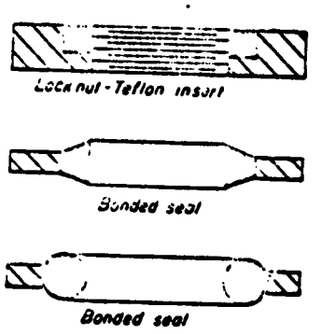

Figure 99 Lock-nut Type Fitting Seals

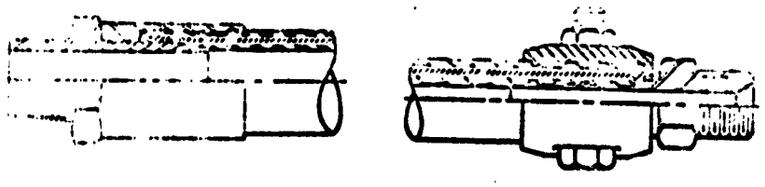

Screw-on type re-usable fitting

Clamp type fitting

Figure 100 Hose Fittings

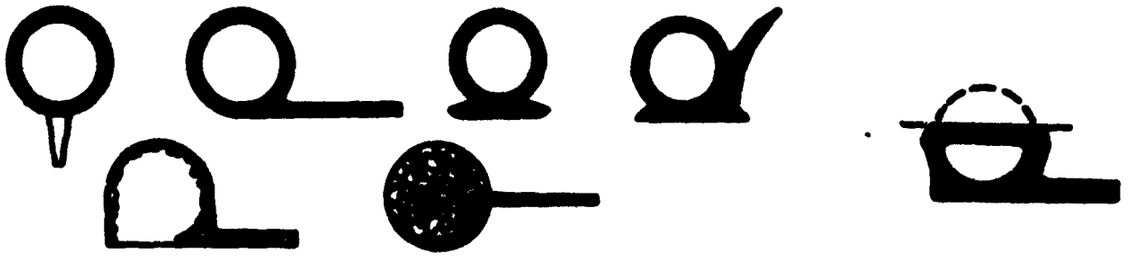

Tubular, bulb, bulb and flap

Flat sponge and miscellaneous flat

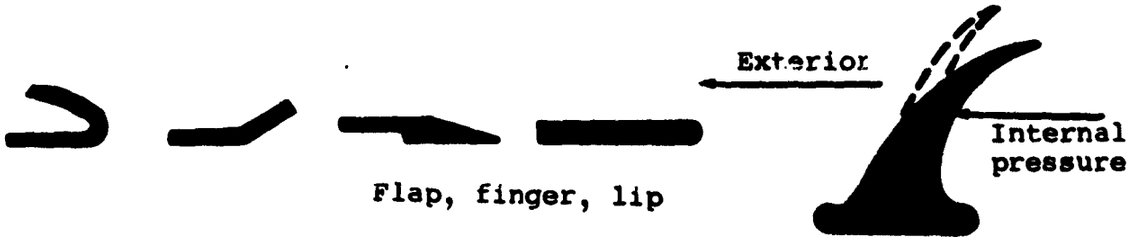

Flap, finger, lip

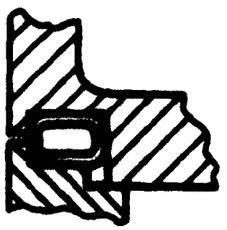

a) Tubular Type Bladder Seal

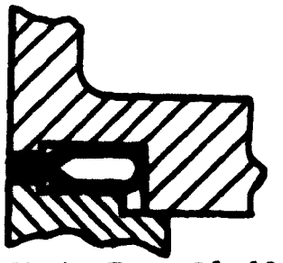

b) Folded Strip Type Bladder Seal

Figure 101 Module Deployment Seals (Ref.39)

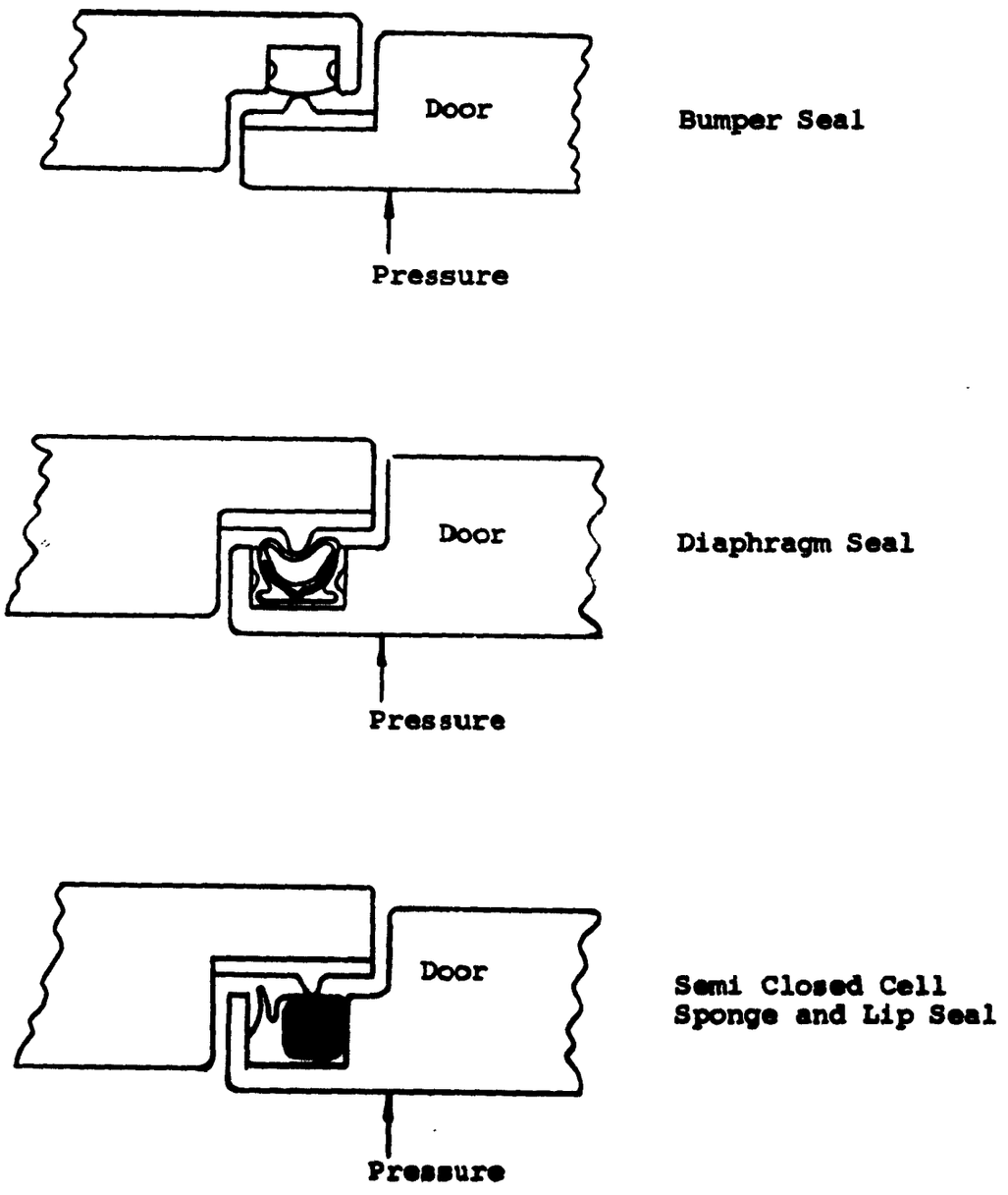

Figure 102 Inward Opening Exist Hatch Seals (Ref.39)

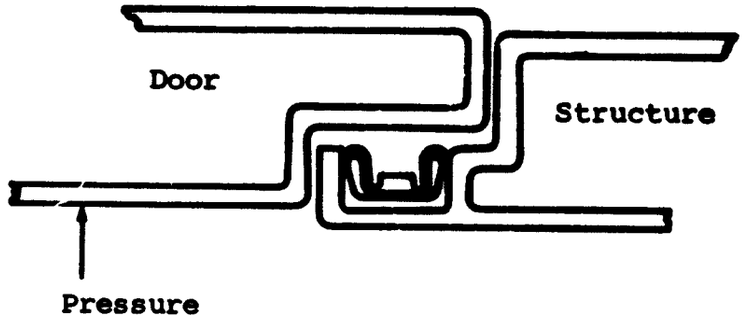

a) Cemented inflatable seal

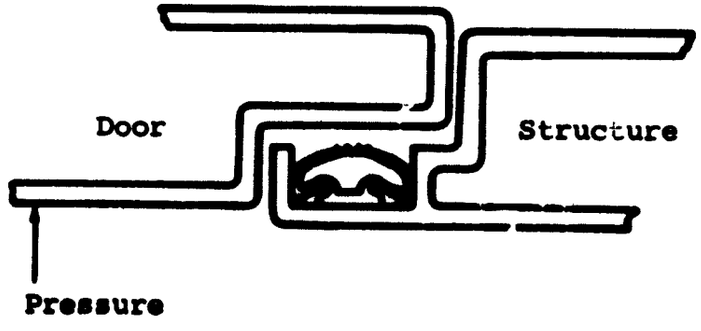

b) Retained inflatable seal

Figure 103 Outward Opening Exist Hatch Seal Configurations (Ref. 39)

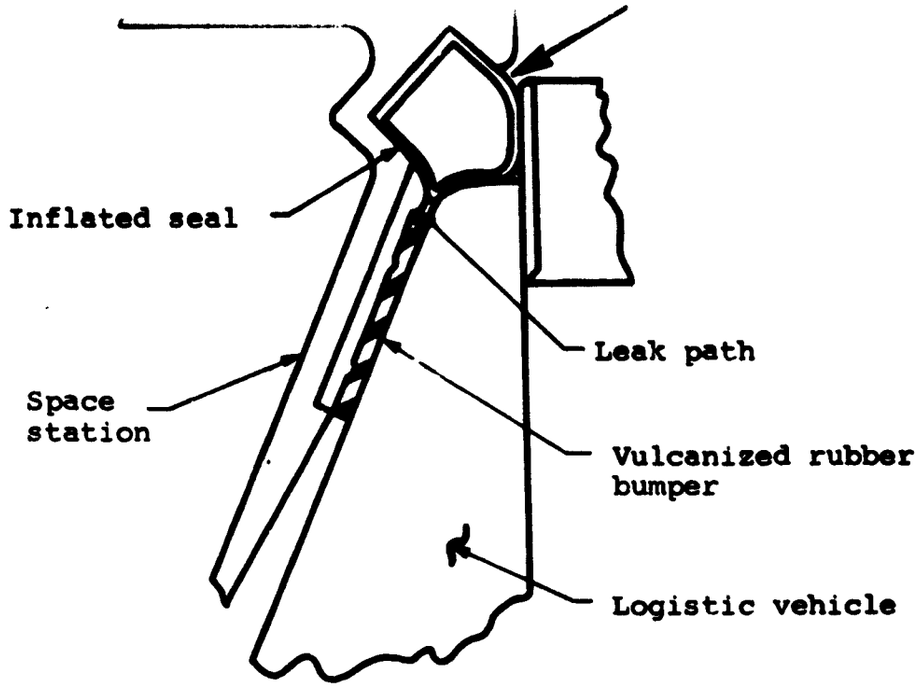

a) Inflatable Docking Seal

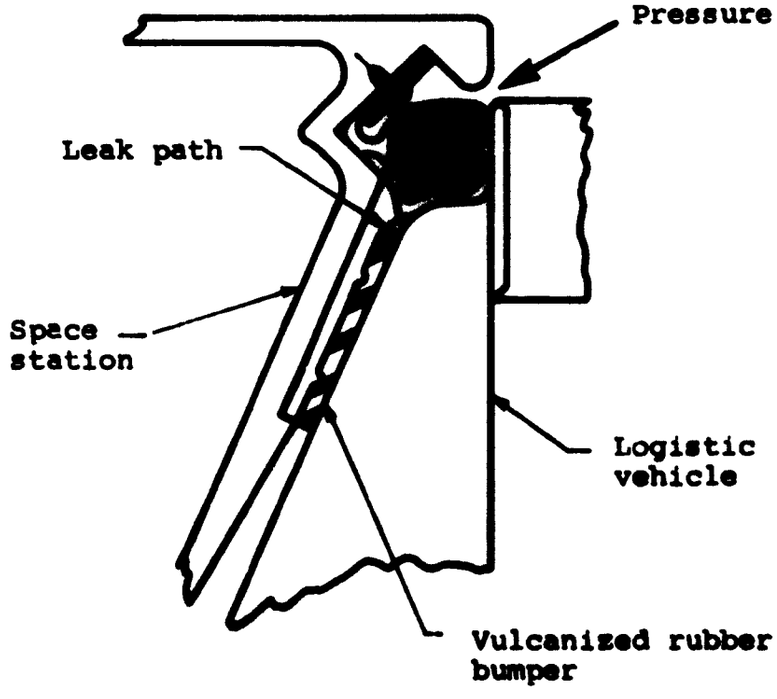

b) Closed Cell Sponge Filled Tubular Docking Seal

Figure 104 Docking Port Seal Configurations (Ref. 39)

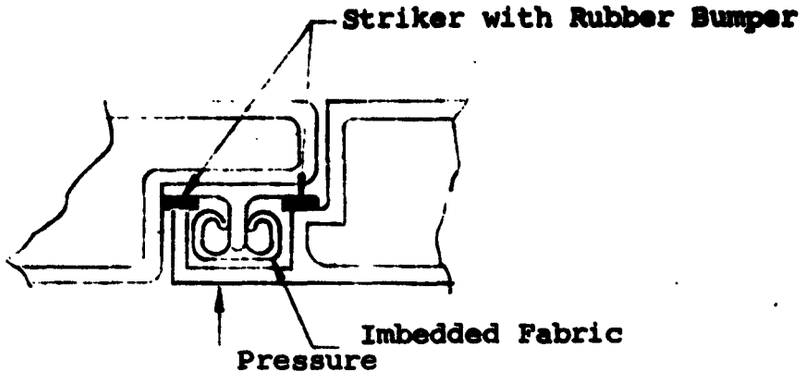

a) Inward Opening Access Door Seal Configuration

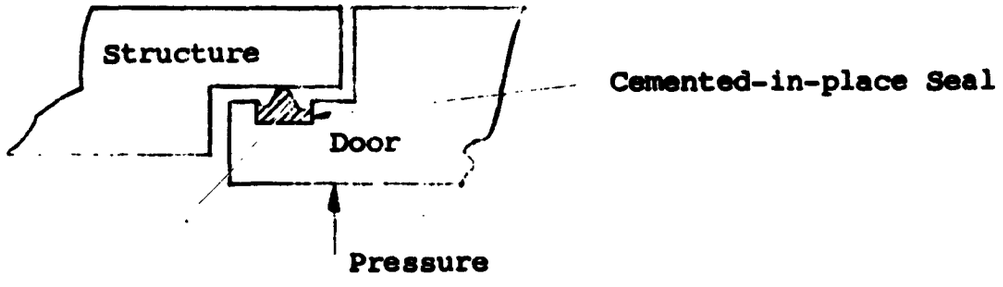

b) Inward or Outward Opening Solid Elastomer Seal

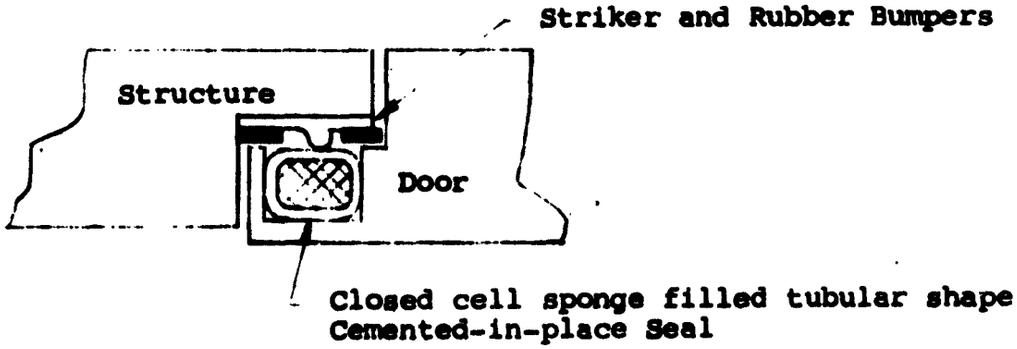

c) Inward and Outward Opening Access Door Seal

Figure 105 Access Door Seal Configurations (Ref.39)

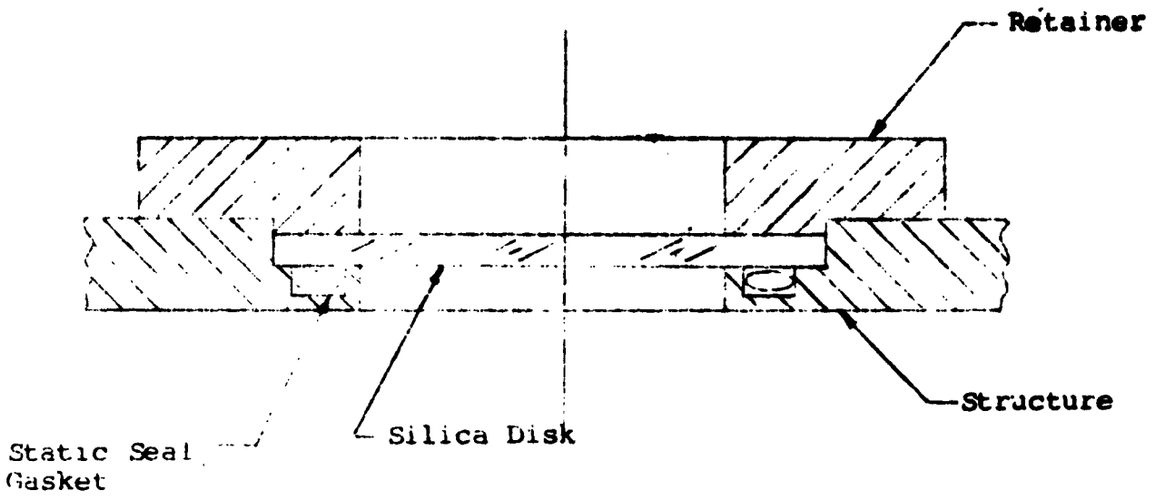

Figure 106 Gasket Type Static Seal Glazing Assembly

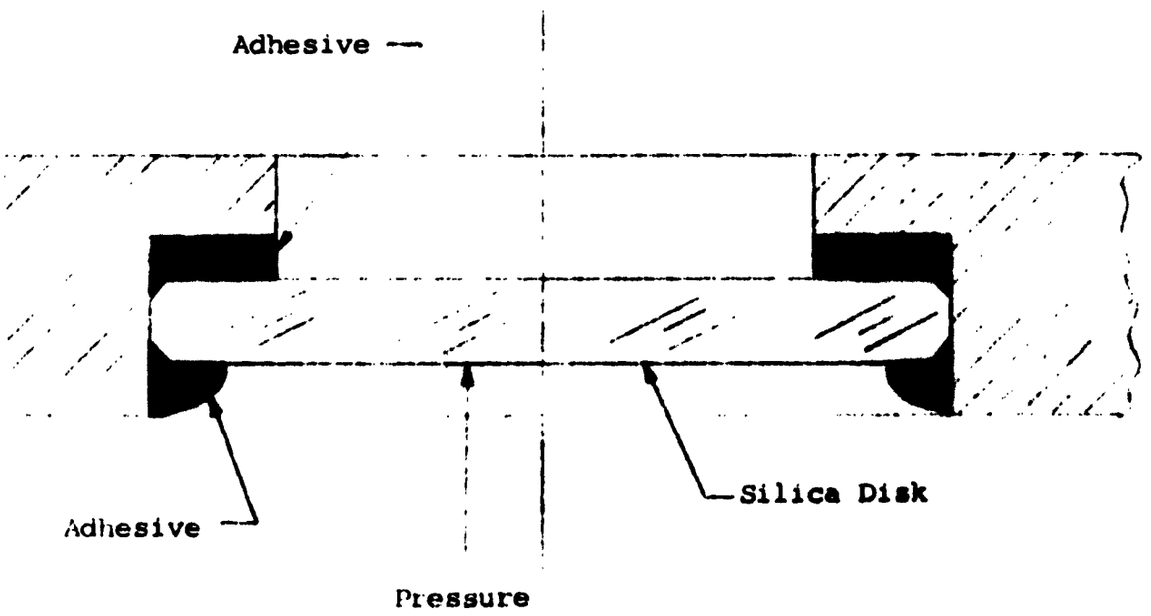

Figure 107 Faying Surface and Fillet Sealed Glazing Assembly (Ref.40)

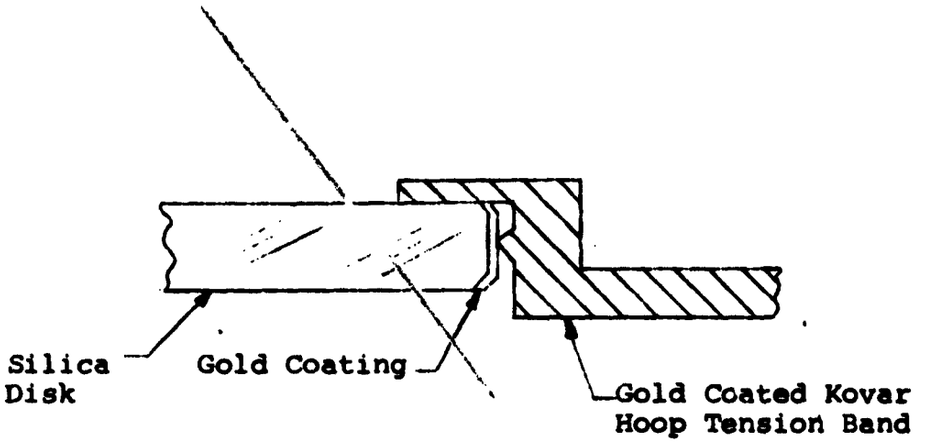

(a) Hoop Tension Glazing Assembly

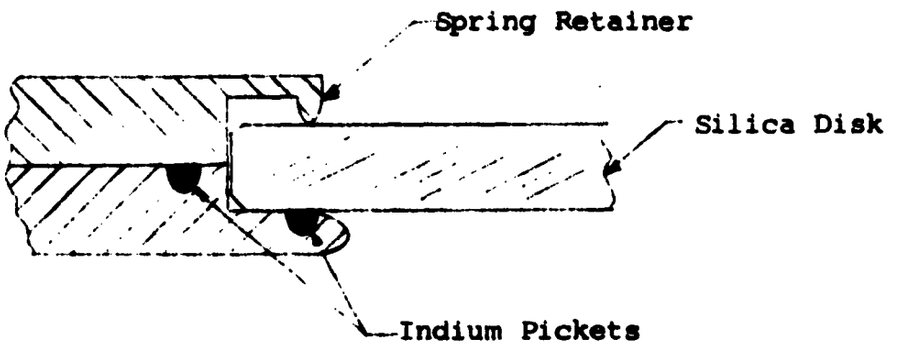

(b) Liquid Indium Seal Glazing Assembly

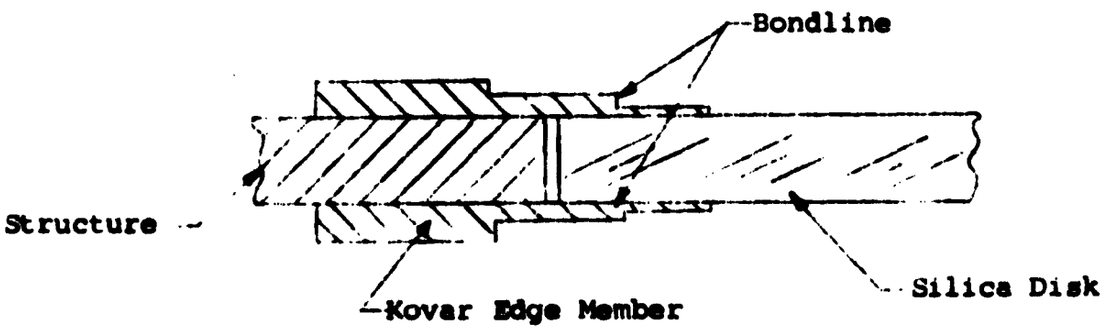

(c) Organically Bonded Glazing Assembly

Figure 108 Glazing Assembly Seal Configuration (Ref.40)

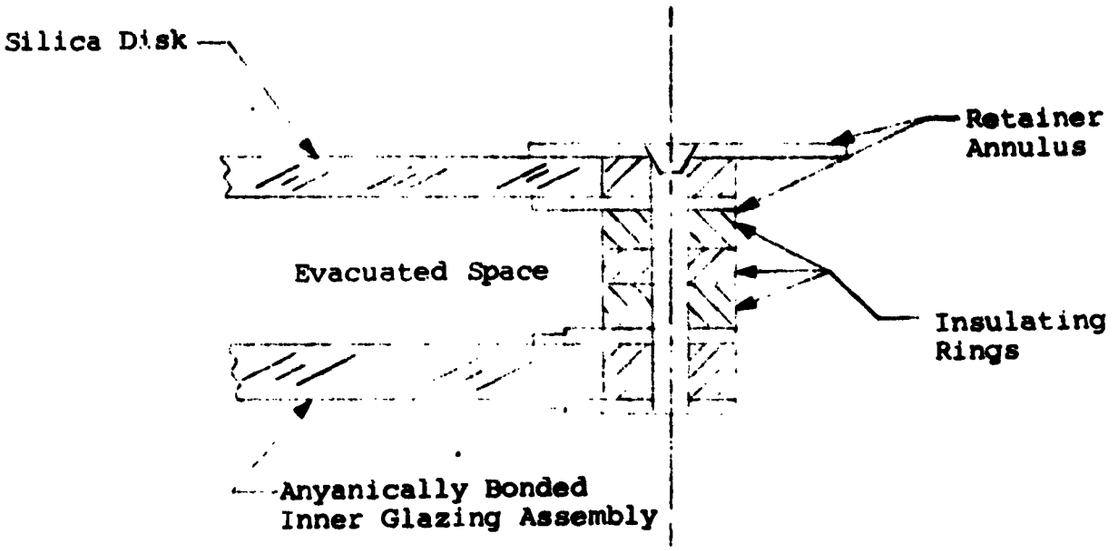

Figure 109 Insulated Edge Multi-Ply Glazing System

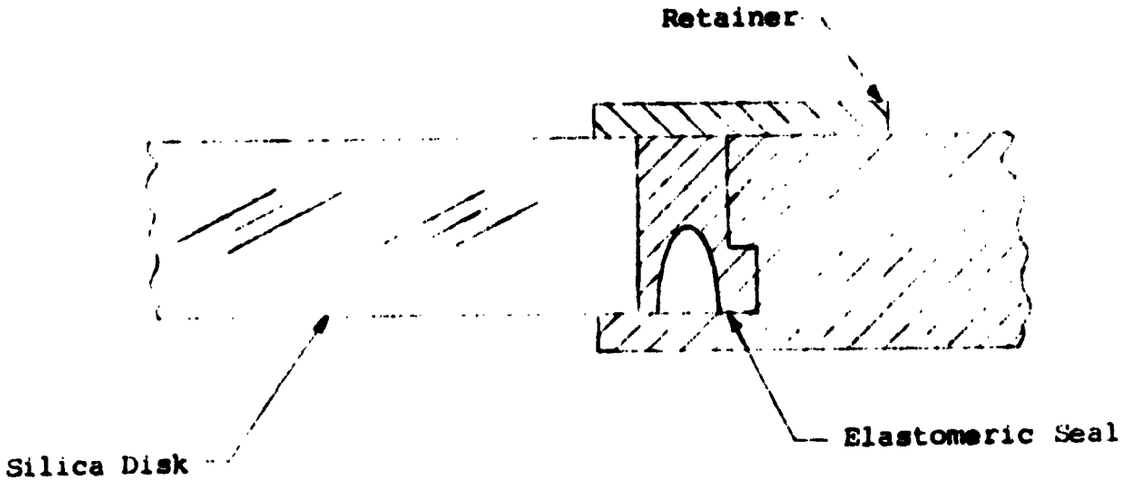

Figure 110 Cemented in Place Elastomer Seal Glazing Assembly (Ref.40)

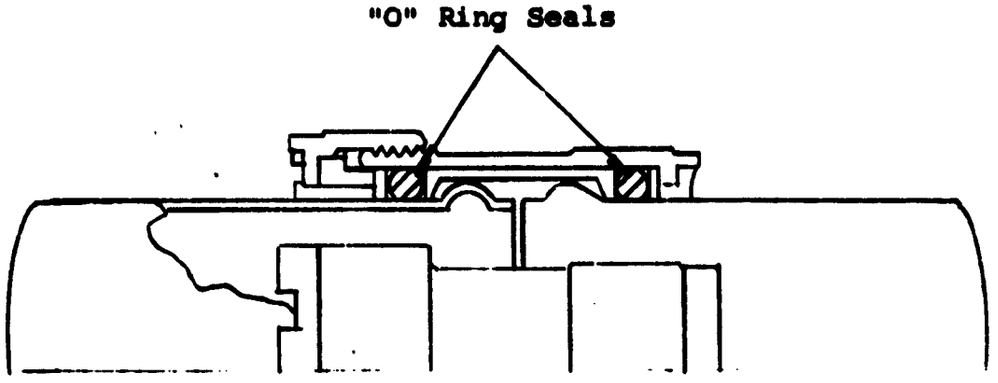

a) Deformed tube

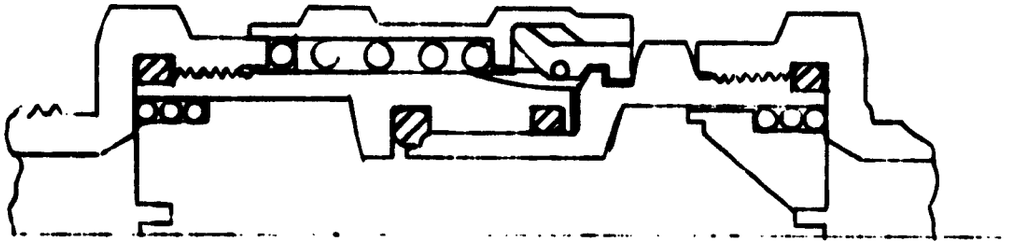

b) Threaded tube

Figure 111 Quick Disconnect Coupling

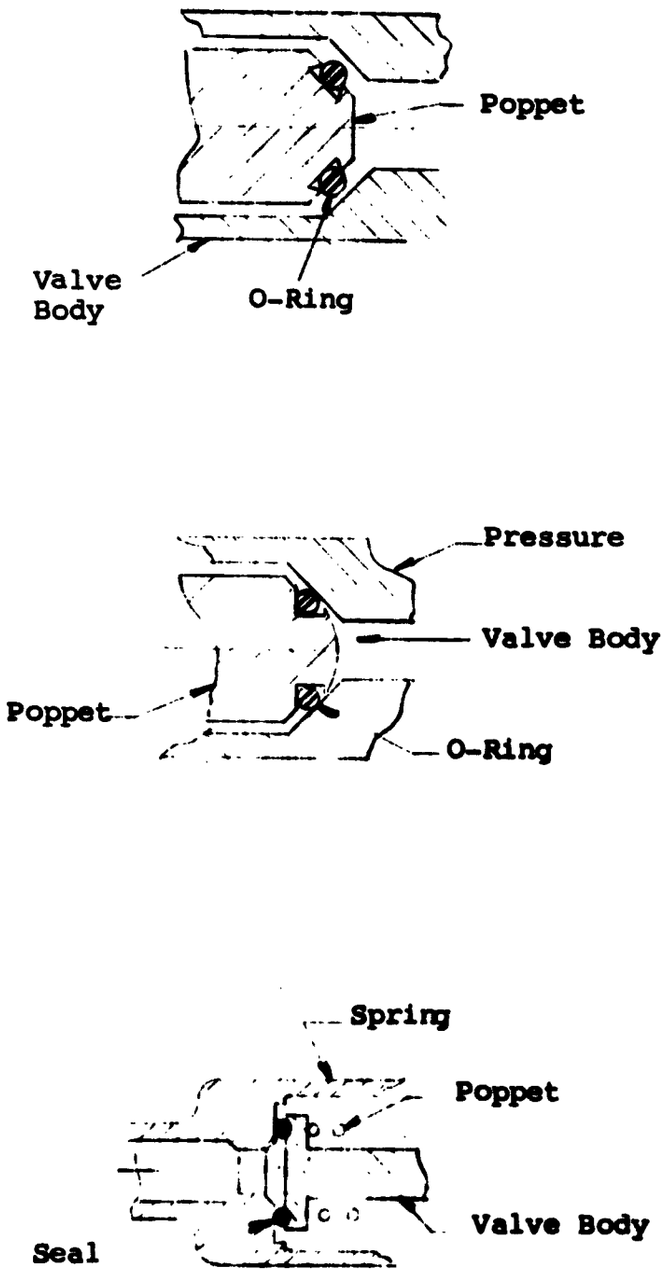

Figure 112 Valve Seat Designs with O-Rings

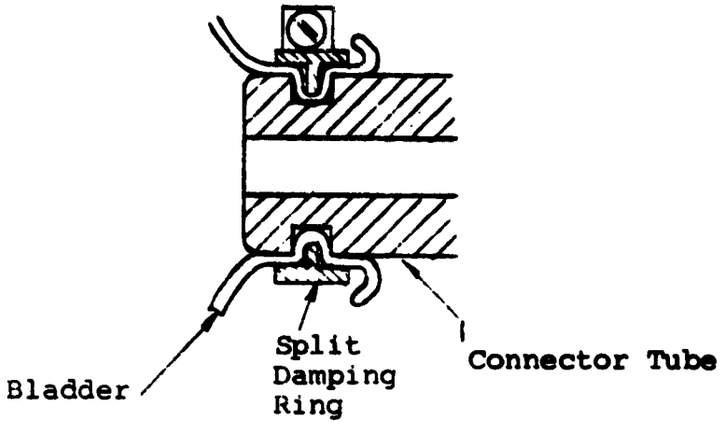

a) Ring type

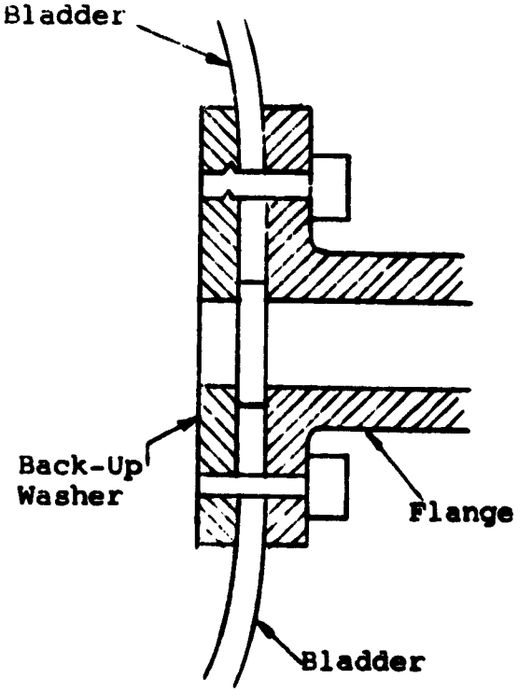

b) Flange type

Figure 113 Clamp Type Bladder Parts

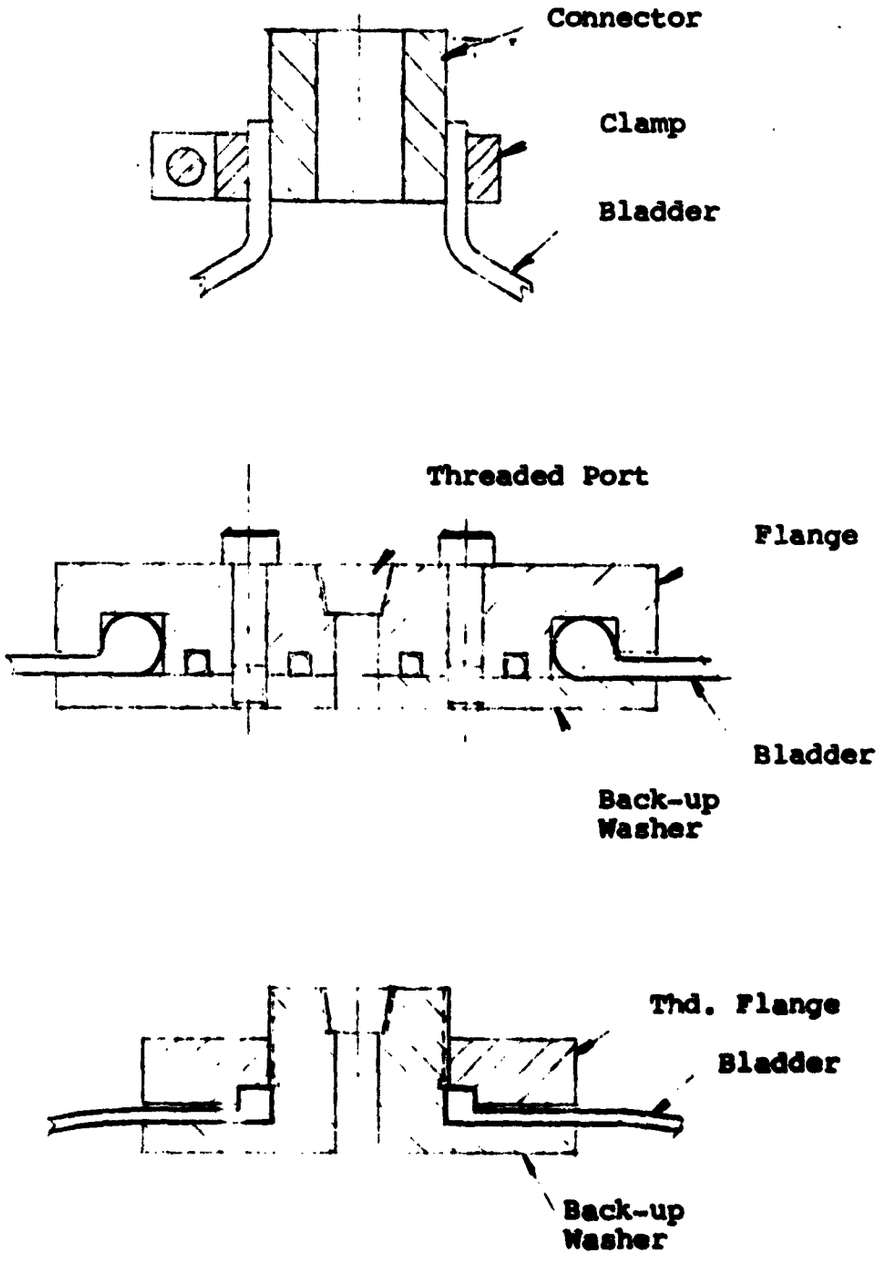

Figure 114 Bladder Attachment Configuration

REFERENCES

1. Norton, F. J., "Permeation of Gases Through Solids," J. of Applied Physics, Vol. 28, p. 28-34 (1957).

2. Cryogenic Seals, Varian Associates, Palo Alto, California.

3. Guerdon, D. A., "Hermetic Magnetic Couplings," Product Engineering, p. 96, November 27, 1961.

4. Trump, J. G., "Vacuum Electrostatic Engineering," D. Sc. Thesis, Massachusetts Inst. of Tech., 1933.

5. Musser, C. W., "Harmonic Drive," Machine Design, p. 160, April 14, 1960 (also United Shoe Machinery Corporation, Beverly, Massachusetts).

6. Denholm, A. S., McCoy, F. J., and C. N. Coenraads, "The Variable Capacitance Vacuum Insulated Generator", Progress Report, Proceedings of Symposium on Electrostatic Energy Conversion, April 1963, Power Information Center, Philadelphia, Pa.

7. Courtney, W. J., Lavelle, J., Britton, R., and A. S. Denholm, "Sealing Techniques for Rotation in Vacuum," AIAA, February 1964.

8. "Elastomers" - Design News Supplement, Design News, March 1965.

9. Bauer, P., Glickman, M., and F. Iwatsuki, "Analytical Techniques for the Design of Static, Sliding, and Rotating Seals for use in Rocket Propulsion Systems," Prepared for Air Force Rocket Propulsion Laboratory, RTD-AFSC, Report No. AFRPL-TDR-65-61.

10. Bauer, P., Glickman, M., and F. Iwatsuki, "Analytical Techniques for the Design of Static, Sliding, and Rotating Seals for use in Rocket Propulsion Systems," Prepared under Air Force Contract No. AF 04(611)-9704, IITRI Project No. K 6062.

11. Dushman, S. and J. M. Lofferty, Scientific Foundation of Vacuum Technique, Second Edition, Wiley & Sons, 1962.

12. Streeter, V., Handbook of Fluid Dynamics, McGraw Hill, 1958.

13. Scheideggan, A. E., The Physics of Flow Through Porous Media, MacMillan, 1957.

14. Kennard, E. H., Kinetic Theory of Gases with an Introduction to Statistical Mechanics, McGraw Hill, 1938.

15. Schlichting, H., Boundary Layer Theory, McGraw Hill, 1955.

16. Liepmann, H. W. and A. Roshko, Element of Gas Dynamics, J. Wiley and Sons, 1957.

17. Espe, W., "Werkstoffkunde der Hochvakuunatechnik," Deutcher Vertag der Wissenschaften, 1959.

18. Kuethe, A. and J. D. Schetzer, Foundations of Aerodynamics, Chapman and Hall, 1950.

19. Pinkus, O. and B. Sternlicht, Theory of Hydrodynamic Lubrication, McGraw Hill, 1961.

20. Pao, Richard H., Fluid Mechanics, John Wiley & Sons, 1961.

21. Hunsaker, J. and B. Rightnuse, Engineering Applications of Fluid Mechanics, McGraw Hill, 1947.

22. Brenhert, Karl, Jr., Elementary Theoretical Fluid Mechanics, John Wiley and Sons, 1960.

23. Hertz, H. and Boussinesq, "The Contact of Elastic Bodies," Gassamelte Werke I, 1881.

24. Timoshenko, S. and J. Goodier, Theory of Elasticity, McGraw Hill, 1951.

25. Love, A. E., Mathematical Theory of Elasticity, 4th edition, Dover Press, 1944.

26. Jones, A. B., New Departure-Analysis of Stresses and Deflections, Vol. I-II, General Motors Corp., 1946.

27. Palmgren, A., Ball and Roller Bearing Engineering, 3rd edition, SKF Industries, 1959.

28. Foppel, A., Technische Mechanik, 4th edition, Vol. 5.

29. Halliday, V. S., Proc. Inst. Mech. Engrs., p. 647, 1957.

30. Dyachenko, R., "Surface Finish," Industrial Diamond Review, June 1952.

31. Tabor, D., The Hardness of Metals, Oxford University Press, 1951.

32. Bowden, F. P. and D. Tabor, The Friction and Lubrication of Solids, Vol. I, Oxford University Press, 1950.

33. Surface Roughness, Waviness, and Lay, MIL-STD-10A, 13 October 1955.

34. Posey, C., "Measurement of Surface Roughness," Mech. Eng. 4, 1946.

35. "Design Criteria for Zero-Leakage Connectors for Launch Vehicles," Vol. 3, F. O. Rathbun, Jr., Editor, General Electric, under Contract NAS 8-4012.

36. Roark, R. J., "Formulas for Stress and Strain," McGraw Hill, New York, 1954.

37. "Pressure Vessel and Piping Design," ASME Collected Papers, 1927-1959, American Society of Mechanical Engineers, New York, 1960.

38. "Space Radiation Effects on Materials," ASTM Special Technical Publication No. 330, American Society for Testing and Materials, Philadelphia, 1962.

39. Silverman, B., and J. C. George, "Space Environment Studies of Seals," Prepared for NASA Manned Spacecraft Center, Contract No. NAS9-1563.

40. Robinson, J., "Research in Extreme Environment Aerospace Vehicle Window Assemblies," ASD-TDR-62-570, April 1963.

SUPPLEMENTARY

INFORMATION

AD 620 044

ERRATA FOR AFFDL-TR-65-88, PART I

NOTICES

When Government drawings, specifications, or other data are used for any purpose other than in connection with a definitely related Government procurement operation, the United States Government thereby incurs no responsibility nor any obligation whatsoever; and the fact that the Government may have formulated, furnished, or in any way supplied the said drawings, specifications, or other data, is not to be regarded by implication or otherwise as in any manner licensing the holder or any other person or corporation, or conveying any rights or permission to manufacture, use, or sell any patented invention that may in any way be related thereto.

This document is subject to special export controls and each transmittal to foreign governments or foreign nationals may be made only with prior approval of the Air Force Flight Dynamics Laboratory (FDTS), Wright-Patterson AFB, Ohio.

Copies of this report should not be returned to the Research and Technology Division unless return is required by security considerations, contractual obligations, or notice on a specific document.